2011

Gene expression in the right ventricle during development of pulmonary hypertension

Jennifer Drake
Virginia Commonwealth University

GENE EXPRESSION IN THE RIGHT VENTRICLE DURING

DEVELOPMENT OF PULMONARY HYPERTENSION

A dissertation submitted in partial fulfillment of the requirements for the degree of Doctor of Philosophy at Virginia Commonwealth University.

by

JENNIFER I. DRAKE
B.S. (Molecular Biology and Biochemistry) University of Wisconsin, Madison, WI, 2002
M.BNFO. Virginia Commonwealth University, Richmond, VA 2006

Director: PAUL M. FAWCETT PH.D.
ASSISTANT PROFESSOR, DEPARTMENT OF INTERNAL MEDICINE, DIVISION OF INFECTIOUS DISEASE AND DIRECTOR OF RESEARCH RESOURCES, MASSEY CANCER CENTER AT VIRGINIA COMMONWEALTH UNIVERSITY

Virginia Commonwealth University
Richmond, VA
September, 2011

Acknowledgements

First, I would like to express my gratitude to my advisor, Paul Fawcett, for his patience, encouragement and support throughout this process. In addition, I would like to thank the members of my Ph.D. committee: Dan Conrad, Alpha (Berry) Fowler, Paul Dent, and Norbert Voelkel – for their advice and continued support. I would also like to thank my program director, Rob Tombes, for his guidance.

Next, I would like to thank my fellow lab members: Jen Fettweis, Joe Bertsche, Nusara Satproedprai, Chris Friedline, Daniela Farkas, Laszlo Farkas, Donatas Kraskauskas, Vita Kraskauskiene, and Jose Gomez Arroyo. Jen provided valuable feedback on the manuscript and technical advice regarding protein studies. Nusara gave me with helpful advice regarding microarray hybridization techniques. Daniela provided technical advice regarding Western Blot techniques. Donatas performed the animal studies.

In addition, I would like to thank Ramesh Natarajan for his valuable advice and help with the RT-PCR and protein studies presented in Chapter 4. Catherine Dumur contributed to the prediction analysis work presented in Chapters 4 and 5. Shirley Helm provided technical advice regarding the cytokine assay. I would also like to thank members of the Voelkel lab, Fowler lab, Buck lab, and anyone else who lent equipment, gifted reagents, provided support, or gave technical advice during my graduate studies.

Lastly, I would like to thank my friends and family for their endless support, especially my husband, Andy Drake, who has been incredibly patient and supportive during my graduate studies.

Table of Contents

Appendices

List of Tables

Page

List of Figures

Page

List of Abbreviations

α	alpha
β	beta
μ	micro
Δ	delta
Ang1	Angiopoietin-1
ANP	Atrial natriuretic peptide
ATII	Angiotensin II
ATP	Adenosine triphosphate
BMP	Bone morphogenetic protein
BMPR2	Bone morphogenetic protein receptor 2
BNP	Brain natriuretic peptide
Camk	Calcium/calmodulin-dependent protein kinase
Ccnd2	Cyclin D2
cDNA	Complementary DNA
cGMP	Cyclic guanosine monophosphate
CHD	Congenital heart disease
CO	Cardiac output

CO_2	Carbon dioxide
COUP-TFII	Chicken ovalbumin upstream promoter transcription factor 2
Creb	Cyclic-AMP response binding element
CTEPH	Chronic thromboembolic pulmonary hypertension
DNA	Deoxyribonucleic acid
E	Embryonic day
Ece1	Endothelin converting enzyme 1
ECM	Extracellular matrix
eNOS	Endothelial nitric oxide synthase
Fat3	FAT tumor suppressor homolog 3
FDR	False discovery rate
Fgf8	Fibroblast growth factor 8
Fgf10	Fibroblast growth factor 10
Gadd45a	Growth arrest and DNA damage-inducible 45, alpha
Glut1	Glucose transporter 1
Hand1	Heart and neural crest derivatives expressed 1
Hand2	Heart and neural crest derivatives expressed 2
Hebp1	Heme binding protein 1
HIF-1α	Hypoxia-inducible factor 1, alpha
HIF-2α	Hypoxia-inducible factor 2, alpha
HIV	Human immunodeficiency virus
Homer2	Homer homolog 1
IGF1	Insulin-like growth factor 1

IL	Interleukin
Irx2	Iroquois related homeobox 2
Isl1	Islet 1
LOOCV	Leave one-out cross-validation
LV	Left ventricle
MAPK	Mitogen-activated kinase-like protein
Mef2	Myocyte enhancer factor 2
Mef2c	Myocyte enhancer factor 2c
MHC-α	Myosin heavy chain, alpha
MHC-β	Myosin heavy chain, beta
mmHg	Millimeters of mercury
MMP	Matrix metalloproteinase
mPAP	Mean pulmonary artery pressure
NAD(P)H	Nicotinamide adenine dinucleotide (phosphate)
Nfat	Nuclear factor of activated T-cells
Nfat3	Nuclear factor of activated T-cells 3
Nkx2-5	Natural killer 2 transcription factor related, locus 5
NO	Nitric oxide
Nppb	Natriuretic peptide precursor b
Nr2f2	Nuclear receptor subfamily 2, group F, member 2
O2	Oxygen
PAB	Pulmonary artery banding
PAH	Pulmonary arterial hypertension

PANTHER	Protein analysis through evolutionary relationships
PCH	Pulmonary capillary hemangiomatosis
PET	Positron emission tomography
PH	Pulmonary hypertension
Pitx2	Paired-like homeodomain transcription factor 2
Pkn1	Protein kinase N1
Ppp3ca	Protein phosphatase 3, catalytic subunit, alpha isoform
Pten	Phosphatase and tensin homolog
PVOD	Pulmonary veno-occlusive disease
qRT-PCR	Quantitative real-time polymerase chain reaction
Rcan1	Regulator of calcineurin 1
RNA	Ribonucleic acid
RNS	Reactive nitrogen species
Rock1	Rho-associated coiled-coil containing protein kinase 1
ROS	Reactive oxygen species
RV	Right ventricle
SAM	Significance analysis of microarrays
Sirt1	Sirtuin 1
SLE	Systemic lupus erythematosus
Smarcd2	SWI/SNF related, matrix associated, actin dependent regulator of chromatin, subfamily d, member 2
Stat3	Signal transducer and activator of transcription 3

SU5416	(3*Z*)-3-[(3,5-dimethyl-1*H*-pyrrol-2-yl)methylidene]-1,3-dihydro-2*H*-indol-2-one
Tbx5	T-box transcription factor 5
Th2	T helper cell 2
Tle3	Transducin-like enhancer of split 3
TNF-α	Tumor necrosis factor alpha
VEGF	Vascular endothelial growth factor
VEGFR2	Vascular endothelial growth factor receptor 2
VCU	Virginia Commonwealth University
Vwf	Von Willebrand factor
Wnt	Wingless-type MMTV integration site family members

Abstract

GENE EXPRESSION PROFILING: A FAILURE SIGNATURE

PREDICTIVE OF RIGHT HEART FAILURE

By Jennifer I. Drake, Ph.D.

A dissertation submitted in partial fulfillment of the requirements for the degree of Doctor of Philosophy at Virginia Commonwealth University.

Virginia Commonwealth University, 2011

Major Director: Paul M. Fawcett, Ph.D.
Assistant Professor, Department of Internal Medicine and Director of Research Resources, Massey Cancer Center at Virginia Commonwealth University

Pulmonary arterial hypertension (PAH) is a disease of the lung vessels that causes severe effects on the right ventricle of the heart; ultimately, most patients with severe PAH die as a result of right heart failure. However, little is known about the causes of right heart failure.

Here, we describe a pattern of gene expression that differs between the normal rat left ventricle (LV) and right ventricle (RV). These genes are known to be involved in the

development of the heart as well as adaptations to the heart during stress. This gene expression pattern is used as a baseline to describe changes in gene expression the occur in the RV as a result of adaptive hypertrophy, stimulated by chronic hypoxia, or right ventricular failure (RVF), caused by administration of Su5416 and hypoxia. The genes differing between RVF and hypertrophy encode glycolytic enzymes, mitochondrial electron transport chain complexes, cell-growth promoting proteins, and angiogenic capillary maintenance proteins. Additionally, we show that RVF is associated with an increase in the serum cytokine production of IL-1β, IL-10, TNF-α, and VEGF. Finally, we show that treatment with the β-adrenergic receptor blocker carvedilol partially changed the gene expression pattern seen with RVF. The most profound effects were on the genes encoding glycolytic enzymes and mitochondrial electron transport chain complexes.

Together, these results show that the normal LV and RV have a distinct pattern of expression and that the failing RV is characterized by changes in cell growth, angiogenesis, and energy utilization. Treatment with carvedilol can partially reverse these gene expression changes in the failing RV.

Chapter 1: Pulmonary Hypertension, the Heart, and their Interactions

1.1 Pulmonary Hypertension

1.1.1 Overview

Pulmonary hypertension refers to an increase in pressure in the lung circulation frequently causing in patients symptoms of dizziness, fatigue, peripheral leg edema, and shortness of breath. It is diagnosed by measurements obtained during right heart catheterization. Patients with pulmonary hypertension have a mean pulmonary artery pressure of greater than 25 mmHg at rest or greater than 30 mmHg with exercise[1]. A normal mean pulmonary artery pressure is 8 – 20 mmHg at rest.

1.1.2 Classification schemes

Pulmonary hypertension is categorized according to a World Health Organization classification scheme, the first of which was proposed in 1973 at an international conference on primary pulmonary hypertension. Based on the presence or absence of

identifiable causes and risk factors, patients were classified as having either primary or secondary pulmonary hypertension[2, 3]. In 1998, the second world symposium on pulmonary arterial hypertension (PAH) was held in Evian, France. Here, five major categories of pulmonary hypertension were created based on shared pathological and clinical features and therapeutic options[4]. The third world symposium was held in Venice, Italy in 2003. During this conference, the primary pulmonary hypertension group was subdivided into idiopathic pulmonary arterial hypertension, familial pulmonary arterial hypertension, or associated pulmonary arterial hypertension[5]. During the fourth world symposium held in Dana Point, California in 2008, modifications of the Venice classifications were made to reflect current publications and treatments[5] (**Table 1**). The groups as described following are based on the Venice classification scheme.

1.1.3 Pulmonary arterial hypertension

Pulmonary arterial hypertension (PAH) may arise spontaneously and have no familial connection (idiopathic PAH), have a familial connection (familial PAH), or be associated with other diseases such as connective tissue disease or HIV (associated PAH). The PAH subgroup of PH adds an additional diagnostic criterion of a mean pulmonary wedge pressure, an indirect measure of left arterial pressure and an indication of left ventricular failure, greater than or equal to 15 mmHg[1]. Idiopathic PAH has an estimated incidence of approximately 2 cases per million per year.[6, 7] The mean age at presentation in adults ranges from 36 – 50, although individuals of any age can be affected.[7, 8] In a

Table 1: Venice classification scheme of pulmonary hypertension

1. Pulmonary arterial hypertension (PAH)
- 1.1 Idiopathic PAH
- 1.2 Heritable PAH
  - 1.2.1 BMPR2
  - 1.2.2 ALK1, endoglin (with or without hereditary hemorrhagic telanglectasia)
  - 1.2.3 unknown
- 1.3 Drug- and toxin-induced
- 1.4 Associated with
  - 1.4.1 Connective tissue diseases
  - 1.4.2 HIV infection
  - 1.4.3 Portal hypertension
  - 1.4.4 Congenital heart diseases
  - 1.4.5 Schistosomiasis
  - 1.4.6 Chronic hemolytic anemia
- 1.5 Persistent pulmonary hypertension of the newborn

1' Pulmonary veno-occlusive disease (PVOD) and/or pulmonary capillary hemangiomatosis (PCH)

2. Pulmonary hypertension owing to left heart disease
- 2.1 Systolic dysfunction
- 2.2 Diastolic dysfunction
- 2.3 Valvular disease

3. Pulmonary hypertension owing to lung diseases and/or hypoxia
- 3.1 Chronic obstructive pulmonary disease
- 3.2 Interstitial lung disease
- 3.3 Other pulmonary diseases with mixed restrictive and obstructive pattern
- 3.4 Sleep-disordered breathing
- 3.5 Alveolar hypoventilation disorders
- 3.6 Chronic exposure to high altitude
- 3.7 Developmental abnormalities

4. Chronic thromboembolic pulmonary hypertension (CTEPH)

5. Pulmonary hypertension with unclear multifactorial mechanisms
- 5.1 Hematologic disorders: myeloproliferative disorders, splenectomy
- 5.2 Systemic disorders: sarcoidosis, pulmonary Langerhans cell histiocytosis, lymphangioleiomyomatosis, neurofibromatosis, vasculitis
- 5.3 Metabolic disorders: glycogen storage disease, Gaucer disease, thyroid disorders
- 5.4 Others: tumoral obstruction, fibrosing mediastinitis, chronic renal failure on dialysis

study of 194 patients with PAH conducted by the NIH from 1981 to 1985, the estimated median life span after diagnosis was 2.8 years with 1-, 3-, and 5-year survival rates of 68%, 48%, and 34%[8]. A more recent study estimates 1-, 2-, and 3-year survival rates at 77%, 69%, and 35%.[9]. Irrespective of the causes, most PAH patients die from intractable right heart failure.

Histological findings of PAH are: intimal hyperplasia, medial hypertrophy, adventitial proliferation and fibrosis, occlusion of small arteries, *in situ* thrombosis, and infiltration of inflammatory and progenitor cells. Plexiform lesions are a hallmark of PAH and are found only in patients with PAH Group 1 and also in patients with myeloproliferative disease and patients with sarcoidosis (Group 5), but not those with other PH categories (**Figure 1**). These complex vascular lesions are typically composed of proliferating endothelial cells and perivascular inflammatory cells and are located downstream from the occluded arteries. They express growth and transcription factors observed in tissues undergoing angiogenesis, including vascular endothelial growth factor (VEGF) and hypoxia inducible factor 1α (HIF-1α)[10]. It is hypothesized that widespread early endothelial apoptosis seen in PAH culminates in selection of apoptosis-resistant endothelial precursor cells that proliferate and eventually form plexiform lesions[11].

In familial PAH patients, bone morphogeneic protein receptor type 2 (BMPR2) germline mutations are seen in 70% of patients[12, 13]. In addition, 11% - 40% of idiopathic PAH patients also have BMPR2 mutations[14, 15]. It has been suggested that patients with BMPR2 mutations may present a subgroup of PAH patients with a more severe form of

Figure 1: Plexiform lesions of pulmonary arterial hypertension

Pulmonary blood vessels in the normal (left) and pulmonary arterial hypertension (right) lung. The plexiform lesions seen in the pulmonary hypertension lung are formed due to increased cell proliferation and decreased apoptosis leading to occlusion of the pulmonary vascular lumen.

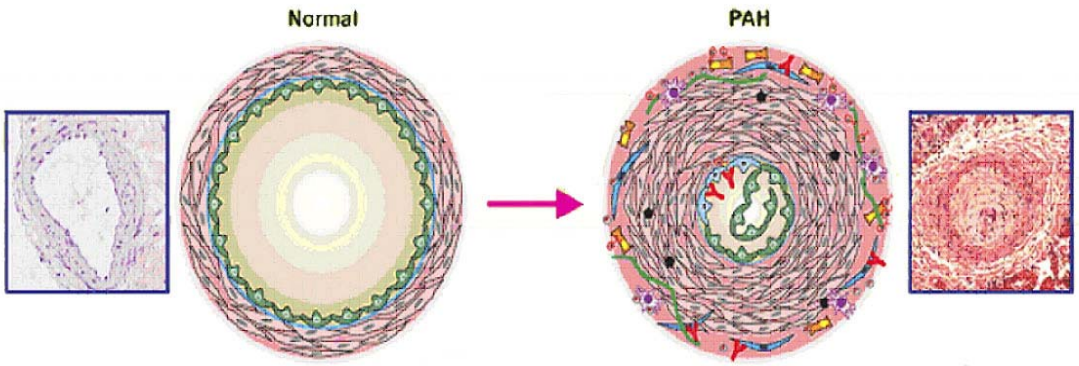
Normal
PAH

the disease and are less likely to demonstrate vasoreactivity than the idiopathic PAH patients without BMPR2 mutations.[16-18] Other, more rare, germline mutations are in endoglin and activin receptor-like kinase type 1 occuring predominantly with hereditary hemorrhagic telangiectasia,[19, 20] also known as Osler-Weber-Rendu disease, which is characterized by abnormal blood vessel formation in the skin and organs.

A number of risk factors relating to drugs or toxins are included in the classifications of PAH and were categorized as "definite," "very likely," "possible," or "unlikely" based on their association with PAH (**Table 2**). A "definite" association is one defined as an epidemic or a large, multi-center epidemiologic study demonstrating an association between the drug and PAH. A "likely" association is one revealed by a single-center, case-controlled study. "Possible" is defined as drugs with similar mechanisms or actions as those in the "definite" or "likely" categories, but has not yet been studied. Those drugs termed "unlikely" have been studied and no association has been revealed.[4] The only identified definite risk factors for PAH are aminorex, amphetamine, fenfluramine, and toxic rapeseed oil[4, 21]. Aminorex and fenfluramine are drugs used in anti-obesity medication. Toxic rapeseed oil is rapeseed oil contaminated with oleoanilide, a chemical by-product formed when industrial grade rapeseed oil interacts with anilide and acetanilide[22]. Between 1998 and 2001, the Surveillance of Pulmonary Hypertension in America (SOPHIA) study enrolled 1,335 patients across the US and determined the association of fenfluramine or dexfenfluramine intake with the development of PAH[23]. It also studied St. John's Wort and over-the-counter anti-obesity drugs containing phenylpropanolamine, both of which were shown to increase the risk of developing

Table 2: Risk factors for development of pulmonary arterial hypertension

Definite
-aminorex
-fenfluramine, dexfenfluramine
-toxic rapeseed oil
Likely
-amphetamines
-methamphetamines
Possible
-chemotherapeutic agents
-cocaine
-phenylpropanolamine
-SSRIs
-St. John's Wort
Unlikely
-cigarette smoking
-estrogen therapy
-oral contraceptives

PAH[23]. While the SOPHIA study showed no increase risk for developing PAH with intake of non-selective monoamine reuptake inhibitors (MAOIs), selective serotonin reuptake inhibitors (SSRIs), antidepressants, or anxiolytics[23], a case-controlled study of pregnant women using SSRIs after 20 weeks of gestation showed an increased risk for the newborn developing persistent PH of the newborn, a form of PH[24]. As such, SSRIs have been placed in the "possible" risk category.

Another subgroup of PAH is the PAH associated with other diseases, including connective tissues diseases, HIV, portal hypertension, congenital heart disease, schistosomiasis, and chronic hemolytic anemias. PAH occurs in 7% - 12% of patients with scleroderma[25, 26], a chronic systemic autoimmune disease characterized by fibrosis and vascular alterations, while the prevalence of PAH associated with systemic lupus erythematosis (SLE), a systemic autoimmune disease that can affect any part of the body[27, 28], and mixed connective tissue disease[29, 30] is unknown, but likely occur less often than with scleroderma. PAH is a rare complication of HIV infection with an incidence of 1 in 200 AIDS patients, and HIV-associated PAH has clinical, hemodynamic, and histological characteristics similar to those found in idiopathic PAH[5]. In the early 1990s before antiretroviral therapy was widely available, 0.5% of patients with HIV also had PAH[31]. A more recent study shows the percent of HIV patients with PAH to be 0.46%[32]. Untreated congenital heart disease (CHD), in particular those patients with systemic-to-pulmonary shunts, presents a significant risk for developing PAH. Eisenmenger syndrome, defined as CHD with an initial large systemic-to pulmonary shunt that induces progressive pulmonary vascular disease and

PAH, presents the most advanced form of PAH associated with CHD[33]. The prevalence of PAH associated with congenital systemic-to-pulmonary shunts in Europe and North America has been estimated to be between 1.6 and 12.5 cases per million adults, 25% - 50% of which have Eisenmenger syndrome[34]. PAH associated with schistosomiasis, an infection caused by a parasitic worm of the genus *Schistosoma*, can have similar clinical presentation to idiopathic PAH[35], including similar histological findings and the development of plexiform lesions[36]. It is estimated that more than 200 million people worldwide are infected by one of the three species of *Schistosoma*, of which 4% - 8% develop hepatosplenic disease, which is characterized by an enlarged liver and spleen and block of portal bloodflow[37]. Of patients with hepatosplenic disease, 4.6% also develop PAH[38]. PAH can also be a complication of chronic hereditary and acquired hemolytic anemias, including sickle cell disease[39, 40]; thalassemia, an autosomal recessive disorder that causes a reduced rate of synthesis or lack of synthesis of globin molecules[41]; hereditary spherocytosis, an autosomal dominant disorder in which red blood cells are sphere-shaped rather than bi-concave disc shaped[42, 43]; stomatocytosis, an autosomal dominant disorder in which the membrane of the red blood cells leak sodium and potassium[44]; and microangiopathic hemolytic anemia, which causes destruction of the red blood cells by a fibrin mesh that forms due to increased coagulation activity[45]. PH has been described most often in patients with sickle cell disease and presents with histological lesions similar to those seen in idiopathic PAH, including plexiform lesions. In the largest study of patients with sickle cell disease, 32% also had PAH[40]. However, a recent study by a French group has revised this incidence to 6%[46].

Three classes of drugs are currently being used to treat PAH: prostanoids, such as prostacyclin, endothelin receptor antagonists, such as bosentan or ambristentan, and phosphodiesterase-5 inhibitors, such as sildenafil. These drugs are used to induce pulmonary vasodilation with the additional hope that they reverse pulmonary vascular remodeling[47, 48]. While these drugs may be advantageous for the lungs, they can have negative effects on the heart by increasing the contractility of the RV. Increased contractility causes an increase oxygen demand and can reduce RV dilation[48]. In addition to vasodilator therapy, based on empirical evidence most patients also receive anti-coagulants, such as warfarin, to prevent thrombosis *in situ* and diuretics to prevent edema[47].

1.1.4 Pulmonary veno-occlusive disease and pulmonary capillary hemangiomatosis

While pulmonary veno-occlusive disease (PVOD) and pulmonary capillary hemangiomatosis (PCH) are very rare, PVOD is increasingly recognized as causes of PAH[49]. PVOD is described as any disease that causes the veins of the lung to become blocked or narrowed. PCH is characterized by thin-walled microvessels infiltrating the perivascular interstitium, the lung parenchyma, and the pleura[50]. Pathological studies indicate that PVOD and PCH are quite similar in terms of development of pulmonary arterial intimal fibrosis and medial hypertrophy, as well as changes in pulmonary parenchyma[5]. PVOD and PCH are often included in PAH classifications because they show similar histological findings in the small pulmonary arteries[5]; clinical

presentation of PVOD, PCH, and PAH are often undistinguishable[21]; and all three diseases share similar risk factors, including scleroderma[51] and HIV infection[52, 53]. Additionally, mutations in the BMPR2 gene have also been seen in patients with PVOD[54, 55].

1.1.5 Pulmonary hypertension due to left heart disease

Left-heart disease may represent the most frequent cause of PH[56]. Ventricular or valvular diseases of the left side of the heart may cause an increase in left atrial pressure leading to an increased pulmonary artery pressure because of passive backwards transmission of the pressure[56]. In this situation, the pulmonary vascular resistance is normal or near normal, unlike in PAH. In approximately 19% to 35% of patients with left heart disease, the increase in pulmonary artery pressure is out of proportion from what is expected by the increase in left arterial pressure, and there is an increase in pulmonary vascular resistance[56, 57]. Currently, no studies of patients with PH due to left heart disease using medications approved for PAH have been conducted; as such, the efficacy and safety of PAH medications in this population remains unknown[5].

1.1.6 Pulmonary hypertension due to lung diseases and/or hypoxemia

Alveolar hypoxia as a result of lung disease, impaired control of breathing, or residence at high altitude is the predominant cause of PH in this category, although the prevalence of PH in these conditions is unknown[5]. PH is generally modest with mean pulmonary

artery pressures from 25 – 35mmHg[58], however some patients can have much larger mean pulmonary artery pressures (35 – 50mmHg)[59]. Diseases including brochiectasis, in which recurrent infection and inflammation of the airways destroy and widen the large airways of the lung; cystic fibrosis, an autosomal recessive disorder that results in accumulation of mucus in the lungs[60]; and a newly identified syndrome characterized by emphysema in the upper portions of the lung and fibrosis in the lower portions of the lung have been shown to cause PH[61]. In those patients with the combined syndrome of fibrosis and emphysema, the prevalence of PAH is approximately 50%[61]. As with the left-heart related PH, PAH drugs have not been tested in this patient population[5].

1.1.7 Chronic thromboembolic pulmonary hypertension

Chronic thromboembolic pulmonary hypertension (CTEPH) is a frequent cause of PH with up to 4% of patients developing PH after an epsidoe of acute pulmonary embolism[62, 63]. Prognosis of CTEPH reflects the degree of associated right ventricular dysfunction and has predictable mortality related to the severity of the underlying PH[64]. Currently, the only cure is pulmonary thromboendarterectomy, removal of the blood clot (thrombus) from the occluded artery[65]. Those patients who are not surgical candidates may benefit from administration of PAH-specific medication[65, 66], but more studies are required.

1.1.8 Pulmonary hypertension with unclear and/or multifactorial mechanisms

The final PH group is composed of several subgroups of PH for which the cause is unclear or multifactorial.

1.1.8.1 Subgroup 1

Several hematological disorders including polycythemia vera, an abnormal increase in the number of red blood cells; essential thrombocytothemia, an over-production of platelets; and chronic myeloid leukemia can cause PH[67]. Chronic myeloproliferative disorders can cause PH by various mechansms, such as high cardiac output; auto or surgical asplenia, absence of normal spleen function; direct obstruction of pulmonary arteries by circulating megakaryocytes[68]; chronic thromboembolic pulmonary hypertension[69]; portopulmonary hypertension; and congestive heart failure[5]. Splenectomy, either as the result of trauma or as a treatment for hematological disorders, can increase the risk of developing PH[70]. Portopulmonary hypertension is a complication of liver disease present in 0.25% to 4% of patients suffering from cirrhosis and in 4% - 6% of those referred for liver transplant[71].

1.1.8.2 Subgroup 2

This subgroup includes systemic disorders that are associated with an increased risk of developing PH. Sarcoidosis is a disease of unknown origin in which abnormal collections of granulomas form as nodules in multiple organs[72]. PH is increasingly recognized as a complication of sarcoidosis[73] with a reported prevalence of 1% - 28%[74]. Severe PH is common in patients with end-stage pulmonary Langerhans cell histocytosis, an abnormal increase in the number of histiocytes[75]. Lymphangioleiomyomatosis is a rare, multisystem disorder predicominantly affecting women that is characterized by lung destruction, lymphatic abnormalities, and abdominal tumors[76]. PH is an uncommon complication in patients with this disease[77, 78]. Neurofibromatosis type 1, also known as von Recklinghausen's disease, is an autosomal dominant disorder characterized by cutaneous fibromas and "café au lait" skin lesions and occasionally complicated by systemic vasculopathy. The neurofibromatosis type 1 gene modulates protein kinase B, which in turn regulates cell proliferation. Several cases of PH have been reported in patients with von Recklinghausen's disease[79-82].

1.1.8.3 Subgroup 3

Subgroup 3 is composed of PH associated with metabolic disorders. PH has been reported in a few cases of type Ia glycogen storage disease, a rare autosomal recessive disorder caused by a deficiency of glucose-6-phosphate[83-85]. Gaucher disease is a rare

disorder characterized by a deficiency of lysosomal β glucosidase resulting in an accumulation of glucocerebroside in reticuloendothelial cells. In a study of 134 patients with Gaucher disease, PH was not common[86]. In addition, an association between thyroid disease, both hypothyroidism and hyperthyroidism, and PH has been reported in several studies[87, 88]. One study reported that more than 40% of patients with thyroid disease also had PH[89]. Another study of PAH patients showed that 49% had autoimmune thyroid disease suggesting a common immunogenetic susceptibility[90].

1.1.8.4 Subgroup 4

Finally, subgroup 4 contains miscellaneous conditions associated with PH. Tumor obstruction may cause PH if a tumor grows into the central pulmonary arteries. However, these cases are rare and occur principally due to pulmonary artery sarcomas and are usually rapidly fatal[91, 92]. Occlusion of the microvasculature by metastatic tumor emboli (mostly caused by gastric cancers) may be another cause of rapidly progressive PH[93]. Patients with mediastinal fibrosis, a late-stage complication of histoplasmosis characterized by invasive calcified fibrosis on lymph nodes that block major vessels and airways[94], may present with severe PH because of compression of both pulmonary arteries and veins[94, 95]. PH has been reported in patients with end-stage renal disease (ESRD) maintained on long-term hemodialysis and may occur in up to 40% of patients in this population[96].

1.2 Heart development and physiology

1.2.1 Heart development

The heart is the first organ to form and function in the embryo. The vertebrate heart forms first from a population of myocardial precursor cells in the primitive streak termed the primary heart field, or first heart field[97, 98] (**Figure 2**). These cells migrate bilaterally into the anterior mesoderm and adopt a crescent shape;[99-101]; this structure is termed the cardiac crescent and is present at embryonic day (E) 7.5 in the mouse, which corresponds to week 2 of human gestation[102]. The cardiac crescent fuses at the midline to form the linear heart tube consisting of an inner endocardial layer and an outer myocardial layer[103] and is normally present at E8.0 in the mouse and gestational week 3 in humans[102]. Rightward looping and differential growth along the outer curvatures of the heart tube ultimately generate the multichambered heart[101]. An additional source of cardiac precursors, the secondary heart field, are derived from the pharyngeal mesoderm located medially to the cardiac crescent and are progressively added to the developing heart to form the outflow tract, right ventricle, and atria[99, 100].

Committed progenitor ISL1+ cells are clustered in the right ventricular outflow tract and right and left atrium, all of which are derived from the secondary heart field. These cells give rise to the endothelial cells, cardiomyocytes, and smooth muscle cells[104-106]. Endothelial cells form the cardiac valves and the endocardium. Cardiomyocytes form the

Figure 2: Heart Development in the Mouse

a) Progenitor cells originate in the primitive streak (PS) and migrate to the anterior of the embryo. **b**) The progenitor cells migrate to under the head folds (HF) and form the cardiac crescent (CC). **c**) The heart tube forms through fusion of the cardiac crescent at the midline. **d**) Rightward looping begins the process of ventricle formation. **e**) By E10.5, the heart has well-defined ventricles. **f**) In the fetal heart, ventricles are separated and connected to the aorta (AO) and the pulmonary trunk (PT) so that normal circulation can occur.

Anterior (A)-posterior (P) and right (R)-left (L) axes are shown. AA, aortic arch; AO, aorta; AVC, atrioventricular canal; CC, cardiac crescent; HF, head folds; IFT, inflow tract; IVC, inferior vena cava; LA, left atria; LV, left ventricle; OFT, outflow tract; PLA, primitive left atria; PRA, primitive right atria; PS, primitive streak; PT, pulmonary trunk; PV pulmonary vein; RA, right atria; RV, right ventricle; SVC, superior vena cava; Tr, trabeculae.

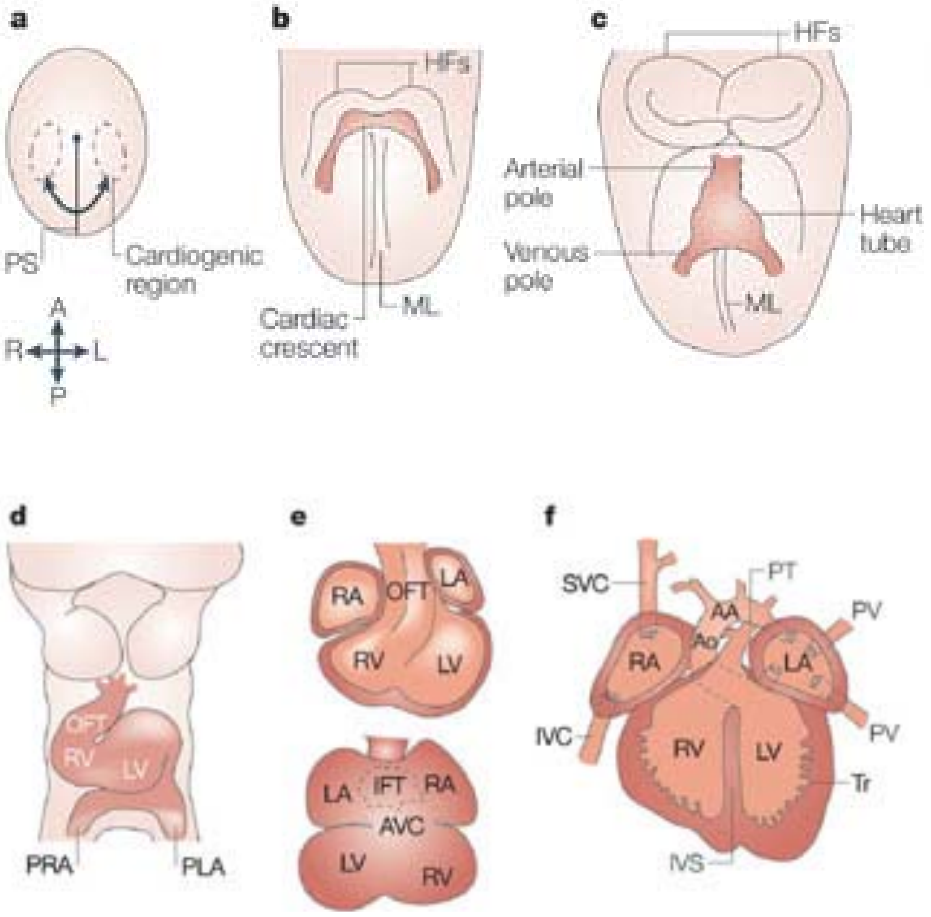
a
PS
Cardiogenic region
A
R
L
P
b
HFs
Cardiac crescent
ML
c
HFs
Arterial pole
Heart tube
Venous pole
ML
d
OFT
RV
LV
PRA
PLA
e
RA
OFT
LA
RV
LV
LA
IFT
RA
AVC
LV
RV
f
SVC
PT
AA
PV
Ao
RA
LA
IVC
PV
RV
LV
Tr
IVS

ventricular and atrial myocytes as well as cells of the conduction system. Smooth muscle cells form arteries and veins.[101]

The transcription factors T-box 5 (*Tbx5*) and hand and neural crest derivatives expressed 1 (*Hand1*) mark the primary heart field, whereas hand and neural crest derivatives expressed 2 (*Hand2*), ISL LIM homeobox 1 (*Isl1*), and fibroblast growth factor (*Fgf10*) are expressed in the secondary heart field[107, 108]. Natural killer 2 transcription factor related, locus 5 (*Nkx2-5*) is expressed in both heart fields[101]. Myocardial transcription factors are first detected in the cardiac crescent where myocardial differentiation is initiated; activation of key myocardial regulatory genes, such as *Nkx2-5* and GATA binding protein 4 (*Gata4*), depends on positive signaling by bone morphogenetic proteins (BMPs) and fibroblast growth factors while wingless-type MMTV integration site family members (Wnts) exert a repressive effect[109].

Mutations of *Gata4* lead to cardiac bifida where the two halves of the cardiac crescent fail to converge at the midline[110-112]. In an *Nkx2-5* knockout, there is loss of ventricular tissue and the absence of *Hand1* expression at the cardiac crescent stage and later in the cardiac tube[113-115]. *Hand1* mutants have a proliferation defect in the left ventricle (LV) and die from extra-embryonic defects[116-118]. Similarly, *Tbx5* mutants show severe defects in the left ventricle and atria-inflow regions of the heart, although *Hand1* is still detectable and the outflow tract and RV continue to grow normally[119]. In contrast, *Hand2* mutants show right-ventricular hypoplasia[120, 121] and extensive cell death in the pharyngeal arches where *Hand2* is normally expressed[122].

Although fibroblast growth factors are necessary for proliferation of cells in the secondary heart field[123], *Fgf10* mutant mice have no apparent early cardiac phenotype and the outflow tract seems to be normal[124, 125]. On the other hand, fibroblast growth factor 8 (*Fgf8*) knockout mice die at gastrulation, but an *Fgf8* hypomorph dies later of cardiac failure that is due to malformation of the outflow region[126, 127]. T-box transcription factor 1 (*Tbx1*) mutant mice show a similar cardiac phenotype to the *Fgf8* hypomorph mice, although the neural crest defect in *Tbx1* mutants is more severe[128-131]. Targeted deletion of *Tbx1* in the secondary heart field causes a proliferation defect[132].

Isl1 may have several roles in the secondary heart field. In its absence, migration of cells into the cardiac tube is not observed, proliferation is affected, and cells undergo apoptosis[107]. In a mutant embryo, the heart tube seems to have only two chambers and the outflow tract is absent. Genetic markers show the presence of an atrial and ventricular myocardium and labeling with *Hand1* and *Tbx5* probes show the left ventricular identity of the anterior compartment. Right ventricular markers are not expressed[100]. Myocyte enhancer factor 2C (*Mef2c*) Is regulated by *Isl1* and *Gata4*[133]. Early expression of *Mef2c* is medial to the cardiac crescent and continues into the secondary heart field[133]. Mutants have a reduced outflow tract and the right ventricle does not develop[134].

1.2.2 The fetal heart

By the third week of gestation, blood begins forming and the primitive heart tube begins beating; active circulation begins by the end of the fourth week of gestation. The right ventricle (RV) and pulmonary circulation begin to separate from the left ventricle (LV) and systemic circulation due to formation of the interventricular septum and formation of valves after the fifth week of gestation. At birth, full septation is normally complete[135-137]. In the fetus and embryo, the RV is the dominant chamber of the heart, accounting for approximately 60% of the total cardiac output; however, only about 15%-25% of the total cardiac output enters the lungs because the embryo receives oxygen from the placenta. The remainder is shunted to either the systemic circulation via the foramen ovale and the LV or the pulmonary artery and aorta via the ductus arteriosis[138, 139]. At birth, the increasing left atrial pressure closes off the formen ovale[140]. Soon after, the ductus arteriosis closes[139], the LV hypertrophies, and the RV involutes becoming thin walled[47].

The fetal heart has different characteristics than the adult heart. Unlike in the adult heart, the RV is as thick as the LV in the fetal heart[141]. A disproportionately smaller LV than RV, which is diagnosed by echocardiography, may be an indication of obstructive left-sided heart disease[142]. The fetal/neonatal RV ejects blood at a higher pressure than systemic circulation. A few days after birth, these pressures fall[143] and, by three weeks of age, the pulmonary artery pressure is usually lower than the systemic pressure[144]. Doppler echocardiography has shown that the RV output in human babies

is slightly larger than that of the LV at a gestational age of 38 weeks (60 ml/min compared to 40 ml/min)[145]. The two ventricles pump in parallel to the systemic circulation and the difference in pressure between the two ventricles is minimal[139].

1.2.3 The adult heart

In adult humans, the right ventricle is the most anterior portion of the heart and is located directly behind the sternum[146]. The RV appears triangular when viewed from the side or has a crescent shape when viewed in a cross section; the entirety of the RV muscle lies between the tricuspid and pulmonary valves. In contrast, the LV has an ellipsoid shape[141, 146]. The interventricular septum is concave towards the LV in the normal RV[141]. The free wall of the RV is normally 1-3mm thick compared to the 10mm thick LV free wall and accounts for approximately one-sixth of the total mass of the human heart – on average $26g/m^2$ compared to $87g/m^2$ of the LV[144, 146]. **Table 3** summarizes the characteristics of the normal RV and LV.

Anatomically, the RV can be divided into three regions: the inflow tract, an apical region, and the outflow tract, which ends at the pulmonic valves. The main pulmonary artery originates from the outflow tract[147] (**Figure 3**). The pulmonary artery is a thin, elastic vessel that branches to supply the various pulmonary arteries, pulmonary arterioles, and alveolar capillaries. Once blood travels through the alveolar capillaries and exchanges CO_2 for O_2, blood returns to the lungs through a system of pulmonary veins and branches to the left atrium. From the left atrium, it goes to the left ventricle and is then pumped to

Table 3: Summary of normal adult RV and LV structure and function

Characteristics	**RV**	**LV**
shape [141, 146]	triangular (side), crescent (cross-section)	ellipsoid
mass index (g/m^2) [146]	26	87
free-wall thickness (mm) [144]	1-3	10
ventricular pressure (mmHg) [148]	25/4	130/8
PVR vs. SVR ($dynes/s/cm^5$) [149]	123	2130
contraction [144, 150]	sequential	concentric and twisting

Figure 3: Pulmonary and systemic circulation

The human circulatory system includes the heart, lungs, and blood vessels. Blood leaves the right ventricle and travels through the pulmonary arteries to the lungs where CO_2 is exchanged from O_2. Blood returns to the left atrium of the heart after passing through the pulmonary veins. After the left atrium, blood pools in the left ventricle where it is pumped through the aorta to the systemic circulation and capillary beds where O_2 is given to the tissues and CO_2 removed from the tissues. It then travels through the veins and venae cavae to the right atrium after which it returns to the right ventricle.

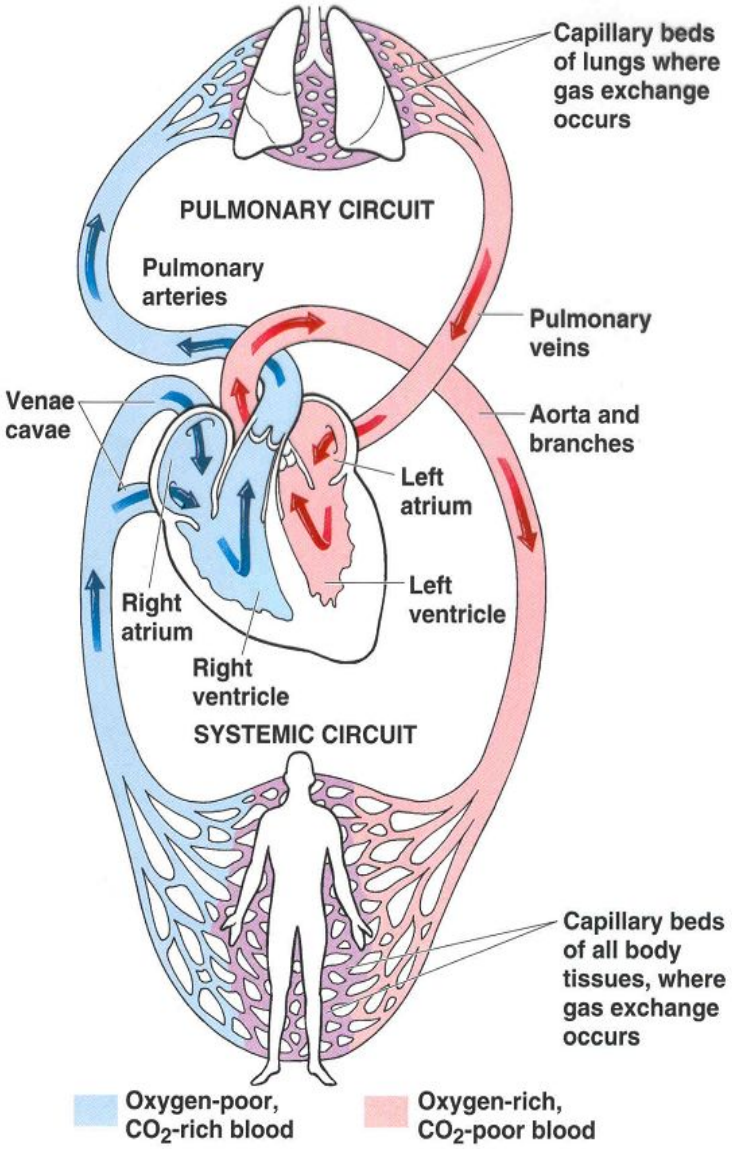
Capillary beds of lungs where gas exchange occurs
PULMONARY CIRCUIT
Pulmonary arteries
Pulmonary veins
Venae cavae
Aorta and branches
Left atrium
Left ventricle
Right atrium
Right ventricle
SYSTEMIC CIRCUIT
Capillary beds of all body tissues, where gas exchange occurs
Oxygen-poor, CO_2-rich blood
Oxygen-rich, CO_2-poor blood

the systemic circulation[149, 151, 152]. Almost the entire cardiac output is pumped by the thin-walled RV through the lung circulation while the oxygenated blood is collected by the four pulmonary veins and emptied into the LV[141]. The RV contracts in a sequential manner, starting with the inflow tract and moving towards the outflow tract in a wave-like manner. In contrast, the LV has a concentric contraction along with a twisting motion[144, 153].

Normally, the pulmonary circulation is a low-resistance, high-capacitance system allowing an increase of RV stroke volume by 3-4 fold without significantly increasing pulmonary pressure[154]. The alveolar membranes of the lung are thin and highly permeable. As such, the pulmonary pressures must remain low to prevent pulmonary edema[155]. In humans, a normal mean pulmonary artery pressure is 14 mmHg with an upper limit of normal of 20.6 mmHg. With exercise, the mean pulmonary artery pressure can have an upper limit of normal as high as 35 mmHg[154]. The average pressure of the RV is 25mmHg/4mmHg (systolic/diastolic) and the LV is 130mmHg/8mmHg[148]. The function of the RV is often determined by measuring the so-called afterload, the pulmonary vascular resistance (PVR). Pulmonary vascular resistance is defined by the ratio of the mean pressure drop from the main pulmonary artery to the left atrium divided by the cardiac output and is given in units of dynes/s/cm^5. It can also be measured in Wood units, which are defined as the mean pulmonary artery pressure minus the mean pulmonary capillary occlusive pressure (both in mmHg) divided by cardiac output (L/min). One Wood unit is equivalent to 80 dynes/s/cm^5[150]. In a normal human heart, pulmonary vascular resistance is approximately 1/20 that of the systemic vascular

resistance – 123 dynes/s/cm^5 in the RV compared to 2130 dynes/s/cm^5 in the systemic circulation[147].

1.3 The heart during progression of pulmonary arterial hypertension

Pulmonary arterial hypertension develops as a consequence of lung vascular lesions that cause an increase in pulmonary vascular resistance against which the right ventricle must pump (**Figure 4**). This increase in afterload is the first trigger for RV adaptation in PAH[48]. Based on the LaPlace relationship, an increase in intraluminal pressure will result in an increase in wall stress unless the thickness of the chamber wall is increased or the internal radius of the chamber is decreased. Because an increase in wall stress would increase myocardial oxygen demand and impede myocardial perfusion, the RV adapts to the increasing afterload pressure through increased wall thickness, both by hypertrophy (increased muscle mass) and assuming a more rounded shape[48] (**Table 4**). Hypertrophy is largely the result of protein synthesis induced by stretch, which is sensed by integrins and stretch-activated ion channels in myocytes, fibroblasts, and endothelial cells of the heart[156]. Integrins are attached to the extracellular matrix (ECM) and the cytoskeleton allowing them to transduce mechanical stress to intracellular chemical signals that increase synthesis of contractile proteins and proteins for autocrine and paracrine signaling[157, 158]. Growth and proliferation of cardiomyocytes is paralleled by ECM synthesis and supporting capillary growth. Angiogenesis, growth of new vessels from existing vessels, is part of this process and can be induced by angiopoietin-1 (Ang1) and vascular endothelial growth factor (VEGF) signaling[48].

Figure 4: Changes in the Heart in PAH

Schematic representation of the heart and lungs in a normal (left) and pulmonary hypertension (right) patient. Pulmonary arteries constrict in pulmonary hypertension due to the formation of plexiform lesions causing an increase in pressure against which the right ventricle must pump. Over time, this causes the right ventricle to hypertrophy.

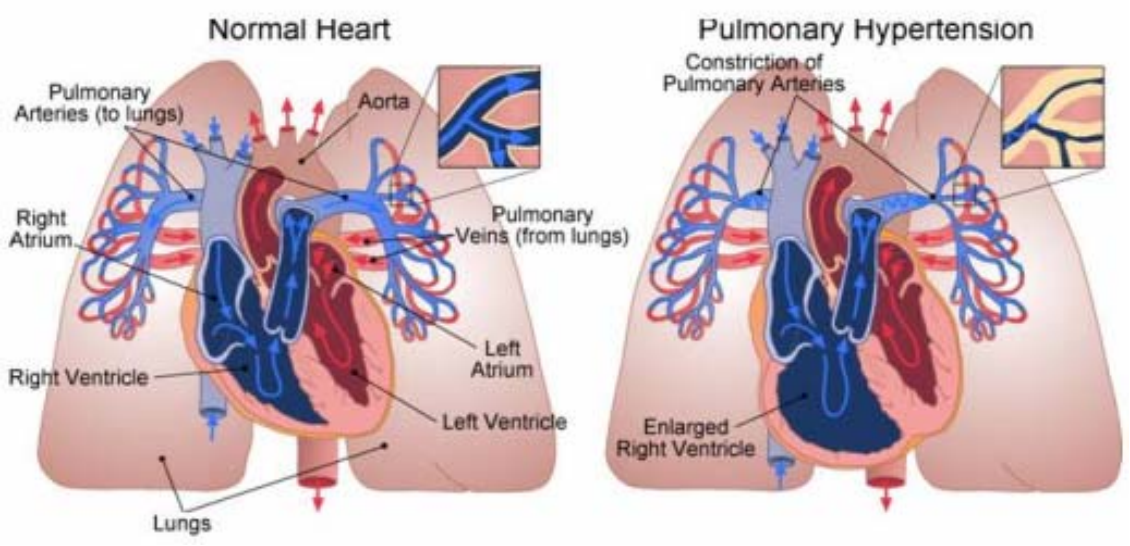
Normal Heart
Pulmonary Arteries (to lungs)
Aorta
Right Atrium
Pulmonary Veins (from lungs)
Left Atrium
Right Ventricle
Left Ventricle
Lungs
Pulmonary Hypertension
Constriction of Pulmonary Arteries
Enlarged Right Ventricle

Table 4: Summary of Changes in the RV and Circulation Associated with PAH

Characteristics	**Normal**	**PAH**
RV shape	triangular (side), crescent (cross-section)	thickened and enlarged
septum position	concave towards right ventricle	paradoxical shift towards left ventricle
energy utilization [47, 159]	varies from fatty acid to glycolysis as needed	reliant on glucose metabolism
RV mass index (g/m^2) [146, 160]	26	68
RV free wall thickness (mm) [144, 160]	1 – 3	5 – 7
RV systolic pressure (mmHg) [148, 160]	25	85
mean pulmonary artery pressure, resting (mmHg) [1, 160]	8 – 20	50
PVR ($dynes/s/cm^5$) [149, 160]	123	240

1.3.1 Adaptive vs. maladaptive hypertrophy

Hypertrophy can be divided into two categories: adaptive, or pathological, and maladaptive, or physiological. Examples of adaptive hypertrophy included athletes' hearts and exercise-induced reversible cardiac enlargement[141]. Hypertrophy is induced in athletes' hearts through aerobic interval training over long periods of time, which causes increased cardiac dimensions and mass as an adaptation to the increase in physical stress; they also show improved myocardial contractility[161-166]. This adaptation allows greater transport of blood and oxygen to the skeletal muscles in order to improve work capacity.[167] Exercise increases secretion of insulin-like growth factor 1 (IGF-1) and growth hormones both systemically and locally in the heart[168-173]. Overexpression of the IGF-1 receptor or an activated form of Akt leads to myocardial hypertrophy with enhanced cardiac function[170, 174]. While exercise training programs induce an improved work capacity and adaptive hypertrophy, pressure overload induces reduced contractile function and maladptive hypertrophy[175]. In maladptive hypertrophy, there can be a doubling of the heart weight, re-expression of fetal genes, and deactivation of the Akt/mTOR signaling cascade[175]. In contrast, adaptive hypertrophy does not reactivate the fetal gene program[176, 177]. Fetal gene re-expression is due to activation of the transcription factors nuclear factor of activated T-cells (*Nfat*) by calcineurin and myocyte enhancer factor 2 (*Mef2*) by calcium/calmodulin-dependent protein kinase (*CaMK*) or mitogen activated kinase-like protein (*MAPK*) [176] and increased protein degradation by the ubiquitin-proteosome system[178]. Molecular

markers have been found that distinguish between adaptive and maladaptive hypertrophy in the LV. *Gata4*, cyclic-AMP response element binding protein (*Creb*), and signal transducer and activator of transcription 3 (*Stat3*) are markers of adaptive hypertrophy while phosphate and tensin homolog (*Pten*), nuclear factor of activated T-cells 3 (*Nfat3*), and *Mef2* are markers of maladaptive hypertrophy[179].

While it is generally believed that sustained pressure overload is enough to induce maladptive hypertrophy and cardiace failure[48], recent studies[180] have shown that increased RV pressure overload alone is not sufficient to cause heart failure. Rats with only pressure overload did not have heart failure or an increase in long-term mortality rates. However, rats with increased RV pressure and angioproliferative pulmonary remodeling, as seen in human PAH, do have heart failure and increased rates of mortality[180]. Those rats with RV failure also have an increase in RV fibrosis, decreased capillary density, and oxidative stress[180].

1.3.2 Transition from hypertrophy to failure

The mechanisms that underlie the transition from hypertrophy to failure in the RV associated with PAH have not been well characterized. Similarly, it is not well understood why some patients with severe PAH rapidly progress to RV failure and others do not[141]. One hallmark of heart failure is the switch from alpha myosin heavy chain (MHC-α) to beta myosin heavy chain (MHC-β) in cardiomyocytes[48]. Normally, in the human RV approximately 25 – 34% of the MHC is in the form of MHC-α and the

remainder is MHC-β. In PAH-associated RV failure, there is approximately 5% MHC-α and 95% MHC-β.[181] MHC-β has lower ATP activity than MHC-α and the reduction in MHC-α causes a decrease in systolic function[182]. Additionally, neurohormonal overdrive, oxidative stress, inflammation, ischemia, and cell death may all contribute to the development of RV dilation and failure[48].

1.3.2.1 Neurohormonal signaling

Heart failure is associated with an activation of the renin-angiotensin system. Angiotensin II (ATII) is the most important factor involved in cardiac remodeling. Adrenergic overstimulation causes increased expression of several peptides including the natriuretic peptides atrial natriuretic peptide (ANP) and brain natriuretic peptide (BNP)[48]. While ATII, ANP, BNP, and aldosterone reach the heart via systemic circulation, they can also be produced locally by myocytes, endothelial cells, and fibroblasts in the heart to affect cardiomyocyte growth, proliferation, and survival[48].

1.3.2.2 Ischemia

Myocardial ischemia occurs when blood flow to the heart muscle is decreased by obstruction of the arteries carrying blood to the heart muscle itself causing a decrease in the oxygen supply of the heart[183]. Exercise-related chest pain, often a symptom of myocardial ischemia, occurs frequently in patients with pulmonary hypertension despite normal coronary angiograms[184]. Systolic right coronary artery flow is reduced in

pulmonary hypertension[185] and can lead to RV ischemia[186] because of a mismatch between the number of capillaries and the size of the cardiomyocytes during development of cardiac hypertrophy and impairment of right coronary artery flow as a consequence of RV wall stress[187]. It has been suggested that the RV coronary circulation becomes more like that in the LV during PAH: greater oxygen extraction at rest and greater dependence on oxygen and an increase in coronary blood flow to meet the myocardial oxygen demand[188].

1.3.2.3 Oxidative and nitrosative stress

Excess reactive oxygen species (ROS) and reactive nitrogen species (RNS) induce contractile dysfunction through suppression of enzymes involved in excitation-contraction coupling. ROS and RNS also favor cardiac remodeling through induction of cell damage, apoptosis, and inflammation[48]. ATII, endothelin1, and other neurohormones can stimulate the formation of ROS to induce hypertrophic pathways within the cardiomyocyte[189]. Activation of ATII leads to ROS formation by upregulation of NAD(P)H oxidases[189]. Neutrophils are recruited to the pressure-overloaded myocardium and may be a source of ROS because they have significant quantities of NAD(P)H oxidases[48]. Other sources of ROS production in heart failure are xanthine oxidase, cytochrome P450, and auto-oxidation of catecholamines[189-191]. RNS in the heart can be hemoglobin dependent and constitutively expressed endothelial nitric oxide (NO) synthase (eNOS). Desaturation of hemoglobin and uncoupling of eNOS can also contribute to ROS generation[192, 193]. Decreased expression of eNOs,

inhibition of eNOS activity, and inhibition of NO by superoxide anions can lead to reduced NO signaling[194]. NO signals through the guanylate cyclase/cyclic guanosine monophosphate (cGMP) pathway and acts as a vasodilator and growth inhibitor; decreased NO activity can cause endothelial cell dysfunction[194].

1.3.2.4 Energy utilization

Otto Warburg proposed that a shift from oxidative phosphorylation to glycolysis and glucose metabolism was a hallmark of malignant cell transformation. It has been observed that, in PAH, the Warburg effect occurs in lung vascular cells[195, 196]. Both cancer and lung vascular cells manifest excessive cell proliferation and impaired apoptosis. While in PAH the lesion cells do not metastasize or disrupt vessel boundaries, lung vascular cells in PAH share a mitochondrial-metabolic abnormality with cancer[197]. Positron emission tomography (PET) studies have shown that there is an increase in glucose uptake in lung tissue of patients and animals with right ventricular hypertrophy[160]. Other studies have shown that there is an increased rate of glycolysis in right ventricular hypertrophy and that the switch from glucose oxidation to glycolysis is associated with impaired RV function in the form of reduced RV contractility and overall cardiac function[198]. This increase in glycolysis is in part due to increased expression in *HIF-1α*, which is known to be increased in animal models of PAH[180]. *HIF-1α* activation causes an increase in transcription of glucose transporter 1 (*Glut1*), hexokinase, and lactate dehydrogenase kinase favoring glycolysis and inhibiting glucose oxidation by activating transcription of pyruvate dehydrogenase kinase genes[199].

Additionally, animal studies of PAH have shown that mitochrondrial function is abnormal due to hyperpolarization of mitochondrial memranes in RV myocytes[200].

1.3.2.5 Apoptosis of cardiac cells

In the normal heart, apoptosis of cardiomyocytes is extremely rare: approximately one apoptotic cardiomyocyte per $10^4 – 10^5$ cells[201]. In human heart failure, the apoptosis rate can increase to up to 1 in 400 cells[202, 203]. Apoptosis rates have been shown to be elevated to 14% in models of ischemia/reperfusion and lower than 1% in models of chronic pressure overload[204]. Even very low rates of apoptosis (approximately 1/5 that of human heart failure rates) have been shown to cause lethal dilated cardiomyopathy in mouse models[205]. Pressure load can induce apoptosis via activation of ATII, ROS, β-adrenoreceptor agonists, and proinflammatory cytokines[206]. Ischemia is another strong activator of apoptosis in the heart[207]. Broad-spectrum caspase inhibitors have been used to block apoptosis after ischemia/reperfusion resulting in reduced infarct size and improved cardiac function[208, 209].

1.3.2.6 Inflammation and immune activation

Patients with chronic heart failure have increased serum levels and myocyte expression of proinflmaatory cytokines: tumor necrosis factor alpha (TNF-α), interleukin 1 (IL-1), and interleukin 6 (IL-6). Elevated levels correlate with disease severity reflected in clinical and hemodynamic parameters[210]. In left-heart failure studies, TNF-α can depress

myocardial contractility[211] and induce apoptosis of endothelial cells[212] and cardiomyocytes[213]. TNF-α is upregulated after trans-aortic contstriction, an experimental model of left-ventricular failure in rodents, and mediates cardiomyocte apoptosis, fibrotic remodeling through inflammatory cell influx, matrix metalloprotease (MMP) upregulation, and activation of IL-6, monocyte chemotactic protein 1, and macrophage inflammatory protein gamma[214]. IL-1 and IL-33 have been shown to be changed during the development of heart failure. IL-1 has a negative inotropic effect on cardiomyocyctes[215] and enhances fetal gene expression[216]. IL-33 is produced by cardiac fibroblasts in response to mechanical strain[217].

In summary, pulmonary arterial hypertension consists of a group of diseases affecting lung circulation with a fatal outcome due to right heart failure. As pulmonary hypertension progresses, there is a shift from adaptive to maladaptive hypertrophy, which can be characterized by pathways involving energy metabolism, inflammation, and apoptosis resulting in ischemia such that the right heart can no longer compensate for the increased strain. While there are some insights into the molecular pathways affected as the disease progresses, there has not been a systematic study of the gene expression changes of pulmonary hypertension or adaptive hypertrophy. A better understanding of the molecular mechanisms of RVF will likely lead to the development of therapeutic strategies to prevent RVF. Because RVF is entirely reversible after single-lung transplantation, other strategies need to be found that will reverse RVF even when the pulmonary artery pressure cannot be lowered by our present treatments.

Chapter 2: Materials and Methods

2.1 Rat models

2.1.1 Su5416

Male Sprague-Dawley rats (Harlan Laboratories Inc., Indianapolis, IN) weighing 200g were injected subcutaneously with SU5416 suspended in 0.5% (w/v) carboxymethylcellulose sodium, 0.9% (w/v) sodium chloride, 0.4% (w/v) polysorbate 80, and 0.9% (v/v) benzyl alcohol in deionized water. Rats were given a single injection of SU5416 (20 mg/kg) at the beginning of the 4-week experiment. The animals were kept at the altitude of Richmond, VA (sea level) for another four weeks.

2.1.2 Chronic hypoxia

Male Sprague-Dawley rats (Harlan Laboratories Inc., Indianapolis, IN) weighing 200g were exposed to chronic hypoxia (simulated altitude of 5,000 m in a nitrogen dilution

chamber) for four weeks; thereafter the animals were kept at the altitude of Richmond, VA (sea level) for another two weeks.

2.1.3 Su5416/hypoxia

Male Sprague-Dawley rats (Harlan Laboratories Inc., Indianapolis, IN) weighing 200g were injected subcutaneously with SU5416 suspended in 0.5% (w/v) carboxymethylcellulose sodium, 0.9% (w/v) sodium chloride, 0.4% (w/v) polysorbate 80, and 0.9% (v/v) benzyl alcohol in deionized water. Rats were given a single injection of SU5416 (20 mg/kg) at the beginning of the 6-week experiment. The animals were then exposed to chronic hypoxia (simulated altitude of 5,000 m in a nitrogen dilution chamber) for four weeks; thereafter the animals were kept at the altitude of Richmond, VA (sea level) for another two weeks.

2.1.4 Carvedilol only

Male Sprague-Dawley rats (Harlan Laboratories Inc., Indianapolis, IN) weighing 200g were given carvedilol (15 mg/kg; Sigma-Aldrich, St. Louis, MO) dissolved in 20% dimethyl sulfoxide and water and administered once daily per oral gavage for 4 weeks.

2.1.5 Su5416/hypoxia and carvedilol

Male Sprague-Dawley rats (Harlan Laboratories Inc., Indianapolis, IN) weighing 200g were injected subcutaneously with SU5416 suspended in 0.5% (w/v) carboxymethylcellulose sodium, 0.9% (w/v) sodium chloride, 0.4% (w/v) polysorbate 80, and 0.9% (v/v) benzyl alcohol in deionized water. Rats were given a single injection of SU5416 (20 mg/kg) at the beginning of the 6-week experiment. The animals were then exposed to chronic hypoxia (simulated altitude of 5,000 m in a nitrogen dilution chamber) for four weeks. Carvedilol (15 mg/kg; Sigma-Aldrich, St. Louis, MO) was dissolved in 20% dimethyl sulfoxide and water and administered once daily per oral gavage for 4 weeks, beginning after return to room air breathing.

2.2 Isolation of total RNA with mortar and pestle

Total RNA was isolated from approximately 30 mg of snap-frozen rat heart tissue using the Qiagen RNeasy Mini Kit (Qiagen, Valencia, CA). Briefly, hearts were homogenized using a mortar and pestle under liquid nitrogen then mixed with Buffer RLT and β-mercaptoethanol in a tissue homogenizer. Samples were then transferred to an Eppendorf tube and spun at full speed for three minutes. Supernatant was transferred to a new 2 ml tube and mixed with an equal volume of 100% ethanol, then placed in an RNeasy spin column. Samples were washed once with buffer RWI and twice with buffer RPE before being eluted in 40 μL RNase-free water. RNA concentration was determined using a

NanoDrop ND-1000 (Thermo Fisher Scientific, Wilmington, DE) spectrophotometer. All samples had an A_{260}/A_{280} ratio between 1.9 and 2.1

2.3 Isolation of total RNA with FastPrep® lysing matrix

Total RNA was isolated from approximately 30 mg of snap-frozen rat heart tissue using the Qiagen RNeasy Mini Kit (Qiagen, Valencia, CA). Briefly, hearts were homogenized with Buffer RLT and β-mercaptoethanol in an MP FastPrep®-24 Lysing Matrix D tube (MP Biomedicals LLC, Solon, OH). Samples were then transferred to an Eppendorf tube and spun at full speed for three minutes. Supernatant was transferred to a new 2 ml tube and mixed with an equal volume of 100% ethanol, then placed in an RNeasy spin column. Samples were washed once with buffer RWI and twice with buffer RPE before being eluted in 40 μL RNase-free water. RNA concentration was determined using a NanoDrop ND-1000 (Thermo Fisher Scientific, Wilmington, DE). All samples had an A_{260}/A_{280} ratio between 1.9 and 2.1

2.4 Microarray hybridization

The amplification and hybridization process is as follows. 500 ng of total RNA was amplified and labeled with Cyanine-5 and 500 ng of universal rat reference RNA (Stratagene, Santa Clara, CA) was amplified and labeled with Cyanine-3 using the Agilent QuickAmp Labeling kit (Agilent Technologies Inc., Santa Clara, CA) to produce labeled cRNA following the manufacturer's protocol. After amplification and labeling,

the dye incorporation was determined using a NanoDrop ND-1000 spectrophotometer (Thermo Fisher Scientific, Wilmington, DE). All ratios were greater than 8.0 pmole dye per μg cRNA per the manufacturer's recommendation. 825 ng of sample and 825 ng of reference RNA were combined and incubated with an Agilent whole rat genome 4x44k microarray slide (Agilent Technologies Inc., Wilmington, DE) for 17 hours at 65°C. Following hybridization, slides were washed following the manufacturer's protocol and scanned using an Axon GenePix 4200A scanner (Axon Instruments, Union City, CA) at a resolution of 5 μM. The raw data will be generated using GenePix Pro 5.0 software (Axon Instruments, Union City, CA) and submitted to the Ramhorn Array Database (http://ramhorn.csbc.vcu.edu). Ramhorn is a VCU-specific implementation of the Longhorn Array Database[218] maintained in the laboratory of Dr. Paul Fawcett.

2.5 Microarray data analysis

Microarray data were retrieved from Ramhorn after filtering the data using a set of spot-quality metrics designed to ensure the reliability of the data. Features were included in the dataset if they have a signal greater than or equal to 1.5 fold above background in both the red and green channels. Those features with less than 50% good data across the set of arrays were eliminated. Technical replicates were averaged together using a best-effort averaging procedure.

Statistical analysis of biological replicates was performed using the Significance Analysis of Microarrays (SAM) algorithm[219] with a two-class paired (for normal RV vs. normal

LV) or unpaired design (normal RV vs. failing RV) to identify differentially expressed genes. Briefly, the SAM algorithm for a two-class comparison is as follows. First, the relative difference in expression between two sets of samples is calculated for each gene; this is the observed relative difference. To calculate the expected relative difference, data labels are permuted and the relative difference is calculated for each gene. The expected relative difference for a gene will be the average relative difference across all permutations. The observed relative difference is plotted against the expected relative difference. Genes that fall outside of a threshold value, Δ, will be called significant. Δ-values were chosen to give an acceptable false discovery rate (FDR) of less than 5% and a 2-fold filter was applied.

The gene list was clustered using hierarchical clustering methods in Cluster 3.0[220] and visualized in Java TreeView[221]. Based on literature search results and pathway analysis results obtained using Ingenuity Pathway Analysis (IPA, Ingenuity Systems, Redwood City, CA) and the PANTHER classification system[222, 223], genes were selected for confirmation by quantitive RT-PCR.

For prediction analyses, raw expression data files were uploaded into R[224] and normalized using the *marray* package[225] by the Lowess normalization algorithm, then exported to BRB Array Tools. Lowess intensity dependent normalization was used to adjust for differences in labeling intensities of the Cy3 and Cy5 dyes. The adjusting factor varied over intensity levels[226]. Genes that were differentially expressed between the three classes were identified using an F test, using an α-level of 0.0001 for univariate

testing, and performing 1,000 permutations for multivariate analysis. The class prediction model was developed using Diagonal Linear Discriminant Analysis[227], Nearest Neighbor Classification[228], and Nearest Centroid Classification. The models incorporated genes that were previously deemed significant. We estimated the prediction error of each model using leave-one-out cross-validation (LOOCV) as descried by Simon et al.[229]. For each LOOCV training set, the entire model building process was repeated, including the gene selection process. We also evaluated whether the cross-validated error rate estimate for a model was significantly less than one would expect from random prediction. The class labels were randomly permuted and the entire LOOCV process was repeated. The significance level is the proportion of the random permutations that gave a cross-validated error rate no greater than the cross-validated error rate obtained with the real data. 2,000 random permutations were used.

2.6 Quantitative real-time polymerase chain reaction

Quantitative real-time polymerase chain reaction (qRT-PCR) was performed using the High-Capacity cDNA Reverse Transcription Kit (Applied Biosystems, Carlsbad, CA) to convert total RNA (1 μg) to cDNA and the Power SYBR® Green PCR Master Mix (Applied Biosystems, Carlsbad, CA) along with rat-specific primers (**Table 5**) (Invitrogen, Carlsbad, CA). A dissociation profile was generated after each run to verify specificy of amplification. All PCR assays were performed in triplicate and no template controls were included. 18S rRNA was used as a housekeeping gene. Automated gene

expression analysis was performed using the Comparative Quantitation model of MxPro QPCR Software (Stratagene, Santa Clara, CA).

2.7 Protein isolation

Protein was isolated from approximately 40 mg of snap-frozen rat heart tissue using RIPA (radio-immunoprecipitation assay) buffer (Sigma-Aldrich, St. Louis, MO) and protease inhibitor cocktail (Sigma-Aldrich, St. Louis, MO) in an MP FastPrep®-24 Lysing Matrix D tube (MP Biomedicals LLC, Solon, OH). Protein concentration was measured using a standard colorimetric protein assay based on the method by Bradford (Bio-Rad, Hercules, CA). A standard curve was generated by measuring the OD595 of the protein reagent mixed with bovine serum albumin (BSA) at concentrations of 2.5 μg/mL, 5 μg/mL, 10 μg/mL, and 20 μg/mL.

2.8 Western blot

Proteins were separated by SDS-PAGE on Novex precast 4-12% Bis-Tris gels using the NuPAGE® system (Invitrogen, Carlsbad, CA). Proteins were transferred to a PVDF membrane (Biorad, Hercules, CA) in NuPAGE® transfer buffer (Invitrogen, Carlsbad, CA) for 1 hour at 50 volts. The membrane was blocked for 45 minutes in TBS-T (20 mM Tris-HCl pH 7.6, 137 mM NaCl, 0.1% Tween-20) containing 5% nonfat dry milk (Carnation, Wilkes-Barre, PA). TBS-T was used for all wash steps. The membranes were incubated overnight at 4°C in TBS-T containing 5% BSA with appropriate rat

antibodies (**Table 6**). The membrane was washed in TBS-T and incubated with a 1/2000 dilution of goat anti-rabbit IgG HRP secondary antibody (Cayman Chemical, Ann Arbor, Michigan). Proteins were detected using Western Lightning™ Plus-ECL chemiluminescent substrate (PerkinElmer Inc., Waltham, MA). The ChemiDoc™ XRS+ Imaging System and Quantity One software (Bio-Rad, Hercules, CA) were used to capture and analyze digital images of chemiluminescent signals.

2.9 Multiplex assay

Levels of 23 cytokines (G-CSF, eotaxin, GM-CSF, IL-1α, leptin, MIP-1α, IL-4, IL-1β, IL-2, IL-6, IL-13, IL-10, IL-12p70, IFN□, IL-5, IL-17, IL-18, MCP-1, IP-10, GRO/KC, VEGF, TNFα, RANTES) were measured in rat serum samples using the Milliplex® rat cytokine/chemokine magnetic bead panel kit (Millipore, Billerica, MA) following the manufacturer's protocol. Briefly, a standard curve at dilutions of 1:1, 1:4, 1:16, 1:64, 1:256, 1:1,024, and 1: 4,096 of each analyte were prepared. Serum samples were diluted 1:4 using serum matrix. Standards, quality control samples, and experimental samples were incubated overnight 4°C with antibody-immobilized magnetic beads. Beads were washed twice with wash buffer, and then incubated with detection antibodies and streptavidin-phycoerythrin. Beads were washed twice again before being resuspended in sheath fluid. The plate was run on a Luminex 100 analyzer (Luminex Corporation, Austin, TX) and results were analyzed using BioPlex Manager Software 4.0 (BioRad, Hercules, CA).

Table 5: qRT-PCR Primers

Name	Sequence 5' to 3'	Product size
Ang-1 forward	AGAAACTTCAGCATCTGGAGC	115bp
Ang-1 reverse	CGCATTCTGTTGTATCTGGG	
ANP forward	CAAGGGCTTCTTCCTCTTCC	124bp
ANP reverse	TCTCCTCCAGGTGGTCTAGC	
Apelin forward	GAATCTGAGTTTCTGCGTGC	108bp
Apelin reverse	CCTTCTTCTAGCCCTTTCCC	
BNP forward	CAATCCACGATGCAGAAGC	84bp
BNP reverse	GCCTTGGTCCTTTGAGAGC	
CAPS1 forward	CAAATGGCAGACCAAATAGC	107bp
CAPS1 reverse	CATGAGTAGGTTGACGGAGG	
CTGF forward	AAATGCTGTGAGGAGTGGG	80bp
CTGF reverse	TTCCAGTCGGTAGGCAGC	
IGF1 forward	GCTCTTCAGTTCGTGTGTGG	106bp
IGF1 reverse	CAACACTCATCCACAATGCC	
Irx2 forward	CCAAGAAAGATGCCAGTGA	73bp
Irx2 reverse	GCTTGGCCCTCCTATAGG	
Klf5 forward	CCAAATATCCAACCTGTCCG	161bp
Klf5 reverse	GCACTTGTAGGGCTTCTCG	
Nr2f2 forward	CTCAAGGCCATAGTCCTGT	61bp
Nr2f2 reverse	CCACGTGGGCTACATC	
Rcan1 forward	ACGGTGATGTCTTCAGCG	119bp
Rcan1 reverse	TGAAGTTTATTCGGACACGC	
VEGF forward	CTGCAATGATGAAGCCCTGGAG	94bp
VEGF reverse	CTATGTGCTGGCTTTGGTGAGG	
Hexokinase2 forward	GAGGTCAACTCCGGATGG	151bp
Hexokinase2 reverse	GAGGTCAACTCCGGATGG	
18s rRNA forward	AGACGGACCAGAGCGAAAGC	309bp
18s rRNA forward	TGTCAATCCTGTCCGTGTCC	

Table 6: Antibodies

Name	Company	Product Number	Species
α-actinin	Cell Signaling	3134	rabbit
AKT	Santa Cruz	sc-8312	rabbit
Ang-1	Santa Cruz	sc-8357	rabbit
Apelin	Santa Cruz	sc-33469	goat
IGF-1	Santa Cruz	sc-9013	rabbit
p-AKT	Santa Cruz	sc-7985	rabbit

Chapter 3: Comparison of the Gene Expression Pattern between the Normal RV and the Normal LV

3.1 Introduction

Although we have concepts and data to explain mechanisms of left ventricular failure, there is little comparable knowledge of mechanisms of right ventricular failure. Right heart failure has not been systematically investigated on the cellular and molecular level most likely because of the widely held opinion that the conditions which govern right ventricular failure and left ventricular failure are identical, or at least very similar. As such, most concepts of right ventricular failure have been shaped by the studies of the left ventricle. However, there exist both embryological and physiological differences between both ventricles that support a hypothesis that the gene expression patters differ between right and left ventricular failure. We first sought to identify gene expression differences in the normal right ventricle (RV) and normal left ventricle (LV). While differences in expression are known for individual genes, there has not been a systematic study of the gene expression differences of the two ventricles. This study served as the basis for the studies of right ventricular failure associated with severe pulmonary arterial hypertension (PAH) in the rat that followed.

The vertebrate heart forms from two populations of cardiac progenitor cells: the primary heart field, or first heart field, and the secondary heart field, or anterior heart field. The primary heart field originates in the anterior splanchnic mesoderm and gives rise to the cardiac crescent, left ventricle, and atria[99-101]. The secondary heart field is derived from the pharyngeal mesoderm, located medial to the cardiac crescent, and gives rise to the outflow tract and large portions of the right ventricle and atria[99, 230]. Progenitor cells from the cardiac crescent migrate medially and form the linear heart tube, which consists of an inner endocardial layer and an outer myocardial layer. Right-ward looping and differential growth along the outer curvatures of the heart tube ultimately generate the multi-chambered heart[101]. Cells from the adjoining secondary heart field are progressively added to the developing heart forming additional structures, such as the right ventricle and atria[99, 100] (**Figure 5).**

During these embryological processes, transcription factors are regionally expressed in the developing heart. While some can be found in both the primary and secondary heart fields, others show specific expression patterns in just one of the developing heart fields. T-box 5 (*Tbx5*) and the basic helix-loop-helix transcription factor heart and neural crest derivatives expressed-1 (*Hand1*) are both expressed in the primary heart field, while heart and neural crest derivatives expressed-2 (*Hand2*), islet-1 (*Isl1*), fibroblast growth factor-8 (Fgf8), fibroblast growth factor-10 (*Fgf10*), paired-like homeodomain-2 (*Pitx2*), and *Tbx5* are expressed in the secondary heart field[107, 108].

Figure 5: Overview of Heart Development

The heart forms from two different heart fields, the primary heart field (shown in blue) and the secondary heart field (shown in purple). a) The cardiac crescent is composed of cells from the primary heart field with cells from the secondary heart field located medially. b) Cells from the cardiac crescent migrate medially and form the linear heart tube. c) Rightward looping of the heard tube ultimately generates the multi-chambered heart (d).

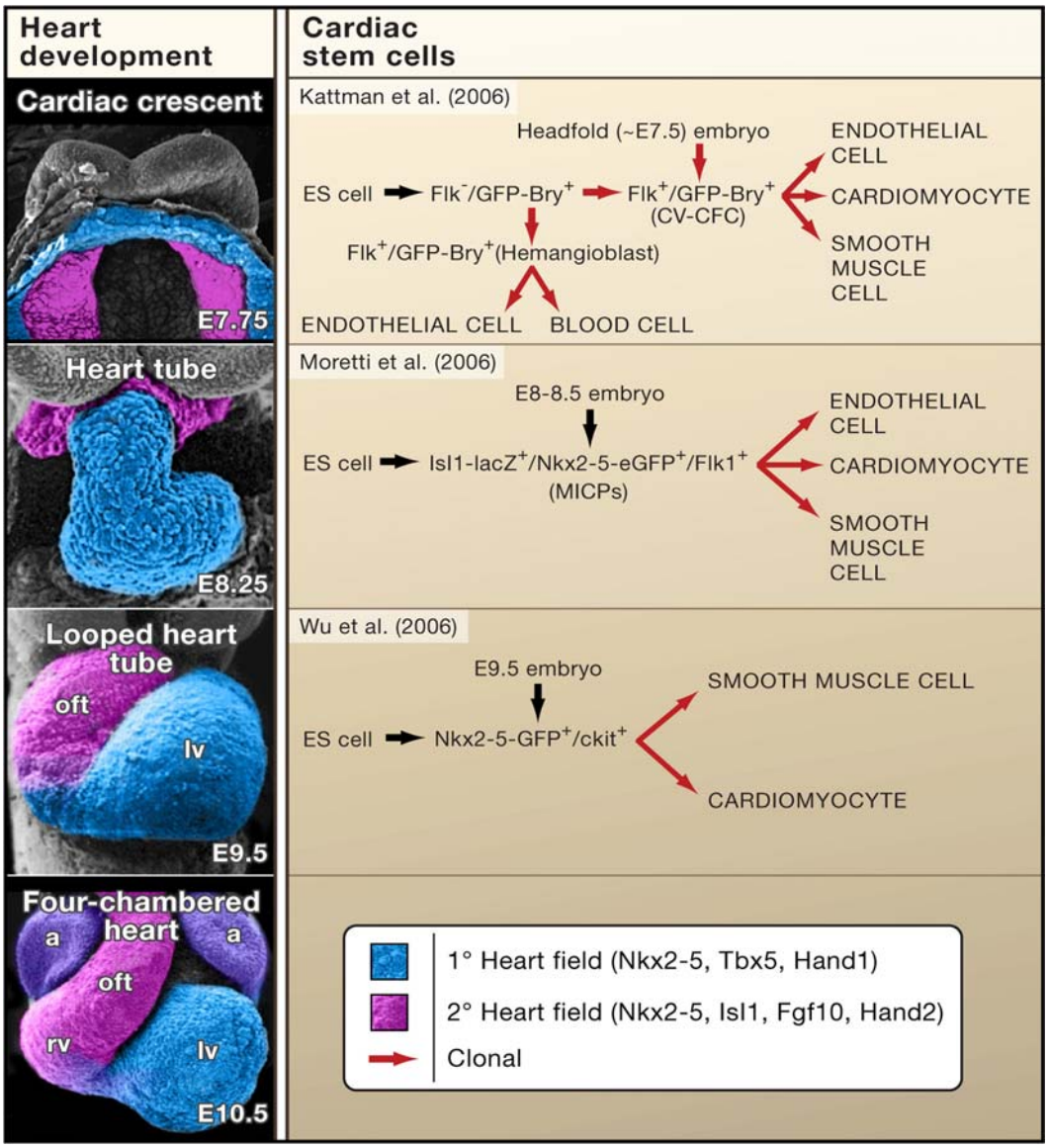
Heart development
Cardiac crescent
E7.75
Heart tube
E8.25
Looped heart tube
oft
lv
E9.5
Four-chambered heart
a
a
oft
rv
lv
E10.5
Cardiac stem cells
Kattman et al. (2006)
Headfold (~E7.5) embryo
ES cell
Flk-/GFP-Bry+
Flk+/GFP-Bry+ (CV-CFC)
Flk+/GFP-Bry+(Hemangioblast)
ENDOTHELIAL CELL
BLOOD CELL
ENDOTHELIAL CELL
CARDIOMYOCYTE
SMOOTH MUSCLE CELL
Moretti et al. (2006)
E8-8.5 embryo
ES cell
Isl1-lacZ+/Nkx2-5-eGFP+/Flk1+ (MICPs)
ENDOTHELIAL CELL
CARDIOMYOCYTE
SMOOTH MUSCLE CELL
Wu et al. (2006)
E9.5 embryo
ES cell
Nkx2-5-GFP+/ckit+
SMOOTH MUSCLE CELL
CARDIOMYOCYTE
1° Heart field (Nkx2-5, Tbx5, Hand1)
2° Heart field (Nkx2-5, Isl1, Fgf10, Hand2)
Clonal

Natural killer cell-associated antigen 2 transcription factor related, locus 5 (*Nkx2-5*) is expressed in both heart fields[101].

Knockout mouse studies of these transcription factors reveal their importance during development of the heart. Loss of *Nkx2-5* was associated with a loss of ventricular tissue and the absence of *Hand1* expression, both at the cardiac-crescent stage and later in the cardiac tube where it would normally mark the left ventricle[113-115]. *Tbx5* mutant mice show severe defects in the atria-inflow region of the heart and left-ventricular hypoplasia; however, *Hand1* and other left-ventricular markers are expressed. Despite the abnormal development of the left ventricle, the outflow tract and right ventricle continue to develop normally[119]. Without expression of *Hand1*, formation of the left ventricle is disrupted due to a proliferation defect, and the mutants die from extra-embryonic effects[116, 118, 231]. In contrast, *Hand2* mutants show right-ventricular hypoplasia[120, 121]. *Isl1* mutants have only two chambers in the heart tube. Labeling with *Hand1* and *Tbx5* probes show that the left ventricle is present; however, markers of the right ventricle and outflow tract are not detected[100]. Chick embryo studies have shown that fibroblast growth factor signaling, including *Fgf8* and *Fgf10*, may be necessary for the proliferation of cells in the secondary heart field[123]. The transcription factor *Pitx2* is expressed during the primitive heart tube stage and is responsible for the left/right specification of the chambers and the outflow tracts. It is co-expressed in the secondary, or anterior, heart field with *Tbx1*, which acts as an enhancer for *Pitx2* and affects asymmetric cardiac morphogenesis[232, 233]. While each of these genes has been identified as playing a role in the development of the heart, there has not

been, to our knowledge, a global study of the gene expression differences between the normal LV and the normal RV.

In addition to considering differences in embryological development between the ventricles, it is also necessary to consider the differences in physiology. The normal pulmonary artery and right ventricular systolic pressure is 1/5 that of the systemic pressure. Additionally, the thickness of the RV free wall is approximately 1/5 less than that of the LV free wall – 2 to 5 mm in the RV compared to 7 – 11mm in the LV[146, 234]. The mass of the RV is 1/6 that of the LV[148]. While the LV has an ellipsoidal shape, the RV has a crescent shape in cross-section and appears triangular from the side[146, 234]. It has been reported that there are regional differences in the size of cardiomyocytes in adult rat hearts[235], and that cardiomyocytes respond differently to changes in hemodynamic load depending on the ventricle in which they are located[236]. During the development of severe pulmonary hypertension (PH), the RV systolic pressure undergoes a 4-5 fold increase above normal[8, 237], whereas the LV systolic pressure in a widely studied model of chronic left ventricular failure, aortic stenosis, increases in pressure by only a few percent[202, 238, 239]. It is also known that α1-adrenergic receptor agonists decrease the contractile force in the normal RV, whereas they increase the force in the corresponding LV[240]. Similarly, long-term infusion of norepinephrine led to LV hypertrophy, but the RV did not respond with hypertrophy[241]. Based on these physiological differences, we postulate that there is a difference in gene expression between the two ventricles.

Rationale: Based on the differences in embryology and physiology, there is sufficient reason to postulate that the normal RV and the normal LV have different gene expression profiles. While many studies have examined the gene expression profile of the LV or the use the nonspecific term "ventricle", none have looked at the differences between the RV and the LV. In fact, many studies do not make the distinction between LV and RV and treat the ventricles as one muscle. However, as explained above, the RV and LV neither respond in the same manner, nor do they arise from the same embryological background. It stands to reason that there is a difference in the normal gene expression patterns in the adult rat that ultimately lead to the differences in the ventricles during right ventricular failure.

3.2 Microarray Analysis

In order to more clearly determine the gene expression changes of the right ventricle during failure caused by PAH, our first goal was search for postulated differences in gene expression between the normal RV and the normal LV. To this end, we adopted DNA microarray technology to elucidate the differences (**Figure 6**). We used the Agilent Whole Rat Genome 4 x 44k chips, a commercially available microarray from Agilent Technologies, Inc. Each array is comprised of probes that have been validated for sequence orientation, accuracy, and clustering assembly classification using the rat genome build m3[242]. In order to obtain an overview of the normal ventricle gene

Figure 6: Clustergram of normal RV and normal LV

Normal RVs and LVs were isolated from the same animal and snap frozen on liquid nitrogen. RNA was isolated from each ventricle and labeled with Cyanine-5 (red). Universal rat reference RNA from Stratagene was labeled with Cyanine-3 (green). Genes were selected using the procedure in the text. The left column shows expression in the LV and the middle column the RV. Genes colored red indicate higher expression than reference RNA, green indicates lower expression, and black indicates equal expression. The column to the right of the grey line is the difference between the RV and LV; in this case, red represents higher expression in the RV, and green represents higher expression in the LV.

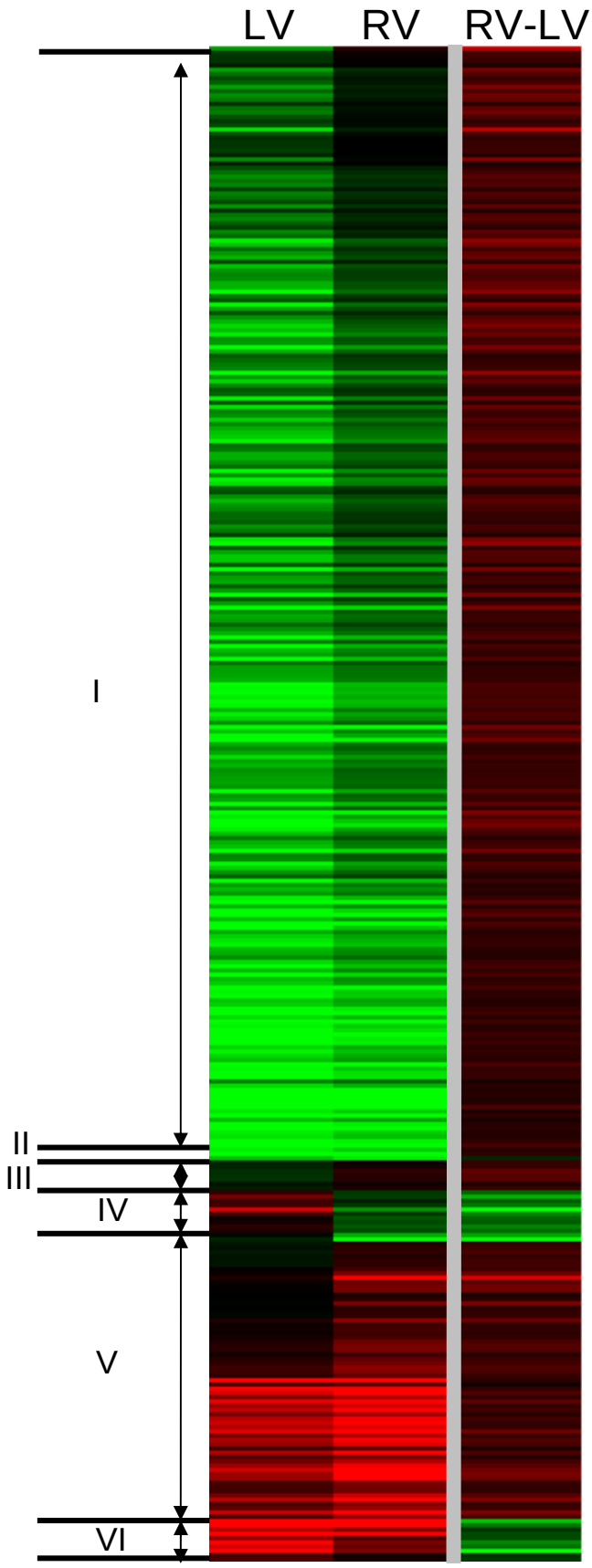
LV
RV
RV-LV
I
II
III
IV
V
VI

expression, we performed a microarray analysis using paired samples, that is, the LV and the RV from six biological replicates (six rats).

Our experimental design utilized a so-called "Type II" approach: each condition was hybridized against a pool of reference RNA from Strategene designed to provide a hybridization signal at each spot and to provide a consistent pool of RNA for each experiment. As such, the expression of the RV and LV as shown is relative to the reference RNA pool and can be considered arbitrary; the important difference comes in the comparison between the two ventricles. All data from the scanned arrays were uploaded to the Ramhorn Array Database, a VCU-specific installation of the Longhorn Array Database[218], for archiving and analysis. To produce the clustergram shown in **Figure 6**, the basic analysis is as follows. Microarray data were retrieved from the Ramhorn Array Database after filtering the data using a set of spot-quality metrics. Spots were included in the dataset if they have a signal greater than or equal to 1.5 fold above background in both the red and green channels and greater than 50% good data across the set of arrays. Technical replicates were averaged together. To determine which genes had a statistically significant difference in their expression between the normal RV and normal LV, we used the Significance Analysis of Microarrays (SAM) algorithm[219] to perform a two-class paired analysis between the data from the normal RV and the normal LV. The SAM analysis was conducted using 64 permutations of the replicate data, the maximum number of permutations given a two-class paired analysis and six biological replicates. Our approach to determining significance was to control the False Discovery Rate (FDR) of the analysis by choosing the lowest delta value resulting in a median FDR of 5% or less; for this analysis, a delta value of 0.92 was chosen giving a median FDR of

4.64%. This results in reporting of genes with q-values (the multiple-comparison adjusted analog of the p-value used by SAM) < 0.05. Of the 20,556 genes that passed filtering conditions, 335 were called significant. The Stanford Unique Intentifiers (SUIDs) representing each significantly regulated gene were retrieved. The expression of biological replicates was averaged for both the RV and LV arrays. The Cluster 3.0 program[220] was used to perform average-linkage hierarchical clustering and exported to the Java TreeView program[221] for visualization. The resulting cluster shown in **Figure 6** is comprised of the 355 genes passing the criteria listed above. The major columns from left to right are: left ventricle average, right ventricle average, and the relative difference between the right ventricle average and the left ventricle average (red means higher expression in the RV than the LV and green means higher expression in the LV than the RV).

Overall, the cluster shows a small number of genes that were differentially expressed. Of the 355 genes with differential expression between the RV and LV, 332 had higher relative expression in the RV than the LV, while only 23 had higher relative expression in the LV than the RV. The clustergram shows the expression in the LV in the first column and the RV expression in the middle column. The third column represents the difference in expression between the RV and LV. In focusing on the third column, smaller clusters become apparent, each with a different pattern of expression that corresponds to different biological functions and pathways. The list of all biological processes associated with these genes that differ in expression was identified using the PANTHER classification

system and is given in **Table 7**[222, 223]. PANTHER was also used to assign the molecular functions of genes in each sub-cluster.

Cluster I This cluster has genes with higher relative expression in the RV than in the LV. Genes in this cluster are involved in binding, catalytic activity, enzyme regulator activity, ion channel activity, receptor activity, structural molecule activity, transcription regulator activity, and transporter activity.

In this cluster are several genes that control the *Wnt* signaling pathway, a signaling pathway that is active during the heart's development in the secondary heart field to promote growth and diversification of precursor cells into the right ventricle and interventricular myocardium[243]. These genes include: FAT tumor suppressor homolog 3 (*Fat3*), SWI/SNF related, matrix associated, actin dependent regulator of chromatin, subfamily d, member 2 (*Smarcd2*), and transducer-like enhancer of split 3 (*Tle3*). Thus, having higher expression of *Wnt* signaling pathways in the RV than the LV is consistent with the different embryological backgrounds of the two ventricles.

In addition, genes involved in the IGF1/insulin signaling pathway can be found in this cluster: insulin-like growth factor 1 (*Igf1*) and insulin-like growth factor binding protein 3 (*Igfbp*). IGF1 signaling has been shown to cause cardiomyocyte growth[244] and control cell differentiation and apoptosis[245].

Table 7: List of biological processes that are differentially expressed between the normal RV and normal LV.

The biological processes were assigned by PANTHER for each gene and summarized here.

Biological Process	# of Genes
Apoptosis	5
Blood circulation and gas exchange	1
Cell adhesion	3
Cell cycle	8
Cell proliferation and differentiation	10
Developmental processes	25
Homeostasis	4
Immunity and defense	15
Neuronal activities	5
Oncogenesis	9
Carbohydrate metabolism	3
Lipid, fatty acid, and steroid metabolism	11
Nucleoside, nucleotide, and nucleic acid metabolism	30
Other metabolism	11
Protein metabolism and modification	22
Protein targeting and localization	1
Cell structure and motility	7
Intracellular protein traffic	5
Transport	16
Sensory perception	3
Signal transduction	46
Miscellaneous	2
Unclassified or unknown	212

Cluster II This cluster is composed of a single gene, heme binding protein 1 (*Hebp1*), which has higher relative expression in the LV than in the RV. *Hebp1* is thought to play a role in heme utilization for hemoprotein synthesis[246]. In addition, it may play a role in the sequestration and extraction of porphyrins from cells[247].

Cluster III Genes in this cluster have higher relative expression in the RV than in the LV. These genes are involved in binding, catalytic activity, and encode structural molecules. Of particular interest, protein phosphatase 3, catalytic subunit, alpha isoform *(Ppp3ca*), also known as calcineurin, is involved in several pathways, including the previously discussed *Wnt* signaling pathway and T-cell activation. Activation of the Ca^{2+}/calcineurin pathway increases Th2 cell development[248]. Additionally, inhibition of calcineurin was shown to be cardioprotective. A decrease in calcineurin was associated with decreased cardiac hypertrophy and improved vascularization[249].

Cluster IV In this cluster there are genes that have lower relative expression in the RV than in the LV. These genes participate in cellular activities such as binding, catalysis, enzyme regulation, and transcription regulation. Both cyclin D2 (*Ccnd2*) and growth arrest and DNA-damage inducible, alpha *(Gadd45a*) are involved in cell cycle regulation. *Gadd45a* acts to repair damaged DNA, while *Ccnd2* induces the transition from G1 to S in the cell cycle. It has been shown that sirtuin (silent mating type information regulation 2 homolog) 1 (*Sirt1*) regulates both genes in the heart. Increased levels of *Sirt1* are associated with oxidative stress and cause induction of *Gadd45a* and repression of *Ccnd2*[250].

Cluster V Genes in this cluster have a higher relative expression in the RV than in the LV. They have functions including: antioxidant activity, binding, catalytic activity, enzyme regulator activity, receptor activity, structural molecule activity, and transcription regulator activity. In addition, two genes play roles in the endothelin signaling pathways: endothelin converting enzyme 1 (*Ece1*) and protein kinase N1 (*Pkn1*). Endothelin signaling is known to stimulate myocyte grown and affect the contractile properties of the heart. It may also increases resistance to apoptosis[251]. Rho-associated coil-coil containing protein kinase 1 (*Rock1*) and von Willebrand factor (*Vwf*) are members of the inflammation by chemokine and cytokine signaling pathway.

Cluster VI In this cluster, the genes have lower relative expression in the RV than the LV. These genes participate in activities of catalysis, structural molecules, and transport.. While there are no significant pathways representative of these genes, several do act as signaling molecules, including homer homolog 2 (*Homer2*), regulator of calcineurin 1 (*Rcan1*), and natriuretic peptide precursor B (*Nppb*).

3.3 Comparison of the gene expression pattern between the normal RV and LV by qRT-PCR

Quantitative real-time polymerase chain reaction (qRT-PCR) was used to validate the microarray expression results of several genes from several different clusters: nuclear receptor subfamily 2, group F, member 2 (*Nr2f2*), *Igf1*, Iroquois homeobox 2 (*Irx2*), and

Nppb. *Igf1* and *Nr2f2* were found in Cluster I, *Irx2* in Cluster IV, and *Nppb* in Cluster VI. The qRT-PCR results (**Figure 7**) were all consistent with the trends seen in the microarray data, giving us confidence in the technique and analysis of those data. *Nr2f2*, also known as COUP-TFII (chicken ovalbumin upstream promoter-transcription factor 2), is required for angiogenesis during heart development[252]. *Nr2f2* is expressed two-fold higher in the normal RV than the LV. *Igf1* was selected for its roles in cardiomyocyte growth and control of cell differentiation and apoptosis[244, 245]. *Igf1* was found to have levels in the normal RV 2.5 fold higher than those in the normal. *Irx2* is a transcription factor expressed in the interventricular septum during heart development where it is thought to play a role in septum specification[253]. *Irx2* was only found to be expressed in the normal LV and was expressed at high levels. *Nppb* is the precursor to the protein *BNP* (brain natriuretic peptide), which is used clinically as a marker of heart failure. Levels of *Nppb* were 7 fold higher in the LV than the RV.

3.4 Discussion

In this chapter, we identify the differences in gene expression between the normal RV and the normal LV. These results are consistent with our understanding of the development and the normal physiology of the heart. While it has been shown previously that chamber-specific gene expression occurs during formation of the LV and the RV[115, 117, 254], it is our understanding that these data represent the first systematic study of the differences in gene expression between the RV and the LV in the adult rat.

Figure 7: Comparison of expression levels of selected genes between the normal RV and normal LV by qRT-PCR

Quantitative real-time PCR analysis of a) Nr2f2 (a, $p<0.05$ vs. LV), b) IGF1 (a, $p<0.01$ vs LV), c) Irx2 (a, $p<0.05$ vs RV), and d) BNP (a, $p<0.005$ vs RV) mRNA in rat normal left and right ventricles. Data were normalized to expression of 18S rRNA and are shown as mean ± s.e.m. (n=3)

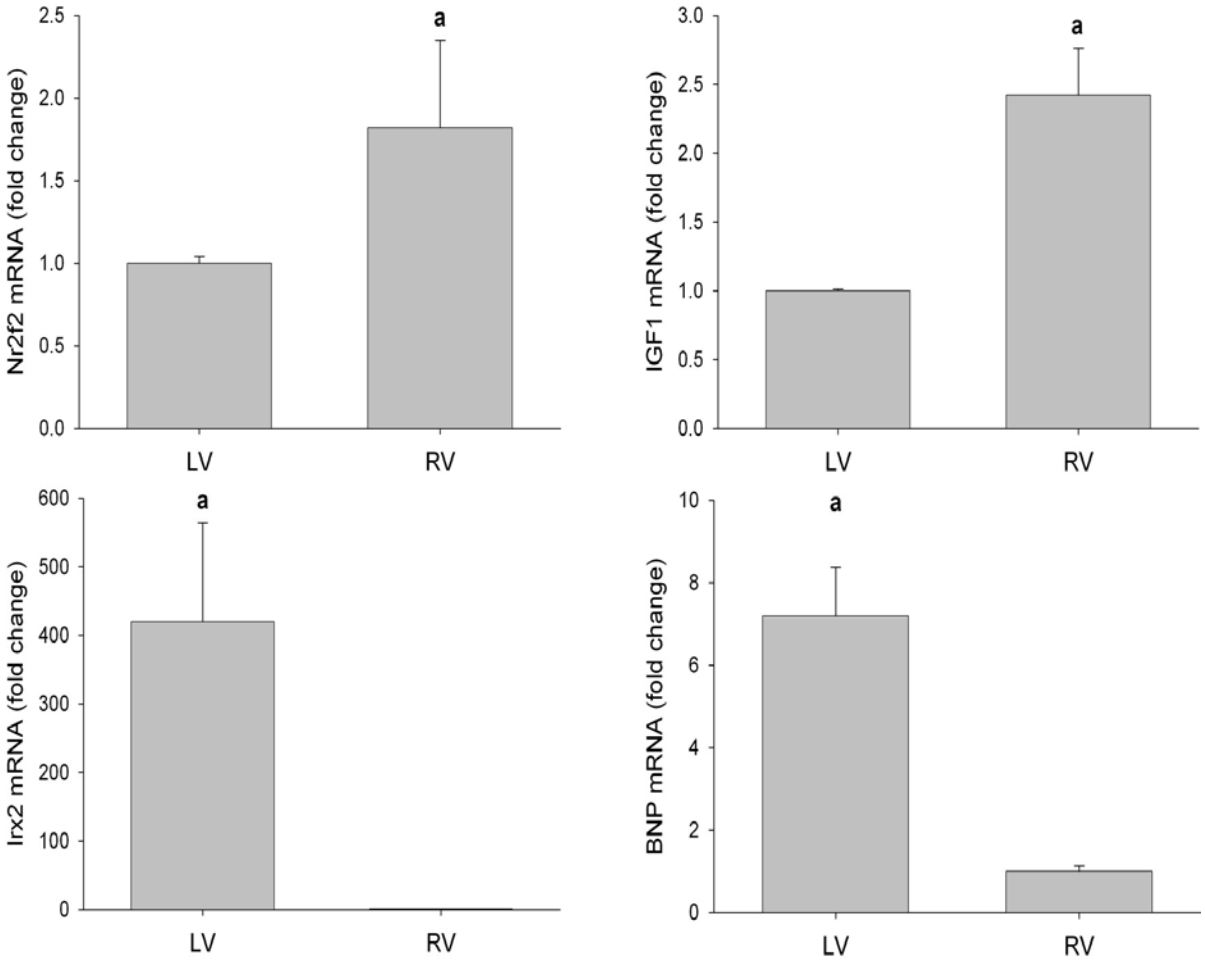
Nr2f2 mRNA (fold change)
2.5
2.0
1.5
1.0
0.5
0.0
a
LV
RV
IGF1 mRNA (fold change)
3.0
2.5
2.0
1.5
1.0
0.5
0.0
a
LV
RV
Irx2 mRNA (fold change)
600
500
400
300
200
100
0
a
LV
RV
BNP mRNA (fold change)
10
8
6
4
2
0
a
LV
RV

While the majority of the genes expressed in the normal rat heart shared gene expression profiles, a relatively small number of genes showed a significant difference in gene expression **(Table 8)**. While the set of differentially expressed genes between the normal LV and normal RV is small, they are enriched for genes and pathways that are known to play a role in the heart. In the case of the transcription factor *Irx2*, the difference was categorical in that there was no expression in the normal RV. Because Irx2 determines interventricular septum specification, absent free wall of the RV tissue expression of Irx2 and high expression in the LV wall may serve as evidence that the interventricular septum is indeed part of the LV rather than the RV as is normally held. For the majority of differentially expressed genes, the difference in expression was a matter of degree, exemplified by *Nr2f2*, *Nppb*, and *Igf1*.

While previous studies investigating right ventricular failure have operated with concepts that were derived from the failing LV, these data make it clear that the RV and LV should be evaluated independently because of differences in gene expression patterns. This notion is supported by the divergent response of the RV and LV to therapeutic agents in particular prostaglandin, which worsens left ventricular failure but improves right ventricular failure[240, 241]. We postulate that a set of gene expression changes associated with right ventricular failure can be identified and this study of the normal RV and the normal LV will serve as the basis for that work.

Table 8: Summary of genes with differential expression in the normal RV and normal LV

Right Ventricle	Left Ventricle
Nr2f2	Irx2
Igf1	Nppb
calcineurin	Hebp1
Ece1	
Vwf	
Rock1	

Chapter 4: Changes in Gene Expression in the RV during Hypertrophy and Failure

4.1 Introduction

Right ventricular failure (RVF) is increasingly recognized as an important clinical problem[255] and most patients with severe and progressive pulmonary arterial hypertension (PAH) die from right-heart failure. Additionally, right ventricular failure is the worst prognostic indicator in patients with left ventricular failure[256, 257]. Acute right ventricular failure in PAH patients can arise due to the progression of the lung vascular disease or neurohormonal activation[154].

During the progression of PAH, the mean pulmonary artery pressure (mPAP) increases progressively as the pulmonary vascular resistance (PVR) increases while the cardiac output (CO) remains the same (**Figure 8**). The right ventricle (RV) usually adapts to the high pressure in the pulmonary artery with an increase in right ventricular wall thickness achieved through muscle hypertrophy[180]. This adaptation is also associated with an increased myocardial oxygen demand[48]. The increase in afterload, defined as the amount of pressure the RV must generated to move blood from the heart to the lungs, is

Figure 8: Progression of PAH

As the pulmonary vascular resistance (PVR, purple line) increases, mean pulmonary artery pressure (PAP, green line) also increases. Cardiac output (CO, blue line) remains constant initially. As resting cardiac output decreases, patients begin to decline. Pulmonary artery pressure eventually decreases.

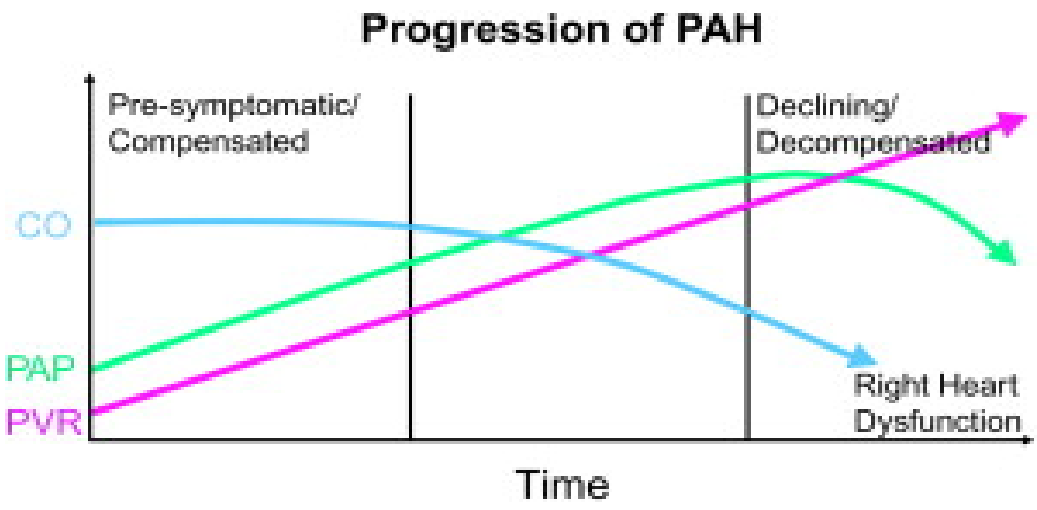
Progression of PAH
Pre-symptomatic/
Compensated
Declining/
Decompensated
CO
PAP
PVR
Right Heart
Dysfunction
Time

sensed by integrins and stretch-activated ion channels in cardiac cells to initiate protein synthesis for the adaptive hypertrophy[156]. Myocardial blood supply must keep up with the hypertrophy. Angiogenesis, the growth of new vessels from existing vessels, is known to be initiated by vascular endothelial growth factor (VEGF), angiopoietin 1 (Ang1), and other growth factors[48].

As the RV begins to fail and is no longer able to overcome the increased pulmonary vascular resistance, the mean pulmonary artery pressure and cardiac output fall [258] (**Figure 8**). As RV end-diastolic volume and pressure increase, RV wall stress also increases, which leads to a reduction in RV stroke volume[154]. While it is often assumed that elevated mean pulmonary artery pressure and increased RV afterload is a sufficient cause of right ventricular failure associated with PAH, it has been shown in animal models of pulmonary hypertension that increased afterload alone does not cause the RV to fail[180]. In animal studies comparing models of elevated pulmonary afterload, achieved through pulmonary artery banding (PAB), with models of failure, the RV hypertrophies but does not fail after PAB[180].

While an increase in afterload is the first trigger for adaptation in the RV, development of RVF in PAH also arises from neurohormonal signaling, oxidative stress, inflammation, ischemia, and cell death[48]. Associated with the changes in pathology are a set of known changes in protein levels. Levels of uric acid increase in hypoxic states and are correlated with functional decline in patients with PAH.[259] Serum levels of BNP are also increased in PAH patients versus control and were inversely correlated with

functional status and survival rates[260]. Troponin levels are often elevated in patients with RVF due to myocardial stretch and ischemia[154]. Reactive oxygen species (ROS), reactive nitrogen species (RNS), and inflammatory responses further the development of right heart failure in PAH[48]. Excessive production of reactive oxygen and reactive nitrogen species induce contractile dysfunction and favor cardiac remodeling through induction of cell damage, apoptosis, and inflammation[48]. Patients with chronic heart failure have increased serum levels of tumor necrosis factor alpha (TNF-α), interleukin 1 (IL-1), and interleukin 6 (IL-6)[210]. The switch from the α- to β-isotype of major thick filament protein myosin heavy chain (MHC) [MHC-α to MHC-β switch] in cardiomyocytes is a known hallmark of maladaptive cardiac growth and is known to be associated with right heart failure in PAH[181]. In addition, contractile dysfunction can be associated with mitochondrial defects, depletion of myocardial ATP, and modifications of myocardial energy metabolism and utilization[48].

Rationale: We have previously shown that the normal RV and normal LV have different gene expression profiles. As such, we hypothesize that the failing RV cannot be examined in terms of known failing LV gene expression profiles. We also hypothesize that the transition from adaptive hypertrophy to right ventricular failure in PAH is associated with a change in gene expression. Using microarray techniology, we will characterize the gene expression of the failing RV and the RV with adaptive hypertrophy.

4.2 Animal models of hypertrophy and failure

Pulmonary hypertension research began in Colorado in the 1950s and 1960s with studies of “brisket disease”, now known as pulmonary hypertension and heart failure, in cattle. In pioneering early PH studies, some cattle were kept at an altitude of 5,000 feet while others were kept at 10,000 feet and hemodynamic measurements were made of both groups. Those cattle kept at the higher altitude developed pulmonary hypertension, while those kept at the lower altitude did not[261]. Later studeies comparing the response in sheep and cattle showed that sheep did not respond to the same extent as cattle to chronic high altitude hypoxia and that the hypoxic pulmonary vascular reponse is species dependent[262].

Roughly at the same time, the monocrotaline model of pulmonary hypertension was being developed. Monocrotaline is a purified pyrollizidine alkaloid found in plants of the genus *Crotalaria* [263] that has been shown to cause hepatotoxicity, pneumotoxicity, and chronic pulmonary hypertension in humans[264-266]. Pathologically, injection of monocrotaline has been shown to cause endothelial cell damage [267, 268]; microvascular leak [269, 270]; arterial thickening; muscularization of small, normally nonvascular arteries; and thickening of the pulmonary artery trunk [271]. A progressive rise in pulmonary artery pressure and development of RVF also result from monocrotaline administration[272]. While the monocrotaline model produces a set of predictable pathological changes in the rat, it has come under criticism in recent years because it also causes myocarditis and pulmonary fibrosis making it difficult for

pulmonary hypertension researchers to correlate the data from this model with human idiopathic pulmonary arterial hypertension [273-276]. As such, it is likely not an appropriate model to for the study of RVF caused by PAH.

A newer model of pulmonary hypertension is the SU5416/hypoxia model[277-279]. It requires administration of the selective vascular endothelial growth factor receptor 2 (VEGFR2) tyrosine kinase inhibitor SU5416 (3-[2,4-dimethylpyrrol-5-yl)methylidenyl]-indolin-2-one) [280] and exposure to chronic hypoxia (10% F_iO_2). This model rests on two components: stress and death of lung vessel endothelial cells and chronic hypoxia. The SU5416/hypoxia model simulates human idiopathic PAH by inducing angioproliferative pulmonary lesions similar to those seen in human patients, severe pulmonary hypertension, and, ultimately, right ventricular failure [281]. The hearts show dilation and hypertrophy of the RV and paradoxical movement of the interventricular septum (**Figure 9**). When SU5416 is given alone, it causes mild pulmonary hypertension and pulmonary vascular remodeling, but neither irreversible PAH nor RVF[282]. Exposure to chronic hypoxia alone for 4 weeks generates moderate pulmonary hypertension and RV hypertrophy, but not right ventricular failure[283]. While the Fulton index (RV/LV+S) increases with both chronic hypoxia and SU5416, the body weight of the animals does not change significantly with treatment (**Figure 10**). SU5416 given alone does not cause a change in the body weight or in the Fulton index. Because of the similarity to human disease, the SU5416/hypoxia model will be used for our studies

Figure 9: Maladaptive remodeling in rat models of right heart failure.

a) The normal RV imaged by echocardiography has a crescent shape (arrow), an interventricular septum that is crescent shaped (dashed line) and a free wall that is difficult to identify by routine echocardiography. b) in the RV failure model (SuHx), echocardiography shows RV hypertrophy (arrow), dilation, and paradoxical movement (towards the LV rather than the RV) of the interventricular septum (dashed line) c) freshly excised normal rat heart d) freshly excised failing (SuHx) rat heart. Arrow points to hypertrophied RV.

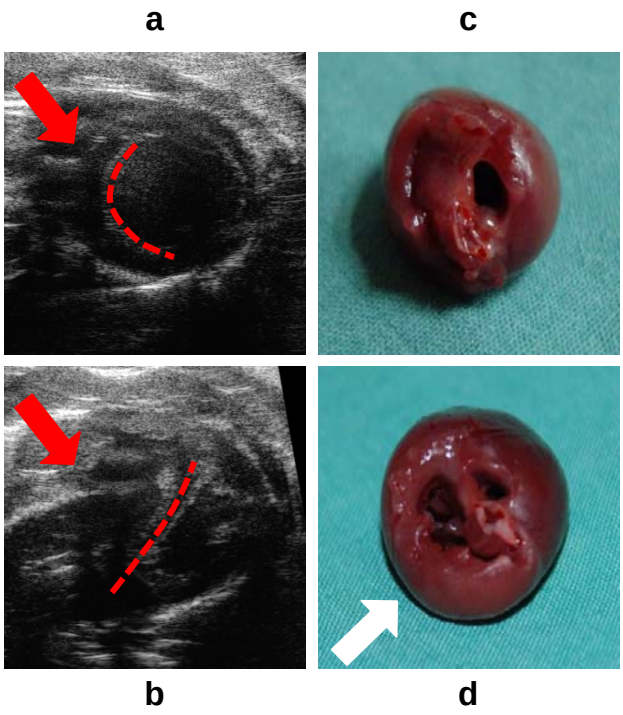
a
c
b
d

Figure 10: Body weight and Fulton index of animal models used in failure study

a) Body weight in grams and b) RV hypertrophy expressed as Fulton index (RV/LV+S) of normal (control), SU5416 (SU5416) treated, hypoxia (hypoxia) treated, and SU5416/hypoxia (SuHx) treated rats (a, $p<0.05$ vs control).

a

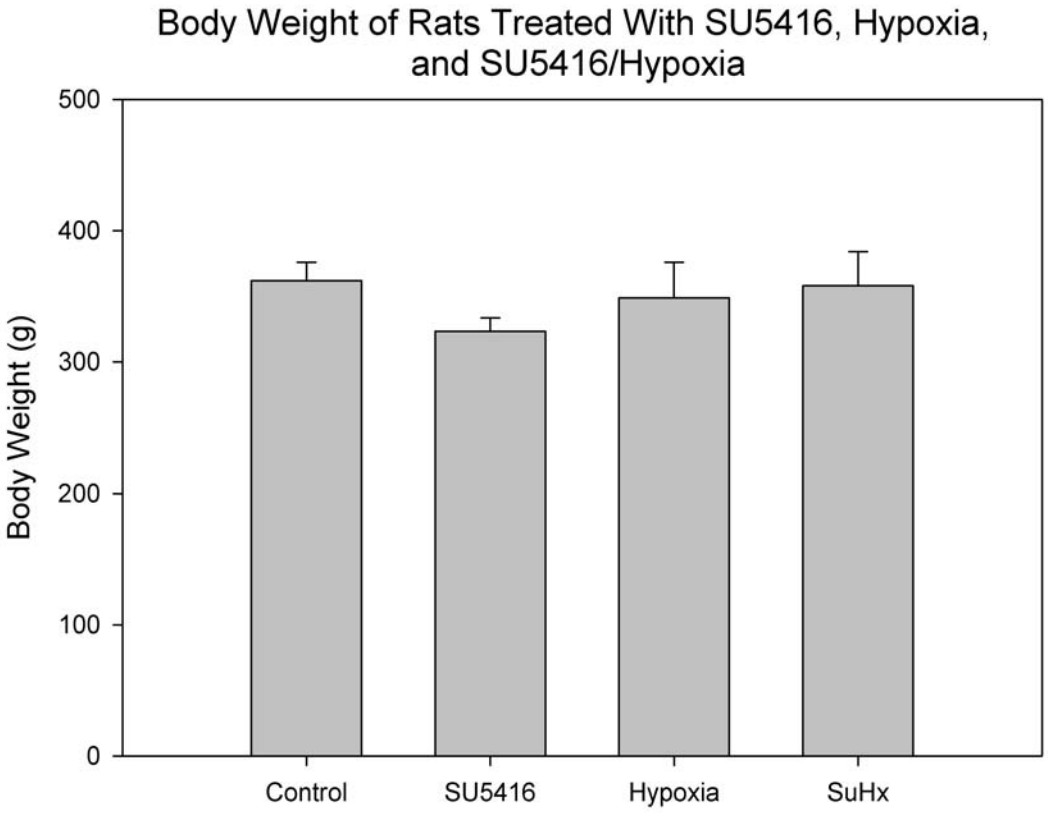
Body Weight of Rats Treated With SU5416, Hypoxia, and SU5416/Hypoxia
Body Weight (g)
500
400
300
200
100
0
Control
SU5416
Hypoxia
SuHx

b

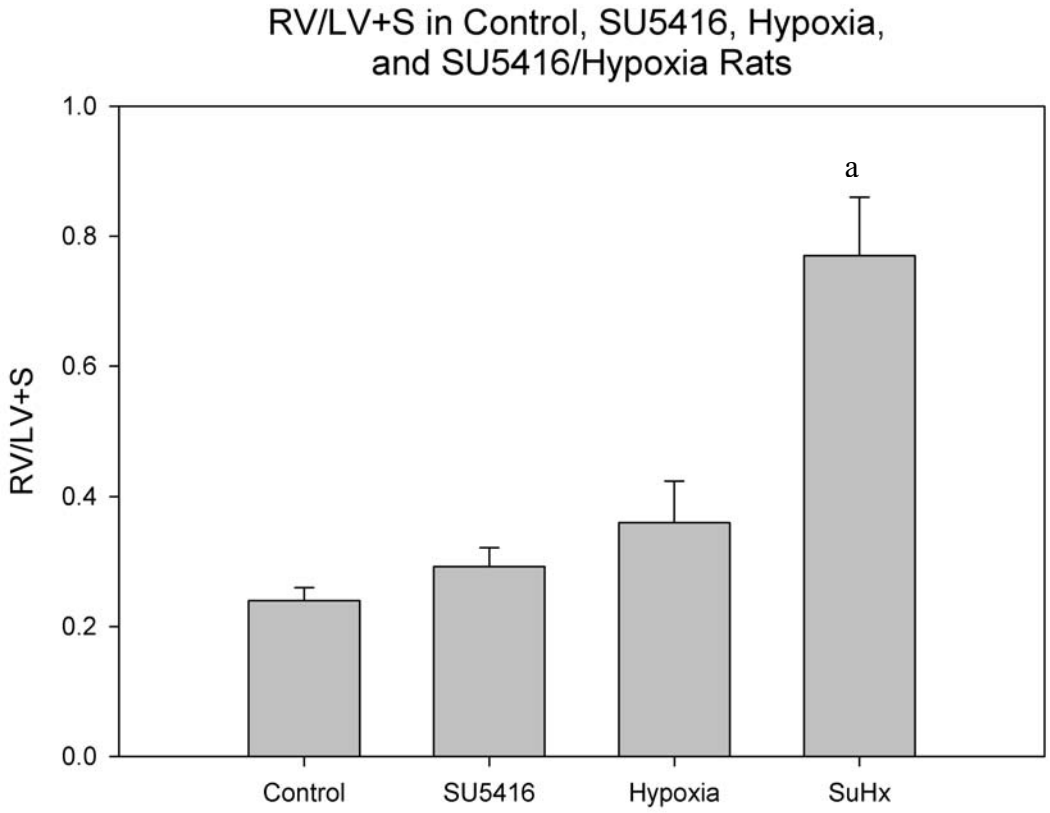
RV/LV+S in Control, SU5416, Hypoxia,
and SU5416/Hypoxia Rats
RV/LV+S
1.0
0.8
0.6
0.4
0.2
0.0
a
Control
SU5416
Hypoxia
SuHx

4.3 Microarray analysis

In order to identify differences in gene expression that occur during right ventricular failure associated with PAH, we used a microarray analysis similar to that employed in the comparison between the normal RV and normal LV. Again, this was a "Type II" approach in which each hybridization was a combination of RNA from an animal model and a pool of commercially available reference RNA. Total RNA was isolated from RV tissue from animals treated with SU5416 alone, chronic hypoxia alone, and SU5416 in combination with chronic hypoxia. Because the normal RV was hybridized against the same pool of reference RNA, it can be used again in this analysis. The expression of each RV treatment as shown is relative to the normal RV.

Total RNA was isolated from the free wall of the RV from rats treated with SU5416 (SU5416) only, rats exposed to chronic hypoxia for 4 weeks, and rats given a combination of SU5416 and chronic hypoxia. RNA was converted to cDNA and fluorescently labeled with either Cyanine-3 (green) or Cyanine-5 (red) dye. The two labeled cDNA samples were mixed together and hybridized to an Agilent Whole Rat Genome 4x44k microarray chip overnight. Six biological replicates and three technical replicates per condition were hybridized. Microarrays were washed and then scanned with an Axon GenePix 4200A scanner and GenePix Pro 5.0 software. All data were uploaded into the Ramhorn Array Database (http://ramhorn.csbc.vcu.edu). Microarray data were retrieved from the Ramhorn Array Database if they had a signal greater than or equal to 1.5 fold above background for both the red and green. A gene was called "good"

and used for analysis if greater than 50% of all arrays for each condition used in the analysis passed the filtering conditions of expression greater than or equal to 1.5 fold above background expression. Technical replicates were averaged together.

To determine which genes had a stastically significant difference in their expression between conditions, we used the Significance Analysis of Microarrays (SAM) algorithm[219] to perform a two-class unpaired analysis with 1,000 permutations of replicate data. To control the False Discovery Rate (FDR), the lowest delta value resulting in a median FDR of 5% or less was chosen to give genes with a q-value < 0.05. First, a pairwise comparison of each condition compared to normal was made. In the comparison between the normal RV and the SU5416-only treated RV, 18,137 genes passed the filtering conditions. Of these, 6,611 were called significant at a delta value of 0.70 and a FDR of 4.83%. When comparing the normal RV and the hypoxia-only RV, 10,967 genes passed filtering conditions and 5,855 of these were significant using a delta value of 0.73 and a FDR of 4.79%. Finally, in a comparison between the normal RV and the SU5416/hypoxia RV, 13,050 genes passed filtering conditions. 3,595 were called significant at a delta value of 0.80 corresponding to a FDR of 4.3%. A venn diagram of the number of genes called significant between each condition and the overlap of those significant genes is shown in **Figure 11**. 493 genes were called significant in all of the pairwise conditions and there was also overlap in the genes called significant between sets of comparisons. However, the majority of genes in each comparison were not shared in another condition and these differences most likely represent the genes causing changes in phenotype by the treatments.

Figure 11: Venn Diagram of Genes Called Significant in Pairwise Comparisons

Pairwise comparisons were made between the normal RV and each condition, SU5416 RV, hypoxia RV, and SU5416/hypoxia RV, using the Significance Analysis of Microarrays two-class unpaired comparison algorithm. For each analysis a delta value was chosen such that the False Discovery Rate was 5% or less. The number of genes called significant in each comparison is shown here as well as the number of significant genes shared between each pairwise comparison. 493 genes were called significant in all pairwise comparisons.

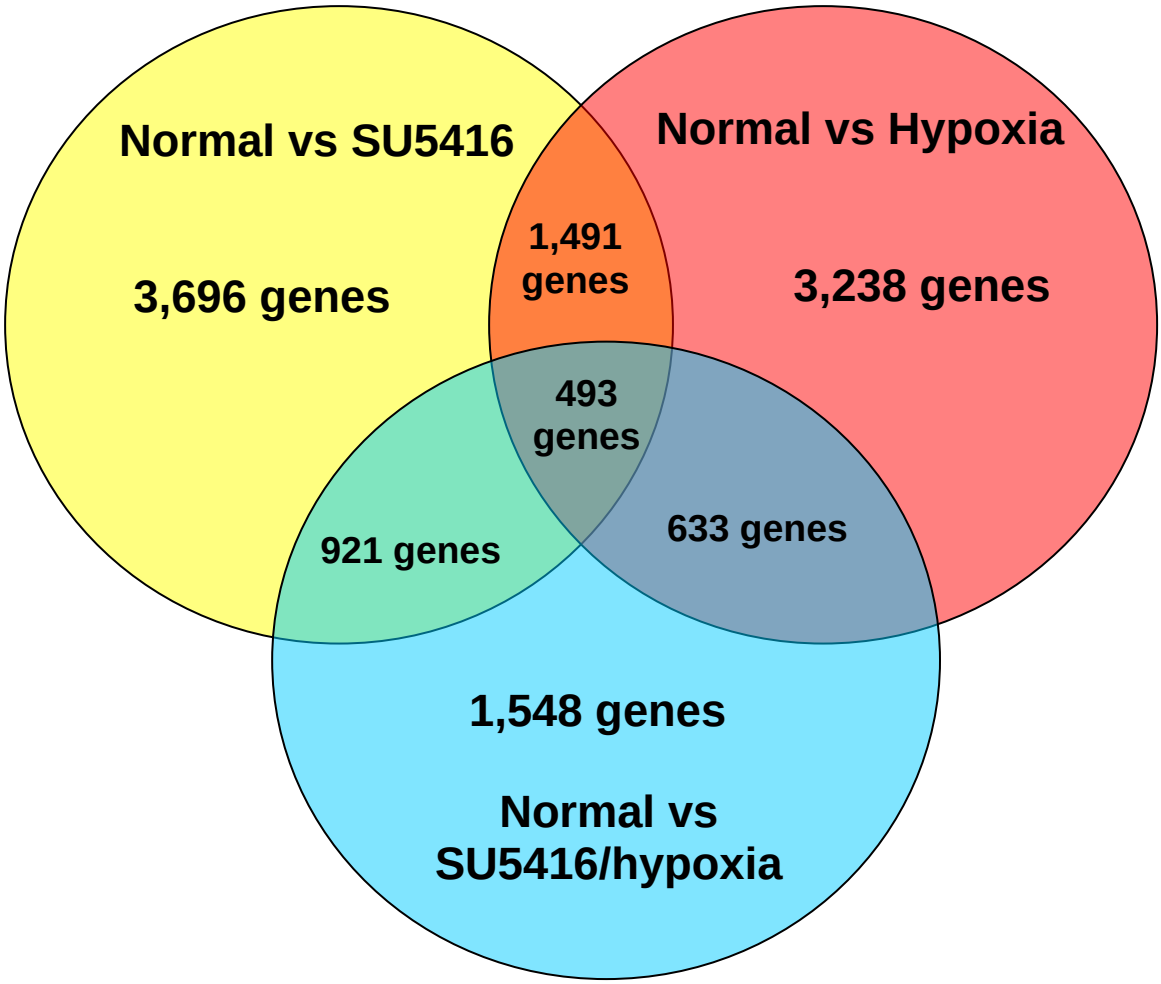
Normal vs SU5416
3,696 genes
Normal vs Hypoxia
3,238 genes
1,491 genes
493 genes
921 genes
633 genes
1,548 genes
Normal vs SU5416/hypoxia

To determine which genes had statistically significant difference in their expression between the normal RV, the failing (SU5416/hypoxia) RV, and the hypoxic RV, a series of two-class unpaired comparisons were made. First, a two-class comparison between the normal RV and the SU5416/hypoxia RV was done to identify 3,595 called significant using the parameters listed previously. Next, a two-class unpaired comparison was made between the SU5416/hypoxia RV and the hypoxia RV for those 3,595 genes called significant between the normal and failing RV. Of the 3,595 genes, 1,980 were called significant between the SU5416/hypoxia RV and hypoxia RV at a delta value 0.74, which gives a FDR of 4.96%. The Stanford Unique Indentifiers representing genes called signficant between both comparisons were compiled and data for all conditions – normal RV, SU5416 RV, Hypoxia RV, and SU5416/hypoxia RV – were retrieved from the Ramhorn Array Database and transformed by subtracting the average expression of the normal RV from each condition. This gives the expression in each experimental condition relative to the normal RV and allows us to visualize the change in expression resulting from the treatment. The Cluster 3.0 program[220] was used to perform average-linkage hierarchichal clustering of the whole dataset and exported to the Java TreeView program[221] for visualization. The resulting cluster shown in **Figure 12** is comprised of the 1,980 genes passing the filtering conditions above. The major columns from left to right are: normal RV, SU5416 RV, Hypoxia RV, and SU5416/hypoxia RV.

Overall, the cluster shows that an approximately equal number of genes were up-regulated and down-regulated in the RV with SU5416/hypoxia treatment as compared to the normal RV. Treatment with SU5416 had a clear pattern of expression in the; this

Figure 12: Clustergram of differentially expressed genes between the normal RV, hypertrophied RV, and failing RV

Six biological replicates per condition were hybridized to Agilent Whole Rat Genome microarrays. RV hypertrophy is generated by treating rats with SU5416 (samples labeled "SU5416") or exposure to chronic hypoxia (samples labeled "Hypoxia"). RV failure (samples labeled "SuHx") is due to the treatment of rats with a combination of SU5416 and chronic hypoxia. Green indicates lower expression in a given condition than in the normal RV, red indicates higher expression in a condition than in the normal RV. Black indicates that the expression in the condition is equal to expression in the normal RV.

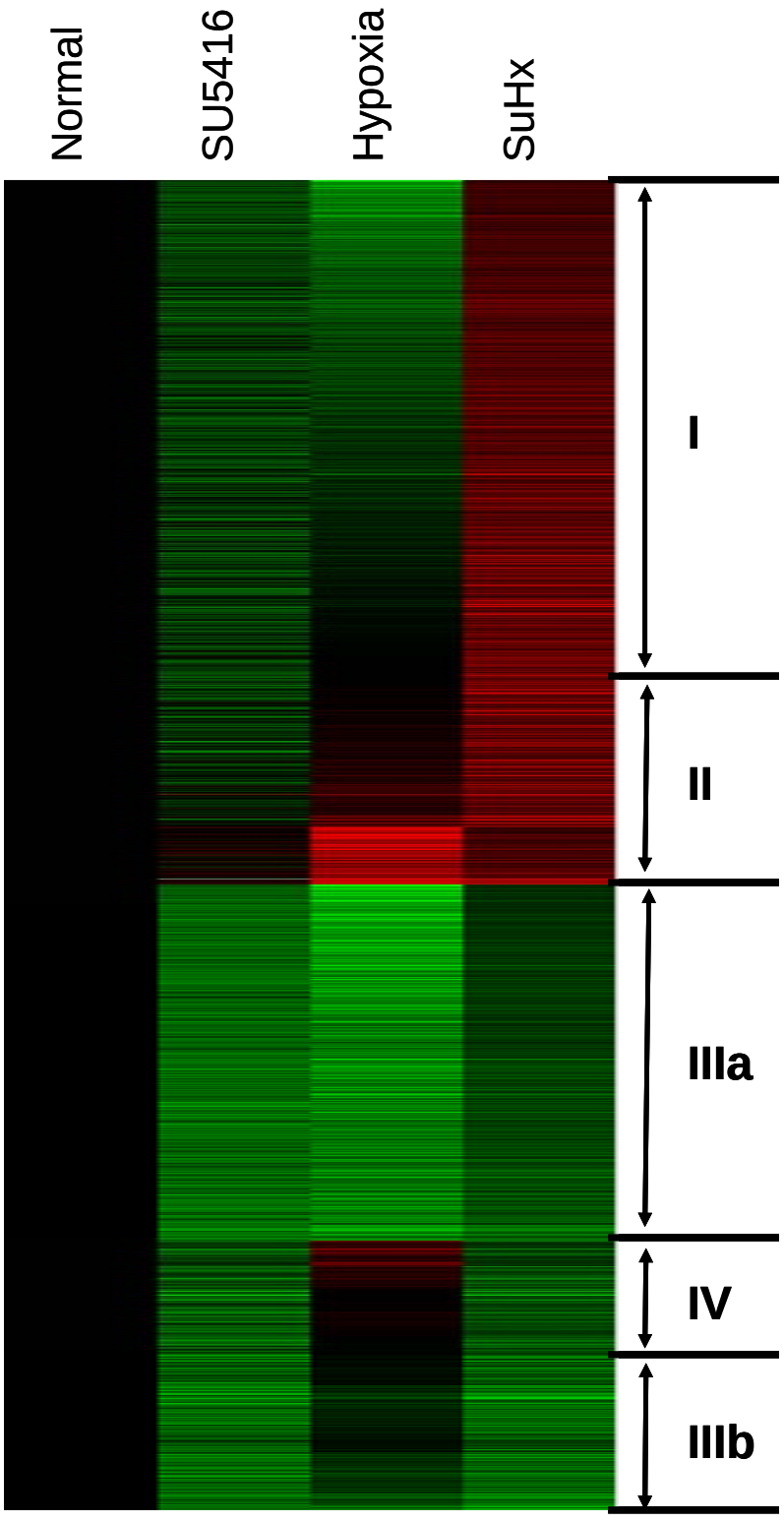
Normal
SU5416
Hypoxia
SuHx
I
II
IIIa
IV
IIIb

pattern was not shared with the chronic hypoxia or SU5416/hypoxia treatment. When contrasting RV hypertrophy caused by chronic hypoxia exposure and RV failure caused by SU5416/hypoxia treatment, there are distinct patterns of expression not shared by the two treatments. Of particular interest are clusters where overexpressed genes in chronic hypoxia are decreased in the failing RV. These genes could indicate a pattern of adaptive hypertrophy gene expression. Ingenuity Pathway Analysis (http://www.ingenuity.com) was used to identify the biological process associated with the genes that differ in expression between the normal RV and the failing RV and is shown in **Table 9**. In focusing on cluster diagram, smaller clusters become apparent, each with a different pattern of expression that corresponds to different biological functions and pathways as determined by Ingenuity Pathway Analysis and the PANTHER Classification System[222, 223].

Subcluster I consists of genes that represent a "frank failure-activated" cluster; they have higher expression in the SU5416/hypoxia RV than the chronically hypoxic RV. The top five canonical pathways as defined by Ingenuity Pathway Analysis for genes in this cluster are listed in **Table 10**. Integrin signaling is known to play a role in the heart's adaptation to pressure overload by increasing synthesis of contractile proteins[157, 158]. Expression of integrin-like kinase (ILK) is highest in the heart and is an essential for regulating cardiac growth, contractility, and repair[284]. Cardiac-specific expression of ILK induces hypertrophy suggesting that ILK is a regulator of hypertrophic signaling pathways[285]. Additionally, levels of α-skeletal mRNA have been shown to increase 10-fold in a calf model of pulmonary hypertension induced by chronic hypoxia[286]. In

Table 9: Biological processes of genes differentially expressed between normal RV and SU5416/hypoxia RV

Biological Process	# of Genes
Apoptosis	261
Blood circulation and gas exchange	61
Muscle contraction	142
Cell adhesion	270
Cell cycle	424
Cell proliferation and differentiation	518
Developmental processes	935
Homeostasis	119
Immunity and defense	731
Neuronal activities	256
Non-vertebrate process	8
Oncogenesis	253
Amino acid metabolism	116
Carbohydrate metabolism	280
Coenzyme and prosthetic group metabolism	97
Lipid, fatty acid and steroid metabolism	417
Nitrogen metabolism	12
Nucleoside, nucleotide and nucleic acid metabolism	1173
Other metabolism	206
Phosphate metabolism	33
Protein metabolism and modification	1240
Sulfur metabolism	33
Protein targeting and localization	105
Cell structure and motility	505
Intracellular protein traffic	400
Transport	613
Electron transport	149
Sensory perception	149
Signal transduction	1522
Miscellaneous	19
Unclassified or unknown	1369

Table 10: Top Five Canonical Pathways of Genes in Subcluster I

Pathway Name	p-value
Integrin Signaling	1.56×10^{-6}
Actin Cytoskeleton Signaling	4.11×10^{-6}
ILK Signaling	6.40×10^{-6}
Nrf2-mediated Oxidative Stress Response	8.35×10^{-6}
IGF-1 Signaling	2.27×10^{-5}

the microarray dataset, expression of several actin genes were increased: actin alpha 1 (*Acta1*) and actin gamma 1 (*Actg1*) were increased 3.5-fold in the SU5416/hypoxia RV over the hypoxic RV while actin beta (*Actb*) was increased 2-fold in the SU5416/hypoxia RV over the hypoxic RV. Rho-kinase (*Rock*), a downstream effector of *RhoA*, plays a role in regulating rearrangement of the actin cytoskeleton[287] and has previously been shown to be increased in expression during pressure overload-induced cardiac hypertrophy[288]. Deletion of *Rock1* was associated with reduced remodeling, including fibrosis, apoptosis, and chamber dilation[287]. *RhoA* was increased 2-fold in the SU5416/hypoxia RV compared to the hypoxic RV in the microarray dataset. Based on these pathways and their involvement in heart disease and hypertrophy, it can be hypothesized that this cluster represents the damaged hearts's attempt to compensate for the increased stress. However, because these genes have higher expression in the SU5416/hypoxic RV than in the hypoxic RV, it is possible that this subcluster represents a maladaptive hypertrophy pattern reflecting damage.

Subcluster II is comprised of genes that reflect a "hypoxia activation cluster" and have increased expression in both the SU5416/hypoxia RV and the hypoxic RV. The top five canonical pathways for genes in this subcluster as defined by Ingenuity Pathway Analysis are listed in **Table 11**. There are several genes in this cluster that are members of the transforming growth factor beta (*Tgf-β*) signaling pathway: inhibin beta B (*Inhba*); mitogen-activated protein kinase 3 (*Mapk3*); and s100 calcium-binding protein A4. *Tgf-β* has been shown to be induced by pressure overload[289] and injury[290] in the heart and increased *Tgf-β1* expression has been identified in the myocardium during cardiac

Table 11: Top Five Canonical Pathways in Subluster II

Pathway Name	p-value
IL-8 Signaling	5.73×10^{-7}
Hepatic Fibrosis/Hepatic Stellate Cell Activation	2.24×10^{-5}
Ovarian Cancer Signaling	6.30×10^{-5}
Pancreatic Adenocarcinoma Signaling	9.05×10^{-5}
Role of Tissue Factor in Cancer	9.71×10^{-5}

hypertrophy and failure[291-293]. *Inhbb* was increased by 3-fold in both the SU5416/hypoxia RV and hypoxic RV relative to normal. *Mapk3* was increased 2-fold in the hypoxic RV and 1-fold in the SU5416/hypoxia RV compared to normal. *S100a4* was increased 1-fold in the hypoxic RV and 3-fold in the SU5416/hypoxia RV compared to the normal RV. Expression of interleukin-8 (IL-8) was increased in the serum of patients with PAH and patients with higher serum levels of IL-8 had lower 1-year and 5-year survival rates than patients with low IL-8 serum levels[294]. While IL-8 is a modulator of immune responses, IL-8 also plays a role in vascular remodeling and modulate smooth muscle and endothelial cell function[295-298]. This expression pattern is most likely an attempt to compensate for stress rather than a failure-specific pattern because genes are expressed almost equally in the hypoxic and SU5416/hypoxia RVs.

Subcluster III consists of genes that make up a "repression cluster" because they have decreased expression in both the hypoxic RV and the SU5416/hypoxia RV. The top five canonical pathways as defined by Ingenuity Pathway Analysis for genes in this subcluster are listed in **Table 12**. The entire mitochondrial biogenesis pathway has been reported to be downregulated in heart failure[299] and the generation of reactive oxygen species (ROS) increases[300-303]. Mitochondria are the source of ROS and they are also damaged by the generated ROS[304]. This ROS damage is associated with mitochondrial dysfunction in failing hearts characterized by increased lipid peroxidation, decreased mitochondrial DNA (mtDNA) copy number, a decrease in mtDNA transcripts, and reduced oxidative capacity[305]. The decrease in oxidative capacity in the heart is caused by defects in the major electron transport chain (ETC) complexes[306]; this is

Table 12: Top Five Canonical Pathways in Subluster III

Pathway Name	p-value
Oxidative Phosphorylation	3.25×10^{-9}
Ubiquinone Biosynthesis	1.83×10^{-6}
Mitochondrial Dysfunction	1.96×10^{-6}
Purine Metabolism	2.06×10^{-5}
Valie, Leucine, and Isoleucine Degradation	8.81×10^{-4}

reflected in our data in **Figure 13**. Additionally, heart failure is characterized by a shift from fatty acid oxidation to glucose oxidation in both clinical[307-309] and experimental[310-312] studies. Furthermore, the ubiquitin proteasome system is involved in cell proliferation and adaptation to stress[313] and increased levels of ubiquitinated proteins are associated with depressed protseasomal activities. Under normal conditions, the ubiquitin proteasome system protects cardiomyocytes by removing pro-apoptotic signaling molecules, but decreased ubiquiting-proteasome system activity allows pro-apoptotic proteins to accumulate and trigger apoptosis[314].

Subcluster IV represents a "loss of hypoxic adaptation cluster;" genes in this cluster have increased expression in the hypoxic RV, but decreased expression in the SU5416/hypoxia RV. Although the top five canonical pathways for genes in this cluster are listed in **Table 13**, none of the pathways has a p-value greater than 0.05. As a result, we looked at specific genes within this subcluster. Of particular interest are the genes caspase 4 (*Casp4*) and transcription factor T-box 3 (*Tbx3*), both of which induce apoptosis signaling. *Casp4* induces apoptosis in response to ER-mediated stress[315, 316] and is expressed 1.6-fold higher in the hypoxic RV than in the SU5416/hypoxia RV. *Tbx3* causes inhibition of cell proliferation and induction of apoptosis[317] and has 2-fold higher expression in the hypoxic RV than the SU5416/hypoxia RV. Patients with PAH have a decrease in proapoptic gene expression and an increase in antiapoptotic gene expression[318]. Additionally, treatment with dichloroacetate in a monocrotaline model of PAH results in induction of mitochondria-dependent aptoptosis and reversal of PAH[319]. This expression pattern could be interpreted as a failure of the

Figure 13: Mitochondrial dysfunction pathway in the failing RV

Canonical pathway analysis indentified the pathways from the Ingenuity Pathway Analysis® library of canonical pathways that were most significant to the dataset. The p-value for the mitochondrial dysfunction canonical pathway is 6.51×10^{-9}. Genes are colored based on fold-change comparison between SU5416/hypoxia (failing) RV and hypoxia (hypertrophy) RV. Red correlates to relatively higher expression in the failing RV than the hypertrophied RV, and green correlates to relatively higher expression in the hypertrophied RV than the failing RV.

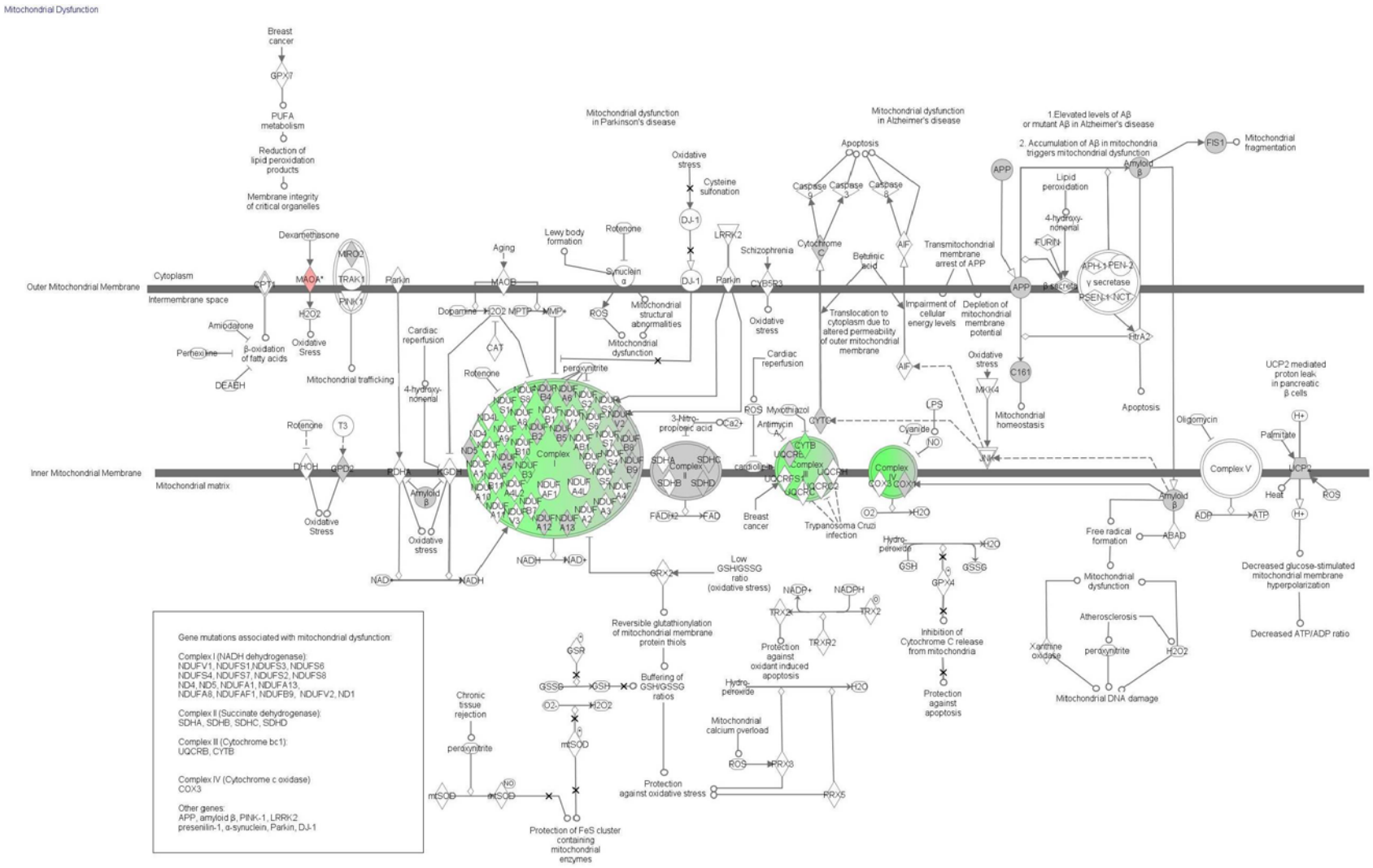

Table 13: Top Five Canonical Pathways in Subcluster IV

Pathway Name	p-value
Purine Metabolism	0.0585
Oxidative Phosphorylation	0.0729
Relaxin Signaling	0.0826
Aldosterone Signaling in Epithelial Cells	0.0961
Endothelin-1 Signaling	0.1150

SU5416/hypoxia heart to sustain stress to the same degree as the hypoxic heart, thus leading to failure.

4.4 Prediction analysis

In order to identify the postulated gene signature that could predict between the three conditions (normal, adaptive hypertrophy, and failing), prediction analyses were performed by applying a leave one-out cross-validation (LOOCV) approach on a dataset comprising six biological replicates in each class (normal RV, chronic hypoxia RV, and SU5416/hypoxia RV), including several technical replicates per class. The LOOCV method takes into account the sample size and is suitable for small sample numbers[227, 229]. Averaging the technical replicates in each class, four prediction algorithms were used: 1-nearest neighbor, 3-nearest neighbors, nearest centroid, and diagonal linear discriminant analysis[228]. We performed 2,000 permutations, which resulted in $p < 0.0005$ for all prediction algorithms. Thus, we found that 499 probes the provided a prediction accuracy of 100% on all four algorithms. In addition, 450 of the 499 probes showed a 100% support of the LOOCV method. These probes were clustered together (**Figure 14**) and are listed in **Appendix A**. These 450 probes, corresponding to 405 different genes, can now be used to predict to which class a new sample belongs and show a gene expression pattern that differentiates RV hypertrophy from right ventricular failure.

Figure 14: **Prediction analysis cluster**.

Dendogram for clustering experiments using centered correlation and average linkage of the 450 probes that showed 100% agreement across LOOCV. Red represents greater relative expression than reference RNA and green represents less relative expression than reference RNA.

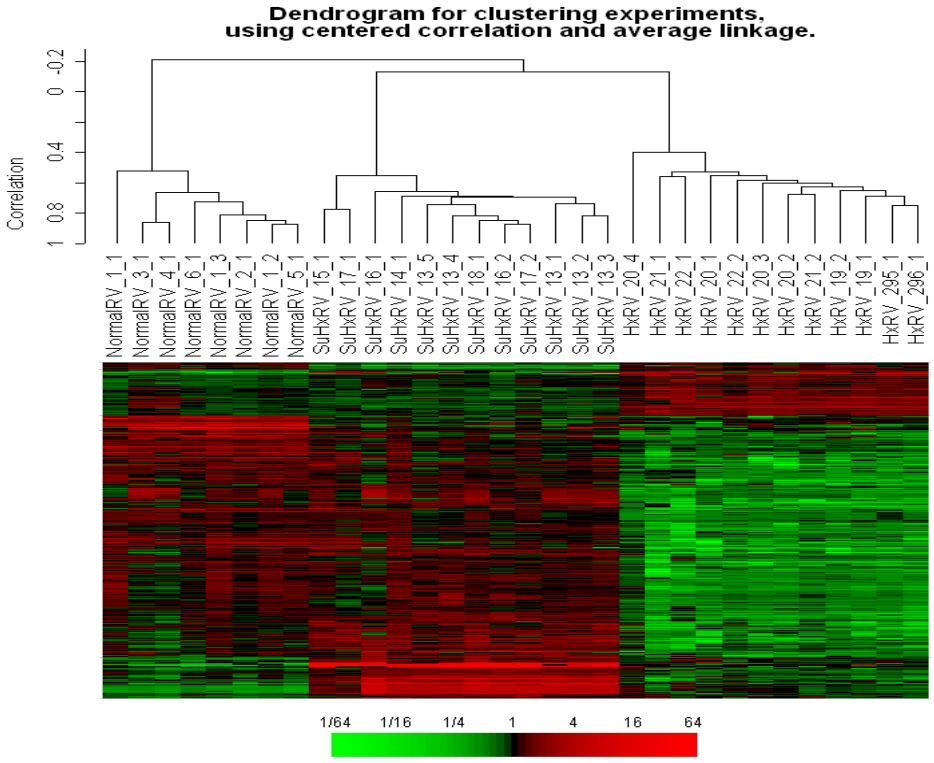
Dendrogram for clustering experiments,
using centered correlation and average linkage.
Correlation
1
0.8
0.4
0
-0.2
NormalRV_1_1
NormalRV_3_1
NormalRV_4_1
NormalRV_6_1
NormalRV_1_3
NormalRV_2_1
NormalRV_1_2
NormalRV_5_1
SuHxRV_15_1
SuHxRV_17_1
SuHxRV_16_1
SuHxRV_14_1
SuHxRV_13_5
SuHxRV_13_4
SuHxRV_18_1
SuHxRV_16_2
SuHxRV_17_2
SuHxRV_13_1
SuHxRV_13_2
SuHxRV_13_3
HxRV_20_4
HxRV_21_1
HxRV_22_1
HxRV_20_1
HxRV_22_2
HxRV_20_3
HxRV_20_2
HxRV_21_2
HxRV_19_2
HxRV_19_1
HxRV_295_1
HxRV_296_1
1/64
1/16
1/4
1
4
16
64

A number of genes that demonstrated a fold-change difference in expression based on microarray analysis between RV hypertrophy and RV failure (**Figure 12, Figure 14**) were selected for qRT-PCR and their corresponding proteins selected for Western Blot (**Figures 15 - 18**). These genes and proteins fell into one of five categories: signals shared between hypertrophy and failure, glycolytic enzymes, cell-growth promoting genes, angiogenesis, and cytoskeletal rearrangement.

4.5 Shared signals between hypertrophy and failure

As expected from previous reports, several genes, including natriuretic peptide prescursor a (*Nppa*), natriuretic peptide prescuror b (*Nppb*), and myosin heavy chain β (*MHC-β),* shared a gene expression pattern between hypoxia (hypertrophy) and SU5416/hypoxia (failure). *Nppa* is the mRNA sequence precursor for atrial natriuretic peptide (ANP) and *Nppb* is the mRNA sequence encoding the precursor for brain natriuretic peptide, both of which are biomarkers of heart failure and increased plasma levels have been reported in patients with PAH[260]. Likewise, an increase in the expression of *MHC-β* is associated with hypertrophy and PAH-associated RV failure[48, 181]. Both *NppA* and *NppB* show increased expression in both hypoxia and SU5416/hypoxia and are not significantly different between hypoxia and SU5416/hypoxia[320]. Hypoxia-inducible factor 2, alpha (*HIF-2α*) is a transcription factor that, like hypoxia-inducible factor 1, alpha (*HIF-1α*), is activated in response to hypoxia. *HIF-2α* recognizes the same DNA consensus sequence in the hypoxia response element (HRE) in promoters of target genes as *HIF-1α*[321]. While both transcription factors recognize the same consensus sequence, they do not

Figure 15: Expression of genes shared between hypertrophy and failure.

Quantitative real time PCR analysis of HIF-2α (a, $p<0.01$ vs SuHx; b, $p<0.01$ vs normal) mRNA in normal (normal), pulmonary artery banding (PAB), hypoxic (hypoxia), and SU5416/Hypoxia (SuHx) rat right ventricles. Data were normalized to expression of 18S rRNA and are shown as mean ± s.d. (n=3).

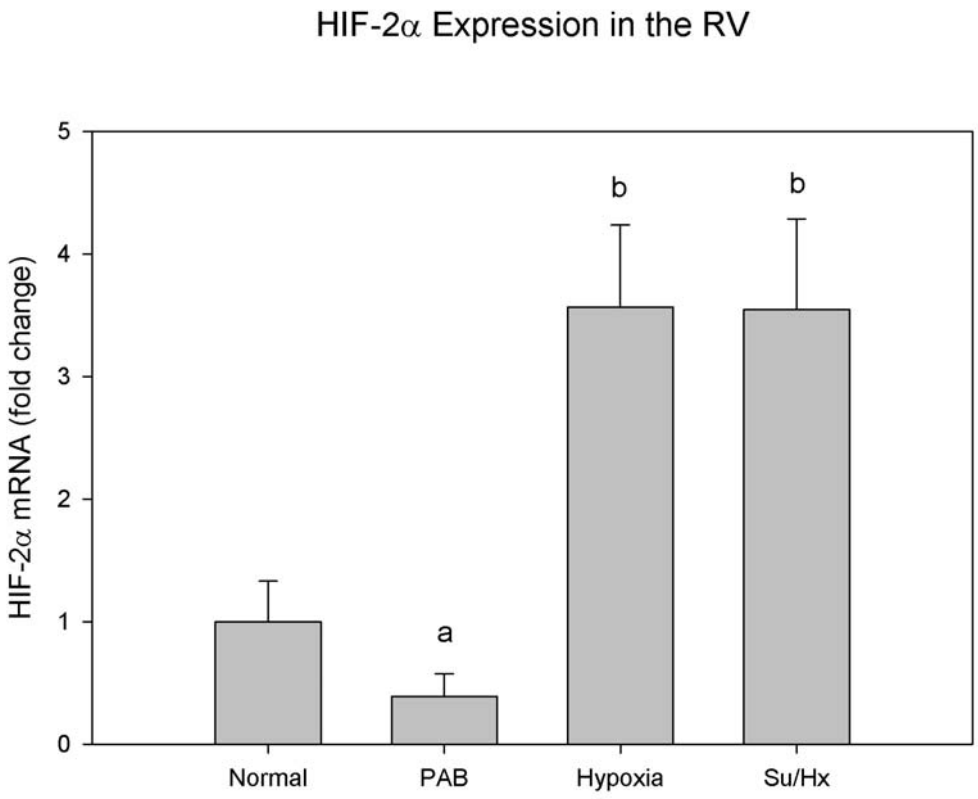
HIF-2α Expression in the RV
HIF-2α mRNA (fold change)
5
4
3
2
1
0
a
b
b
Normal
PAB
Hypoxia
Su/Hx

transactivate the same genes nor can they compensate for each other[322, 323]. *HIF-2α* is mainly expressed in endothelial cells, where it enhances transcription of endothelial-specific genes related to angiogenesis and vessel maturation, such as vascular endothelial growth factor receptors 1 and 2 (*Vegfr1* and *Vegfr2*), endothelium-specific receptor tyrosine kinase 2 (*Tie2*), and angiopoietin-1 (*Ang1*)[324-326]. In addition, *HIF-2α* maintains mitochondrial homeostasis by regulating the production of cellular factors to alleviate oxidative stress[327, 328]. The *HIF-2α* null phenotype shows increased oxidative stress because of decreased expression of genes encoding antioxidant enzymes, including *Sod2*[328]. *HIF-2α* can promote *VEGF* expression in some tumors that lack *HIF-1α* expression[329] and an activation mutant of *HIF-2α* dysregulates erythropoietin production in humans leading to PAH.[330] As shown in **Figure 15,** *HIF-2α* expression increases 3.5 fold over normal in both the hypoxia and SU5416/hypoxia RVs, suggesting that *HIF-2α* may be important for adaptive hypertrophy. While these data do not distinguish between hypertrophy and failure, they do show that the models produce the expected markers of hypertrophy and failure.

4.6 Loss of cell-growth promoting genes

Expression of growth factors, including insulin-like growth factor 1 (IGF-1), has been shown to increase in response to exercise[168-173] and overexpression of IGF-1 receptor or activated Akt leads to myocardial hypertrophy[170, 174]. In the hypoxic RV tissues, mRNA expression of *Igf1* was increased 3-fold compared to normal; however, *Igf1* was not increased in the SU5416/hypoxia RV compared to normal (**Figure 16**).

Figure 16: Expression of cell-growth promoting genes

Quantitative real time PCR analysis of a) IGF-1 (a, $p<0.05$ vs normal; b, $p<0.01$ vs SuHx) and b) KLF-5 (a, $p<0.01$ vs normal; b, $p<0.01$ vs SuHx; c, $p<0.05$ vs SuHx) mRNA in normal (normal), pulmonary artery banding (PAB), hypoxic (hypoxia), and SU5416/Hypoxia (SuHx) rat right ventricles. Data were normalized to expression of 18S rRNA and are shown as mean ± s.d. (n=3). c) Western blot for expression of IGF-1 from these normal, hypoxia, and SU5416/hypoxia. d) Densitometry was performed using Quantity One 1-D Analysis software (Bio-Rad) for normalized IGF-1 (a, $p<0.001$ vs Hx)

a

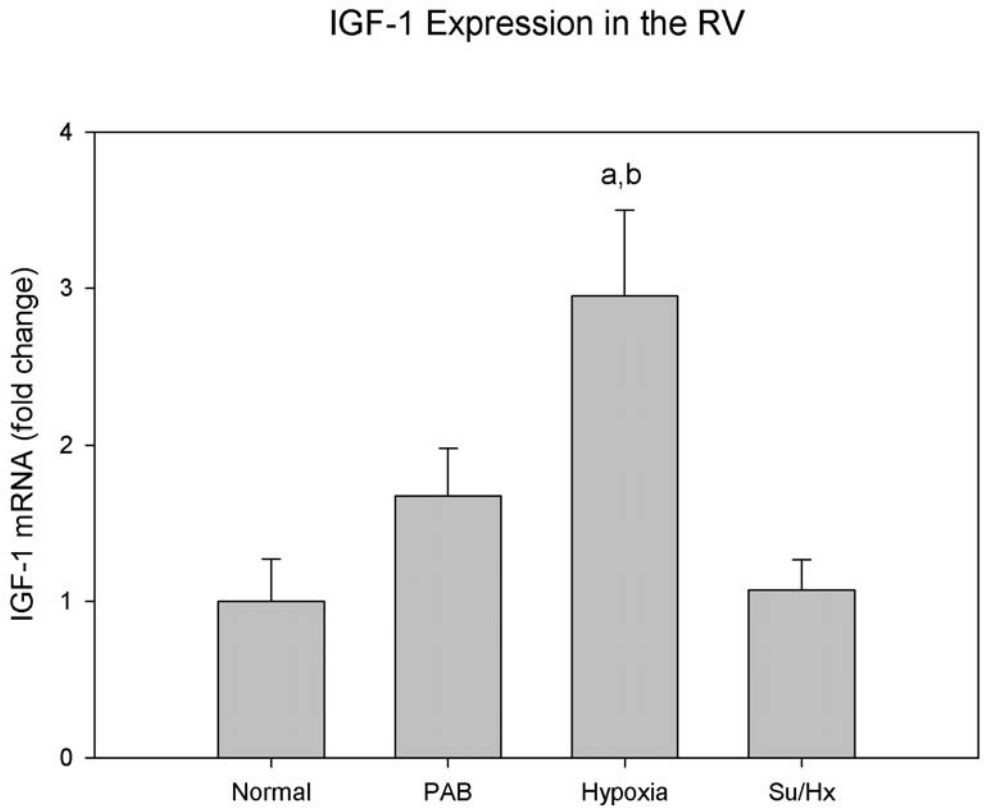
IGF-1 Expression in the RV
IGF-1 mRNA (fold change)
0
1
2
3
4
a,b
Normal
PAB
Hypoxia
Su/Hx

b

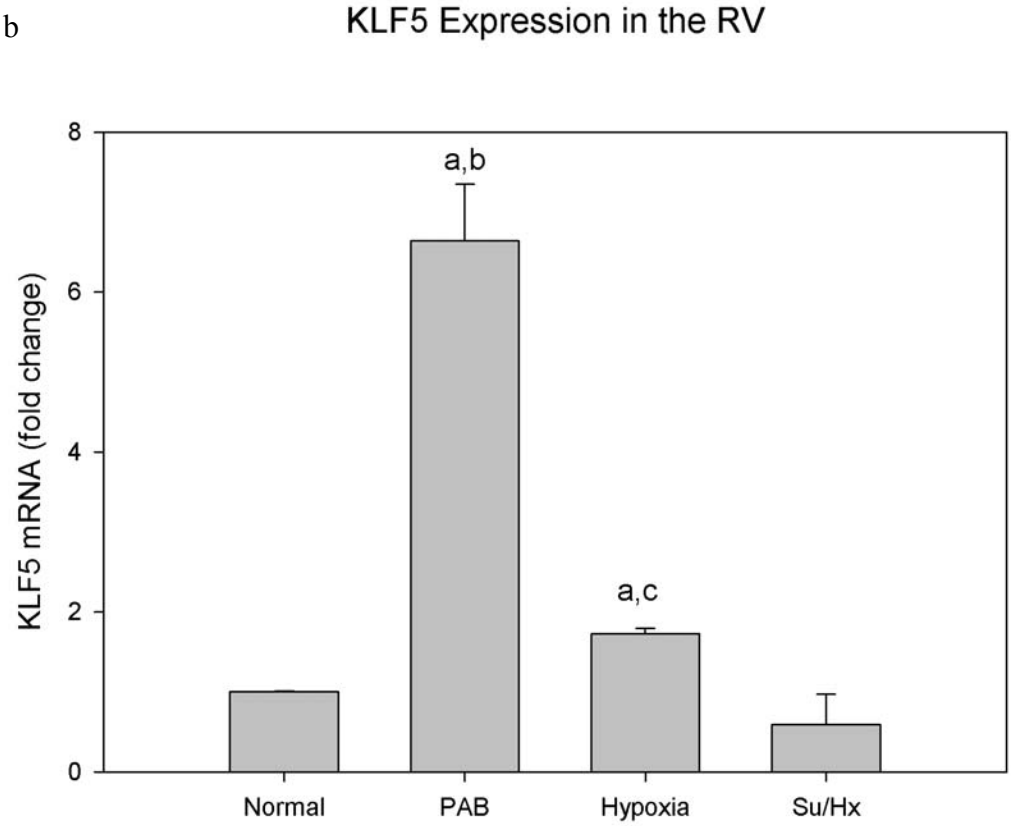
KLF5 Expression in the RV
KLF5 mRNA (fold change)
0
2
4
6
8
a,b
a,c
Normal
PAB
Hypoxia
Su/Hx

c

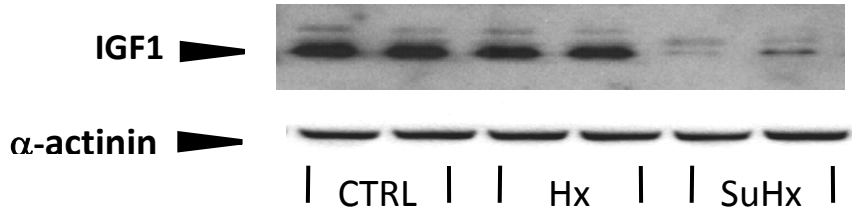
IGF1
α-actinin
CTRL
Hx
SuHx

d

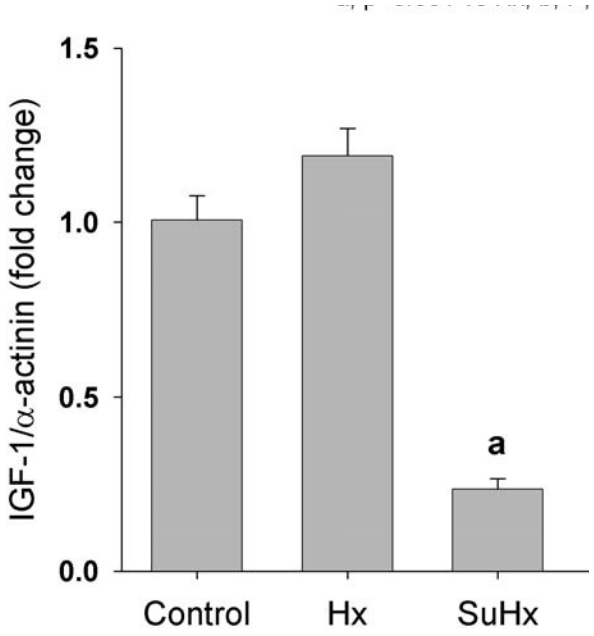
IGF-1/α-actinin (fold change)
1.5
1.0
0.5
0.0
a
Control
Hx
SuHx

Importantly, the expression of IGF-1 protein was decreased in the SU5416/hypoxia RV in comparison to the normal and hypoxic RV. Kruppel-like factor 5 (*Klf5*) has been identified as a factor that transactivates IGF-1 in cardiac fibroblasts; the secreted protein stimulates cardiomyocyte growth[244] and controls cell differentiation and apoptosis[245]. *Klf5* expression also increased in the hypoxic RV (2 fold increase over normal), but not in the failing (SuHx) RV. Together, these results suggest that in the failing RV cell growth is impaired.

4.7 Impairment of angiogenic capillary maintenance

HIF-1α also plays a role in the development of cardiac hypertrophy[331]. In addition, capillary rarefaction, the loss of capillaries, occurs in the failing RV[180]. While the expression of *HIF-1α* mRNA did not differ between RV hypertrophy and RV failure[180], downstream signaling molecules transcribed by *HIF-1α* were affected in the failing RV in comparison to the hypertrophied RV. *VEGF*[320], *Ang1*, and *apelin* expression were reduced in the SU5416/hypoxia RV compared to the hypoxic RV tissue (**Figure 17**). Similarly, apelin protein levels were also decreased in the SU5416/hypoxia RV when compared to the hypoxia RV (**Figure 17**). Reduced *apelin* expression can impair capillary growth and maintenance[332], which is consistent with the results seen in the failing RV. The combined effect of reduced expression of *VEGF*, *Ang1*, and *apelin* is that of a loss of capillary vessels and reduced angiogenesis. Whereas *HIF-1α* gene expression cannot explain the decreased angiogenesis factor gene and protein expression, *HIF-1α* protein stability may account for the impaired angiogenesis profile.

Figure 17: Expression of angiogenic capillary maintenance genes

Quantitative real time PCR analysis of a) Angiopoietin-1 (a, $p<0.05$ vs normal; b, $p<0.05$ vs SuHx) and b) apelin (a, $p<0.01$ vs normal; b, $p<0.01$ vs SuHx) mRNA in normal (normal), hypoxic (hypoxia), pulmonary artery banded (PAB), and SU5416/hypoxia (SuHx) rat right ventricles. Data were normalized to expression of 18S rRNA and are shown as mean ± s.d. (n=3). c) Representative Western blots for expression of angiopoietin-1, apelin and α-actinin from these groups. Densitometry was performed using Quantity One 1-D Analysis software (Bio-Rad) for normalized d) Ang1 (no significant difference) and e) apelin (a, $p<0.005$ vs control; b, $p<0.001$ vs Hx).

a

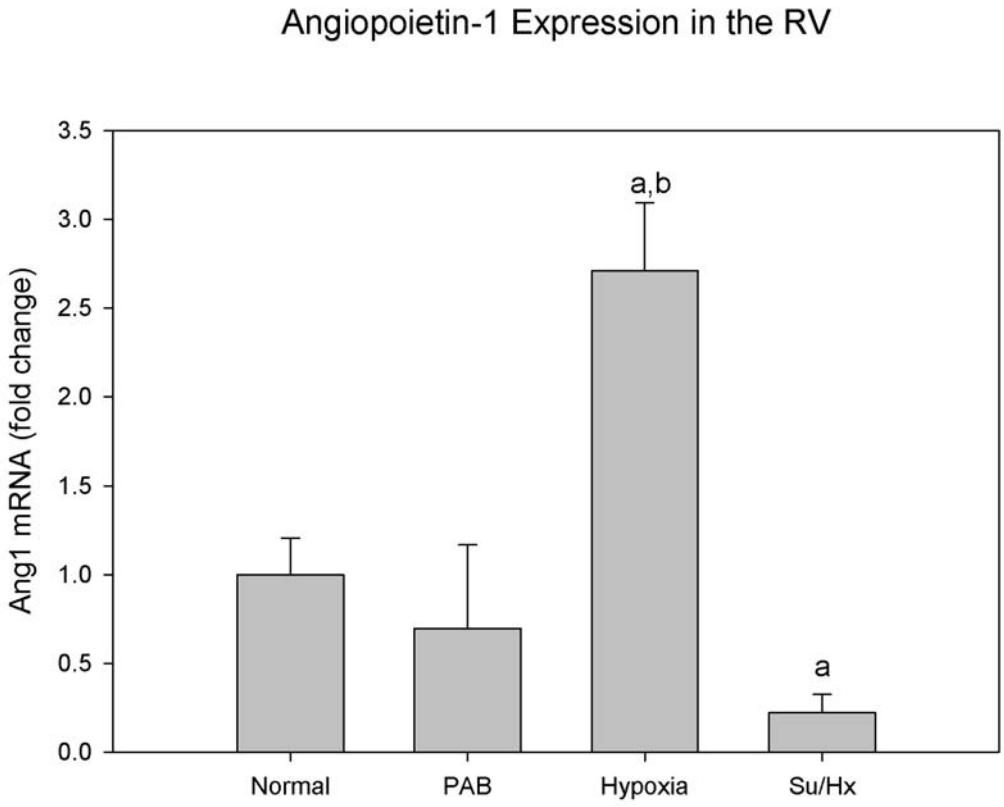
Angiopoietin-1 Expression in the RV
Ang1 mRNA (fold change)
3.5
3.0
2.5
2.0
1.5
1.0
0.5
0.0
a,b
a
Normal
PAB
Hypoxia
Su/Hx

b

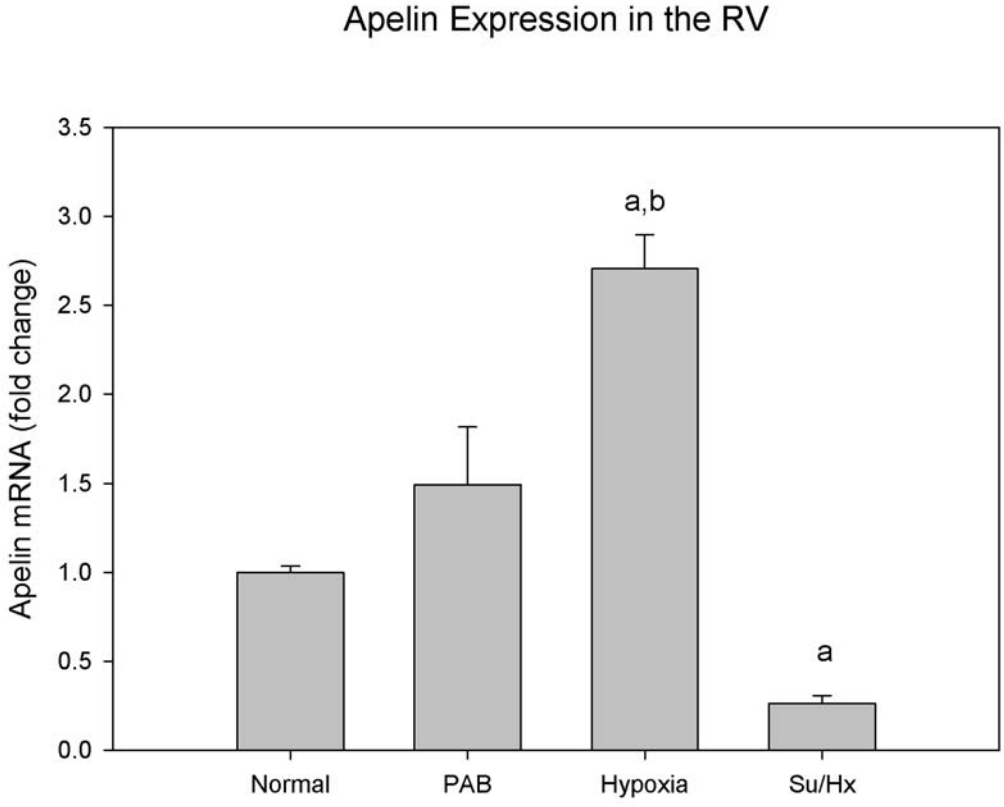
Apelin Expression in the RV
Apelin mRNA (fold change)
3.5
3.0
2.5
2.0
1.5
1.0
0.5
0.0
a,b
a
Normal
PAB
Hypoxia
Su/Hx

c

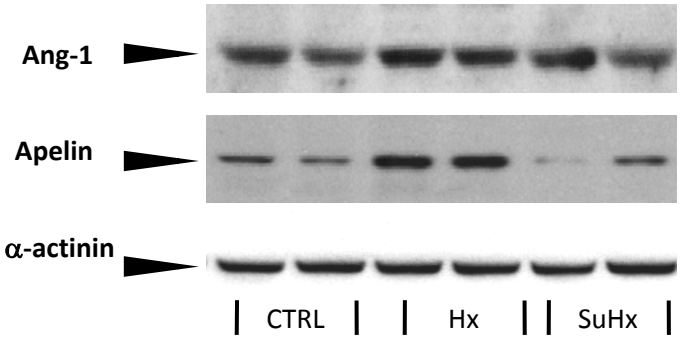
Ang-1
Apelin
α-actinin
CTRL
Hx
SuHx

d

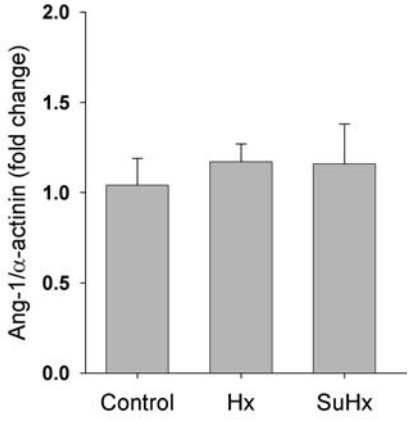
Ang-1/α-actinin (fold change)
2.0
1.5
1.0
0.5
0.0
Control
Hx
SuHx

e

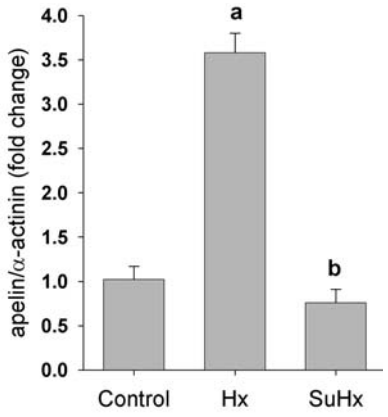
apelin/α-actinin (fold change)
4.0
3.5
3.0
2.5
2.0
1.5
1.0
0.5
0.0
a
b
Control
Hx
SuHx

4.8 Cytoskeletal rearrangement

CTGF is an extracellular matrix-secreted protein that is induced by TGF-β[333, 334]. Increased levels of CTGF are associated with cardiac fibrosis in a mouse model of cardiomyopathy[335]. CTGF can cause hypertrophy in cardiomyocytes and induce apoptosis via an activated caspase-3 pathway[336]. Induction of CTGF may be important in an initial beneficial adaptive response to cardiac stress; however, long-term activation of CTGF leads to dilation of ventricles and loss of cardiomyocytes[337]. As shown in **Figure 18**, expression of *Ctgf* increases 19-fold over normal in the hypoxic RV and then further increases in the SU5416/hypoxia RV – 46 fold over normal – consistent with the theory that CTGF can have both a beneficial and detrimental role in the RV. Adducin 3 (*Add3*) encodes the γ subunit of the adducin protein, a heterodimeric cytoskeletal protein[338, 339]. Mutations in Adducin 1, encoding the α subunit of adducin, and *Add3* have been associated with the development of hypertension[340]. Adducin has been reported to positively regulate the intercellular junction of epithelial cells[341]. Overexpression of *Add3* in cardiomyocytes blocks cell elongation and results in a more rounded structure[342]. While *Add3* is expressed in the fetal heart, it is not typically expressed in the adult heart; microRNA (miR)-143 supresses expression of *Add3*[342]. *Add3* is re-activated in the RV during development of pulmonary hypertension associated with RVF. In hypoxic RV tissues, *Add3* was increased by 8-fold over normal and increased 13-fold over normal in the SU5416/hypoxia tissues. PAB, a model of increased afterload alone, did not increase levels of *Add3* suggesting that this is an important adaptation to a hypoxic response. Expression of miR-143 in the SU5416/hypoxia RV was approximately one-half that of the normal RV (**Figure 19**).

Figure 18: Expression of cytoskeletal rearrangement genes

Quantitative real time PCR analysis of a) CTGF (a, $p<0.05$ vs normal; b, $p<0.05$ vs SuHx; c, $p<0.01$ vs normal) and b) Add3 (a, $p<0.01$ vs SuHx; b, $p<0.001$ vs normal; c, $p<0.05$ vs SuHx) mRNA in normal (normal), pulmonary artery banding (PAB), hypoxic (hypoxia), and SU5416/Hypoxia (SuHx) rat right ventricles. Data were normalized to expression of 18S rRNA and are shown as mean ± s.d. (n=3).

a

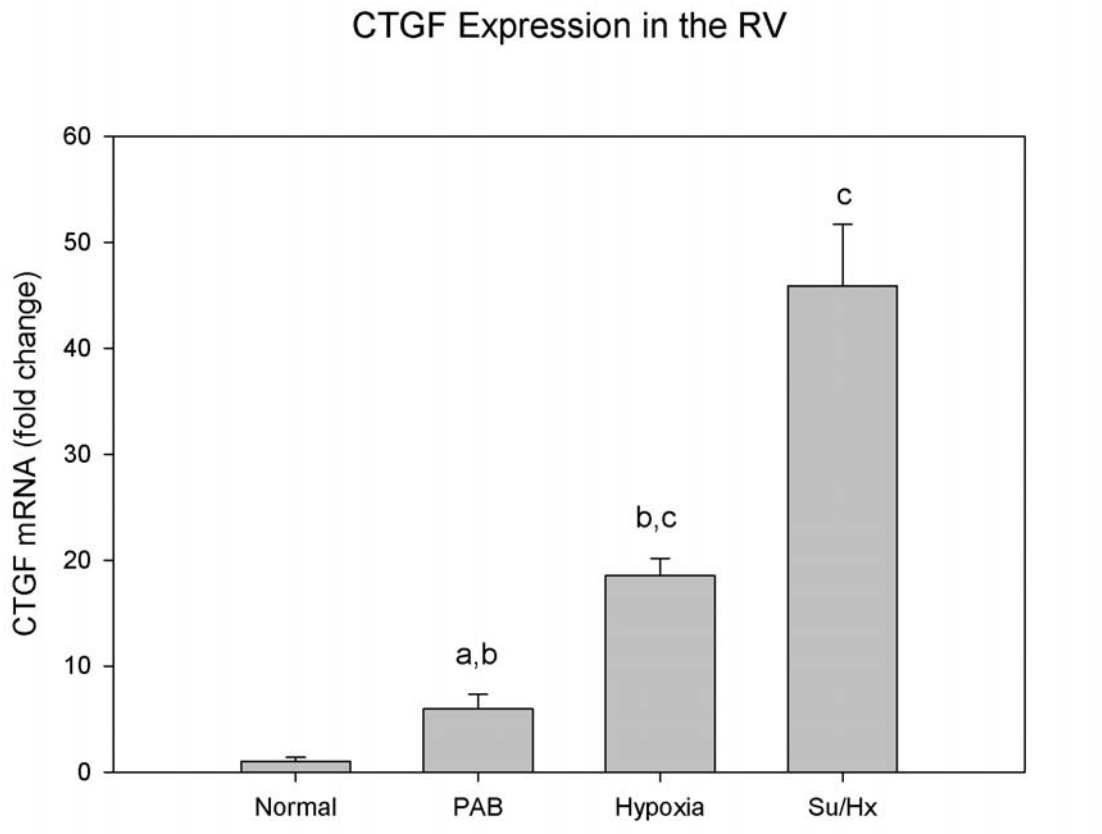
CTGF Expression in the RV
CTGF mRNA (fold change)
60
50
40
30
20
10
0
c
b,c
a,b
Normal
PAB
Hypoxia
Su/Hx

b

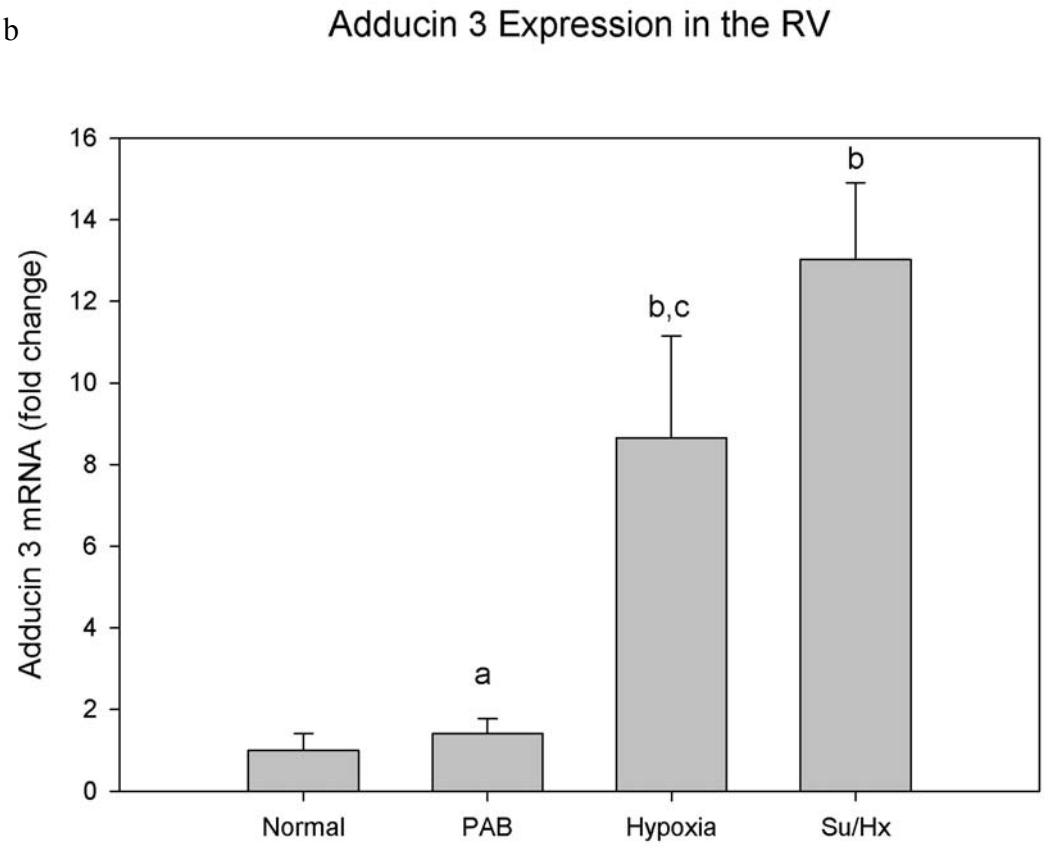
Adducin 3 Expression in the RV
Adducin 3 mRNA (fold change)
16
14
12
10
8
6
4
2
0
b
b,c
a
Normal
PAB
Hypoxia
Su/Hx

Figure 19: Expression of miR-143 expression in the RV

Quantitative real-time PCR analysis of miR-143 (a, $p<0.01$ vs control) in normal (control), hypoxic (Hx), and Sugen/hypoxia (SuHx) rat right ventricle. Data were normalized to expression of SNORA73A and are shown as mean ± s.d. (n=3).

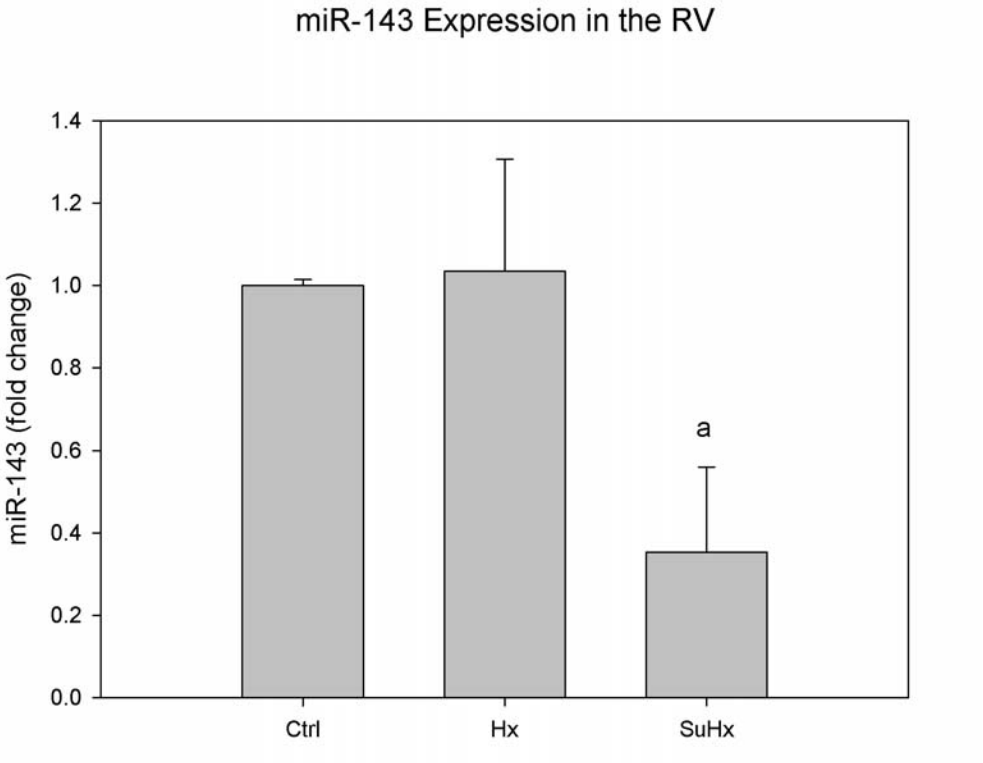
miR-143 Expression in the RV
miR-143 (fold change)
1.4
1.2
1.0
0.8
0.6
0.4
0.2
0.0
a
Ctrl
Hx
SuHx

4.9 Elevated expression of glycolytic enzymes

We used the Ingenuity Pathway Analysis program (http://www.ingenuity.com) to further explore the microarray gene expression data with respect to the pathways involved in the different response to hypertrophy and failure. Canonical pathways analysis identified the pathways from the Ingenuity Pathways Analysis library of canonical pathways that were most significant to the data set. Molecules from the dataset that had a fold-change greater than 2 between failing and hypertrophied RV were included in the analysis. The significance of the association between the data set and the canonical pathway was measured in 2 ways: 1) A ratio of the number of molecules from the data set that map to the pathway divided by the total number of molecules that map to the canonical pathway is displayed. 2) Fisher's exact test was used to calculate a p-value determining the probability that the association between the genes in the dataset and the canonical pathway is explained by chance alone. The expression pattern of the glycolysis/gluconeogensis canonical pathway had a p-value of 0.009 (**Figure 20**) and seven different genes encoding glycolytic enzymes were found to be differentially expressed (**Table 14**). Of particular interest, hexokinase 1 (*Hk1*) gene expression was five-fold greater in the SU5416/hypoxia RV compared to the hypertrophied RV, and phosphofructokinase (*Pfkb*) was increased 3-fold in expression between SU5416/hypoxia and hypoxia. In contrast, alcohol dehydrogenase 7 (*Adh7*) was decreased two-fold in the SU5416/hypoxia RV compared to hypoxia RV. Additionally, *Ucp2*, a marker of mitochondrial function, was increased 3-fold in SU5416/hypoxia RV compared to hypoxia RV supporting the concept of impaired metabolism and energy utilization.

Figure 20: Glycolysis and gluconeogenesis pathway in the failing RV

Canonical pathway analysis indentified the pathways from the Ingenuity Pathway Analysis® library of canonical pathways that were most significant to the dataset. The p-value for the glycolysis and gluconeogenesis canonical pathway is 0.00923. Genes are colored based on fold-change comparison between SU5416/hypoxia (failing) RV and hypoxia (hypertrophy) RV. Red correlates to relatively higher expression in the failing RV than the hypertrophied RV, and green correlates to relatively higher expression in the hypertrophied RV than the failing RV. Enzyme classification (EC) numbers reported by Ingenuity were converted to recommended names using the BRENDA enzyme database[343]; these names were then incorporated into the Ingenuity canonical pathway using the MyPathway® feature

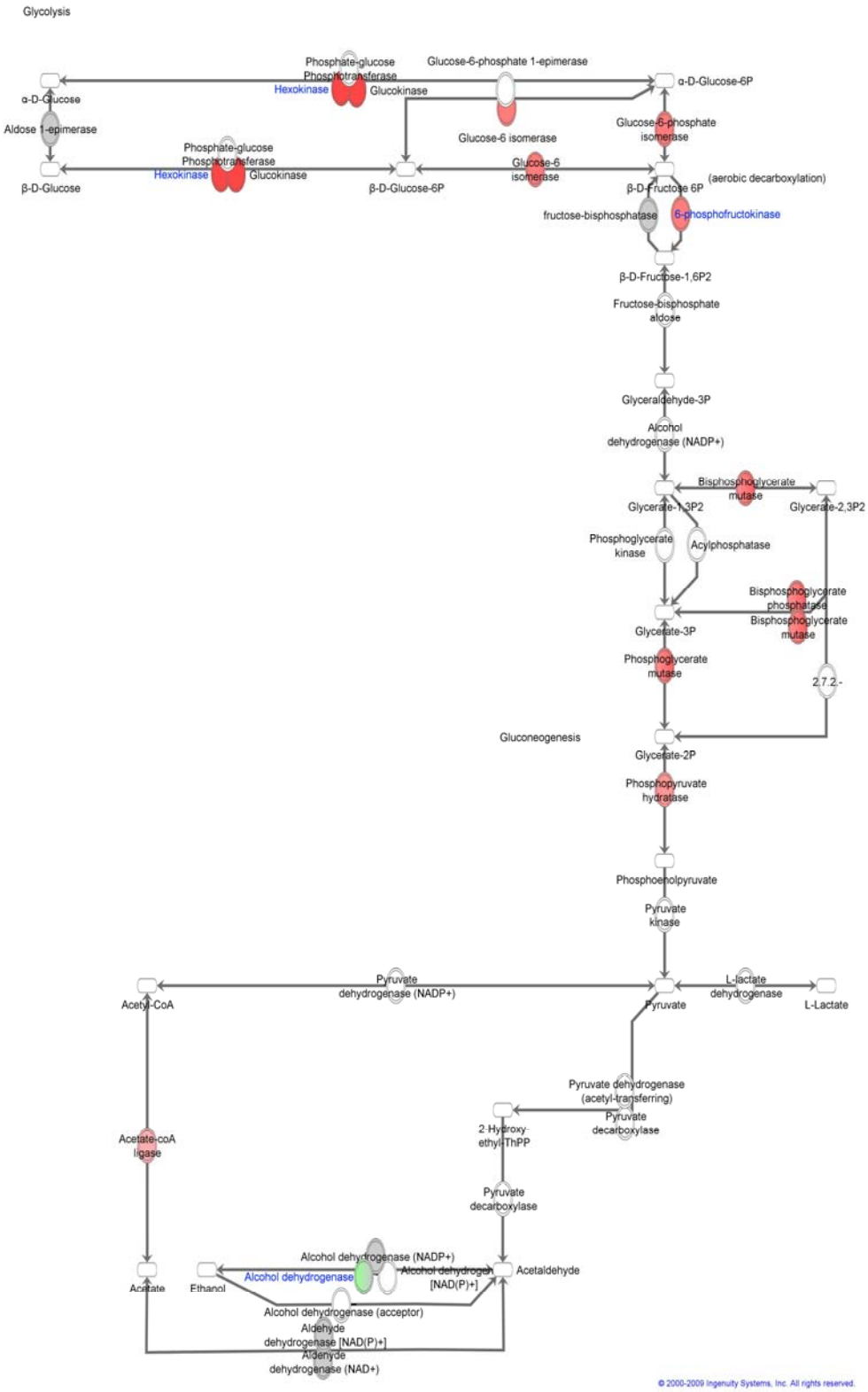
Glycolysis
Phosphate-glucose Phosphotransferase
Hexokinase
Glucokinase
Glucose-6-phosphate 1-epimerase
α-D-Glucose-6P
α-D-Glucose
Aldose 1-epimerase
Glucose-6 isomerase
Glucose-6-phosphate isomerase
β-D-Glucose
β-D-Glucose-6P
β-D-Fructose 6P
(aerobic decarboxylation)
fructose-bisphosphatase
6-phosphofructokinase
β-D-Fructose-1,6P2
Fructose-bisphosphate aldose
Glyceraldehyde-3P
Alcohol dehydrogenase (NADP+)
Bisphosphoglycerate mutase
Glycerate-1,3P2
Glycerate-2,3P2
Phosphoglycerate kinase
Acylphosphatase
Bisphosphoglycerate phosphatase
Glycerate-3P
Phosphoglycerate mutase
2,7,2,-
Gluconeogenesis
Glycerate-2P
Phosphopyruvate hydratase
Phosphoenolpyruvate
Pyruvate kinase
Pyruvate dehydrogenase (NADP+)
L-lactate dehydrogenase
Acetyl-CoA
Pyruvate
L-Lactate
Pyruvate dehydrogenase (acetyl-transferring)
Pyruvate decarboxylase
2-Hydroxy-ethyl-ThPP
Acetate-coA ligase
Pyruvate decarboxylase
Alcohol dehydrogenase (NADP+)
Alcohol dehydrogenase
Alcohol dehydrogen [NAD(P)+]
Acetaldehyde
Acetate
Ethanol
Alcohol dehydrogenase (acceptor)
Aldehyde dehydrogenase [NAD(P)+]
Aldehyde dehydrogenase (NAD+)
© 2000-2009 Ingenuity Systems, Inc. All rights reserved.

Table 14: Expression of genes encoding glycolytic enzymes

Hypertrophy fold change is given relative to the normal RV and failure fold change is given relative to the hypertrophied RV. Hexokinase 1 (Hk1) mRNA is clearly overexpressed in the failing RV when compared to the hypertrophied RV of the chronically hypoxic rats (Hx); likewise, phosphofructokinase (Pfkm) is overexpressed in the failing RV.

	FOLD CHANGE	
GENES	**HYPERTROPHY**	**FAILURE**
Adh7	3.45	1.59
HK1	-3.73	1.33
PfkB	-1.48	2.31
Ucp2	-1.25	1.86

These results are consistent with the observations that in tissues and cells from patients with PAH there is a shift from oxidative phosphorylation to glucose metabolism and glycolysis[195, 196].

4.10 Cytokine production in plasma samples

The levels of inflammatory cytokines were measured in rat serum using a multiplex ELISA kit. Patients with chronic heart failure have increased serum levels of IL-1, IL-6, and TNF-α[210]. Similarly, patients with PAH have increased serum levels of IL-8[294], IL-1β, IL-6, and TNF-α[344] in comparison to healthy controls. Treatment with an IL-1 receptor agonist reduced right ventricular hypertrophy and PH in a rat monocrotaline model of PH[345]. Mice overexpressing IL-6 develop spontaneous pulmonary vascular remodeling and PH[346], while mice overexpressing TNF-α develop right ventricular hypertrophy and severe PH[347]. Additionally, levels of VEGF are significantly higher in the serum of patients with PAH than in control patients[348]. These studies suggest that serum levels of these cytokines may be increased in the rat models of PH studied here.

In fact, levels of IL-1β, IL-10, IL-13, IL-17, TNF-α, and VEGF were increased significantly in serum samples from the SU5416/hypoxia rats when compared with normal (**Figure 21**), whereas only VEGF and IL-13 were also significantly increased in the samples from hypoxia-only rats. Levels of IL-6 were out-of-range for this assay (data not shown). The increased levels of IL-1β, TNF-α, and VEGF are consistent with

Figure 21: Expression of cytokines in rat serum from normal, hypertrophy, and failing models

Multiplex ELISA analysis of a) IL-1α, b) IL-1β, c) IL-2, d) IL-4, e) IL-5, f) IL-10, g) IL-13, h) IL-17, i) IL-18, j) TNF-α, and k) VEGF protein in normal (normal), pulmonary artery banded (PAB), hypoxic (hypoxia), and SU5416/hypoxia (SuHx) rat serum samples (a, $p<0.05$ vs normal; b, $p<0.01$ vs normal). Data are shown as mean ± s.d. (n=3).

a

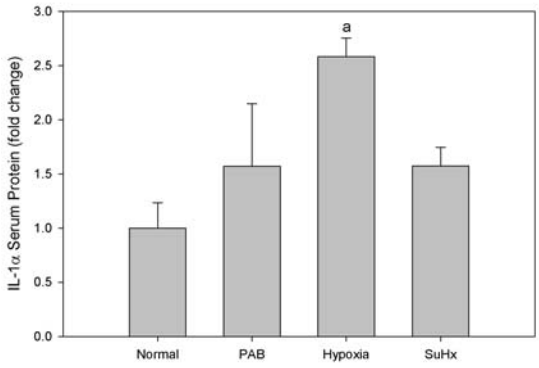
IL-1α Expression in Rat Serum
IL-1α Serum Protein (fold change)
3.0
2.5
2.0
1.5
1.0
0.5
0.0
a
Normal
PAB
Hypoxia
SuHx

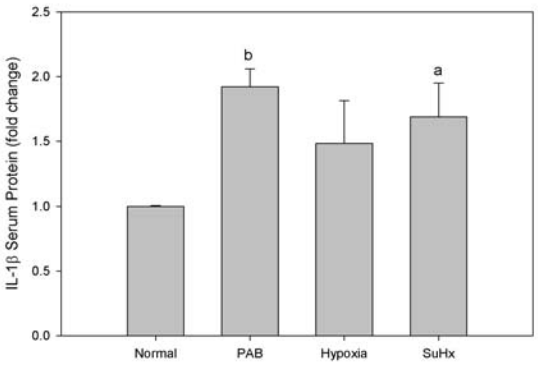
IL-1β Expression in Rat Serum
IL-1β Serum Protein (fold change)
2.5
2.0
1.5
1.0
0.5
0.0
b
a
Normal
PAB
Hypoxia
SuHx

c

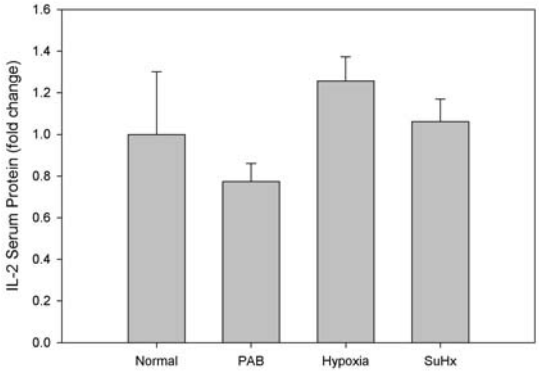
IL-2 Expression in Rat Serum
IL-2 Serum Protein (fold change)
1.6
1.4
1.2
1.0
0.8
0.6
0.4
0.2
0.0
Normal
PAB
Hypoxia
SuHx

d

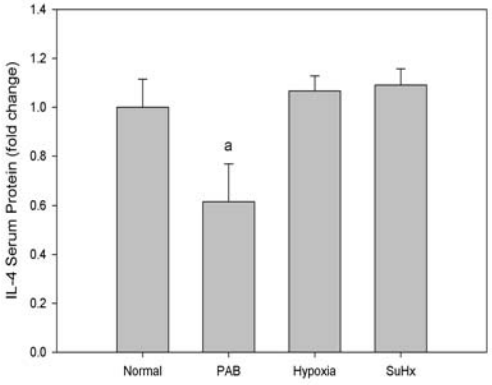
IL-4 Expression in Rat Serum
IL-4 Serum Protein (fold change)
1.4
1.2
1.0
0.8
0.6
0.4
0.2
0.0
a
Normal
PAB
Hypoxia
SuHx

e

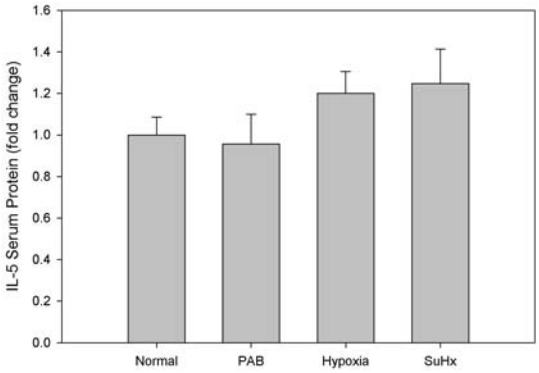
IL-5 Expression in Rat Serum
IL-5 Serum Protein (fold change)
1.6
1.4
1.2
1.0
0.8
0.6
0.4
0.2
0.0
Normal
PAB
Hypoxia
SuHx

f

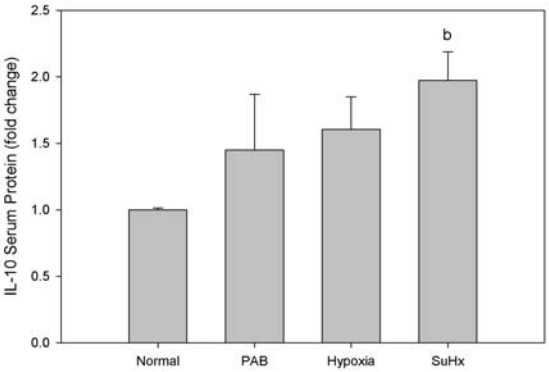
IL-10 Expression in Rat Serum
IL-10 Serum Protein (fold change)
2.5
2.0
1.5
1.0
0.5
0.0
b
Normal
PAB
Hypoxia
SuHx

g

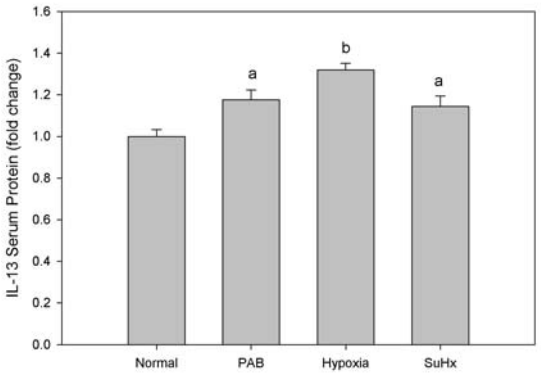
IL-13 Expression in Rat Serum
IL-13 Serum Protein (fold change)
1.6
1.4
1.2
1.0
0.8
0.6
0.4
0.2
0.0
a
b
a
Normal
PAB
Hypoxia
SuHx

h

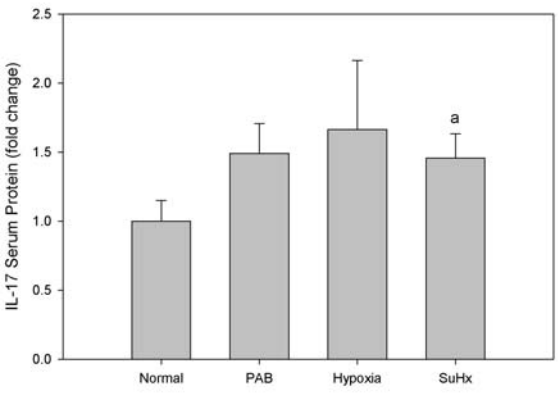
IL-17 Expression in Rat Serum
IL-17 Serum Protein (fold change)
2.5
2.0
1.5
1.0
0.5
0.0
a
Normal
PAB
Hypoxia
SuHx

i

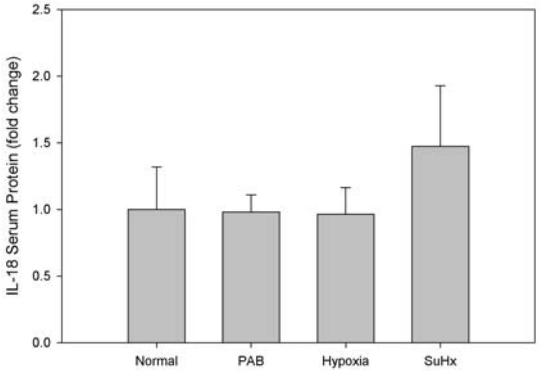
IL-18 Expression in Rat Serum
IL-18 Serum Protein (fold change)
2.5
2.0
1.5
1.0
0.5
0.0
Normal
PAB
Hypoxia
SuHx

j

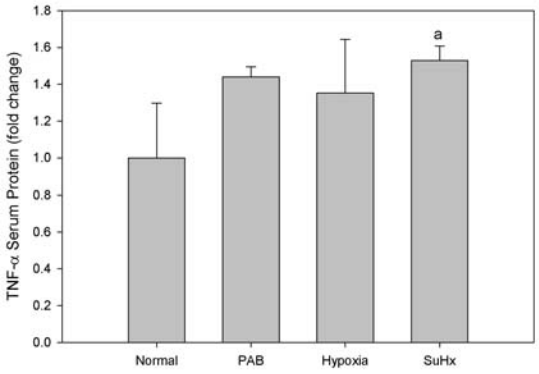
TNF-α Expression in Rat Serum
TNF-α Serum Protein (fold change)
1.8
1.6
1.4
1.2
1.0
0.8
0.6
0.4
0.2
0.0
a
Normal
PAB
Hypoxia
SuHx

k

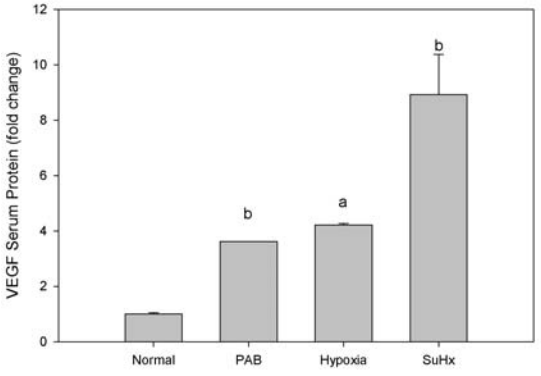
VEGF Expression in Rat Serum
VEGF Serum Protein (fold change)
12
10
8
6
4
2
0
b
b
a
Normal
PAB
Hypoxia
SuHx

reported increases in serum levels of these cytokines in PAH patients. Although levels of IL-13 and IL-17 have not been investigated in the serum of patients with PH or animal models of PH, they do have previously characterized roles. IL-13 is upregulated in schistosomiasis-induced PH[349] and dysregulation of IL-13 signaling in PAH may play a role in vascular remodeling[350]. IL-17 is increased in lung samples from PAH patients[351]. Given these results, increased levels of IL-1β, IL-13, IL-17, TNF-α, and VEGF are to be expected in serum from SU5416/hypoxia rats. However, IL-10 is an anti-inflammatory cytokine and is typically decreased in animal models of PH[349]. IL-10 expression may be a compensatory mechanism and levels in the SU5416/hypoxia serum may not be high enough to exert and anti-inflammatory effect.

4.11 Discussion

Here, we identify changes in gene expression between the normal, hypertrophied, and failing RV in an attempt to understand the mechanisms leading to RV failure associated with PAH. A major assumption underlying our experimental strategy has been that adaptive hypertrophy without failure exists. The rat PAB and chronic hypoxia models both support this concept. We induced hypertrophy in rats by exposing the animals to chronic hypoxia, and we induced right heart failure by combining chronic VEGF receptor blockade (SU5416) with chronic hypoxia[180, 283]. RV hypertrophy without failure was characterized by a normal cardiac output, while RV failure was characterized by a decrease in cardiac output and by RV dilation[180]. The gene expression pattern was analyzed by microarray analysis (**Figure 12**) and prediction analysis (**Figure 14**) to

identify genes that can distinguish between RV hypertrophy and RVF. While some signals, such as ANP, BNP, and HIF-2α, are shared between hypertrophy and failure (**Figure 15**), it is also clear from **Figure 12** that there are large differences in the overall gene expression patterns between hypertrophy and RV failure. Through use of pathway analysis tools, we can characterize these changes in terms of several categories: loss of cell-growth promoting genes, changes in energy metabolism, impairment of angiogenesis, and cytoskeletal rearrangement.

Several genes associated with cell growth are increased in expression in the hypoxic RV, but are decreased in the failing RV. Although *Igf1* has been reported to increase in cardiomyopathy[352] and in myocardial biopsies from patients with LV failure[353], *Igf1* and its transcription factor *Klf5*[244] are both decreased in the failing rat RV. *Klf5* transactivates *Igf1* in cardiac fibroblasts to activate cardiomyocte growth[244] and *Igf1* controls cell differentiation and apoptosis[245]. That *Klf5* and *Igf1* are increased in the hypertrophied RV (chronic hypoxia model), but not in the failing RV, suggests an important loss of cell-growth promoting genes, which may be maladaptive.

The changes in energy metabolism as the RV progresses from hypertrophy to failure are associated with a shift from fatty acid oxidation to glycolysis and downregulated expression of mitochondrial electron transport chain complexes. A switch from fatty acid oxidation to glycolysis has been reported in left ventricular failure (LVF) [354] and has been hypothesized to occur in the transition from RV hypertrophy to RVF[198]. The increased expression of glycolytic enzymes and the mitochondrial uncoupling protein

Ucp2[355] in the failing RV suggests energy limitation and impaired energy utilization as described in LVF[356]. An increase in glycolytic enzymes and natriuretic peptides (including ANP and BNP)[357, 358] may be "attempts of the RV" to survive and maintain contractile function. Furthermore, impairment of mitochondrial respiratory chain complexes is characteristic of damaged and dysfunctional mitochondria in failing hearts[305], mostly likely caused by increased generation of reactive oxygen species[300-303]. **Figure 13** shows the decreased expression of genes encoding mitochondrial electron transport chain complexes; this combined with an increase in the expression of genes encoding glycolytic enzymes (**Figure 20**) indicates that there are indeed drastic changes in the energy generation and ultilization in the failing RV.

Like the failing LV, the failing RV is characterized by capillary rarefaction[180], and here we show that the loss of expression of a number of angiogenic capillary maintenance. VEGF signaling is important for the maintenance of normal cardiac function[359]. *VEGF* also induces expression of anti-hypertrophy signals, including regulator of calcineurin 1 (*Rcan1*) [360]. *Apelin* is induced by *Ang1* and controls blood vessel diameter during angiogenesis[332]. Increases in *apelin* expression due to hypoxic stimuli have been linked to endothelial cell proliferation and angiogenesis[361, 362]. Additionally, increased apelin expression has been shown in the hypoxic RV[363] consistent with the results seen here. Similarly, *Ang1* promotes both cardiac myocyte survival[364] and endothelial cell survival[365]. Without expression of these genes, there is most likely an impairment of capillary growth and maintenance in the failing RV.

In addition to changes in capillary maintenance, the switch from RV hypertrophy to RVF is associated with changes in the cytoskeletal arrangement. Integrins are activated to compensate from the pressure overload in the RV and induce expression of contractile proteins[157, 158]. ILK regulates cell hypertrophy signaling[285] and RhoA, via ROCK, regulates rearrangement of the cytoskeleton[287]. In addition, *Add3*, normally only expressed in the fetal tissue, is re-expressed in the failing RV and miR-143, expressed in the normal heart to suppress expression of *Add3*[342], is turned off (**Figures 18 and 19)**. With increased expression of *Add3*, cardiomyocytes have a less elongated phenotype and hypertrophy[342], as is seen in the failing RV. Finally, CTGF is typically seen as a hypertrophy signal, but long-term signaling leads to dilation of the ventricle and loss of cardiomyocytes[338]. These changes may be initially beneficial in the hypertrophied RV, but with long-term expression of these signals, the heart undergoes changes that are maladaptive and lead to RVF.

Taken together, the data define a gene expression pattern that can robustly distinguish between adaptive RV hypertrophy and RV failure in a rat model of PAH. To thoroughly assess the clinical importance of the gene expression set, it will be necessary to confirm the expression of these genes in human heart tissue. However, this expression set also provides a basis for understanding the reversal of gene expression changes in the SU5416/hypoxia model of severe PAH using various therapeutic strategies.

Chapter 5: Reversibility of Right Ventricular Failure

5.1 Introduction

Although pulmonary arterial hypertension (PAH) is a disease originating in the lungs, most patients with PAH die from right-heart failure. The three-year mortality rate for patients with PAH ranges from 20% for patients with heart disease to 80% for patients with PAH associated with scleroderma[366]. The response of the right ventricle (RV) typically determines the outcome of the disease[8, 367]. Current treatment for PAH includes the use of vasodilators, endothelin receptor blockers, and phosphodiesterase-5 inhibitors[47, 48], but these do not specifically focus on reversing right ventricular failure (RVF).

It is known from studies of post-lung transplant PAH patients that the RV is not irreversibly damaged by enlargement and hypertrophy[368]. In the 1980s, heart-lung transplant was the surgical treatment for PAH patients[369]. However, in the early 1990s, this shifted towards lung transplant only[370]. A significant improvement in right

ventricular function occurs soon after lung transplantation – either single or double lung transplant[371-374]. Additionally, patients receiving living-donor lobar lung transplant have similar improvements within two months after transplantation[368]. After lung transplantation, the 1-, 3-, and 5-year survival rates for PAH patients have been reported as 77%, 62.6%, and 53.6%[375], with slightly higher rates for patients receiving a double-lung transplant than a single-lung transplant.[376] Three years after transplant, 89.6% of patients report no activity limitations[377]. These findings show that the right ventricular failure (RVF) associated with PAH is reversible and motivates the search for a non-surgical intervention that can reverse RVF.

β-adrenergic receptor blockers are often used in the treatment of patients with left ventricular failure[378]. The β-adrenergic receptors are G-protein coupled receptors that activate c-AMP mediated protein kinase A[379, 380]. Long-term activation of the receptor leads to maladaptive cardiac remodeling and receptor down-regulation[381, 382]. However, β-adrenergic receptors can also recruit β-arrestins to initiate a second wave of signaling that is independent of the G-protein signaling pathway[383, 384] and promote mitogenic and anti-apoptotic effects[385, 386]. Signaling through β-arrestins also transactivates epidermal growth factor receptor (EGFR) to promote cardioprotective signals in response to mechanical stress[387].

The effects of β-blockers in left heart failure include: improved ventricular remodeling, preserved cardiac contractility, reduced oxidative stress, and reduced cardiac expression of proinflammatory cytokines[388, 389]. However, β-adrenergic receptor blockers are

not currently used as a treatment for PAH. Reasons for this could be the potentially detrimental effects on hemodynamics and exercise capacity. PAH patients increase cardiac output through increased heart rate because they have a decreased stroke volume and contractility problems prevent its increase[390]. A small group of patients with PAH due to portopulmonary hypertension was treated with propanalol, a non-specific β-adrenergic receptor blocker, or atenolol, a β_1-adrenergic receptor agonist. Upon withdrawal of the adrenergic receptor blockers, patients had an improved exercise capacity[391] leading researchers to conclude that the adrenergic receptor blockers were not beneficial to the patients. However, this study was limited due to small size – 10 patients – and propanalol or atenalol are presently not used to treat left ventricular failure.

Carvedilol, an $\alpha_1/\beta_1/\beta_2$-adrenergic receptor blocker that also has anti-oxidant properties[392], has been used to treat left-heart failure and to treat an animal model of PAH[360]. In post-myocardial infarction (MI) studies of the left ventricle, carvedilol treatment is associated with improved ventricular function, reduced left ventricular dilation, and there is improved survival in post-MI patients[393, 394]. Similarly, treatment with carvedilol of patients with chronic heart failure caused by ischemia has also improved survival when given in combination with conventional heart failure treatments[393, 395].

In animal studies of carvedilol treatment in the Su5416/hypoxia model of pulmonary hypertension, carvedilol had no effect on pulmonary vascular remodeling[360] and did not change the number of occluded small pulmonary vessels[277], but did have effects in

the heart. While the amount of pressure overload was the same in both Su5416/hypoxia rats and Su5416/hypoxia rats treated with carvedilol, those that were given carvedilol treatment had decreased cardiac hypertrophy[360]. In addition, carvedilol treatment was associated with increased cardiac output, decreased RV dilation, increased stroke volume, decreased cardiomyocyte death, and decreased fibrosis[360]. Clinically, the SU5416/hypoxia + carvedilol rats have increased exercise capactity and increased survival when compared with the SU5416/hypoxia animals[360], suggesting that carvedilol treatment benefits the heart and reduces PAH symptoms. A decrease in fibrosis was also reported with carvedilol treatment of pressure overload in the LV[396, 397]. While some changes in gene expression have been reported in carvedilol-treated rats[360], a systematic study of the gene expression changes in the heart as a consequence of carvedilol treatment does not exist.

Rationale: We have previously demonstrated the changes in gene expression associated with the development of right ventricular failure caused by PAH. We hypothesize that right heart failure is reversible and that treatment of the failing RV with carvedilol will show a different gene expression profile than a non-treated failing RV. Using microarray technology, quantitative real-time polymerase chain reaction (qRT-PCR), and multiplex enzyme-linked immunosorbent assays (ELISAs), we characterized the changes in gene expression due to the carvedilol treatment and reversal of RVF.

5.2 Physiological and gene expression changes with carvedilol treatment

We first investigated the effects of carvedilol treatment on normal (control) rats. There was no change in body weight in the carvedilol-treatment animals, and there was no significant difference in the Fulton index (RV/LV + S) between normal and carvedilol-treated animals (**Figure 22**). As previously reported by Bogaard *et al*., carvedilol treatment of normal rats had no effect on the resting hemodynamics of the heart, with the exception of a small change in heart rate[360].

We then examined the changes in gene expression in the RV of the carvedilol-treated animals in comparison to normal animals using quantitative real-time polymerase chain reaction (qRT-PCR). Genes were selected based on their inclusion in previous analyses in Chapter 4 (**Figure 23**). Although there was no significant difference in expression between normal and carvedilol-treated animals for the genes natriuretic peptide precursor A (*Nppa*, mRNA for the atrial natriuretic peptide [ANP]); natriuretic peptide precursor B (*Nppb*, mRNA for brain natriuretic peptide [BNP]); and connective tissue growth factor (*Ctgf*), there was a significant difference ($p<0.05$) for the remaining genes analyzed. As previously discussed, insulin-like growth factor 1 (*Igf1*) and kruppel like factor 5 (*Klf5*) serve to promote cell growth in the heart; *Igf1* expression was increased 2.8-fold and *Klf5* was increased almost 9-fold in the carvedilol treated control RV compared to the untreated normal RV. Hypoxia-inducible factor 1α (*HIF-1α*), hypoxia-inducible factor 2α (*HIF-2α*), vascular endothelial growth factor (*VEGF*), angiopoietin 1 (*Ang1*) and apelin are angiogenic and can increase capillary density in the heart. Both

Figure 22: Body Weight and Fulton Index of Animal Models Used in Study

a) Body weight in grams and b) Fulton index (RV/LV+S) (a, $p<0.05$ vs normal) of normal (control), SU5416 (SU5416) treated, hypoxia (hypoxia) treated, SU5416/hypoxia (SuHx) treated, carvedilol (carvedilol) treated, and SU5416/hypoxia + carvedilol (SuHx + carv) treated rats. Data are shown as mean mean ± s.d. (n=6).

a

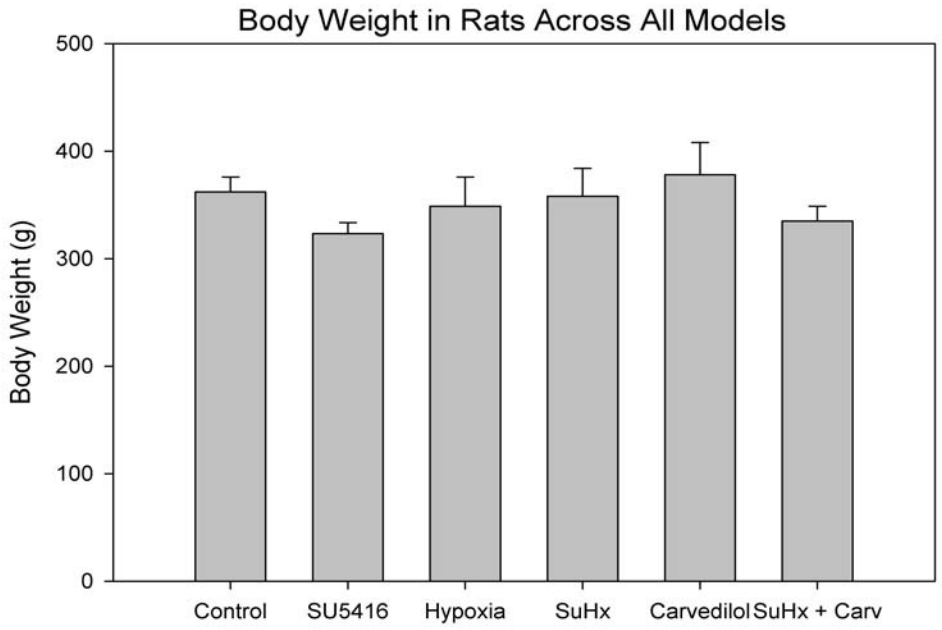
Body Weight in Rats Across All Models
Body Weight (g)
500
400
300
200
100
0
Control
SU5416
Hypoxia
SuHx
Carvedilol
SuHx + Carv

b

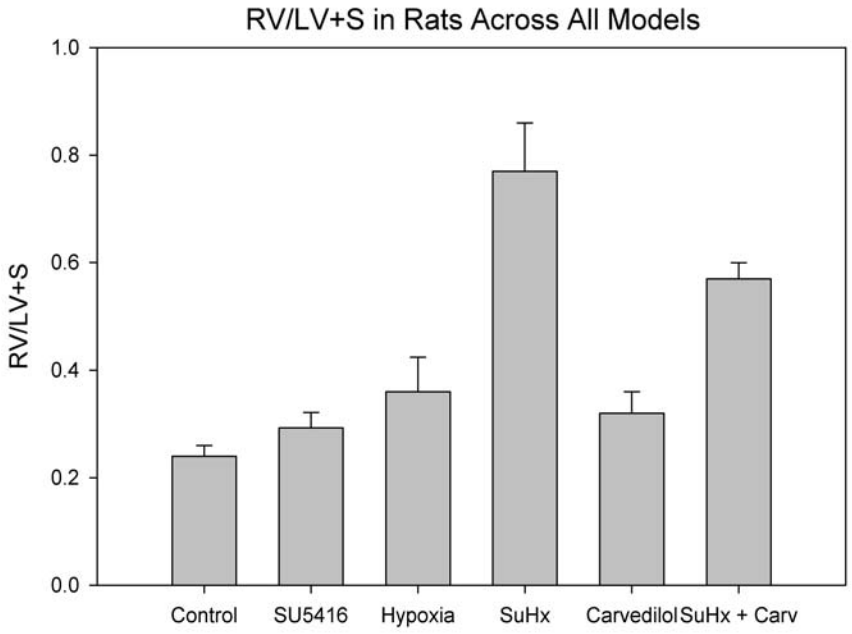
RV/LV+S in Rats Across All Models
RV/LV+S
1.0
0.8
0.6
0.4
0.2
0.0
Control
SU5416
Hypoxia
SuHx
Carvedilol
SuHx + Carv

Figure 23: Effects of Carvedilol on Gene Expression in the Normal Right Ventricle

Quantitative real-time PCR analysis of Add3, Ang1, ANP, Apelin, BNP, CTGF, HIF-1α, HIF-2α, IGF-1, KLF5, MHC-α, MHC-β, and VEGF mRNA in normal and carvedilol rat right ventricles (a, $p<0.05$ vs normal; b, $p<0.01$ vs normal; c, $p<0.005$ vs normal). Data were normalized to expression of 18S rRNA and are shown as mean ± s.d. (n=3).

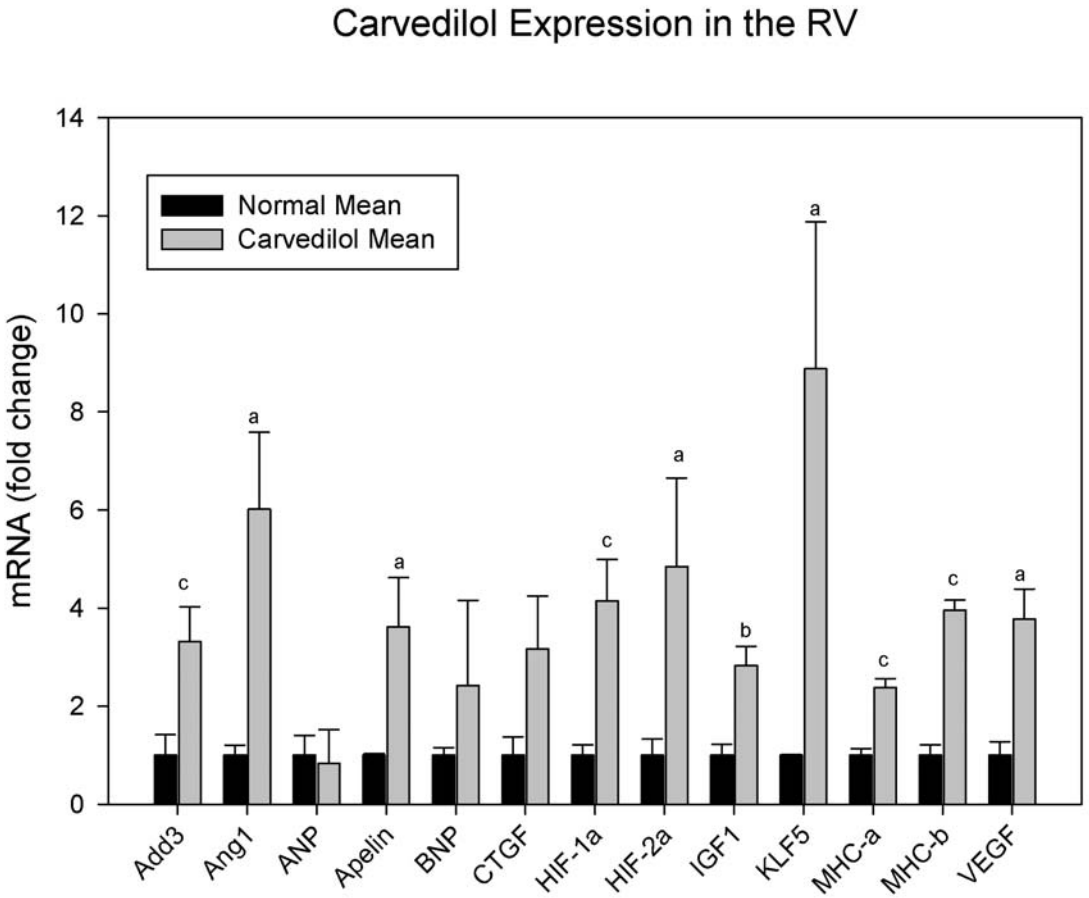
Carvedilol Expression in the RV
Normal Mean
Carvedilol Mean
mRNA (fold change)
0
2
4
6
8
10
12
14
c
a
a
a
c
b
a
c
c
a
Add3
Ang1
ANP
Apelin
BNP
CTGF
HIF-1a
HIF-2a
IGF1
KLF5
MHC-a
MHC-b
VEGF

HIF-1α and *HIF-2α* were increased by over 4-fold in the carvedilol-treated RV compared to the normal RV, VEGF and apelin increased by approximately 3.5-fold, and *Ang1* increased by 6-fold. Adducin 3 (*Add3*), myosin heavy chain alpha (*MHC-α*), and myosin heavy chain beta (*MHC-β*) all function in cytoskeletal rearrangement. *Add3*, *MHC-α*, and *MHC-β* were increased by 3.3-, 2.5-, and 4-fold respectively in the carvedilol-treated RV compared to the normal RV.

5.3 Microarray analysis

In order to identify differences in gene expression that occur during right ventricular failure associated with PAH, we used a microarray analysis similar to that employed in the comparison between the normal RV and normal LV and the models of adaptive hypertrophy and RVF. Again, this was a "Type II" approach in which each hybridization was between RNA from an animal model and a pool of commercially available reference RNA. Total RNA was isolated from RV tissue from animals subjected to the SU5416/hypoxia protocol for four weeks, then treated with carvedilol for four weeks. Because the SU5416/hypoxia RVs from previous studies in Chapter 4 were hybridized against the same pool of reference RNA, they can be used again in this analysis.

Total RNA was isolated from the free wall of the RV from rats treated with a combination of SU5416 and chronic hypoxia for four weeks to establish RVF. The animals were then treated with carvedilol for four weeks[360]. RNA was first converted

to cDNA and fluorescently labeled with either Cyanine-3 (green) or Cyanine-5 (red) dye and then the two samples were mixed together for overnight hybridization. Six biological replicates per condition were hybridized to an Agilent Rat Whole Genome 4 x 44k microarray chip. Microarrays were washed and scanned with an Axon GenePix 4200A Scanner and GenePix Pro 5.0 Software. All data were uploaded into the Ramhorn Array Database (http://ramhorn.csbc.vcu.edu). Microarray data were retrieved from the Ramhorn Array Database if they had a signal greater than or equal to 1.5 fold above background for both the red and green channels. A gene was called "good" if greater than 50% of arrays for each condition (SU5416/hypoxia and SU5416/hypoxia + carvedilol) passed the filtering conditions of expression greater than or equal to 1.5 fold above the background expression. Technical replicates were averaged together.

To determine which genes had a statistically significant difference in their expression between the SU5416/hypoxia (failing) RV and the SU5416/hypoxia treated for four weeks with carvedilol (treated) RV, we used the Significance Analysis of Microarrays (SAM) algorithm[219] to perform a two-class unpaired analysis with 1,000 permutations of replicate data. To control for the False Discovery Rate (FDR), the lowest delta value resulting in a median FDR of 5% or less was chosen. For this analysis, a delta value of 0.645 was selected corresponding to an FDR of 4.59%. This results in reporting of genes with q-values < 0.05. Of the genes passing initial filtering conditions, 4,714 were identified as significantly different in expression. The Stanford Unique Indentifiers representing significantly regulated genes were compiled and data for the following conditions: normal RV, SU5416/Hypoxia RV, and SU5416/hypoxia + carvedilol RV

were retrieved from the Ramhorn Array Database. The replicates for each condition were averaged and transformed by subtracting the average expression of the normal RV from each condition. This gives the expression in each experimental condition relative to the normal RV and allows us to visualize the change in expression resulting from the treatment. The Cluster 3.0 program[220] was used to perform average-linkage hierarchichal clustering by gene of the whole dataset, and clustered data was exported to the Java TreeView program[221] for visualization.

The resulting cluster shown in **Figure 24** is comprised of the 4,714 genes called significant by SAM between the SU5416/hypoxia RV and the SU5416/hypoxia + carvedilol RV. The major columns from left to right are: normal RV, SU5416/Hypoxia RV, SU5416/hypoxia + carvedilol RV and the difference in SU5416/Hypoxia RV + carvedilol and SU5416/hypoxia RV (shown to the right of the grey line). This final column allows us to focus in on the genes that are changing in the attempt to reverse right heart failure due to carvedilol treatment. The subclusters seen in the figure are based on the Pearson correlation coefficient for similarity of genes in that cluster. Using a threshold correlation value of 0.8 generates the four smaller clusters seen in **Figure 24**.

Subcluster 1 is comprised of genes that have increased expression in the SU5416/hypoxia and the SU5416/hypoxia + carvedilol RV and could represent a pattern of expression associated with increased hypertrophy in the heart. The top five canonical pathways for genes in this cluster are listed in **Table 15**. Of these, the hepatic fibrosis and hepatic stellate cell activation pathway stood out because fibrosis is known to increase in

Figure 24: Microarray Cluster

Six biological replicates per condition were hybridized to Agilent Whole Rat Genome microarrays. Failing RV (samples labeled "SuHx") is obtained by treating rats with a combination of SU5416 and chronic hypoxia. Carvedilol treatment given after a combination of SU5416 and chronic hypoxia (samples labeled "SuHx + Carv) is an attempt to reverse right heart failure. Genes to the right of the grey line (column labeled "-") show the difference in expression between the average SuHx + carvedilol RV and the average SuHx RV. The small columns represent different animals treated with the same condition. Each row represents a gene called significant by the SAM algorithm. Green indicates lower expression in a given condition than in the normal RV, red indicates higher expression in a condition than in the normal RV. Black indicates that the expression in the condition is equal to expression in the normal RV.

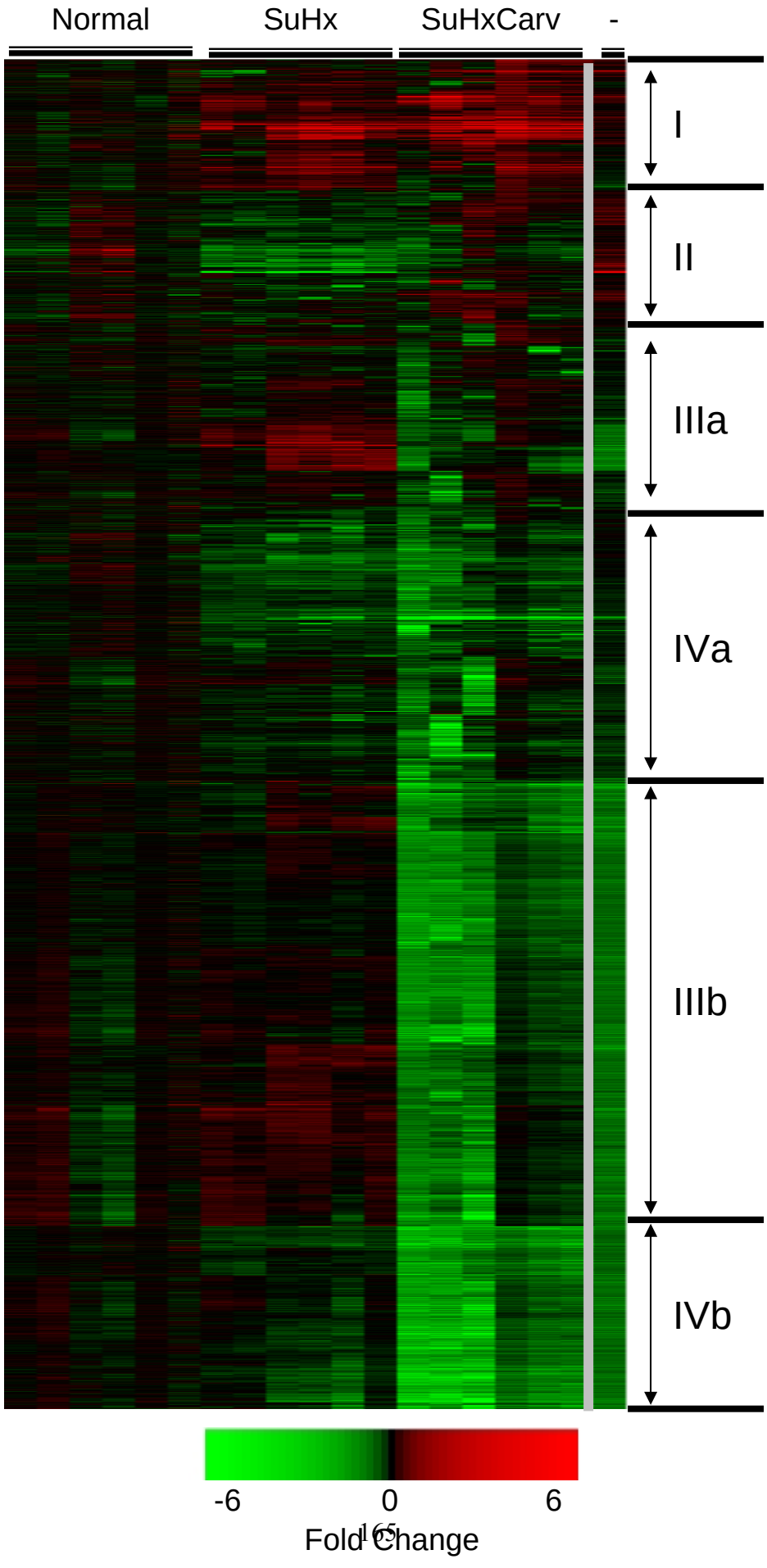
Normal
SuHx
SuHxCarv
-
I
II
IIIa
IVa
IIIb
IVb
-6
0
6
Fold Change

Table 15: Top Five Canonical Pathways of Genes in Subcluster 1

Pathway Name	**p-value**
Hepatic Fibrosis/Hepatic Stellate Cell Activation	6.01×10^{-8}
Calcium Signaling	1.09×10^{-5}
ILK Signaling	2.40×10^{-5}
VEGF Signaling	1.13×10^{-4}
Actin Cytoskeleton Signaling	1.13×10^{-4}

PAH and in the SU5416/hypoxia model of PAH[291-293]. In the microarray data set, expression of transforming growth factor alpha (*TGF-α*) was increased 1.5-fold in the SU5416/hypoxia RV compared to the normal RV and 3-fold in the SU5416/hypoxia + carvedilol RV compared to the normal RV. Similarly, transforming growth factor beta 2 (*TGF-β2*) was increased 3-fold and 2.5-fold, respectively, in the SU5416/hypoxia RV and SU5416/hypoxia + carvedilol RV compared to the normal RV. In addition, another of the pathways – Integrin-like kinase (ILK) signaling – has been implicated as a regulator of hypertrophic signaling pathways because cardiac-specific expression of ILK has been shown to induce hypertrophy[285]. ILK expression is highest in the heart and is essential for mediating repair, growth, and contractility in the heart[284]. Actin cytoskeleton rearrangement is mediated by rho-kinase (ROCK), a downstream mediator of *RhoA*[286]. Levels of ROCK have been reported to increase in expression during pressure overload-induced hypertrophy[288]. Deletion of *Rock1* is assocated with reduced fibrosis, apoptosis, and chamber dilation in the heart[287]. *RhoA* was increased 1.02-fold in the SU5416/hypoxia RV and 1.25-fold in the SU5416/hypoxia + carvedilol RV compared to normal. Additionally, two actin molecules also showed increased expression: cardiac alpha actin 1 (*Actc1*) was increased 1.1-fold in the SU5416/hypoxia RV and 2-fold in the SU5416/hypoxia + carvedilol RV compared to normal and alpha actinin 2 (*Actn2*) was increased 1.8-fold in the SU5416/hypoxia RV and 2.1-fold in the SU5416/hypoxia + carvedilol RV compared to normal. Overall, genes in this cluster have increased levels of expression in the SU5416/hypoxia and SU5416/hypoxia + carvedilol RVs (**Figure 24, subcluster 2**) suggesting that these pathways are a mechanism of compensation for stress in the right ventricle.

Subcluster 2 is made up of genes that might be characterized as having a "reversal of failure" expression pattern; these genes have increased expression in the carvedilol-treated SU5416/hypoxia RV when compared with the SU5416/hypoxia RV. The top five canonical pathways for these genes are listed in **Table 16.** Of particular interest are the oxidative phosphorylation and mitochondrial dysfunction pathways. The failing RV is known to be associated with a shift in energy metabolism towards glucose oxidation and away from fatty acid oxidation in clinical and experimental studies[307-312]. In addition, mitochondrial biogenesis is downregulated in the failing heart[299] along with an increase in the generation of reactive oxygen species[300-303]. A decrease in the genes encoding proteins of the electron transport chain complexes is associated with a decrease in oxidative capacity[306]. These changes in metabolism were reflected in the failing RV in the SU5416/hypoxia RV (**Chapter 4, Figure 13**). With carvedilol treatment after SU5416/hypoxia, there is an increase in expression of genes encoding mitochondrial enzymes (**Figures 25 and 26**). Cytochrome c oxidase (Complex IV of the electron transport chain) is the last enzyme in the electron transport chain and catalyzes the oxidation of cytochrome c and reduction of oxygen to water. Four subunits of cytochrome c oxidase are increased in the microarray dataset: cytochrome c oxidase subunit I (*Cox1*), cytochrome c oxidase subunit II (*Cox2*), cytochrome c oxidase subunit VIa polypeptide 2 (*Cox6a2*), and cytochrome c oxidase subunit VIIIb (*Cox8b*). *Cox1* is increased 1.5-fold, *Cox2* is increased 1.7-fold, *Cox6a2* is increased 1.2-fold, and *Cox8b* is increased 1.6-fold in the SU5416/hypoxia + carvedilol RV compared to SU5416/hypoxia RV. We can conclude that these alterations in metabolism are beneficial to the heart and reflect the beginning of a return towards normal metabolism in the heart.

Table 16: Top Five Canonical Pathways of Genes in Subcluster 2

Pathway Name	p-value
Oxidative Phosphorylation	1.86×10^{-3}
Mitochondrial Dysfunction	5.16×10^{-3}
Phospholipase C Signaling	1.07×10^{-3}
G Protein Signaling Mediated by Tubby	1.46×10^{-2}
Non-Small Cell Lung Cancer Signaling	1.88×10^{-2}

Figure 25: Mitochondrial Dysfunction Genes in Subcluster 2

Microarray gene expression of genes encoding proteins involved in mitochondrial dysfunction in subcluster 2. The first three major columns on the left labeled "normal," "SuHx", and "SuHxCarv" denote expression in the normal, SU5416/hypoxia, and SU5416/hypoxia + carvedilol RVs. Red coloration indicates increased expression compared to the average normal RV expression level while green indicates reduced expression. The small columns represent different animals treated with the same condition. The last major column on the right of the grey line labeled "-" denotes the difference in expression between the SU5416/hypoxia + carvedilol and SU5416/hypoxia RVs. Red coloration indicates increased expression in the SU5416/hypoxia RV with carvedilol treatment compared to an untreated SU5416/hypoxia RV, and green indicates reduced expression in the SU5416/hypoxia + carvedilol RV compared to the SU5416/hypoxia RV.

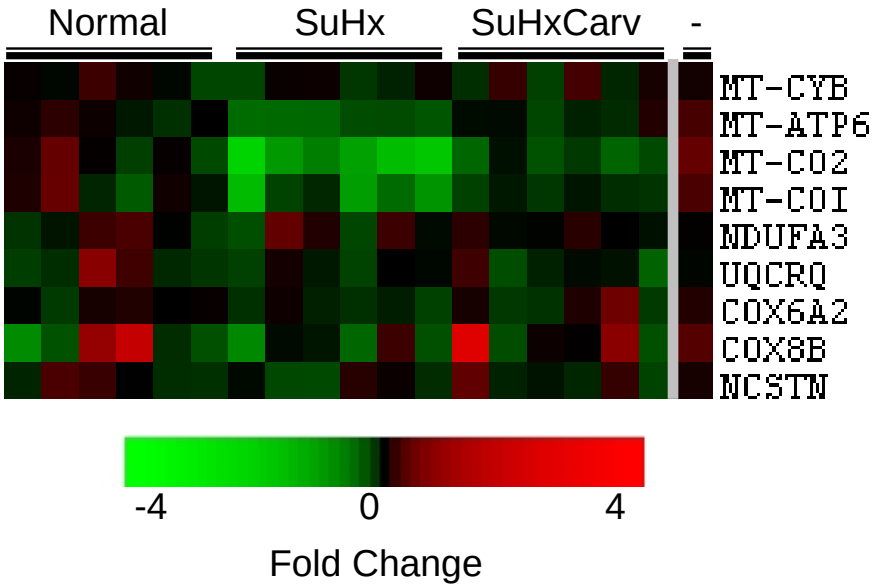
Normal
SuHx
SuHxCarv
-
MT-CYB
MT-ATP6
MT-CO2
MT-COI
NDUFA3
UQCRQ
COX6A2
COX8B
NCSTN
-4
0
4
Fold Change

Figure 26: Mitochondrial Dysfunction Canonical Pathway

Canonical pathway analysis indentified the pathways from the Ingenuity Pathway Analysis® library of canonical pathways that were most significant to the dataset. The p-value for the mitochondrial dysfunction canonical pathway is 5.16×10^{-3}. Genes are colored based on fold-change comparison between the SU5416/hypoxia + carvedilol (treated) RV and the SU5416/Hypoxia (failing) RV. Red correlates to relatively higher expression in the treated RV than the failing RV, and green correlates to relatively higher expression in the failing RV than the treated RV.

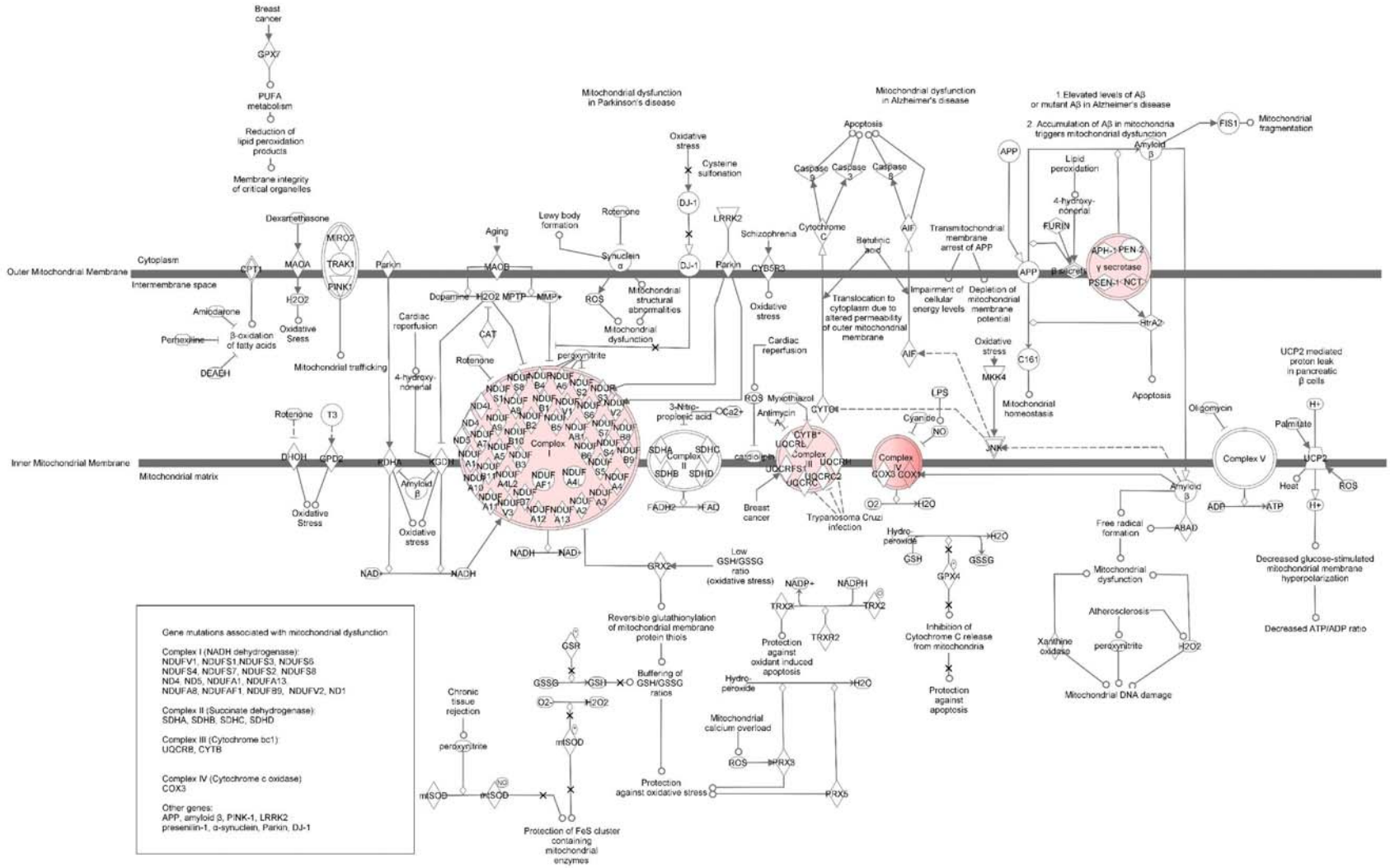

Subcluster 3 contains genes that could represent a "reversal of failure" expression pattern; these genes have increased expression in the SU5416/hypoxia RV and decreased expression in the SU5416/hypoxia + carvedilol RV. The top canonical pathways for genes in this cluster are shown in **Table 17**. Two pathways, Regulation of eIF4 and p70S6k and eIF2 Signaling, will be discussed in more detail in section 5 of this chapter, while the protein ubiquitination pathway will be discussed further as part of subcluster 4. One of the main biological functions of genes in this pathway is cardiac hypertrophy (**Figure 27**); a reduction in genes encoding cardiac hypertrophy functions is consistent with studies reporting that carvedilol reduces hypertrophy in the SU5416/hypoxia RV[360]. Of particular importance to pulmonary hypertension are the genes HIF-1α and angiopoietin-2 (*Ang2*). Hypoxia-driven activation of HIFs plays a role in the pathogenesis of experimental PH[398, 399] by increasing angiogenesis[400] and the metabolic switch towards glycolysis[401]. HIF-1α, along with HIF-2α and VEGF, is found in plexiform lesions[10] and pulmonary artery smooth muscle cells[196] suggesting that HIF-dependent signaling contributes to proliferative activities in PAH. In a HIF-1α heterozygous mouse there was impaired vascular remodeling, decreased RV hypertrophy, and decreased pulmonary artery pressure[399]. *HIF-1α* expression is decreased 2.1-fold in the SU5416/hypoxia + carvedilol RV in comparison to the SU5416/hypoxia RV. *Ang2* is also known to play a role in PAH. *Ang2* has pro-angiogenic properties when expressed in high concentrations[402] or in combination with VEGF[403, 404]. Patients with idiopathic PAH had increased plasma levels of Ang2, and these levels correlated with cardiac index and pulmonary vascular resistance; increased Ang2 was an independent risk factor for mortality[405]. *Ang2* expression is decreased

Table 17: Top Five Canonical Pathways in Subcluster 3

Pathway Name	**p-value**
Protein Ubiquitination Pathway	1.13×10^{-9}
Estrogen Receptor Signaling	6.59×10^{-8}
Androgen Signaling	3.54×10^{-6}
Regulation of eIF4 and p70S6k Signaling	4.06×10^{-6}
eIF2 Signaling	5.61×10^{-6}

Figure 27: Cardiac Hypertrophy Genes

Microarray gene expression of genes involved in cardiac hypertrophy functions in subcluster 3. The first three major columns on the left labeled "normal," "SuHx", and "SuHxCarv" denote expression in the normal, SU5416/hypoxia, and SU5416/hypoxia + carvedilol RVs. Red coloration indicates increased expression compared to the average normal RV expression level while green indicates reduced expression. The small columns represent different animals treated with the same condition. The last major column on the right of the grey line labeled "-" denotes the difference in expression between the SU5416/hypoxia + carvedilol and SU5416/hypoxia RVs. Red coloration indicates increased expression in the SU5416/hypoxia RV with carvedilol treatment compared to an untreated SU5416/hypoxia RV, and green indicates reduced expression in the SU5416/hypoxia + carvedilol RV compared to the SU5416/hypoxia RV.

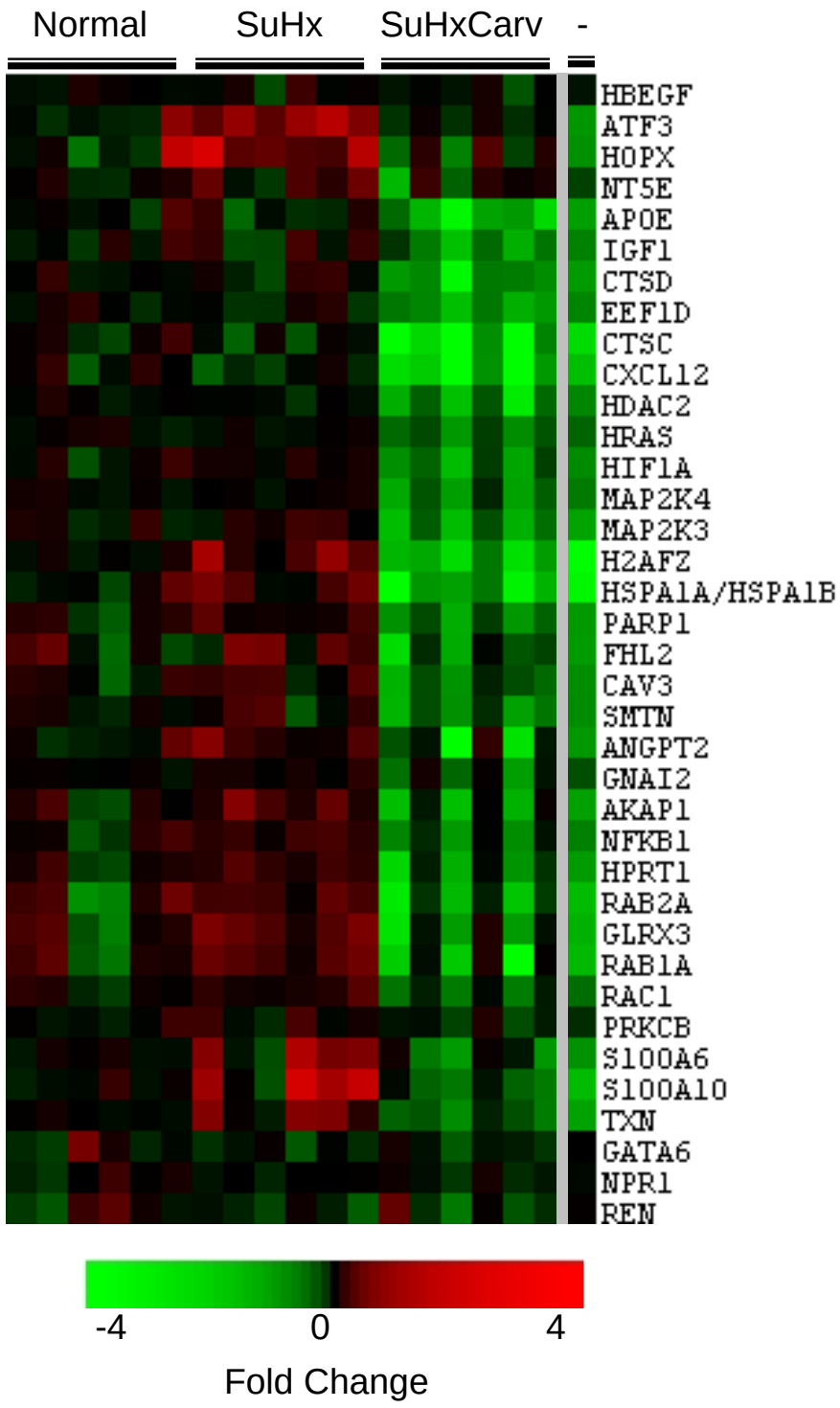
Normal
SuHx
SuHxCarv
-
HBEGF
ATF3
HOPX
NT5E
APOE
IGF1
CTSD
EEF1D
CTSC
CXCL12
HDAC2
HRAS
HIF1A
MAP2K4
MAP2K3
H2AFZ
HSPA1A/HSPA1B
PARP1
FHL2
CAV3
SMTN
ANGPT2
GNAI2
AKAP1
NFKB1
HPRT1
RAB2A
GLRX3
RAB1A
RAC1
PRKCB
S100A6
S100A10
TXN
GATA6
NPR1
REN
-4
0
4
Fold Change

2.3-fold in the SU5416/hypoxia + carvedilol RV in comparison to the SU5416/hypoxia RV. A reduction in these genes, as seen in the SU5416/hypoxia + carvedilol RV, could lead to reduced cardiac hypertrophy and improved myocardial function.

Subcluster 4 is composed of genes that have a "repression" expression pattern and have reduced expression in the SU5416/hypoxia RV and in the SU5416/hypoxia + carvedilol RV. The top five canonical pathways for these genes are listed in **Table 18**, of which 2 are related: ubiquinone biosynthesis and the protein ubiquitination pathway. As previously discussed, the protein ubiquination system is cardioprotective because it removes pro-apoptotic signaling molecules from the cell[314]. Decreased expression of ubiquitination proteins leads to reduced proteasomal activities[313] and allows accumulation of pro-apoptotic proteins[314]. While carvedilol treatment of the SU5416/hypoxia RV does not change expression of these pathway genes compared to SU5416/hypoxia RV, they may not be essential for reversal of RV failure.

5.4 Prediction analysis

The prediction set generated in Chapter 4 was used to evaluate the SU5416/hypoxia + carvedilol data set. The prediction set is made up of those 450 genes that had expression patterns that were most discriminatory between normal, hypertrophy, and failure in the RV. By comparing the expression of carvedilol-treated failing RVs to the prediction set, we can determine which expression pattern carvedilol most resembles and see the effects that carvedilol had on this small subset of genes.

Table 18: Top Five Canonical Pathways in Subcluster 4

Pathway Name	p-value
Ubiquinone Biosynthesis	4.03×10^{-11}
Pyruvate Metabolism	2.49×10^{-06}
Protein Ubiquitination Pathway	1.62×10^{-05}
Citrate Cycle	1.19×10^{-04}
AMPK Signaling	8.65×10^{-04}

This is a supervised learning method; the initial data set applies the knowledge represented by data label to create a class predictor that can classify samples in a new data set. The previous data set, composed of the normal, hypoxia, and SU5416/hypoxia microarrays, acts as a training data set against which the SU5416/hypoxia + carvedilol data set – the prediction data set – is compared. Using the 1-nearest neighbor, 3-nearest neighbors, nearest centroid, and linear discriminant analysis algorithms[228], each of the arrays in the SU5416/hypoxia + carvedilol data set was assigned a label of either "normal," "hypertrophy," or "failure" based on the similarity of the 450 genes in the training data set to the 450 genes in the prediction data set.

As seen in **Table 19**, each of the SU5416/hypoxia + carvedilol arrays was classified as "failure" by all of the algorithms. It is evident from **Figure 28**, that the expression of the genes in the SU5416/hypoxia + carvedilol set has a great deal of similarity to the failure gene set, but that there are also some genes with distinct expression patterns. Although the SU5416/hypoxia + carvedilol data were classified as being most similar to failure (SU5416/hypoxia), it is important to remember that this is based on a small set of genes rather than the data set as a whole.

However, there are some genes with a distinct gene expression pattern between the SU5416/hypoxia and SU5416/hypoxia + carvedilol RVs which may represent the genes that are responsible for reversal of failure. *Cox1*, as previously discussed, was increased 1.5-fold in the SU5416/hypoxia + carvedilol RV compared to the SU5416/hypoxia RV

Table 19: Summary of Prediction Analysis Results
Description of how the SU5416/hypoxia + carvedilol microarrays were classified by the prediction analysis set generated in Chapter 4.

Array ID	Number of genes in classifier	1-Nearest Neighbor	3-Nearest Neighbors	Nearest Centroid	Linear Discriminant Analysis
237	435	Failure	Failure	Failure	Failure
238	435	Failure	Failure	Failure	Failure
239	435	Failure	Failure	Failure	Failure
526	435	Failure	Failure	Failure	Failure
527	435	Failure	Failure	Failure	Failure
604	435	Failure	Failure	Failure	Failure

Figure 28: Prediction Analysis Results

Dendogram for clustering experiments using centered correlation and average linkage of the 450 probes that showed 100% agreement across LOOCV. The first three major columns on the left labeled "normal," "SuHx", and "SuHxCarv" denote expression in the normal, SU5416/hypoxia, and SU5416/hypoxia + carvedilol RVs. Red coloration indicates increased expression compared to the average normal RV expression level while green indicates reduced expression. The small columns represent different animals treated with the same condition. Each row represents a gene from the prediction set. The last major column on the right of the grey line labeled "-" denotes the difference in expression between the SU5416/hypoxia + carvedilol and SU5416/hypoxia RVs. Red coloration indicates increased expression in the SU5416/hypoxia RV with carvedilol treatment compared to an untreated SU5416/hypoxia RV, and green indicates reduced expression in the SU5416/hypoxia + carvedilol RV compared to the SU5416/hypoxia RV.

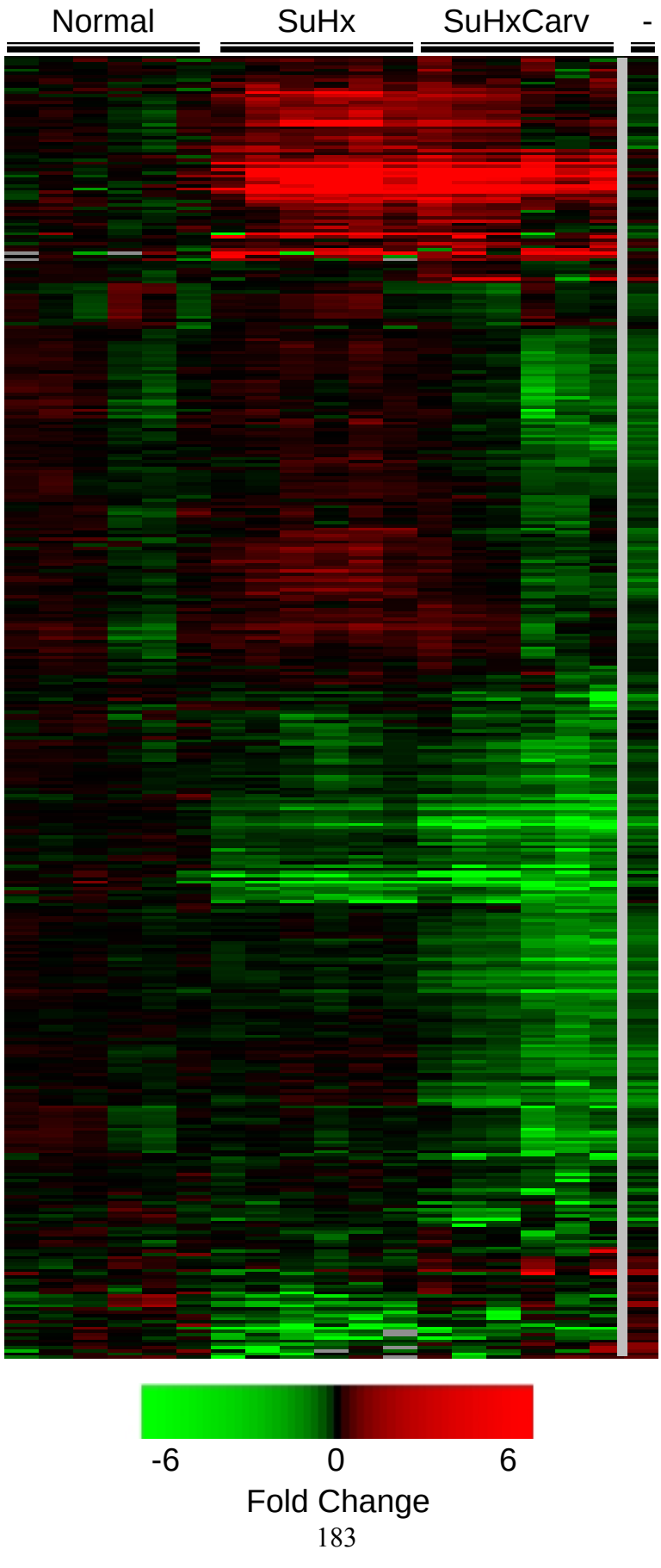
Normal
SuHx
SuHxCarv
-
-6
0
6
Fold Change

demonstrating that there are effects of carvedilol on the complexes of the electron transport chain. In addition, endothelin 2 (*Edn2*) was decreased 2.6-fold in the SU5416/hypoxia + carvedilol RV when compared to the SU5416/hypoxia RV; in several cancer cell lines, hypoxia triggers production of *Edn2*[406-408]. *Edn2* has strong vasoconstricting activity[409] similar to endothelin 1, which has been implicated as a mediator of vascular tone and vascular remodeling in pulmonary hypertension[410]. Similarly, expression of beta 5 tubulin (*Tubb5*) were decreased 2.9-fold in the SU5416/hypoxia + carvedilol RV in comparison to the SU5416/hypoxia RV. Levels of β-tubulin increase in rat models of cardiac hypertrophy and pulmonary hypertension induced by monocrotaline[411], which has been associated with contractile dysfunction[412]. It may be that only a few differences in gene expression such as these can have a positive outcome on the function of the RV.

5.5 Class comparison analysis

Although the class prediction set classified all of the SU5416/hypoxia + carvedilol microarrays as "failure" because of similarities to the SU5416/hypoxia data set, there are a few significant changes in gene expression in that dataset. In addition, the microarray analysis showed a large number of genes that were differentially expressed between the SU5416/hypoxia + carvedilol and SU5416/hypoxia microarrays. As such, there is reason to believe that we can identify the genes that had the greatest difference in expression between the two data sets. To do so, we employed a class comparison algorithm, which uses a T-test to compare the expression of each gene between the two classes in the data

set[413]. Those genes with a p-value below a given threshold value are called significant. In addition, multivariate permutation testing can be used to control the false discovery rate[226, 414]. For each permutation in the multivariate permutation testing algorithm, the data labels are changed and the p-value is re-calculated for each gene. The genes are then ordered by their p-value and the number of genes with a p-value below the threshold is recorded. The process is repeated for all permutations. For a given p-value, the number of genes selected via permutation testing is known and is the false discovery rate. A threshold p-value is chosen to minimize the false discovery rate.

When comparing the SU5416/hypoxia (failing) and SU5416/hypoxia + carvedilol (treatment) microarrays, a two-sample T-test was used to compare the two classes. The p-value threshold was set at 0.001 to allow no more than 10 false-positive genes and a proportion of false-positive genes less than 5%. Of the 43,379 probes in the data set, 489 were selected as significant given the chosen test conditions. The probability of selecting at least 489 probes by chance at the threshold p-value of 0.001 if there was no difference between the classes is 0.216%. The list of these genes is given in **Appendix 2** and the cluster showing their expression is shown in **Figure 29**. Two clear subclusters are apparent in the cluster diagram and will be explained in more detail.

Subcluster 1 is composed of 282 probes that correspond to 275 different genes. The top five canonical pathways for genes in this cluster are given in **Table 20**. Two of these pathways, regulation of eIF4 and p70S6k signaling and eIF2 signaling, are involved in common biological processes. Eukaryotic initiation factor (eIF)-2 and 4 are both

Figure 29: Class Comparison between SU5416/hypoxia and SU5416/hypoxia + carvedilol

Cluster for class comparison analysis between SU5416/hypoxia RV (failure) and SU5416/hypoxia + carvedilol RV (Tx = treatment) microarray data sets. 489 probes were called significant at an $\alpha<0.001$ level and multivariate permutation testing gives a false discover rate less than 5%. Red represents greater relative expression than reference RNA and green represents less relative expression than reference RNA.

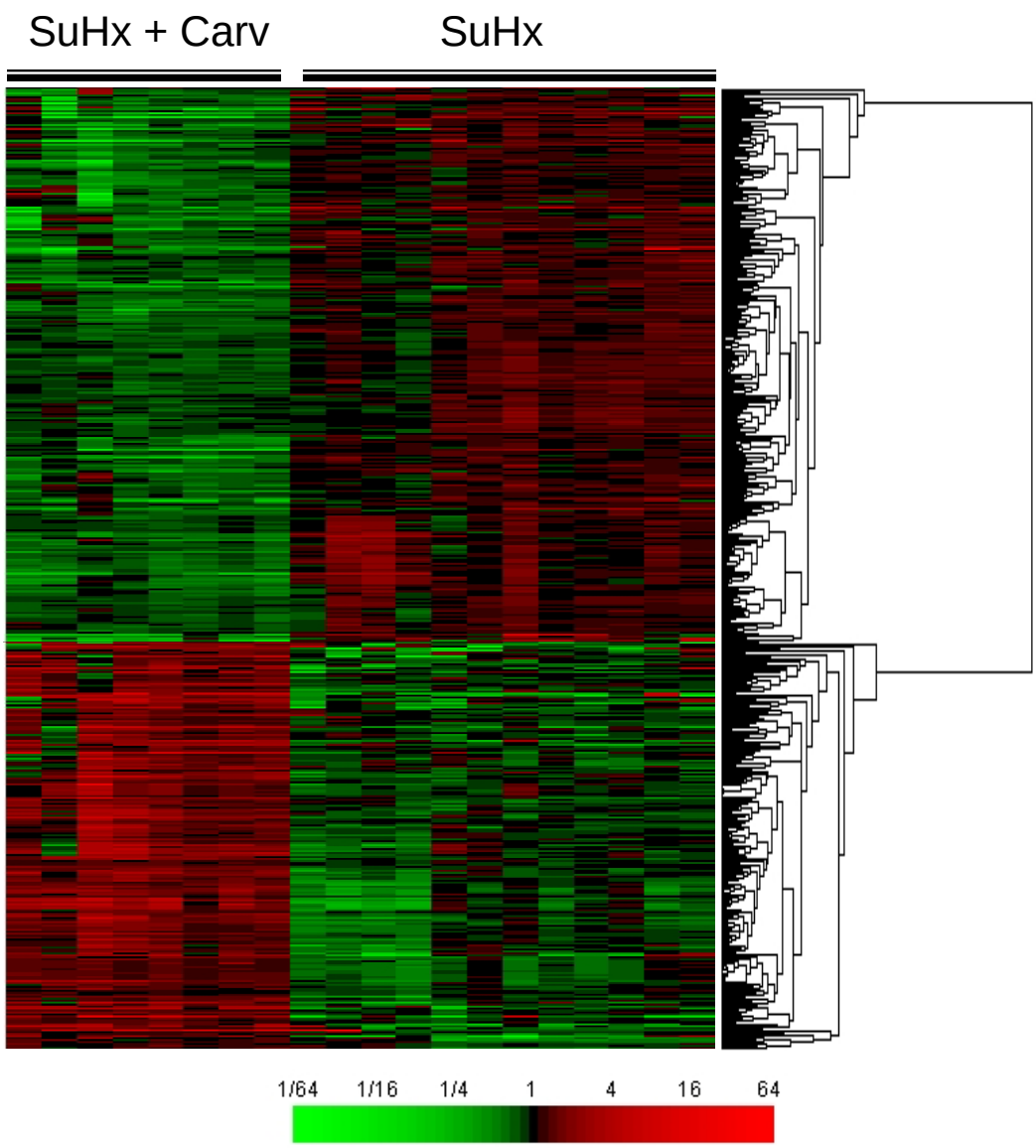
SuHx + Carv
SuHx
1/64
1/16
1/4
1
4
16
64

Table 20: Top Five Canonical Pathways of Genes in Subcluster 1 of Multivariate Analysis

Pathway Name	p-value
Regulation of eIF4 and p70S6k Signaling	1.98×10^{-4}
Glucocorticoid Receptor Signaling	2.61×10^{-4}
Ceramide Signaling	4.04×10^{-4}
EGF Signaling	4.94×10^{-4}
eIF2 Signaling	5.68×10^{-4}

required for the initiation of translation. *eIF2* forms a complex with GTP and methionyl tRNA, which binds to the 40S ribosomal subunit to form the 43S preinitiation complex. The 43S preinitiation complex binds to mRNA. Mammalian target of rapamycin (mTOR) phosphorylates *eIF4e* binding protein allowing *eIF4e* to separate from its binding protein and to bind to the mRNA and begin translation[415]. It is known that cardiac hypertrophy requires an increase in protein synthesis by individual cardiomyocytes[416], thus would require greater activity of the eIFs. In a model of cardiac hypertrophy caused by chronic alcohol intake, *eIF2* levels were increased[417]. *eIF4b* has been shown to regulate translation of proliferative and pro-survival mRNAs[418]. Similarly, decreased expression of *eIF4e* leads to reduced rates of cell growth[419]. In the microarray dataset, several of the eIF genes were decreased in expression in the SU5416/hypoxia + carvedilol RV compared to the SU5416/hypoxia RV: *eIF2B3* was decreased 1.51-fold, *eIF3F* was decreased 2.19-fold, and *eIF4G2* was decreased 2.46-fold, which should lead to decreased protein synthesis in the SU5416/hypoxia + carvedilol RV. Another pathway, EGF Signaling, also plays a known role in the heart. Transactivation of the epidermal growth-factor receptor (EGF-R) activates G protein-coupled receptors to mediate proliferation and mitogenic effects, including hypertension, vascular inflammation, tissue remodeling, and left ventricular hypertophy[380, 420-422]. Activation of EGF-R induces expression of interferon regulatory factor (IRF1) via phosphorylation of signal transducer and activator of transcription 1 and 3 (STAT1 and STAT3)[423]; in the microarray dataset, expression of *Stat1* is decreased by 3.36-fold in the SU5416/hypoxia + carvedilol RV compared to the SU5416/hypoxia RV. Another member of the EGF-R signaling pathway, mitogen-

activated protein kinase 4 (*Mapk4*), was also decreased by 1.96-fold in the SU5416/hypoxia + carvedilol RV compared to the SU5416/hypoxia RV in the microarray dataset. Disruption of EGF signaling has been shown to be protective against cardiac hypertrophy[424, 425]. In addition, EGF-R signaling mediated the development of PAH in mice overexpressing transforming growth factor alpha (TGF-α)[426]. As shown in **Figure 29**, the eIF2-, eIF4-, and EGF signaling pathways are increased in the SU5416/hypoxia model when compared with the SU5416/hypoxia + carvedilol model. This suggests that these pathways have been affected by carvedilol to decrease hypertrophy and return the heart to a more normal state.

Subcluster 2 is made up of 207 probes that represent 192 different genes. The top five canonical pathways for genes in this cluster are listed in **Table 21**. Of these pathways, three – PPAR signaling, PPARα/RXRα activation, and Nrf2-mediated oxidative stress response – have common functions in the heart. Peroxisome proliferator-activator receptor (PPAR) alpha and gamma are both activated by PPAR coactivator-1 alpha (PGC-1α) and signal through nuclear factor-like 2 (*Nrf2*). Both PGC-1α and PPAR-α are preferentially expressed in tissues with high oxidative capacity, including the heart[427]. Through co-activation of PPAR-α and estrogen-related receptor alpha (ERRα), PGC-1α activates genes involved in the cellular uptake and mitochondrial activation of fatty acids[428]. As shown in gene knock-out studies, both ERRα and PPARα have been shown to play an important role in the functional adaptation of the heart to pressure overload[427, 429]. In PGC-1α knockout mice, there is a reduction of fatty acid oxidation and a reduction in expression of mitochondrial genes in the

Table 21: Top Five Canonical Pathways of Genes in Subcluster 2 of Multivariate Analysis

Pathway Name	p-value
PPAR Signaling	2.59×10^{-5}
PPARα/RXRα Activation	5.75×10^{-4}
Agrin Interactions at Neuromuscular Junction	8.10×10^{-4}
NRF2-mediated Oxidative Stress Response	8.76×10^{-4}
Prostate Cancer Signaling	1.56×10^{-3}

heart[430, 431]. It has been shown that levels of PGC-1α, PPAR-α, and ERR-α genes and protein are decreased in the SU5416/hypoxia RV and that this reduction in mRNA expression is correlated with RV function[432]. The reactive oxygen species created during oxidative stress increase levels of nuclear factor kappa B (NF-κB), which subsequently increases levels of pro-inflammatory cytokines such as IL-1, IL-6, and TNF-α[433]. Increased expression of NF-κB inhibitor alpha (*NF-κBIA*) suppresses the transcriptional activity of *NF-κB*; in the microarray data set, expression of *NF-κBIA* is increased 2.1-fold in the SU5416/hypoxia RV compared to the SU5416/hypoxia RV. Additionally, *NF-κB* activation prevents changes in expression of ATP-binding cassette subfamily C member 1 (*Abcc1*, also called multidrug-resistance associated protein 1 (*Mrp1*)), which protects against oxidative stress[434, 435]. Further confirming this protective role, patients with COPD have decreased expression of Abcc1 compared with healthy patients[436]. In the SU5416/hypoxia + carvedilol RV, *Abcc1* is expressed 1.4-fold higher than that of the Su5416/hypoxia RV. As shown in **Figure 29**, genes in these pathways are returning towards normal expression levels in the RV with carvedilol treatment, indicating that a change in energy metabolism and mitochondrial function is associated with the reversal of RVF.

5.6 qRT-PCR and additional pathway analysis

We next examined the changes in gene expression in RV tissue samples in rats treated with SU5416/hypoxia and carvedilol for genes previously examined by quantitative real-time polymerase chain reaction (qRT-PCR) (**Figure 30**). Treatment of the

Figure 30: RT-PCR Results

Quantitative real-time PCR analysis of a) Add3 (a, $p<0.01$ vs SuHx; b, $p<0.01$ vs normal; c, $p<0.05$ vs SuHx), b) Ang1 (a, $p<0.05$ vs normal; b, $p<0.05$ vs SuHx; c, $p<0.01$ vs normal), c) apelin (a, $p<0.01$ vs normal; b, $p<0.01$ vs SuHx; c, $p<0.05$ vs normal; d, $p<0.05$ vs SuHx), d) HIF-2α (a, $p<0.01$ vs SuHx; b, $p<0.01$ vs normal; c, $p<0.05$ vs normal; d, $p<0.05$ vs SuHx), e) IGF-1 (a, $p<0.05$ vs normal; b, $p<0.05$ vs SuHx; c, $p<0.01$ vs SuHx), and f) KLF5 (a, $p<0.01$ vs normal; b, $p<0.01$ vs SuHx; c, $p<0.05$ vs SuHx; d, $p<0.05$ vs normal) mRNA in normal and carvedilol rat right ventricles. Data were normalized to expression of 18S rRNA and are shown as mean ± s.d. (n=3).

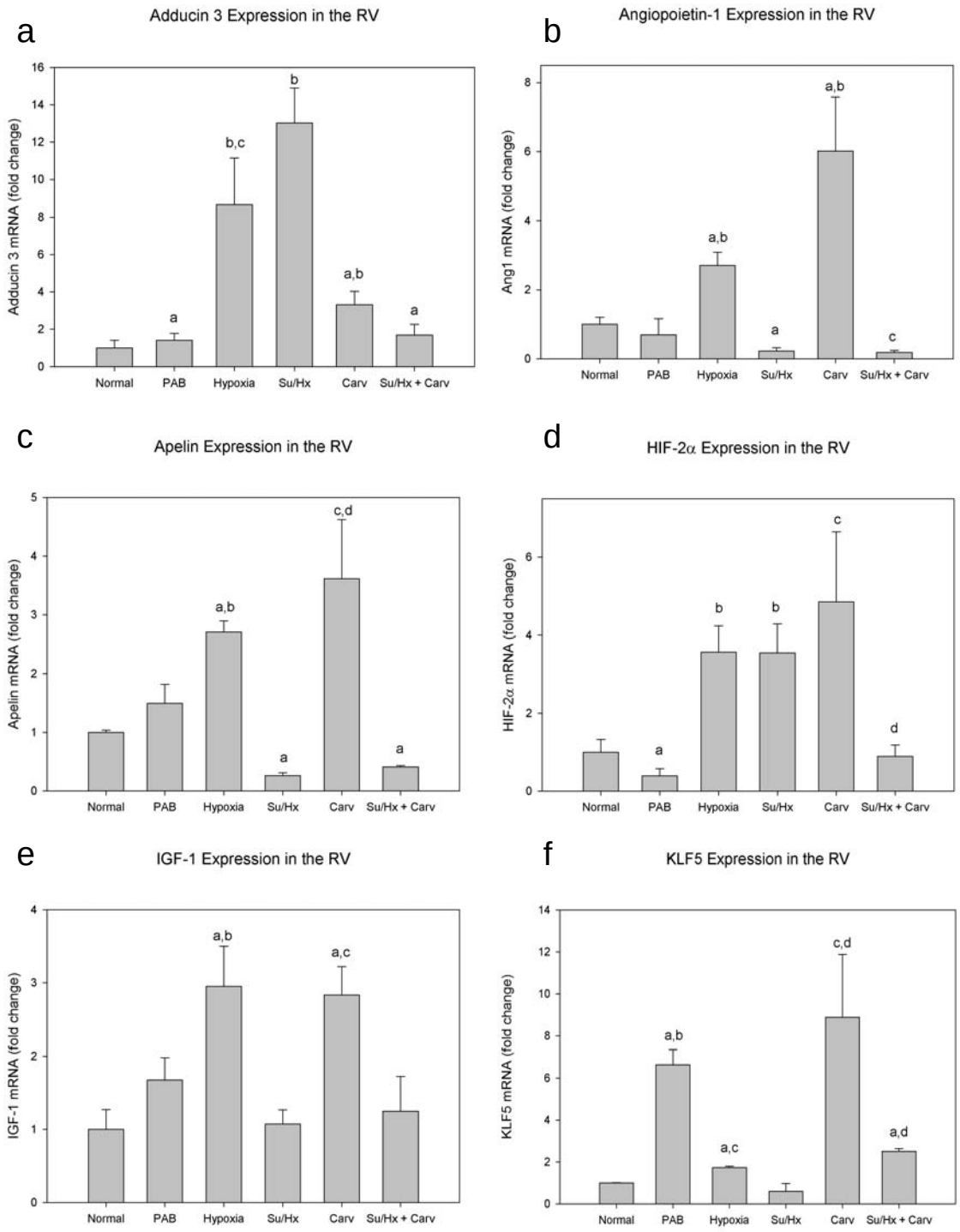
a
Adducin 3 Expression in the RV
Adducin 3 mRNA (fold change)
16
14
12
10
8
6
4
2
0
a
b,c
b
a,b
a
Normal
PAB
Hypoxia
Su/Hx
Carv
Su/Hx + Carv
b
Angiopoietin-1 Expression in the RV
Ang1 mRNA (fold change)
8
6
4
2
0
a,b
a,b
a
c
Normal
PAB
Hypoxia
Su/Hx
Carv
Su/Hx + Carv
c
Apelin Expression in the RV
Apelin mRNA (fold change)
5
4
3
2
1
0
a,b
c,d
a
a
Normal
PAB
Hypoxia
Su/Hx
Carv
Su/Hx + Carv
d
HIF-2α Expression in the RV
HIF-2α mRNA (fold change)
6
4
2
0
a
b
b
c
d
Normal
PAB
Hypoxia
Su/Hx
Carv
Su/Hx + Carv
e
IGF-1 Expression in the RV
IGF-1 mRNA (fold change)
4
3
2
1
0
a,b
a,c
Normal
PAB
Hypoxia
Su/Hx
Carv
Su/Hx + Carv
f
KLF5 Expression in the RV
KLF5 mRNA (fold change)
14
12
10
8
6
4
2
0
a,b
a,c
c,d
a,d
Normal
PAB
Hypoxia
Su/Hx
Carv
Su/Hx + Carv

SU5416/hypoxia RV with carvedilol was associated with a decrease in the expression of *Add3* and *HIF-2α;* both genes returned towards normal levels of expression. Similarly, expression of *Ang1* and *apelin* also both returned towards normal RV expression levels and were increased in comparison to SU5416/hypoxia RV levels. In contrast, levels of *Aqp1*, *Nppb*, and *Klf5* increased above the SU5416/hypoxia RV levels, which were also increased in comparison to normal RV levels. There was no significant effect on the expression of IGF-1 in the SU5416/hypoxia + carvedilol RV tissue.

In addition, we examined the glycolysis/gluconeogenesis pathways (**Figure 31**) with respect to carvedilol treatment on the failing RV. Genes that were up-regulated by SU5416/hypoxia treatment (**Chapter 4, Figure 20**) are now down regulated by carvedilol treatment. In patients with PAH, there is a shift from oxidative phosphorylation to glycolysis in the heart[195, 196], which is associated with reduced RV contractility and impairment of cardiac function[198]. A reduction in expression of genes encoding glycolytic enzymes in the carvedilol-treated failing RV may be an indication that the heart is switching from glycolysis back to oxidative phosphorylation and may be consistent with some degree of myocardial metabolic recovery.

5.7 Inflammatory genes

On a molecular level, carvedilol treatment has been shown to affect inflammatory cytokines and apoptosis. In post-MI rats that were treated with carvedilol, there was: preservation of myocardial contractility, reduced cardiac expression of IL-1β, and

Figure 31: Glycolysis and Gluconeogenesis Canonical Pathway

Canonical pathway analysis identified the pathways from the Ingenuity Pathway Analysis® library of canonical pathways that were most significant to the dataset. The p-value for the glycolysis and gluconeogenesis canonical pathway is 0.00929. Genes are colored based on fold-change comparison between Sugen/Hypoxia (failing) RV and Sugen/Hypoxia with carvedilol treatment (treated) RV. Carvedilol was given to rats for four weeks at a dose of 15 mg/kg. Red correlattes to relatively higher expression in the treated RV than the failing RV, and green correlates to relatively higher expression in the failing RV than the treated RV. Enzyme classification (EC) numbers reported by Ingenuity were converted to recommended names using the BRENDA enzyme database (32); these names were then incorporated into the Ingenuity canonical pathway using the MyPathway® feature.

Path Designer Glycolysis/Gluconeogenesis SuHxCSuHx

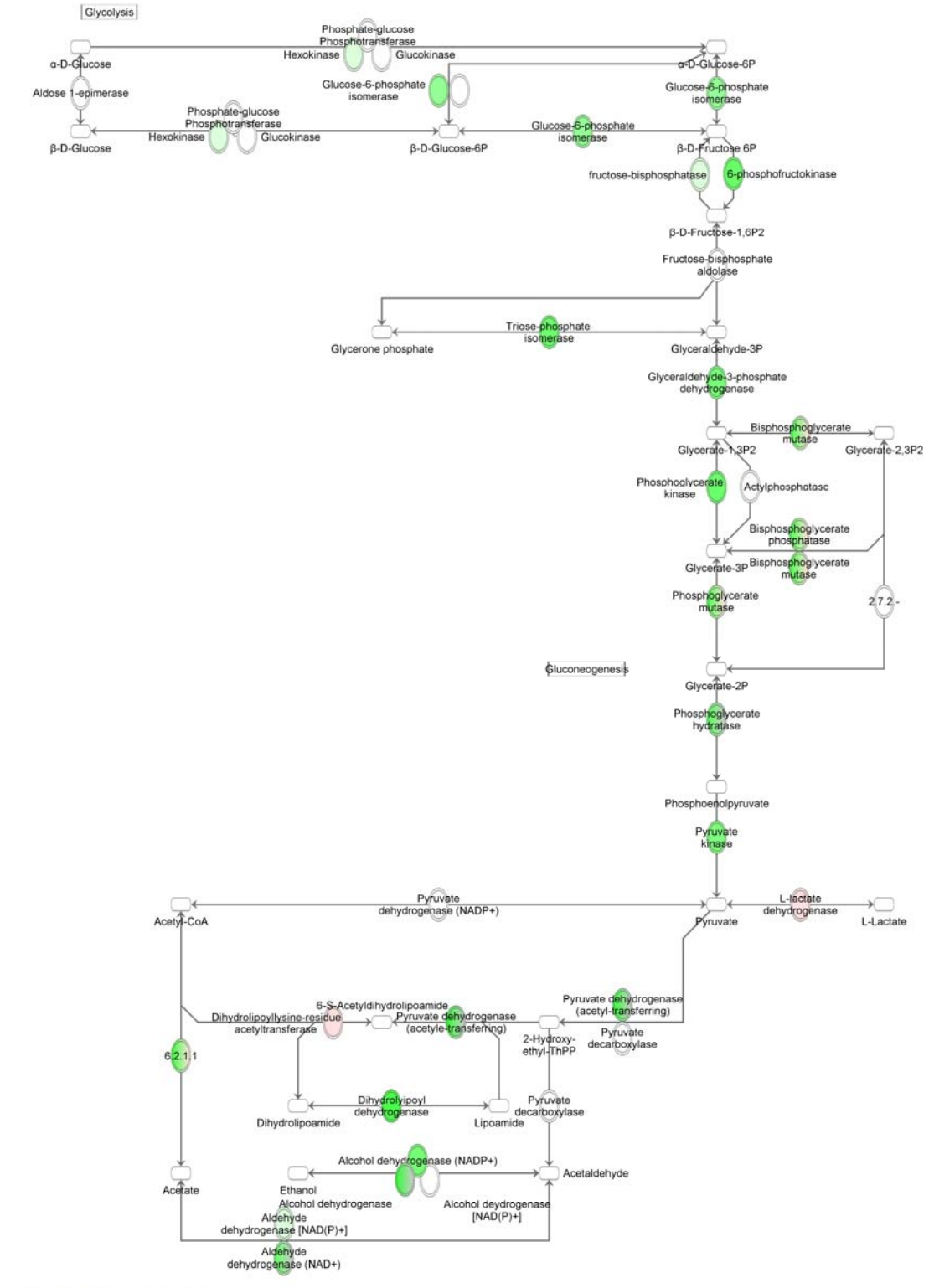

beneficial effects on ventricular remodeling; however, no effect on cardiac oxidative stress was seen[437]. Additionally, four weeks of treatment with carvedilol after MI reduced expression of the pro-inflammatory cytokines TNF-α, IL-1β, IL-6, and TGF-β while increasing levels of the anti-inflammatory cytokine IL-10[438]. Similarly, carvedilol as a treatment for myocarditis reduced expression of IL-1β and TNF-α and increased expression of IL-10[439]. Furthermore, carvedilol suppressed the activation of caspase3 via downregulation of TNF-α and inhibition of mitochondrial cytochrome c release, resulting in reduced endothelial cell apoptosis induced by congestive heart failure[440]. Because neither prazosin, an α1-adrenergic receptor blocker, or propanolol, a non-specific β-blocker, were able to induce the same effect but an antioxidant did, it is speculated that this effect is due to the antioxidant properties of carvedilol[440]. Finally, carvedilol has been shown to inhibit proliferation of pulmonary artery smooth muscle cells isolated from patients with idiopathic pulmonary arterial hypertension (PAH)[441].

We examined the effect of carvedilol on the production of cytokines using a multiplex ELISA. As shown in **Figure 32**, there was no significant difference in the expression of cytokines between the normal rat and carvedilol-only treated normal rat serum samples. These signals activated by carvedilol may play a cardioprotective role and contribute to the beneficial effects seen with carvedilol treatment in the right ventricular failure animal models. Whether carvedilol also affects the expression of the above-mentioned genes in the normal and carvedilol-treated LV will be investigated.

Figure 32: Effects of carvedilol on cytokine production in serum samples

Multiplex ELISA analysis of IL-1α, IL-1β, IL-2, IL-4, IL-5, IL-10, IL-13, IL-17, IL-18, TNF-α, and VEGF protein in normal and carvedilol rat serum samples (no significant difference). Data are shown as mean ± s.d. (n=3).

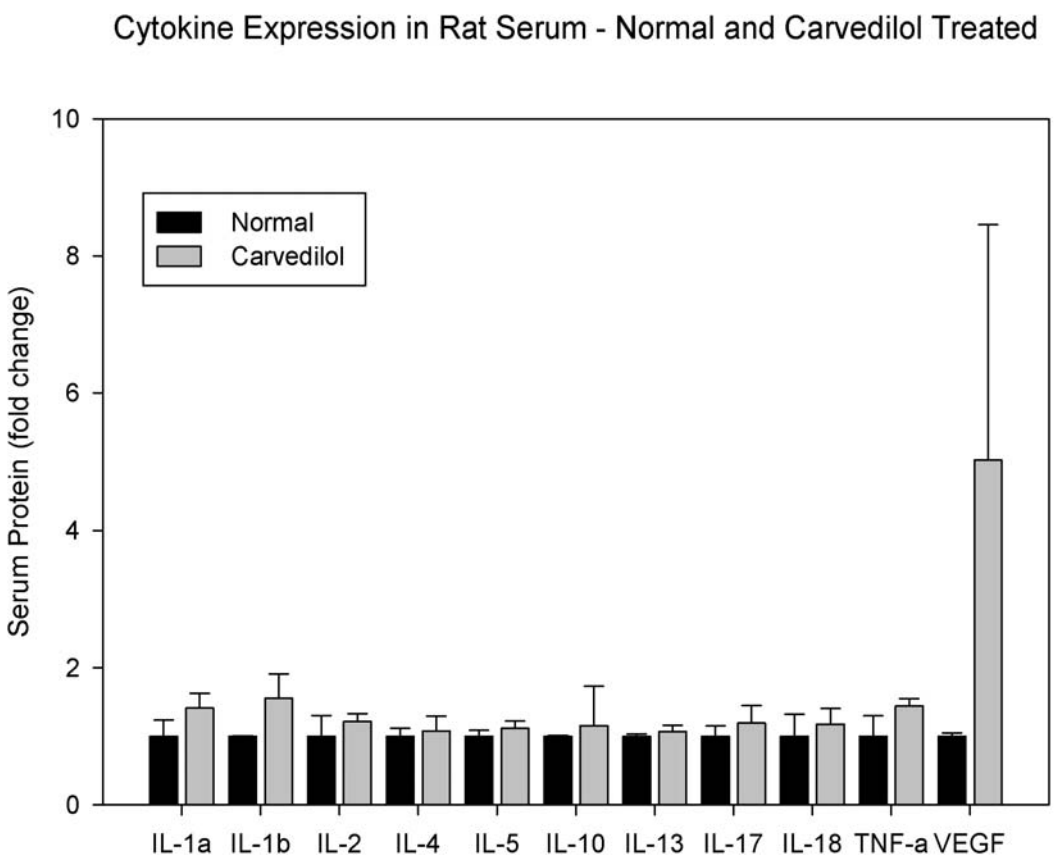
Cytokine Expression in Rat Serum - Normal and Carvedilol Treated
Serum Protein (fold change)
10
8
6
4
2
0
Normal
Carvedilol
IL-1a
IL-1b
IL-2
IL-4
IL-5
IL-10
IL-13
IL-17
IL-18
TNF-a
VEGF

In addition, we analyzed the expression of cytokines in the serum taken from different rat models (**Figure 33**). Of the previously analyzed cytokines **(Chapter 4, Figure 21)**, only IL-1β and VEGF had increased expression in the SU5416/hypoxia + carvedilol samples when compared to normal rat serum samples. Additionally, there was no significant difference in cytokine expression in serum samples between the SU5416/hypoxia samples and the SU5416/hypoxia + carvedilol samples. It is possible that there is a change in cytokine levels in the tissues of the heart that is not reflected in the serum samples.

To determine if there were effects on the expression of cytokines in the RV, the microarray data were analyzed with respect to inflammatory genes (**Figure 34**). Several genes were affected by carvedilol in the manner expected based on previously published literature results. VEGF forms B and C were decreased by 1.5-fold and 1.3-fold respectively in the SU5416/hypoxia + carvedilol RV compared to the SU5416/hypoxia RV. IL-18 also decreased by 1.4-fold and IL-10 increased 1.2-fold, consistent with previously published literature that shows IL-10 decreases with carvedilol treatment[438, 439]. VEGF-A did have a different expression in the two conditions. However, other pro-inflammatory cytokines were increased in expression with carvedilol treatment in the SU5416/hypoxia RV compared to the SU5416/hypoxia RV, including IL-1α (1.6-fold increase), IL-1β (1.3-fold increase), IL-2 (6.5-fold increase), IL-4 (1.8-fold increase), IL-5 (1.4-fold increase), IL-6 (1.6-fold increase), IL-13 (2-fold increase), and TNF-α (1.5-fold increase). However, unlike the cytokine assay that measures protein levels, the

Figure 33: Expression of cytokines in rat serum from normal, failing, and carvedilol-treated models

Multiplex ELISA analysis of a) IL-1α, b) IL-1β, c) IL-2, d) IL-4, e) IL-5, f) IL-10, g) IL-13, h) IL-17, i) IL-18, j) TNF-α, and k) VEGF protein in normal (normal), pulmonary artery banded (PAB), hypoxic (hypoxia), SU5416/hypoxia (SuHx), carvedilol (Carv), and SU5416/hypoxia + carvedilol (SuHx + Carv) rat serum samples (a, $p<0.05$ vs normal; b, $p<0.01$ vs normal). Data are shown as mean ± s.d. (n=3).

a

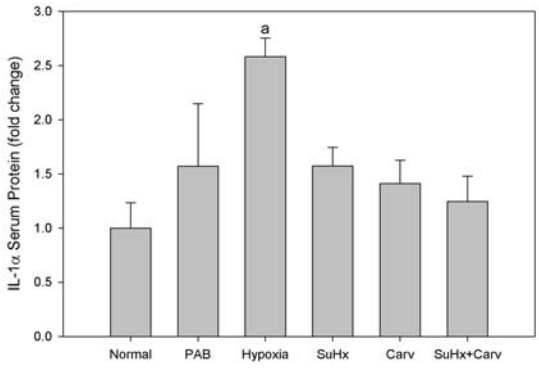
IL-1α Expression in Rat Serum
IL-1α Serum Protein (fold change)
3.0
2.5
2.0
1.5
1.0
0.5
0.0
a
Normal
PAB
Hypoxia
SuHx
Carv
SuHx+Carv

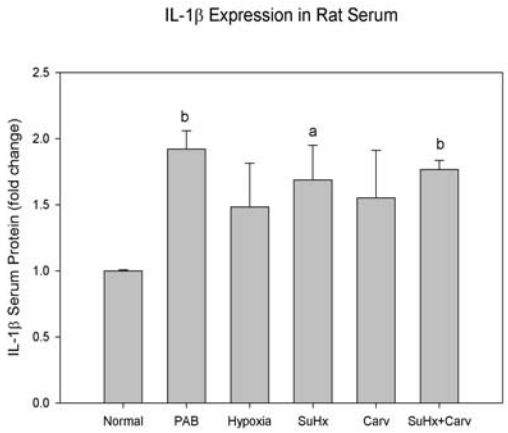
IL-1β Expression in Rat Serum
IL-1β Serum Protein (fold change)
2.5
2.0
1.5
1.0
0.5
0.0
b
a
b
Normal
PAB
Hypoxia
SuHx
Carv
SuHx+Carv

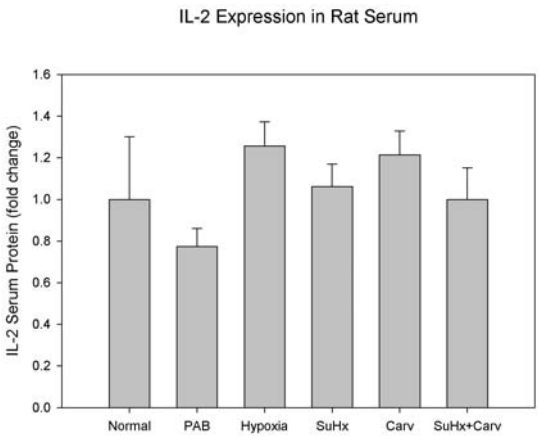
IL-2 Expression in Rat Serum
IL-2 Serum Protein (fold change)
1.6
1.4
1.2
1.0
0.8
0.6
0.4
0.2
0.0
Normal
PAB
Hypoxia
SuHx
Carv
SuHx+Carv

d

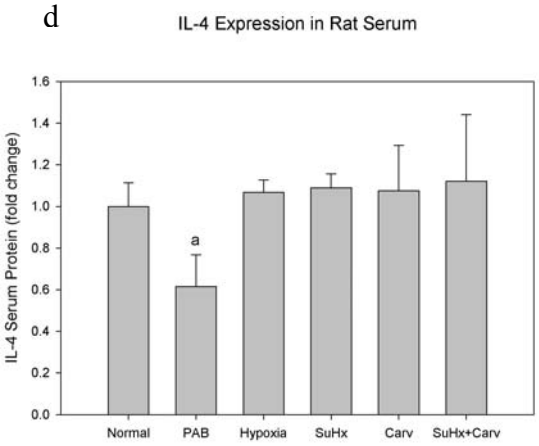
IL-4 Expression in Rat Serum
IL-4 Serum Protein (fold change)
1.6
1.4
1.2
1.0
0.8
0.6
0.4
0.2
0.0
a
Normal
PAB
Hypoxia
SuHx
Carv
SuHx+Carv

e

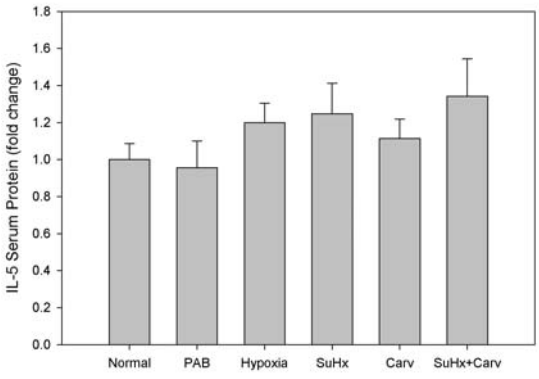
IL-5 Expression in Rat Serum
IL-5 Serum Protein (fold change)
1.8
1.6
1.4
1.2
1.0
0.8
0.6
0.4
0.2
0.0
Normal
PAB
Hypoxia
SuHx
Carv
SuHx+Carv

f

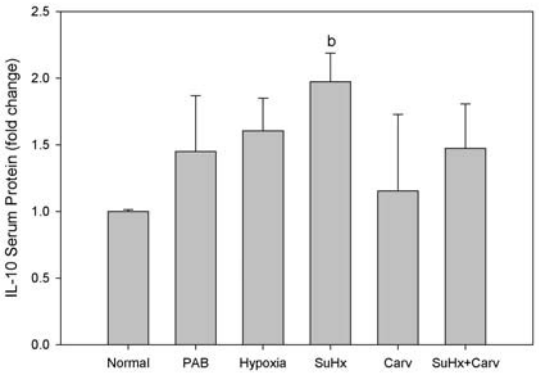
IL-10 Expression in Rat Serum
IL-10 Serum Protein (fold change)
2.5
2.0
1.5
1.0
0.5
0.0
b
Normal
PAB
Hypoxia
SuHx
Carv
SuHx+Carv

g

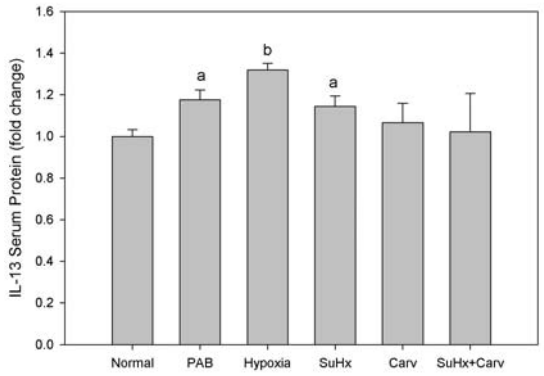
IL-13 Expression in Rat Serum
IL-13 Serum Protein (fold change)
1.6
1.4
1.2
1.0
0.8
0.6
0.4
0.2
0.0
a
b
a
Normal
PAB
Hypoxia
SuHx
Carv
SuHx+Carv

h

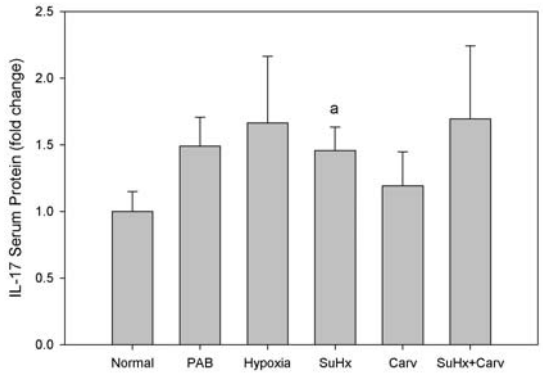
IL-17 Expression in Rat Serum
IL-17 Serum Protein (fold change)
2.5
2.0
1.5
1.0
0.5
0.0
a
Normal
PAB
Hypoxia
SuHx
Carv
SuHx+Carv

i

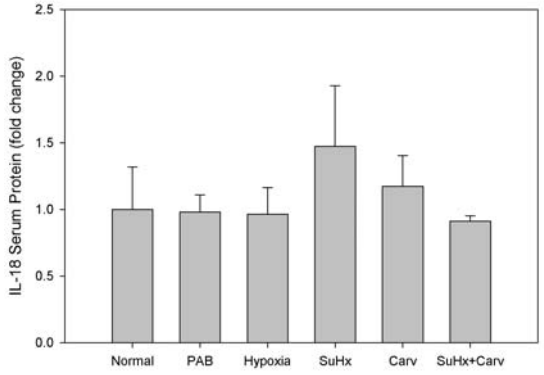
IL-18 Expression in Rat Serum
IL-18 Serum Protein (fold change)
2.5
2.0
1.5
1.0
0.5
0.0
Normal
PAB
Hypoxia
SuHx
Carv
SuHx+Carv

j

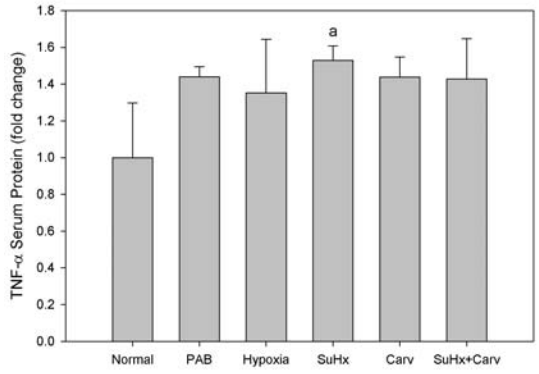
TNF-α Expression in Rat Serum
TNF-α Serum Protein (fold change)
1.8
1.6
1.4
1.2
1.0
0.8
0.6
0.4
0.2
0.0
a
Normal
PAB
Hypoxia
SuHx
Carv
SuHx+Carv

k

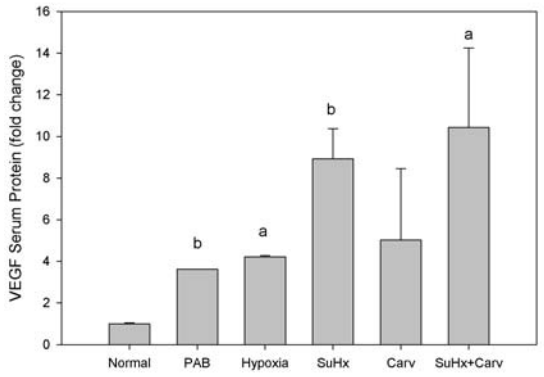
VEGF Expression in Rat Serum
VEGF Serum Protein (fold change)
16
14
12
10
8
6
4
2
0
b
a
b
a
Normal
PAB
Hypoxia
SuHx
Carv
SuHx+Carv

Figure 34: Clustergram of inflammatory genes

Microarray gene expression of inflammatory genes in microarray dataset. The first three major columns on the left labeled "normal," "SuHx", and "SuHxC" denote expression in the normal, SU5416/hypoxia, and SU5416/hypoxia + carvedilol RVs. Red coloration indicates increased expression compared to the average normal RV expression level while green indicates reduced expression. The small columns represent different animals treated with the same condition. The last major column on the right of the grey line labeled "-" denotes the difference in expression between the SU5416/hypoxia + carvedilol and SU5416/hypoxia RVs. Red coloration indicates increased expression in the SU5416/hypoxia RV with carvedilol treatment compared to an untreated SU5416/hypoxia RV, and green indicates reduced expression in the SU5416/hypoxia + carvedilol RV compared to the SU5416/hypoxia RV.

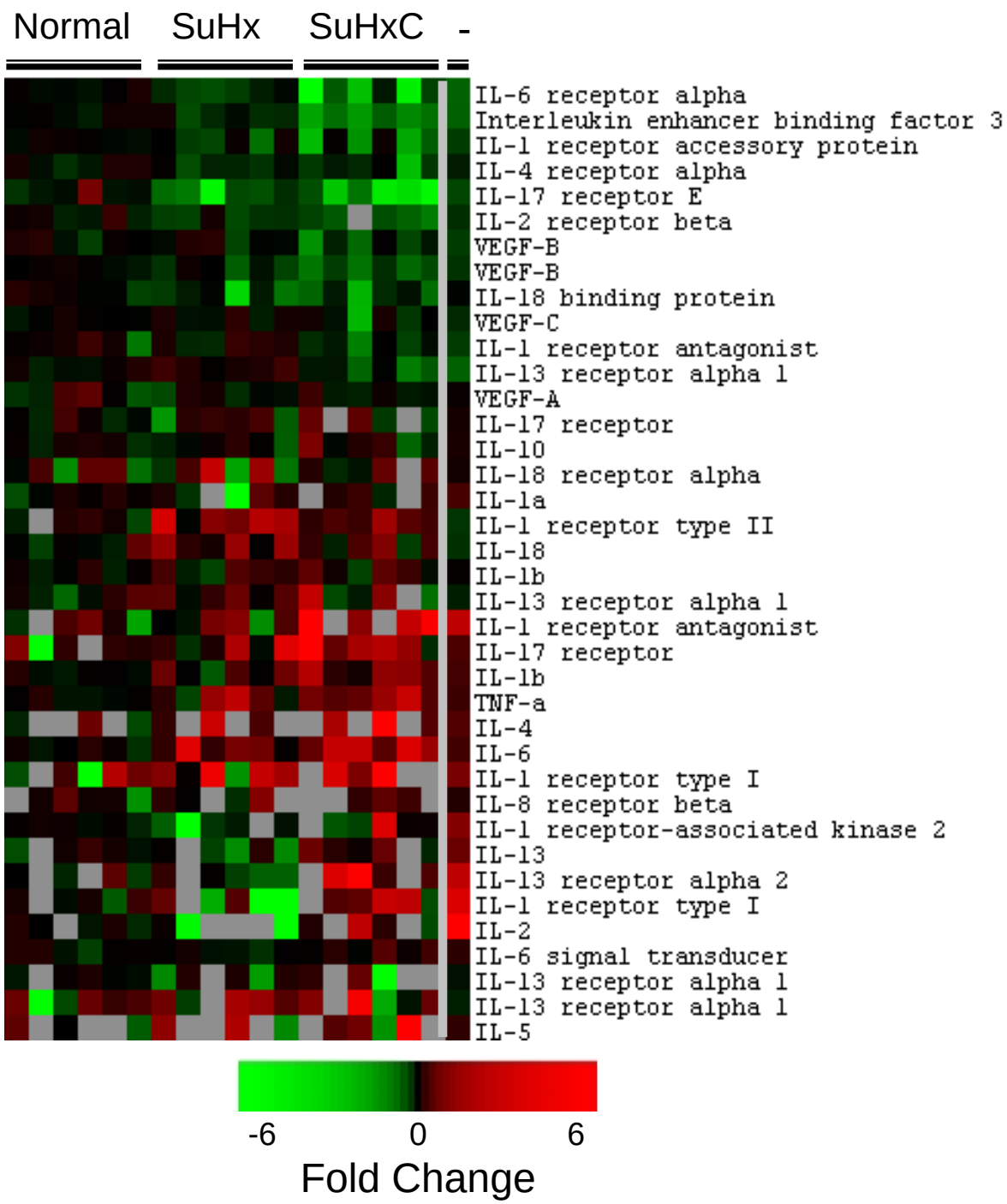
Normal
SuHx
SuHxC
-
IL-6 receptor alpha
Interleukin enhancer binding factor 3
IL-1 receptor accessory protein
IL-4 receptor alpha
IL-17 receptor E
IL-2 receptor beta
VEGF-B
VEGF-B
IL-18 binding protein
VEGF-C
IL-1 receptor antagonist
IL-13 receptor alpha 1
VEGF-A
IL-17 receptor
IL-10
IL-18 receptor alpha
IL-1a
IL-1 receptor type II
IL-18
IL-1b
IL-13 receptor alpha 1
IL-1 receptor antagonist
IL-17 receptor
IL-1b
TNF-a
IL-4
IL-6
IL-1 receptor type I
IL-8 receptor beta
IL-1 receptor-associated kinase 2
IL-13
IL-13 receptor alpha 2
IL-1 receptor type I
IL-2
IL-6 signal transducer
IL-13 receptor alpha 1
IL-13 receptor alpha 1
IL-5
-6
0
6
Fold Change

microarray only measures mRNA expression and the actual protein levels of these cytokines in the RV may be different due to post-translational mRNA modifications.

5.8 Discussion

Carvedilol, an $\alpha_1/\beta_1/\beta_2$-specific adrenergic receptor blocker, has been shown to improve the hemodynamics in the failing RV of the SU5416/hypoxia model, as well as reduce RV hypertrophy and dilation, myocardial fibrosis, and increase RV capillarization. Animals given carvedilol treatment after development of PAH from SU5416/hypoxia had an increased exercise capacity and survival rate. Here, we test whether the partial reversal of the RV failure in the SU5416/hypoxia model by carvedilol was also associated with a change of the RV-associated gene expression pattern. The gene expression pattern was analyzed by microarray analysis (**Figure 24**), prediction analysis (**Figure 28**), and class comparison analysis (**Figure 29**) to identify those signals that reverse failure.

Although the prediction analysis classified the SU5416/hypoxia + carvedilol predictor set as being most similar to the expression of the failing RV, it is clear from the class comparison analysis in **Figure 28** that there are distinct changes in gene expression between the failing and treated RVs, including genes involved in endothelin signaling and genes encoding mitochondrial electron transport chain complexes. Carvedilol treatment is associated with a reduction in translation initiation and epidermal growth factor receptor signaling, both of which are involved in the cardiac response to hypertrophy. A reduction in EGF signaling leads to reduced cardiac hypertrophy[424,

425]; similarly, a reduction in translation will also lead to a decrease in hypertrophy[416]. Treatment with carvedilol also increased expression of genes involved in PPAR and Nrf2-mediated signaling. These signaling pathways are activated while the heart compensates for increased pressure afterload[427, 429]. Additionally, the mitochondrial dysfunction pathway (**Figure 26**) and glycolysis/gluconeogenesis pathway (**Figure 31**) have been affected by carvedilol treatment. In both, there is a higher expression of genes in the failing (SU5416/hypoxia) RV than in the treated (SU5416/hypoxia + carvedilol) RV. As it is known that PAH causes a shift from oxidative phosphorylation to glucose metabolism and glycolysis[195, 196], this may be a return towards normal metabolism in the RV.

Treatment of the failing RV with carvedilol also changed the expression of the genes that were previously examined. While some, including *Ang1*, *Add3*, *apelin*, and *HIF-2a*, returned towards normal RV expression levels with carvedilol treatment, others, including *Aqp1*, *BNP*, and *Klf5*, increased further above normal RV and SU5416/hypoxia RV levels with carvedilol treatment. There was no change in *Igf1* expression in the SU5416/hypoxia + carvedilol RV. Although there is a change in some of the genes analyzed, it is unclear whether they are responsible for the functional improvement seen in the heart or whether they are a consequence of the RV functional improvement.

Carvedilol has been reported to decrease expression of pro-inflammatory cytokines and increase expression of anti-inflammatory cytokines[438, 439]. Microarray analysis (Figure 13) reflected these results in the expression of IL-18, which decreased with

carvedilol treatment, and increased expression of IL-10. However, an increase in mRNA expression of IL-1α, IL-1β, IL-2, IL-4, IL-5, IL-6, IL-13, and TNF-α was also found and is not consistent with literature results. There may be differences in protein levels in the RV that are not reflected in the mRNA results. In the serum, there were no significant differences in the expression of cytokines between the SU5416/hypoxia and SU5416/hypoxia + carvedilol samples. As such, the reported anti-inflammatory effects of carvedilol may not play a role in the reversal of RVF.

In the SU5416/hypoxia model of PAH, carvedilol treatment has improved RV function and reversed maladaptive RV remodeling. On a gene expression level, carvedilol affected key signaling pathways, including mitochondrial dysfunction, oxidative stress, and glycolysis. These changes in energy utilization should be studied further to examine the extent of metabolic remodeling caused by carvedilol treatment. In addition, further characterization of the signaling pathway activated by carvedilol in the heart to change gene expression should be undertaken. Silencing RNA (siRNA) has been used against β-arrestin to characterize the signaling pathway[442]; such a strategy could be employed to effectively knock-out β-arrestin in the carvedilol-treated rat model and compare the resulting RVF in the normal and knock-out rats. Finally, these results indicate the promise in using carvedilol to treat PAH in human patients. A Phase I/Phase II clinical trial on the safety and efficacy of carvedilol in PAH was started at Virginia Commonwealth University in 2011 (NCT00964678). Based on the results of these and additional trials, carvedilol may become a standard treatment for PAH patients.

Chapter 6: Discussion and Future Directions

6.1 Introduction

Pulmonary arterial hypertension (PAH) is associated with changes in gene expression in the right ventricle (RV) of the heart corresponding to physiological changes such as hypertrophy, capillary rarefaction, and reduced contractility. Identifying a therapeutic intervention that targets these changes in the RV has been a challenge for researchers. We show that carvedilol, a β-adrenergic receptor blocker, reduces hypertrophy, induces angiogenesis, and increases contractility; these physiological changes are associated with a change in gene expression. Here, we provide a brief overview of PAH before focusing more in-depth on the three aims of this study and its implications on future research directions.

PAH is a disease of the lung vessels in which vascular changes increase the pulmonary vascular resistance (PVR) which, in turn, leads to increase afterload in the right ventricle (RV) of the heart. Patients are diagnosed with PH if they have a mean pulmonary artery pressure of greater than 25 mmHg at rest or greater than 30 mmHg during exercise; a

normal mean pulmonary artery pressure is 8 – 20 mmHg at rest[1]. The mean pulmonary artery pressure increases in PAH patients as the PVR increases. The RV can adapt to the increase in pressure by hypertrophying – an increase in RV wall thickness through increased muscle mass and a more rounded shape[180]. The RV begins to fail as PH progresses, which is usually associated with RV dilation, a decrease in cardiac output[258], and a reduction in RV stroke volume[154]. Right ventricular failure (RVF) is the leading cause of death in patients with PH[255]. The estimated mean life span after diagnosis of PAH prior to the period of drug treatment is 2.8 years[8] with a 1-, 2-, and 3-year survival rate of 77%, 69%, and 35%[9].

Three classes of drugs are current standards of treatment for PH: prostanoids (prostacyclin and analogues like iloprost), endothelin receptor blocks (bosentan or ambristentan), and phosphodiesterase-5 inhibitors (sildenafil)[47, 48]. These drugs act as pulmonary vasodilators and there had been the hope that they would also reverse pulmonary vascular remodeling[47, 48]. However, they can have negative effects on the heart by increasing RV contractility, which causes an increase in oxygen[48]. While these treatments for PH focus on controlling symptoms and inducing pulmonary vasodilation, they do not address the aspect of RVF associated with PH. RVF is known to be reversible from studies of patients that have undergone lung transplant[368]. After lung transplant, a significant improvement in both pulmonary artery pressure and right ventricular function occur[374]. In addition, the 1-, 3-, and 5-year survival rates for PH patients after lung transplant increase to 77%, 62.6%, and 53.6%[375]. These studies

demonstrate that PH-associated RVF is reversible and motivate the search for pharmacological interventions that can reverse RVF.

In order to investigate the effectiveness of drugs on reversing right ventricular failure, it was necessary to first understand the changes in the RV that occur with hypertrophy and failure associated with PAH. The studies here aimed to address these questions in the following ways: 1) identifying the differences in gene expression between the normal right ventricle and normal left ventricle, 2) identifying changes in gene expression between the normal, hypertrophied, and failing right ventricle in animal models of pulmonary hypertension, and 3) identifying changes in gene expression in the failing right ventricle after treatment with carvedilol, an $\alpha_1/\beta_1/\beta_2$-adrenergic receptor blocker.

6.2 Identifying differences in gene expression between the normal LV and RV

Given that there are differences in embryology and physiology between the normal RV and normal LV, we identified a small, but significant, number of genes that were differentially expressed between the normal RV and normal LV using DNA microarray technology. These genes were indentified using the Significance Analysis of Micorarrays (SAM) two-class paired analysis[219]; 335 genes with identified as having significantly different patterns of expression between the normal RV and normal LV from the total 20,556 genes. These genes were clustered together using average-linkage hierarchical clustering[220] and pathway analysis using the PANTHER classification system[222,

223] and Ingenuity Pathway Analysis (http://www.ingenuity.com) identified molecular functions and differentially expressed pathways.

Differentially expressed genes are associated with known cardiac functions. The Wnt signaling pathway is active during development in the secondary heart field and helps promote growth and diversification of precursor cells in the RV[243]. Genes in this pathway had higher expression in the normal RV than the normal LV. Additionally, genes in the IGF-1/insulin signaling pathway are more highly expressed in the normal RV than the normal LV. Activation of this pathway leads to cardiomyocyte growth[244] and can control cell differentiation and apoptosis[245]. In contrast, genes involved in cell-cycle regulation and DNA damage repair were more highly expressed in the normal LV than the normal RV.

From cluster and pathway analysis, several genes were selected for follow-up by quantitative real-time polymerase chain reaction (qRT-PCR): *Nr2f2*, *Igf1*, *Irx2*, and *Nppb*. *Nr2f2*, also known as COUP-TFII (chicken ovalbumin upstream promoter-transcription factor 2) is required during development for angiogenesis[252]. *Igf1*, as previously mentioned, controls cardiomyocyte growth, differentiation, and apoptosis[244, 245]. *Irx2* is expressed during development in the interventricular septum and is thought to play a role in septum specification[253]. *Nppb* is the precursor to BNP, which is commonly used as a clinical marker of heart failure. These genes may provide insight into gene expression changes that occur during heart failure.

This study sought to identify differences in gene expression between the normal RV and normal LV. These data support the concept that the RV and LV should be evaluated independently rather than using the LV as the basis for studies of the RV. This study also serves as the basis for studies of changes in gene expression in the RV caused by hypertrophy and right ventricular failure associated with PH. Another unanswered question is whether the interventricular septum is part of the right or left ventricle. Microarray studies similar to those used above can answer this question both for the normal, unstressed heart and for the heart in PAH where the interventricular septum is shifted into the LV cavity impairing LV filling.

6.3 Identifying changes in gene expression between the normal, hypertrophied, and failing RV in animal models of PAH

Given that the normal RV and normal LV have different gene expression profiles, it can be hypothesized that RVF cannot *a priori* be described by known patterns of gene expression in the failing LV. In addition, we hypothesize that the transition from adaptive hypertrophy to RVF associated with the development of PAH will be associated with a change in gene expression. Using DNA microarray technology, the gene expression patterns associated with the normal RV, hypertrophied RV, and failing RV were examined in a rat model. Hypertrophy was induced by exposure to chronic hypoxia[283] while failure was induced by a combination of chronic hypoxia and administration of a vascular endothelial growth factor receptor (VEGFR) blocker SU5416[281]. Echocardiography and hemodynamic studies showed that the RV was fully functional in the chronically hypoxic and pulmonary hypertension rats, but that the

RV failed (had decreased cardiac output) in the SU5416/hypoxia rats. The SAM two-class unpaired analysis[219] was used to identify 3,595 genes with significantly different expression between the normal RV and the failing RV. In addition, a prediction set of 450 probes corresponding to 405 different genes that distinguish between the normal RV, hypertrophied RV, and failing RV was developed using four algorithms and leave one-out cross-validation[226-229]. These genes were analyzed with cluster analysis[220], the PANTHER classification system[222, 223], and Ingenuity Pathway Analysis (http://www.ingenuity.com) to identify biological functions and pathways associated with the differences in gene expression as the RV transitions from hypertrophy to failure.

There were several genes with shared expression patterns between the failing RV and the hypertrophied RV, including ANP, BNP, and hypoxia-inducible factor 2, alpha (*HIF-2*α). Increased expression of ANP and BNP can be expected from previously described reports[48, 181] as they are markers of heart stress and failure. *HIF-2*α expression is increased in response to hypoxia signaling[321] and enhances transcription of endothelial-specific genes related to angiogenesis and vessel maturation[324, 325]. Because these genes have increased expression in both the hypertrophied and failing RVs, it suggests that they are important to the adaptation to hypertrophy, but may not play a role in the transition to RVF. Several themes with different expression patterns between the failing RV and the hypertrophied RV became apparent in the analysis steps: elevated expression of glycolytic enzymes, loss of cell-growth promoting genes, impaired angiogenic capillary maintenance, and cytoskeletal rearrangement.

A switch from fatty acid oxidation to glycolysis has been reported in studies of left ventricular failure[354] and has been hypothesized to occur in the failing RV associated with PAH[198]. The increased expression of genes encoding glycolytic enzymes in the failing RV in this study suggests a shift in energy metabolism that has been described in left ventricular failure. In addition, the data show a downregulation of genes encoding mitochondrial electron transport chain complexes, which is known to be a characteristic of damaged and dysfunctional mitochondria in the failing heart[305]. These findings indicated that there are drastic changes in energy utilization as the RV transitions from hypertrophy to failure.

The studies described here as well as previous studies suggest that there is a shift from fatty acid oxidation to glycolysis in the failing RV. However, these are based on expression of mRNA of genes involved in the glycolytic and mitochondrial dysfunction pathways rather than studies of respiration in intact cardiac mitochondria. Single populations of cardiac mitochondria can be isolated from the normal and failing RVs[443]. Oxygen consumption by these intact mitochondria can be measured to determine the ADP/O ratio[444-446]. A lower ADP/O ratio indicates more oxygen used per unit of ADP provided in the assay and is an indication of impaired mitochondrial efficiency. We would expect to find that the failing RV from the SU5416/hypoxia rat has a lower ADP/O2 ratio than the normal rat based on our microarray results showing increased mitochondrial dysfunction and decreased expression of genes encoding mitochondrial electron transport chain subunits in the SU5416/hypoxia RV on the mRNA level.

Several genes, including *Igf1* and Kruppel-like factor 5 (*Klf5*), had an increased expression in the hypertrophied RV, but a decrease in expression in the failing RV. *Igf1* is transactivated by *Klf5* in cardiac fibroblasts and secreted to activated cardiomyocyte growth[244] and control cell differentiation and apoptosis[245]. Although increased expression of *Igf1* has been reported in cardiomyopathy[352] and in myocardial biopsies from failing hearts[353], we did not find an increase in *Igf1* expression in the failing rat RV. This suggests that cell-growth promoting genes are important in triggering a response to hypertrophy, and that a reduction in the expression of cell-growth promoting genes may characterize RV failure.

Based on these results, increasing expression of IGF-1 may prove to be beneficial to the failing heart. Mecasermin is a recombinant human insulin-like growth factor I (rhIGF-1) approved by the United States Food and Drug Administration in the fall of 2005 for use in treating severe primary IGF-1 deficiency[447]. Patients with growth hormone and IGF-1 deficiency have increased cardiac mortality[448], and studies are ongoing to see whether rhIGF-1 has a beneficial effect on heart failure in humans[449]. rhIGF-1 may also prove beneficial in the treatment of pulmonary hypertension because of the role of IGF-1 in adaptive, or beneficial, hypertrophy that is lost in the failing heart. We could induce PAH using the SU5416/hypoxia model as described in our studies here and then treat with mecasermin. After mecasermin treatment, hemodynamic measurements would be taken and the gene expression profile analyzed using microarrays and analysis techniques similar to those described here. We would expect to see a gene expression

profile more closely resembling the hypertrophied RV. However, mecasermin may need to be administered in combination with an existing therapy for PAH, such as sildenafil, to improve the hemodynamic performance in the heart. Future studies may also address the aspects of combination therapy of rhIGF-1 and another treatment.

This study sought to identify differences in RV gene expression between normal, hypertrophy, and failure. A set of genes that were descriptive of those changes and a set of genes that could predict those differences was identified and analyzed for common themes among the differences in gene expression. Our data show that there is a difference in expression between the hypertrophied and failing RV and the key pathways that may govern the transition from hypertrophy to failure associated with PAH. This data set also provides a basis for evaluating any changes in gene expression in the RV as a result of a pharmacological intervention, a treatment goal for PAH.

One possible pharmacological intervention for PAH is dexamethasone, an anti-inflammatory and immunosuppressive glucocorticoid used to treat inflammatory and autoimmune disorders[450]. Dexamethasone inhibits secretion of T-helper 1 (Th1) cells and enhances production of T-helper 2 (Th2) cytokines both in vitro and in vivo[451-453]. Small groups of patients with PAH due to connective tissue disorders including scleroderma, systemic lupus erythematosus (SLE), and mixed connective tissue diseases have been treated with a combination of immunosuppressant drugs and glucocorticoids resulting in an improvement of PAH symptoms[454]. Additionally, dexamethasone was used to prevent development of PAH in a rat monocrotaline model; these rats had

significantly decreased pulmonary artery pressure and RV hypertrophy compared to the monocrotaline-induced PAH rats[455]. While the prevention of PAH shows promising results, treatment with dexamethasone after development of PAH would be the most clinically relevant study. PAH could be induced using the SU5416/hypoxia model as described in our studies here followed by treatment with dexamethasone. Following several weeks of dexamethasone treatment, hemodynamic measurements would be taken and the gene expression profile analyzed using microarrays and analysis techniques similar to those described here. We would expect to see a decrease in RV hypertrophy compared to the untreated SU5416/hypoxia RV and a gene expression profile more closely resembling the normal or hypertrophied RV.

6.4 Identifying changes in gene expression in the failing RV after treatment with carvedilol

Treatment for PAH is currently focused on the use of vasodilators, endothelin-receptor blockers, and phosphodiesterase-5 inhibitors[47, 48], but none of these drugs have effects on reversing RVF. One possible pharmacological intervention is the use of β-adrenergic receptor blockers, which are often used in treatment of patients with left ventricular failure[378]. In recent animal studies, carvedilol, an $\alpha_1/\beta_1/\beta_2$-adrenergic receptor blocker[360], was tested as a treatment for PAH. Carvedilol had no effect on the pulmonary vascular remodeling in these animals, but did reduce RV hypertrophy and reverse the capillary rarefaction; increase cardiac output and stroke volume; and decrease fibrosis and cardiomyocyte apoptosis[360].

Although some changes in gene expression due to carvedilol treatment have been reported[360], a systematic study of the gene expression changes in the RV as a result of carvedilol treatment of a failing RV had not been done. Carvedilol was given to rats for four weeks after SU5416/chronic hypoxia treatment and the carvedilol-treated RV was compared to the untreated failing RV using DNA microarrays. Although the previously described prediction set classified the carvedilol-treated data set as being similar to the failing RV, other methods were used to identify genes that were different between the failing and carvedilol treated RV. A two-class unpaired SAM analysis[219] identified 4,714 genes that were differentially expressed between the failing RV and the carvedilol-treated RV. Additionally, a class comparison analysis[226, 413, 414] identified 489 genes that were significantly different between the failing and carvedilol-treated RV at a p-value < 0.001. The genes from these two analyses were analyzed with clustering algorithms[220], the PANTHER classification system[222, 223], and Ingenuity Pathway Analysis (http://www.ingenuity.com).

Previously discussed results demonstrate that the failing RV was characterized by a shift from fatty acid oxidation to glycolysis[197] and a decrease in expression of genes encoding mitochondrial electron transport chain complexes[198, 305]. With carvedilol treatment, there was an increase in the expression of mitochondrial electron transport chain genes and a decrease in expression of glycolytic enzymes, suggesting that there was a return towards normal myocardial metabolism in the heart after treatment with carvedilol. In addition, there was an increase in expression in genes in the peroxisome proliferator-acitvator receptor (PPAR) and nuclear factor-like 2 (*Nrf2*) signaling

pathways. PPAR-α is activated by PPAR coactivator-1, alpha (PGC-1α) and signals via Nrf2. PGC-1α and PPAR-α are preferentially expressed in the heart[427] and activate genes involved in the cellular uptake and mitochondrial activation of fatty acids[428]. PPAR-α plays an important role in the functional adaptation in the heart to pressure overload[427, 429]. An increase in the expression of genes in these signaling pathways in the carvedilol-treated RV suggests that a change in energy metabolism and mitochondrial function is important in reversing RVF. Targeting mitochondrial function pharmacologically may be an important aspect of clinical treatment for PAH.

In addition, signaling for fibrosis and integrin-like kinase (ILK) were increased in both the SU5416/hypoxia RV and the SU5416/hypoxia + carvedilol RV. TGF-β-mediated cardiac fibrosis can be induced by increased pressure afterload[289] and injury[214]. Similarly, increased pressure or afterload induces expression of rho-kinase (ROCK), which induces cardiac hypertrophy[288]. These pathways may be involved in mechanisms of cardiac compensation. Conversely, the SU5416/hypoxia RV and SU5416/hypoxia + carvedilol RV also show the same expression pattern for downregulated pathways, including protein ubiquitination and ERK/MAPK signaling. Without protein ubquitination pathway, pro-apoptotic proteins accumulate in the RV[314]. ERK signaling induces adaptive hypertrophic responses, such as cardiomyocyte growth and cytoskeletal rearrangement[456-458]. ERK signaling can also prevent myocardial damage, as is evident from studies of pre-ischemic conditioning[459]. Although these pathways may be maladaptive, changes in expression may or may not be required for “beneficial effects” of carvedilol on the overall function of the RV.

Carvedilol treatment of the failing RV also affected the expression of genes that were previously examined. mRNA expression of *Ang1*, *Add3*, *apelin*, and *HIF-2α* returned towards normal expression levels in the carvedilol-treated RV. However, *Aqp1*, *BNP*, and *Klf5* increased in expression further above normal RV and failing RV levels with carvedilol treatment. However, carvedilol had no apparent effect on changing serum cytokine levels from those observed in the SU5416/hypoxia animals, although there was a significant increase in the expression of IL-1β and VEGF from normal serum levels.

Although our data demonstrate that carvedilol changes gene expression in the failing RV, they are not descriptive of the mechanism by which carvedilol acts. Carvedilol acts as an $\alpha_1/\beta_1/\beta_2$-adrenergic receptor blocker, but also has antioxidant properties. Whether carvedilol-induced gene expression changes occur mainly via adrenergic receptor activity or via antioxidant activity in the failing heart has yet to be examined. In addition, the adrenergic receptors may signal either through G protein-coupled receptors to promote anti-apoptotic and mitogenic effects[383-386] or via β-arrestin to promote cardioprotective signals in response to mechanical stress[387]. The role of these two signaling pathways could be elucidated in future research by using siRNA to β-arrestin in the rat or by using β-arrestin knockout mice. We have demonstrated here that carvedilol treatment of normal rats is associated with increased mRNA expression of angiogeneic and growth factor genes. If these are a consequence of β-arrestin signaling rather than signaling through G-protein coupled receptors, there should be no increase in mRNA expression of those genes in animals lacking β-arrestin.

The data described here characterize a set of expressed genes that distinguishes between the normal RV and failing RV and between a failing RV and a carvedilol-treated RV. While changes in specific genes and pathways have been characterized, these changes are by no means a complete list of all of the genes associated with failure and recovery from RVF. In addition, it is unclear whether the genes and pathways described after carvedilol treatment are directly responsible for the functional improvement seen in the RV or are a consequence of functional RV improvement. Further examination of the present data set as well as time course studies to characterize the transition phase from compensated hypertrophy to RVF are necessary to more rigorously describe the mechanisms governing failure and recovery.

Although these data describe differences in the gene expression pattern between the normal, hypertrophies, failing, and treated RV, they are derived from an animal model of pulmonary hypertension (PH). As such, the same changes may or may not be present in other animal models of PH or in human heart tissue samples. These data may serve as the basis and reference for comparison to other animal models and to heart tissue samples from patients with PAH. Correlating these data with human sample data will be important for developing therapeutic strategies for human PAH.

Literature Cited

Literature Cited

1. Badesch, D.B., et al., *Diagnosis and assessment of pulmonary arterial hypertension.* J Am Coll Cardiol, 2009. **54**(1 Suppl): p. S55-66.
2. Hatano, S. and T. Strasser, *Primary pulmonary hypertension: report on a WHO meeting, Geneva, 15-17 October 1973*. 1975: World Health Organization.
3. Wagenvoort, C.A. and N. Wagenvoort, *Primary Pulmonary Hypertension: A Pathologic Study of the Lung Vessels in 156 Clinically Diagnosed Cases.* Circulation, 1970. **42**(6): p. 1163-1184.
4. Fishman, A.P., *Clinical classification of pulmonary hypertension.* Clin Chest Med, 2001. **22**(3): p. 385-91, vii.
5. Simonneau, G., et al., *Updated clinical classification of pulmonary hypertension.* J Am Coll Cardiol, 2009. **54**(1 Suppl): p. S43-54.
6. Gaine, S.P. and L.J. Rubin, *Primary pulmonary hypertension.* Lancet, 1998. **352**(9129): p. 719-25.
7. Humbert, M., et al., *Pulmonary arterial hypertension in France: results from a national registry.* Am J Respir Crit Care Med, 2006. **173**(9): p. 1023-30.
8. D'Alonzo, G.E., et al., *Survival in patients with primary pulmonary hypertension. Results from a national prospective registry.* Ann Intern Med, 1991. **115**(5): p. 343-9.
9. Hopkins, W.E., et al., *Comparison of the hemodynamics and survival of adults with severe primary pulmonary hypertension or Eisenmenger syndrome.* J Heart Lung Transplant, 1996. **15**(1 Pt 1): p. 100-5.
10. Tuder, R.M., et al., *Expression of angiogenesis-related molecules in plexiform lesions in severe pulmonary hypertension: evidence for a process of disordered angiogenesis.* J Pathol, 2001. **195**(3): p. 367-74.
11. Sakao, S., et al., *Initial apoptosis is followed by increased proliferation of apoptosis-resistant endothelial cells.* Faseb J, 2005. **19**(9): p. 1178-80.
12. Aldred, M.A., et al., *BMPR2 gene rearrangements account for a significant proportion of mutations in familial and idiopathic pulmonary arterial hypertension.* Hum Mutat, 2006. **27**(2): p. 212-3.
13. Cogan, J.D., et al., *High frequency of BMPR2 exonic deletions/duplications in familial pulmonary arterial hypertension.* Am J Respir Crit Care Med, 2006. **174**(5): p. 590-8.
14. Machado, R.D., et al., *Mutations of the TGF-beta type II receptor BMPR2 in pulmonary arterial hypertension.* Hum Mutat, 2006. **27**(2): p. 121-32.

15. Thomson, J.R., et al., *Sporadic primary pulmonary hypertension is associated with germline mutations of the gene encoding BMPR-II, a receptor member of the TGF-beta family.* J Med Genet, 2000. **37**(10): p. 741-5.
16. Elliott, C.G., et al., *Relationship of BMPR2 mutations to vasoreactivity in pulmonary arterial hypertension.* Circulation, 2006. **113**(21): p. 2509-15.
17. Rosenzweig, E.B., et al., *Clinical implications of determining BMPR2 mutation status in a large cohort of children and adults with pulmonary arterial hypertension.* J Heart Lung Transplant, 2008. **27**(6): p. 668-74.
18. Sztrymf, B., et al., *Clinical outcomes of pulmonary arterial hypertension in carriers of BMPR2 mutation.* Am J Respir Crit Care Med, 2008. **177**(12): p. 1377-83.
19. Chaouat, A., et al., *Endoglin germline mutation in a patient with hereditary haemorrhagic telangiectasia and dexfenfluramine associated pulmonary arterial hypertension.* Thorax, 2004. **59**(5): p. 446-8.
20. Trembath, R.C., et al., *Clinical and molecular genetic features of pulmonary hypertension in patients with hereditary hemorrhagic telangiectasia.* N Engl J Med, 2001. **345**(5): p. 325-34.
21. Simonneau, G., et al., *Clinical classification of pulmonary hypertension.* J Am Coll Cardiol, 2004. **43**(12 Suppl S): p. 5S-12S.
22. Garcia-Dorado, D., et al., *An epidemic of pulmonary hypertension after toxic rapeseed oil ingestion in Spain.* J Am Coll Cardiol, 1983. **1**(5): p. 1216-22.
23. Walker, A.M., et al., *Temporal trends and drug exposures in pulmonary hypertension: an American experience.* Am Heart J, 2006. **152**(3): p. 521-6.
24. Chambers, C.D., et al., *Selective serotonin-reuptake inhibitors and risk of persistent pulmonary hypertension of the newborn.* N Engl J Med, 2006. **354**(6): p. 579-87.
25. Hachulla, E., et al., *Early detection of pulmonary arterial hypertension in systemic sclerosis: a French nationwide prospective multicenter study.* Arthritis Rheum, 2005. **52**(12): p. 3792-800.
26. Mukerjee, D., et al., *Prevalence and outcome in systemic sclerosis associated pulmonary arterial hypertension: application of a registry approach.* Ann Rheum Dis, 2003. **62**(11): p. 1088-93.
27. Asherson, R.A., et al., *Pulmonary hypertension in a lupus clinic: experience with twenty-four patients.* J Rheumatol, 1990. **17**(10): p. 1292-8.
28. Tanaka, E., et al., *Pulmonary hypertension in systemic lupus erythematosus: evaluation of clinical characteristics and response to immunosuppressive treatment.* J Rheumatol, 2002. **29**(2): p. 282-7.
29. Burdt, M.A., et al., *Long-term outcome in mixed connective tissue disease: longitudinal clinical and serologic findings.* Arthritis Rheum, 1999. **42**(5): p. 899-909.
30. Jais, X., et al., *Immunosuppressive therapy in lupus- and mixed connective tissue disease-associated pulmonary arterial hypertension: a retrospective analysis of twenty-three cases.* Arthritis Rheum, 2008. **58**(2): p. 521-31.
31. Opravil, M., et al., *HIV-associated primary pulmonary hypertension. A case control study. Swiss HIV Cohort Study.* Am J Respir Crit Care Med, 1997. **155**(3): p. 990-5.

32. Sitbon, O., et al., *Prevalence of HIV-related pulmonary arterial hypertension in the current antiretroviral therapy era.* Am J Respir Crit Care Med, 2008. **177**(1): p. 108-13.
33. Wood, P., *The Eisenmenger syndrome or pulmonary hypertension with reversed central shunt. I.* Br Med J, 1958. **2**(5098): p. 701-9.
34. Galie, N., et al., *Management of pulmonary arterial hypertension associated with congenital systemic-to-pulmonary shunts and Eisenmenger's syndrome.* Drugs, 2008. **68**(8): p. 1049-66.
35. Lapa, M.S., et al., *[Clinical characteristics of pulmonary hypertension patients in two reference centers in the city of Sao Paulo].* Rev Assoc Med Bras, 2006. **52**(3): p. 139-43.
36. Chaves, E., *The pathology of the arterial pulmonary vasculature in manson's schistosomiasis.* Dis Chest, 1966. **50**(1): p. 72-7.
37. Warren, K.S., *Hepatosplenic schistosomiasis mansoni: an immunologic disease.* Bull N Y Acad Med, 1975. **51**(4): p. 545-50.
38. Lapa, M., et al., *Cardiopulmonary manifestations of hepatosplenic schistosomiasis.* Circulation, 2009. **119**(11): p. 1518-23.
39. Castro, O., M. Hoque, and B.D. Brown, *Pulmonary hypertension in sickle cell disease: cardiac catheterization results and survival.* Blood, 2003. **101**(4): p. 1257-61.
40. Gladwin, M.T., et al., *Pulmonary hypertension as a risk factor for death in patients with sickle cell disease.* N Engl J Med, 2004. **350**(9): p. 886-95.
41. Aessopos, A., et al., *Pulmonary hypertension and right heart failure in patients with beta-thalassemia intermedia.* Chest, 1995. **107**(1): p. 50-3.
42. Smedema, J.P. and V.J. Louw, *Pulmonary arterial hypertension after splenectomy for hereditary spherocytosis.* Cardiovasc J Afr, 2007. **18**(2): p. 84-9.
43. Kumar, V., et al., *Red blood cells and bleeding disorders*, in *Robbins and Cotran Pathologic Basis of Disease, Professional Edition, 8th Edition*, V. Kumar, et al., Editors. 2010, Saunders, an imprint of Elsevier, Inc.: Philadelphia, PA.
44. Jais, X., et al., *An extreme consequence of splenectomy in dehydrated hereditary stomatocytosis: gradual thrombo-embolic pulmonary hypertension and lung-heart transplantation.* Hemoglobin, 2003. **27**(3): p. 139-47.
45. Stuard, I.D., R.S. Heusinkveld, and A.J. Moss, *Microangiopathic hemolytic anemia and thrombocytopenia in primary pulmonary hypertension.* N Engl J Med, 1972. **287**(17): p. 869-70.
46. Parent, F., et al., *A hemodynamic study of pulmonary hypertension in sickle cell disease.* N Engl J Med, 2011. **365**(1): p. 44-53.
47. Archer, S.L., E.K. Weir, and M.R. Wilkins, *Basic science of pulmonary arterial hypertension for clinicians: new concepts and experimental therapies.* Circulation, 2010. **121**(18): p. 2045-66.
48. Bogaard, H.J., et al., *The right ventricle under pressure: cellular and molecular mechanisms of right-heart failure in pulmonary hypertension.* Chest, 2009. **135**(3): p. 794-804.
49. Montani, D., et al., *Pulmonary veno-occlusive disease.* Eur Respir J, 2009. **33**(1): p. 189-200.

50. Almagro, P., et al., *Pulmonary capillary hemangiomatosis associated with primary pulmonary hypertension: report of 2 new cases and review of 35 cases from the literature.* Medicine (Baltimore), 2002. **81**(6): p. 417-24.
51. Dorfmuller, P., et al., *Fibrous remodeling of the pulmonary venous system in pulmonary arterial hypertension associated with connective tissue diseases.* Hum Pathol, 2007. **38**(6): p. 893-902.
52. Escamilla, R., et al., *Pulmonary veno-occlusive disease in a HIV-infected intravenous drug abuser.* Eur Respir J, 1995. **8**(11): p. 1982-4.
53. Ruchelli, E.D., et al., *Pulmonary veno-occlusive disease. Another vascular disorder associated with human immunodeficiency virus infection?* Arch Pathol Lab Med, 1994. **118**(6): p. 664-6.
54. Montani, D., et al., *Pulmonary veno-occlusive disease: clinical, functional, radiologic, and hemodynamic characteristics and outcome of 24 cases confirmed by histology.* Medicine (Baltimore), 2008. **87**(4): p. 220-33.
55. Runo, J.R., et al., *Pulmonary veno-occlusive disease caused by an inherited mutation in bone morphogenetic protein receptor II.* Am J Respir Crit Care Med, 2003. **167**(6): p. 889-94.
56. Oudiz, R.J., *Pulmonary hypertension associated with left-sided heart disease.* Clin Chest Med, 2007. **28**(1): p. 233-41, x.
57. Costard-Jackle, A. and M.B. Fowler, *Influence of preoperative pulmonary artery pressure on mortality after heart transplantation: testing of potential reversibility of pulmonary hypertension with nitroprusside is useful in defining a high risk group.* J Am Coll Cardiol, 1992. **19**(1): p. 48-54.
58. Weitzenblum, E., et al., *Prognostic value of pulmonary artery pressure in chronic obstructive pulmonary disease.* Thorax, 1981. **36**(10): p. 752-8.
59. Thabut, G., et al., *Pulmonary hemodynamics in advanced COPD candidates for lung volume reduction surgery or lung transplantation.* Chest, 2005. **127**(5): p. 1531-6.
60. Fraser, K.L., et al., *Pulmonary hypertension and cardiac function in adult cystic fibrosis: role of hypoxemia.* Chest, 1999. **115**(5): p. 1321-8.
61. Cottin, V., et al., *Combined pulmonary fibrosis and emphysema: a distinct underrecognised entity.* Eur Respir J, 2005. **26**(4): p. 586-93.
62. Pengo, V., et al., *Incidence of chronic thromboembolic pulmonary hypertension after pulmonary embolism.* N Engl J Med, 2004. **350**(22): p. 2257-64.
63. Tapson, V.F. and M. Humbert, *Incidence and prevalence of chronic thromboembolic pulmonary hypertension: from acute to chronic pulmonary embolism.* Proc Am Thorac Soc, 2006. **3**(7): p. 564-7.
64. Hoeper, M.M., et al., *Chronic thromboembolic pulmonary hypertension.* Circulation, 2006. **113**(16): p. 2011-20.
65. Dartevelle, P., et al., *Chronic thromboembolic pulmonary hypertension.* Eur Respir J, 2004. **23**(4): p. 637-48.
66. Jamieson, S.W., et al., *Pulmonary endarterectomy: experience and lessons learned in 1,500 cases.* Ann Thorac Surg, 2003. **76**(5): p. 1457-62; discussion 1462-4.
67. Dingli, D., et al., *Unexplained pulmonary hypertension in chronic myeloproliferative disorders.* Chest, 2001. **120**(3): p. 801-8.

68. Marvin, K.S. and R.D. Spellberg, *Pulmonary hypertension secondary to thrombocytosis in a patient with myeloid metaplasia.* Chest, 1993. **103**(2): p. 642-4.
69. Nand, S. and E. Orfei, *Pulmonary hypertension in polycythemia vera.* Am J Hematol, 1994. **47**(3): p. 242-4.
70. Peacock, A.J., *Pulmonary hypertension after splenectomy: a consequence of loss of the splenic filter or is there something more?* Thorax, 2005. **60**(12): p. 983-4.
71. Torregrosa, M., et al., *Role of Doppler echocardiography in the assessment of portopulmonary hypertension in liver transplantation candidates.* Transplantation, 2001. **71**(4): p. 572-4.
72. Iannuzzi, M.C., B.A. Rybicki, and A.S. Teirstein, *Sarcoidosis.* N Engl J Med, 2007. **357**(21): p. 2153-65.
73. Gluskowski, J., et al., *Pulmonary haemodynamics at rest and during exercise in patients with sarcoidosis.* Respiration, 1984. **46**(1): p. 26-32.
74. Shorr, A.F., et al., *Pulmonary hypertension in advanced sarcoidosis: epidemiology and clinical characteristics.* Eur Respir J, 2005. **25**(5): p. 783-8.
75. Dauriat, G., et al., *Lung transplantation for pulmonary langerhans' cell histiocytosis: a multicenter analysis.* Transplantation, 2006. **81**(5): p. 746-50.
76. Aubry, M.C., et al., *Pulmonary lymphangioleiomyomatosis in a man.* Am J Respir Crit Care Med, 2000. **162**(2 Pt 1): p. 749-52.
77. Taveira-DaSilva, A.M., et al., *Pulmonary artery pressure in lymphangioleiomyomatosis: an echocardiographic study.* Chest, 2007. **132**(5): p. 1573-8.
78. Harari, S., et al., *Prognostic value of pulmonary hypertension in patients with chronic interstitial lung disease referred for lung or heart-lung transplantation.* J Heart Lung Transplant, 1997. **16**(4): p. 460-3.
79. Aoki, Y., et al., *von Recklinghausen disease complicated by pulmonary hypertension.* Chest, 2001. **119**(5): p. 1606-8.
80. Engel, P.J., et al., *Pulmonary hypertension in neurofibromatosis.* Am J Cardiol, 2007. **99**(8): p. 1177-8.
81. Samuels, N., et al., *Pulmonary hypertension secondary to neurofibromatosis: intimal fibrosis versus thromboembolism.* Thorax, 1999. **54**(9): p. 858-9.
82. Simeoni, S., et al., *Type 1 neurofibromatosis complicated by pulmonary artery hypertension: a case report.* J Med Invest, 2007. **54**(3-4): p. 354-8.
83. Hamaoka, K., et al., *Pulmonary hypertension in type I glycogen storage disease.* Pediatr Cardiol, 1990. **11**(1): p. 54-6.
84. Humbert, M., et al., *Pulmonary arterial hypertension and type-I glycogen-storage disease: the serotonin hypothesis.* Eur Respir J, 2002. **20**(1): p. 59-65.
85. Inoue, S., et al., *[Pulmonary hypertension due to glycogen storage disease type II (Pompe's disease): a case report].* J Cardiol, 1989. **19**(1): p. 323-32.
86. Elstein, D., et al., *Echocardiographic assessment of pulmonary hypertension in Gaucher's disease.* Lancet, 1998. **351**(9115): p. 1544-6.
87. Ferris, A., et al., *Pulmonary arterial hypertension and thyroid disease.* Chest, 2001. **119**(6): p. 1980-1.
88. Li, J.H., et al., *Pulmonary hypertension and thyroid disease.* Chest, 2007. **132**(3): p. 793-7.

89. Merce, J., et al., *Cardiovascular abnormalities in hyperthyroidism: a prospective Doppler echocardiographic study.* Am J Med, 2005. **118**(2): p. 126-31.
90. Chu, J.W., et al., *High prevalence of autoimmune thyroid disease in pulmonary arterial hypertension.* Chest, 2002. **122**(5): p. 1668-73.
91. Anderson, M.B., et al., *Primary pulmonary artery sarcoma: a report of six cases.* Ann Thorac Surg, 1995. **59**(6): p. 1487-90.
92. Mayer, E., et al., *Surgical treatment of pulmonary artery sarcoma.* J Thorac Cardiovasc Surg, 2001. **121**(1): p. 77-82.
93. Roberts, K.E., et al., *Pulmonary tumor embolism: a review of the literature.* Am J Med, 2003. **115**(3): p. 228-32.
94. Davis, A.M., R.N. Pierson, and J.E. Loyd, *Mediastinal fibrosis.* Semin Respir Infect, 2001. **16**(2): p. 119-30.
95. Loyd, J.E., et al., *Mediastinal fibrosis complicating histoplasmosis.* Medicine (Baltimore), 1988. **67**(5): p. 295-310.
96. Yigla, M., et al., *Pulmonary hypertension in patients with end-stage renal disease.* Chest, 2003. **123**(5): p. 1577-82.
97. Garcia-Martinez, V. and G.C. Schoenwolf, *Primitive-streak origin of the cardiovascular system in avian embryos.* Dev Biol, 1993. **159**(2): p. 706-19.
98. Hatada, Y. and C.D. Stern, *A fate map of the epiblast of the early chick embryo.* Development, 1994. **120**(10): p. 2879-89.
99. Abu-Issa, R. and M.L. Kirby, *Heart field: from mesoderm to heart tube.* Annu Rev Cell Dev Biol, 2007. **23**: p. 45-68.
100. Buckingham, M., S. Meilhac, and S. Zaffran, *Building the mammalian heart from two sources of myocardial cells.* Nat Rev Genet, 2005. **6**(11): p. 826-35.
101. Garry, D.J. and E.N. Olson, *A common progenitor at the heart of development.* Cell, 2006. **127**(6): p. 1101-4.
102. Srivastava, D., *Making or breaking the heart: from lineage determination to morphogenesis.* Cell, 2006. **126**(6): p. 1037-48.
103. Srivastava, D. and E.N. Olson, *A genetic blueprint for cardiac development.* Nature, 2000. **407**(6801): p. 221-6.
104. Bu, L., et al., *Human ISL1 heart progenitors generate diverse multipotent cardiovascular cell lineages.* Nature, 2009. **460**(7251): p. 113-7.
105. Kattman, S.J., T.L. Huber, and G.M. Keller, *Multipotent flk-1+ cardiovascular progenitor cells give rise to the cardiomyocyte, endothelial, and vascular smooth muscle lineages.* Dev Cell, 2006. **11**(5): p. 723-32.
106. Moretti, A., et al., *Multipotent embryonic isl1+ progenitor cells lead to cardiac, smooth muscle, and endothelial cell diversification.* Cell, 2006. **127**(6): p. 1151-65.
107. Cai, C.L., et al., *Isl1 identifies a cardiac progenitor population that proliferates prior to differentiation and contributes a majority of cells to the heart.* Dev Cell, 2003. **5**(6): p. 877-89.
108. Kelly, R.G., N.A. Brown, and M.E. Buckingham, *The arterial pole of the mouse heart forms from Fgf10-expressing cells in pharyngeal mesoderm.* Dev Cell, 2001. **1**(3): p. 435-40.
109. Brand, T., *Heart development: molecular insights into cardiac specification and early morphogenesis.* Dev Biol, 2003. **258**(1): p. 1-19.

110. Kuo, C.T., et al., *GATA4 transcription factor is required for ventral morphogenesis and heart tube formation.* Genes Dev, 1997. **11**(8): p. 1048-60.
111. Li, S., et al., *Advanced cardiac morphogenesis does not require heart tube fusion.* Science, 2004. **305**(5690): p. 1619-22.
112. Molkentin, J.D., et al., *Requirement of the transcription factor GATA4 for heart tube formation and ventral morphogenesis.* Genes Dev, 1997. **11**(8): p. 1061-72.
113. Lyons, I., et al., *Myogenic and morphogenetic defects in the heart tubes of murine embryos lacking the homeo box gene Nkx2-5.* Genes Dev, 1995. **9**(13): p. 1654-66.
114. Tanaka, M., et al., *Complex modular cis-acting elements regulate expression of the cardiac specifying homeobox gene Csx/Nkx2.5.* Development, 1999. **126**(7): p. 1439-50.
115. Yamagishi, H., et al., *The combinatorial activities of Nkx2.5 and dHAND are essential for cardiac ventricle formation.* Dev Biol, 2001. **239**(2): p. 190-203.
116. Firulli, A.B., et al., *Heart and extra-embryonic mesodermal defects in mouse embryos lacking the bHLH transcription factor Hand1.* Nat Genet, 1998. **18**(3): p. 266-70.
117. McFadden, D.G., et al., *The Hand1 and Hand2 transcription factors regulate expansion of the embryonic cardiac ventricles in a gene dosage-dependent manner.* Development, 2005. **132**(1): p. 189-201.
118. Riley, P., L. Anson-Cartwright, and J.C. Cross, *The Hand1 bHLH transcription factor is essential for placentation and cardiac morphogenesis.* Nat Genet, 1998. **18**(3): p. 271-5.
119. Bruneau, B.G., et al., *A murine model of Holt-Oram syndrome defines roles of the T-box transcription factor Tbx5 in cardiogenesis and disease.* Cell, 2001. **106**(6): p. 709-21.
120. Srivastava, D., P. Cserjesi, and E.N. Olson, *A subclass of bHLH proteins required for cardiac morphogenesis.* Science, 1995. **270**(5244): p. 1995-9.
121. Srivastava, D., et al., *Regulation of cardiac mesodermal and neural crest development by the bHLH transcription factor, dHAND.* Nat Genet, 1997. **16**(2): p. 154-60.
122. Thomas, T., et al., *A signaling cascade involving endothelin-1, dHAND and msx1 regulates development of neural-crest-derived branchial arch mesenchyme.* Development, 1998. **125**(16): p. 3005-14.
123. Waldo, K.L., et al., *Conotruncal myocardium arises from a secondary heart field.* Development, 2001. **128**(16): p. 3179-88.
124. Min, H., et al., *Fgf-10 is required for both limb and lung development and exhibits striking functional similarity to Drosophila branchless.* Genes Dev, 1998. **12**(20): p. 3156-61.
125. Sekine, K., et al., *Fgf10 is essential for limb and lung formation.* Nat Genet, 1999. **21**(1): p. 138-41.
126. Abu-Issa, R., et al., *Fgf8 is required for pharyngeal arch and cardiovascular development in the mouse.* Development, 2002. **129**(19): p. 4613-25.
127. Frank, D.U., et al., *An Fgf8 mouse mutant phenocopies human 22q11 deletion syndrome.* Development, 2002. **129**(19): p. 4591-603.

128. Garg, V., et al., *Tbx1, a DiGeorge syndrome candidate gene, is regulated by sonic hedgehog during pharyngeal arch development.* Dev Biol, 2001. **235**(1): p. 62-73.
129. Jerome, L.A. and V.E. Papaioannou, *DiGeorge syndrome phenotype in mice mutant for the T-box gene, Tbx1.* Nat Genet, 2001. **27**(3): p. 286-91.
130. Lindsay, E.A., et al., *Tbx1 haploinsufficieny in the DiGeorge syndrome region causes aortic arch defects in mice.* Nature, 2001. **410**(6824): p. 97-101.
131. Merscher, S., et al., *TBX1 is responsible for cardiovascular defects in velo-cardio-facial/DiGeorge syndrome.* Cell, 2001. **104**(4): p. 619-29.
132. Xu, H., et al., *Tbx1 has a dual role in the morphogenesis of the cardiac outflow tract.* Development, 2004. **131**(13): p. 3217-27.
133. Dodou, E., et al., *Mef2c is a direct transcriptional target of ISL1 and GATA factors in the anterior heart field during mouse embryonic development.* Development, 2004. **131**(16): p. 3931-42.
134. Lin, Q., et al., *Control of mouse cardiac morphogenesis and myogenesis by transcription factor MEF2C.* Science, 1997. **276**(5317): p. 1404-7.
135. Anderson, R.H., et al., *Development of the heart: (2) Septation of the atriums and ventricles.* Heart, 2003. **89**(8): p. 949-58.
136. Anderson, R.H., et al., *Development of the heart: (3) formation of the ventricular outflow tracts, arterial valves, and intrapericardial arterial trunks.* Heart, 2003. **89**(9): p. 1110-8.
137. Moorman, A., et al., *Development of the heart: (1) formation of the cardiac chambers and arterial trunks.* Heart, 2003. **89**(7): p. 806-14.
138. Heymann, M.A., *Control of the pulmonary circulation in the fetus and during the transitional period to air breathing.* Eur J Obstet Gynecol Reprod Biol, 1999. **84**(2): p. 127-32.
139. Kiserud, T. and G. Acharya, *The fetal circulation.* Prenat Diagn, 2004. **24**(13): p. 1049-59.
140. Rudolph, A.M., *The changes in the circulation after birth. Their importance in congenital heart disease.* Circulation, 1970. **41**(2): p. 343-59.
141. Voelkel, N.F., et al., *Right Ventricle in Pulmonary Hypertension.* Comprehensive Physiology, 2011. **1**: p. 525-540.
142. Rudolph, A.M., *Myocardial growth before and after birth: clinical implications.* Acta Paediatr, 2000. **89**(2): p. 129-33.
143. Emmanouilides, G.C., et al., *Pulmonary Arterial Pressure Changes In Human Newborn Infants From Birth To 3 Days Of Age.* J Pediatr, 1964. **65**: p. 327-33.
144. Dell'Italia, L.J., *The right ventricle: anatomy, physiology, and clinical importance.* Curr Probl Cardiol, 1991. **16**(10): p. 653-720.
145. Quartermain, M.D., et al., *Left ventricle to right ventricle size discrepancy in the fetus: the presence of critical congenital heart disease can be reliably predicted.* J Am Soc Echocardiogr, 2009. **22**(11): p. 1296-301.
146. Ho, S.Y. and P. Nihoyannopoulos, *Anatomy, echocardiography, and normal right ventricular dimensions.* Heart, 2006. **92 Suppl 1**: p. i2-13.
147. Greyson, C.R., *The right ventricle and pulmonary circulation: basic concepts.* Rev Esp Cardiol, 2010. **63**(1): p. 81-95.

148. Lorenz, C.H., et al., *Normal human right and left ventricular mass, systolic function, and gender differences by cine magnetic resonance imaging.* J Cardiovasc Magn Reson, 1999. **1**(1): p. 7-21.
149. Huang, W., et al., *Morphometry of the human pulmonary vasculature.* J Appl Physiol, 1996. **81**(5): p. 2123-33.
150. Grant, B.J. and L.J. Paradowski, *Characterization of pulmonary arterial input impedance with lumped parameter models.* Am J Physiol, 1987. **252**(3 Pt 2): p. H585-93.
151. Paredi, P. and P.J. Barnes, *The airway vasculature: recent advances and clinical implications.* Thorax, 2009. **64**(5): p. 444-50.
152. Singhal, S., et al., *Morphometry of the human pulmonary arterial tree.* Circ Res, 1973. **33**(2): p. 190-7.
153. Meier, G.D., et al., *Contractile function in canine right ventricle.* Am J Physiol, 1980. **239**(6): p. H794-804.
154. Matthews, J.C. and V. McLaughlin, *Acute right ventricular failure in the setting of acute pulmonary embolism or chronic pulmonary hypertension: a detailed review of the pathophysiology, diagnosis, and management.* Curr Cardiol Rev, 2008. **4**(1): p. 49-59.
155. Homik, L.A., et al., *Effect of alveolar hypoxia on pulmonary fluid filtration in in situ dog lungs.* J Appl Physiol, 1988. **65**(1): p. 46-52.
156. Mann, D.L., *Basic mechanisms of left ventricular remodeling: the contribution of wall stress.* J Card Fail, 2004. **10**(6 Suppl): p. S202-6.
157. Katsumi, A., et al., *Integrins in mechanotransduction.* J Biol Chem, 2004. **279**(13): p. 12001-4.
158. Ross, R.S., et al., *Beta1 integrins participate in the hypertrophic response of rat ventricular myocytes.* Circ Res, 1998. **82**(11): p. 1160-72.
159. Sharma, S., et al., *Dynamic changes of gene expression in hypoxia-induced right ventricular hypertrophy.* Am J Physiol Heart Circ Physiol, 2004. **286**(3): p. H1185-92.
160. Oikawa, M., et al., *Increased [18F]fluorodeoxyglucose accumulation in right ventricular free wall in patients with pulmonary hypertension and the effect of epoprostenol.* J Am Coll Cardiol, 2005. **45**(11): p. 1849-55.
161. Ferguson, S., et al., *Cardiac performance in endurance-trained and moderately active young women.* Med Sci Sports Exerc, 2001. **33**(7): p. 1114-9.
162. Gledhill, N., D. Cox, and R. Jamnik, *Endurance athletes' stroke volume does not plateau: major advantage is diastolic function.* Med Sci Sports Exerc, 1994. **26**(9): p. 1116-21.
163. Pelliccia, A. and B.J. Maron, *Outer limits of the athlete's heart, the effect of gender, and relevance to the differential diagnosis with primary cardiac diseases.* Cardiol Clin, 1997. **15**(3): p. 381-96.
164. Pluim, B.M., et al., *The athlete's heart. A meta-analysis of cardiac structure and function.* Circulation, 2000. **101**(3): p. 336-44.
165. Schaible, T.F. and J. Scheuer, *Cardiac function in hypertrophied hearts from chronically exercised female rats.* J Appl Physiol, 1981. **50**(6): p. 1140-5.
166. Wiebe, C.G., et al., *Exercise cardiac function in endurance-trained males versus females.* Clin J Sport Med, 1998. **8**(4): p. 272-9.

167. Richardson, R.S., *Oxygen transport: air to muscle cell.* Med Sci Sports Exerc, 1998. **30**(1): p. 53-9.
168. Dorn, G.W., 2nd and T. Force, *Protein kinase cascades in the regulation of cardiac hypertrophy.* J Clin Invest, 2005. **115**(3): p. 527-37.
169. Godfrey, R.J., Z. Madgwick, and G.P. Whyte, *The exercise-induced growth hormone response in athletes.* Sports Med, 2003. **33**(8): p. 599-613.
170. Latronico, M.V., et al., *Regulation of cell size and contractile function by AKT in cardiomyocytes.* Ann N Y Acad Sci, 2004. **1015**: p. 250-60.
171. McMullen, J.R., et al., *Phosphoinositide 3-kinase(p110alpha) plays a critical role for the induction of physiological, but not pathological, cardiac hypertrophy.* Proc Natl Acad Sci U S A, 2003. **100**(21): p. 12355-60.
172. Neri Serneri, G.G., et al., *Increased cardiac sympathetic activity and insulin-like growth factor-I formation are associated with physiological hypertrophy in athletes.* Circ Res, 2001. **89**(11): p. 977-82.
173. Walsh, K., *Akt signaling and growth of the heart.* Circulation, 2006. **113**(17): p. 2032-4.
174. McMullen, J.R., et al., *The insulin-like growth factor 1 receptor induces physiological heart growth via the phosphoinositide 3-kinase(p110alpha) pathway.* J Biol Chem, 2004. **279**(6): p. 4782-93.
175. Kemi, O.J., et al., *Activation or inactivation of cardiac Akt/mTOR signaling diverges physiological from pathological hypertrophy.* J Cell Physiol, 2008. **214**(2): p. 316-21.
176. Frey, N. and E.N. Olson, *Cardiac hypertrophy: the good, the bad, and the ugly.* Annu Rev Physiol, 2003. **65**: p. 45-79.
177. Molkentin, J.D. and G.W. Dorn, 2nd, *Cytoplasmic signaling pathways that regulate cardiac hypertrophy.* Annu Rev Physiol, 2001. **63**: p. 391-426.
178. Willis, M.S. and C. Patterson, *Into the heart: the emerging role of the ubiquitin-proteasome system.* J Mol Cell Cardiol, 2006. **41**(4): p. 567-79.
179. Morisco, C., et al., *Is treating cardiac hypertrophy salutary or detrimental: the two faces of Janus.* Am J Physiol Heart Circ Physiol, 2003. **284**(4): p. H1043-7.
180. Bogaard, H.J., et al., *Chronic pulmonary artery pressure elevation is insufficient to explain right heart failure.* Circulation, 2009. **120**(20): p. 1951-60.
181. Lowes, B.D., et al., *Changes in gene expression in the intact human heart. Downregulation of alpha-myosin heavy chain in hypertrophied, failing ventricular myocardium.* J Clin Invest, 1997. **100**(9): p. 2315-24.
182. Herron, T.J. and K.S. McDonald, *Small amounts of alpha-myosin heavy chain isoform expression significantly increase power output of rat cardiac myocyte fragments.* Circ Res, 2002. **90**(11): p. 1150-2.
183. Opie, L.H., *Mechanisms of Cardiac Contraction and Relaxation*, in *Braunwald's Heart Disease: A Textbook of Cardiovascular Medicine*, P. Libby, et al., Editors. 2008, Saunders Elsevier: Philadelphia, PA. p. 509-539.
184. Ross, R.S., *Right ventricular hypertension as a cause of precordial pain.* Am Heart J, 1961. **61**: p. 134-5.
185. van Wolferen, S.A., et al., *Right coronary artery flow impairment in patients with pulmonary hypertension.* Eur Heart J, 2008. **29**(1): p. 120-7.

186. Gomez, A., et al., *Right ventricular ischemia in patients with primary pulmonary hypertension.* J Am Coll Cardiol, 2001. **38**(4): p. 1137-42.
187. Tomanek, R.J., *Response of the coronary vasculature to myocardial hypertrophy.* J Am Coll Cardiol, 1990. **15**(3): p. 528-33.
188. Saito, D., et al., *Oxygen metabolism of the hypertrophic right ventricle in open chest dogs.* Cardiovasc Res, 1991. **25**(9): p. 731-9.
189. Giordano, F.J., *Oxygen, oxidative stress, hypoxia, and heart failure.* J Clin Invest, 2005. **115**(3): p. 500-8.
190. Cappola, T.P., et al., *Allopurinol improves myocardial efficiency in patients with idiopathic dilated cardiomyopathy.* Circulation, 2001. **104**(20): p. 2407-11.
191. Heymes, C., et al., *Increased myocardial NADPH oxidase activity in human heart failure.* J Am Coll Cardiol, 2003. **41**(12): p. 2164-71.
192. Hare, J.M. and J.S. Stamler, *NO/redox disequilibrium in the failing heart and cardiovascular system.* J Clin Invest, 2005. **115**(3): p. 509-17.
193. Kuzkaya, N., et al., *Interactions of peroxynitrite, tetrahydrobiopterin, ascorbic acid, and thiols: implications for uncoupling endothelial nitric-oxide synthase.* J Biol Chem, 2003. **278**(25): p. 22546-54.
194. Morrell, N.W., et al., *Cellular and molecular basis of pulmonary arterial hypertension.* J Am Coll Cardiol, 2009. **54**(1 Suppl): p. S20-31.
195. Archer, S.L., et al., *Mitochondrial metabolism, redox signaling, and fusion: a mitochondria-ROS-HIF-1alpha-Kv1.5 O2-sensing pathway at the intersection of pulmonary hypertension and cancer.* Am J Physiol Heart Circ Physiol, 2008. **294**(2): p. H570-8.
196. Bonnet, S., et al., *An abnormal mitochondrial-hypoxia inducible factor-1alpha-Kv channel pathway disrupts oxygen sensing and triggers pulmonary arterial hypertension in fawn hooded rats: similarities to human pulmonary arterial hypertension.* Circulation, 2006. **113**(22): p. 2630-41.
197. Voelkel, N.F., et al., *Primary pulmonary hypertension between inflammation and cancer.* Chest, 1998. **114**(3 Suppl): p. 225S-230S.
198. Piao, L., G. Marsboom, and S.L. Archer, *Mitochondrial metabolic adaptation in right ventricular hypertrophy and failure.* J Mol Med, 2010. **88**(10): p. 1011-20.
199. Dang, C.V., et al., *The interplay between MYC and HIF in cancer.* Nat Rev Cancer, 2008. **8**(1): p. 51-6.
200. Nagendran, J., et al., *A dynamic and chamber-specific mitochondrial remodeling in right ventricular hypertrophy can be therapeutically targeted.* J Thorac Cardiovasc Surg, 2008. **136**(1): p. 168-78, 178 e1-3.
201. Soonpaa, M.H. and L.J. Field, *Survey of studies examining mammalian cardiomyocyte DNA synthesis.* Circ Res, 1998. **83**(1): p. 15-26.
202. Hein, S., et al., *Progression from compensated hypertrophy to failure in the pressure-overloaded human heart: structural deterioration and compensatory mechanisms.* Circulation, 2003. **107**(7): p. 984-91.
203. Olivetti, G., et al., *Apoptosis in the failing human heart.* N Engl J Med, 1997. **336**(16): p. 1131-41.
204. Kang, P.M. and S. Izumo, *Apoptosis in heart failure: is there light at the end of the tunnel (TUNEL)?* J Card Fail, 2000. **6**(1): p. 43-6.

205. Wencker, D., et al., *A mechanistic role for cardiac myocyte apoptosis in heart failure.* J Clin Invest, 2003. **111**(10): p. 1497-504.
206. Foo, R.S., K. Mani, and R.N. Kitsis, *Death begets failure in the heart.* J Clin Invest, 2005. **115**(3): p. 565-71.
207. Black, S.C., et al., *Co-localization of the cysteine protease caspase-3 with apoptotic myocytes after in vivo myocardial ischemia and reperfusion in the rat.* J Mol Cell Cardiol, 1998. **30**(4): p. 733-42.
208. Holly, T.A., et al., *Caspase inhibition reduces myocyte cell death induced by myocardial ischemia and reperfusion in vivo.* J Mol Cell Cardiol, 1999. **31**(9): p. 1709-15.
209. Yaoita, H., et al., *Attenuation of ischemia/reperfusion injury in rats by a caspase inhibitor.* Circulation, 1998. **97**(3): p. 276-81.
210. Mann, D.L., *Inflammatory mediators and the failing heart: past, present, and the foreseeable future.* Circ Res, 2002. **91**(11): p. 988-98.
211. Bozkurt, B., et al., *Pathophysiologically relevant concentrations of tumor necrosis factor-alpha promote progressive left ventricular dysfunction and remodeling in rats.* Circulation, 1998. **97**(14): p. 1382-91.
212. Madge, L.A. and J.S. Pober, *TNF signaling in vascular endothelial cells.* Exp Mol Pathol, 2001. **70**(3): p. 317-25.
213. Krown, K.A., et al., *Tumor necrosis factor alpha-induced apoptosis in cardiac myocytes. Involvement of the sphingolipid signaling cascade in cardiac cell death.* J Clin Invest, 1996. **98**(12): p. 2854-65.
214. Sun, M., et al., *Tumor necrosis factor-alpha mediates cardiac remodeling and ventricular dysfunction after pressure overload state.* Circulation, 2007. **115**(11): p. 1398-407.
215. Hosenpud, J.D., S.M. Campbell, and D.J. Mendelson, *Interleukin-1-induced myocardial depression in an isolated beating heart preparation.* J Heart Transplant, 1989. **8**(6): p. 460-4.
216. Thaik, C.M., et al., *Interleukin-1 beta modulates the growth and phenotype of neonatal rat cardiac myocytes.* J Clin Invest, 1995. **96**(2): p. 1093-9.
217. Sanada, S., et al., *IL-33 and ST2 comprise a critical biomechanically induced and cardioprotective signaling system.* J Clin Invest, 2007. **117**(6): p. 1538-49.
218. Killion, P.J., G. Sherlock, and V.R. Iyer, *The Longhorn Array Database (LAD): an open-source, MIAME compliant implementation of the Stanford Microarray Database (SMD).* BMC Bioinformatics, 2003. **4**: p. 32.
219. Tusher, V.G., R. Tibshirani, and G. Chu, *Significance analysis of microarrays applied to the ionizing radiation response.* Proc Natl Acad Sci U S A, 2001. **98**(9): p. 5116-21.
220. Eisen, M.B., et al., *Cluster analysis and display of genome-wide expression patterns.* Proc Natl Acad Sci U S A, 1998. **95**(25): p. 14863-8.
221. Saldanha, A.J., *Java Treeview--extensible visualization of microarray data.* Bioinformatics, 2004. **20**(17): p. 3246-8.
222. Mi, H., et al., *PANTHER version 6: protein sequence and function evolution data with expanded representation of biological pathways.* Nucleic Acids Res, 2007. **35**(Database issue): p. D247-52.

223. Thomas, P.D., et al., *PANTHER: a library of protein families and subfamilies indexed by function.* Genome Res, 2003. **13**(9): p. 2129-41.
224. R Development Core Team, *R: A Language and Environment for Statistical Computing}*. 2010, R Foundation for Statistical Computing: Vienna, Austria.
225. Yee, H.Y., A. Paquet, and S. Dudoit, *Exploratory analysis for two-color spotted microarray data.* 2007, R package version 1.20.0.
226. Simon, R., et al., *Design and Analysis of DNA Microarray Investigations*. 2003, New York: Springer-Verlag.
227. Radmacher, M.D., L.M. McShane, and R. Simon, *A paradigm for class prediction using gene expression profiles.* J Comput Biol, 2002. **9**(3): p. 505-11.
228. Dudoit, S., J. Fridyland, and T.P. Speed, *Comparison of discrimination methods for the classification of tumors using gene expression data.* Journal of the American Statistical Association, 2002. **97**(457): p. 77-87.
229. Simon, R., et al., *Pitfalls in the use of DNA microarray data for diagnostic and prognostic classification.* J Natl Cancer Inst, 2003. **95**(1): p. 14-8.
230. Meilhac, S.M., et al., *The clonal origin of myocardial cells in different regions of the embryonic mouse heart.* Dev Cell, 2004. **6**(5): p. 685-98.
231. McFadden, D.G., et al., *A GATA-dependent right ventricular enhancer controls dHAND transcription in the developing heart.* Development, 2000. **127**(24): p. 5331-41.
232. Harvey, R.P., S.M. Meilhac, and M.E. Buckingham, *Landmarks and lineages in the developing heart.* Circ Res, 2009. **104**(11): p. 1235-7.
233. Nowotschin, S., et al., *Tbx1 affects asymmetric cardiac morphogenesis by regulating Pitx2 in the secondary heart field.* Development, 2006. **133**(8): p. 1565-73.
234. Jiang, L., *Right Ventricle*. Principle and Practice of Echocardiolgraphy., ed. A. Weyman. 1994, Baltimore, MD: Lippincott Williams & Wilkings. 901-921.
235. Gerdes, A.M., et al., *Regional differences in myocyte size in normal rat heart.* Anat Rec, 1986. **215**(4): p. 420-6.
236. Campbell, S.E., B. Korecky, and K. Rakusan, *Remodeling of myocyte dimensions in hypertrophic and atrophic rat hearts.* Circ Res, 1991. **68**(4): p. 984-96.
237. Michelakis, E., et al., *Oral sildenafil is an effective and specific pulmonary vasodilator in patients with pulmonary arterial hypertension: comparison with inhaled nitric oxide.* Circulation, 2002. **105**(20): p. 2398-403.
238. Ling, H., et al., *Requirement for Ca2+/calmodulin-dependent kinase II in the transition from pressure overload-induced cardiac hypertrophy to heart failure in mice.* J Clin Invest, 2009. **119**(5): p. 1230-40.
239. Willis, M.S., et al., *Cardiac muscle ring finger-1 increases susceptibility to heart failure in vivo.* Circ Res, 2009. **105**(1): p. 80-8.
240. Wang, G.Y., et al., *Contrasting inotropic responses to alpha1-adrenergic receptor stimulation in left versus right ventricular myocardium.* Am J Physiol Heart Circ Physiol, 2006. **291**(4): p. H2013-7.
241. Irlbeck, M., et al., *Different response of the rat left and right heart to norepinephrine.* Cardiovasc Res, 1996. **31**(1): p. 157-62.
242. Gibbs, R.A., et al., *Genome sequence of the Brown Norway rat yields insights into mammalian evolution.* Nature, 2004. **428**(6982): p. 493-521.

243. Ai, D., et al., *Canonical Wnt signaling functions in second heart field to promote right ventricular growth.* Proc Natl Acad Sci U S A, 2007. **104**(22): p. 9319-24.
244. Takeda, N., et al., *Cardiac fibroblasts are essential for the adaptive response of the murine heart to pressure overload.* J Clin Invest, 2010. **120**(1): p. 254-65.
245. Dong, J.T. and C. Chen, *Essential role of KLF5 transcription factor in cell proliferation and differentiation and its implications for human diseases.* Cell Mol Life Sci, 2009. **66**(16): p. 2691-706.
246. Taketani, S., et al., *Molecular characterization of a newly identified heme-binding protein induced during differentiation of urine erythroleukemia cells.* J Biol Chem, 1998. **273**(47): p. 31388-94.
247. Jacob Blackmon, B., et al., *Characterization of a human and mouse tetrapyrrole-binding protein.* Arch Biochem Biophys, 2002. **407**(2): p. 196-201.
248. Yamashita, M., et al., *T cell receptor-induced calcineurin activation regulates T helper type 2 cell development by modifying the interleukin 4 receptor signaling complex.* J Exp Med, 2000. **191**(11): p. 1869-79.
249. Di Marco, G.S., et al., *Cardioprotective effect of calcineurin inhibition in an animal model of renal disease.* Eur Heart J, 2011. **32**(15): p. 1935-45.
250. Ferrara, N., et al., *Exercise training promotes SIRT1 activity in aged rats.* Rejuvenation Res, 2008. **11**(1): p. 139-50.
251. Sugden, P.H., *An overview of endothelin signaling in the cardiac myocyte.* J Mol Cell Cardiol, 2003. **35**(8): p. 871-86.
252. Pereira, F.A., et al., *The orphan nuclear receptor COUP-TFII is required for angiogenesis and heart development.* Genes Dev, 1999. **13**(8): p. 1037-49.
253. Christoffels, V.M., et al., *Patterning the embryonic heart: identification of five mouse Iroquois homeobox genes in the developing heart.* Dev Biol, 2000. **224**(2): p. 263-74.
254. Bruneau, B.G., *The developmental genetics of congenital heart disease.* Nature, 2008. **451**(7181): p. 943-8.
255. Zornoff, L.A., et al., *Right ventricular dysfunction and risk of heart failure and mortality after myocardial infarction.* J Am Coll Cardiol, 2002. **39**(9): p. 1450-5.
256. Ghio, S., et al., *Independent and additive prognostic value of right ventricular systolic function and pulmonary artery pressure in patients with chronic heart failure.* J Am Coll Cardiol, 2001. **37**(1): p. 183-8.
257. Meyer, P., et al., *Effects of right ventricular ejection fraction on outcomes in chronic systolic heart failure.* Circulation, 2010. **121**(2): p. 252-8.
258. Friedman, E., H. Palevsky, and D. Taichman, *Classification and prognosis of pulmonary arterial hypertension*, in *Pulmonary vascular disease*, J. Mandel and D. Taichman, Editors. 2006, Elsevier Science: Philadelphia. p. 66-82.
259. Nagaya, N., et al., *Serum uric acid levels correlate with the severity and the mortality of primary pulmonary hypertension.* Am J Respir Crit Care Med, 1999. **160**(2): p. 487-92.
260. Nagaya, N., et al., *Plasma brain natriuretic peptide as a prognostic indicator in patients with primary pulmonary hypertension.* Circulation, 2000. **102**(8): p. 865-70.
261. Will, D.H., et al., *High altitude-induced pulmonary hypertension in normal cattle.* Circ Res, 1962. **10**: p. 172-7.

262. Reeves, J.T., E.B. Grover, and R.F. Grover, *Pulmonary circulation and oxygen transport in lambs at high altitude.* Journal of Applied Physiology, 1963. **18**(3): p. 560-566.
263. Barnes, J.M., P.N. Magee, and R. Schoental, *Lesions In The Lungs And Livers Of Rats Poisoned With The Pyrrolizidine Alkaloid Fulvine And Its N-Oxide.* J Pathol Bacteriol, 1964. **88**: p. 521-31.
264. Brooks, S.E., et al., *Acute veno-occlusive disease of the liver. Fine structure in Jamaican children.* Arch Pathol, 1970. **89**(6): p. 507-20.
265. Schultze, A.E. and R.A. Roth, *Chronic pulmonary hypertension--the monocrotaline model and involvement of the hemostatic system.* J Toxicol Environ Health B Crit Rev, 1998. **1**(4): p. 271-346.
266. Wilson, D.W., et al., *Mechanisms and pathology of monocrotaline pulmonary toxicity.* Crit Rev Toxicol, 1992. **22**(5-6): p. 307-25.
267. Merkow, L. and J. Kleinerman, *An electron microscopic study of pulmonary vasculitis induced by monocrotaline.* Lab Invest, 1966. **15**(3): p. 547-64.
268. Valdivia, E., et al., *Alterations in pulmonary alveoli after a single injection of monocrotaline.* Arch Pathol, 1967. **84**(1): p. 64-76.
269. Plestina, R. and H.B. Stoner, *Pulmonary oedema in rats given monocrotaline pyrrole.* J Pathol, 1972. **106**(4): p. 235-49.
270. Sugita, T., et al., *Lung vessel leak precedes right ventricular hypertrophy in monocrotaline-treated rats.* J Appl Physiol, 1983. **54**(2): p. 371-4.
271. Altiere, R.J., J.W. Olson, and M.N. Gillespie, *Altered pulmonary vascular smooth muscle responsiveness in monocrotaline-induced pulmonary hypertension.* J Pharmacol Exp Ther, 1986. **236**(2): p. 390-5.
272. Ghodsi, F. and J.A. Will, *Changes in pulmonary structure and function induced by monocrotaline intoxication.* Am J Physiol, 1981. **240**(2): p. H149-55.
273. Akhavein, F., et al., *Decreased left ventricular function, myocarditis, and coronary arteriolar medial thickening following monocrotaline administration in adult rats.* J Appl Physiol, 2007. **103**(1): p. 287-95.
274. Correia-Pinto, J., et al., *Time course and mechanisms of left ventricular systolic and diastolic dysfunction in monocrotaline-induced pulmonary hypertension.* Basic Res Cardiol, 2009. **104**(5): p. 535-45.
275. Stenmark, K.R., et al., *Animal models of pulmonary arterial hypertension: the hope for etiological discovery and pharmacological cure.* Am J Physiol Lung Cell Mol Physiol, 2009. **297**(6): p. L1013-32.
276. Usui, S., et al., *Upregulated neurohumoral factors are associated with left ventricular remodeling and poor prognosis in rats with monocrotaline-induced pulmonary arterial hypertension.* Circ J, 2006. **70**(9): p. 1208-15.
277. Taraseviciene-Stewart, L., et al., *Inhibition of the VEGF receptor 2 combined with chronic hypoxia causes cell death-dependent pulmonary endothelial cell proliferation and severe pulmonary hypertension.* Faseb J, 2001. **15**(2): p. 427-38.
278. Taraseviciene-Stewart, L., et al., *Simvastatin causes endothelial cell apoptosis and attenuates severe pulmonary hypertension.* Am J Physiol Lung Cell Mol Physiol, 2006. **291**(4): p. L668-76.

279. Taraseviciene-Stewart, L., et al., *Treatment of severe pulmonary hypertension: a bradykinin receptor 2 agonist B9972 causes reduction of pulmonary artery pressure and right ventricular hypertrophy.* Peptides, 2005. **26**(8): p. 1292-300.
280. Fong, T.A., et al., *SU5416 is a potent and selective inhibitor of the vascular endothelial growth factor receptor (Flk-1/KDR) that inhibits tyrosine kinase catalysis, tumor vascularization, and growth of multiple tumor types.* Cancer Res, 1999. **59**(1): p. 99-106.
281. Abe, K., et al., *Formation of plexiform lesions in experimental severe pulmonary arterial hypertension.* Circulation, 2010. **121**(25): p. 2747-54.
282. Kasahara, Y., et al., *Inhibition of VEGF receptors causes lung cell apoptosis and emphysema.* J Clin Invest, 2000. **106**(11): p. 1311-9.
283. Oka, M., et al., *Rho kinase-mediated vasoconstriction is important in severe occlusive pulmonary arterial hypertension in rats.* Circ Res, 2007. **100**(6): p. 923-9.
284. Hannigan, G.E., et al., *Regulation of cell adhesion and anchorage-dependent growth by a new beta 1-integrin-linked protein kinase.* Nature, 1996. **379**(6560): p. 91-6.
285. Hannigan, G.E., J.G. Coles, and S. Dedhar, *Integrin-linked kinase at the heart of cardiac contractility, repair, and disease.* Circ Res, 2007. **100**(10): p. 1408-14.
286. Bakerman, P.R., K.R. Stenmark, and J.H. Fisher, *Alpha-skeletal actin messenger RNA increases in acute right ventricular hypertrophy.* Am J Physiol, 1990. **258**(4 Pt 1): p. L173-8.
287. Shi, J., L. Zhang, and L. Wei, *Rho-kinase in development and heart failure: insights from genetic models.* Pediatr Cardiol, 2011. **32**(3): p. 297-304.
288. Zhang, Y.M., et al., *Targeted deletion of ROCK1 protects the heart against pressure overload by inhibiting reactive fibrosis.* Faseb J, 2006. **20**(7): p. 916-25.
289. Kuwahara, F., et al., *Transforming growth factor-beta function blocking prevents myocardial fibrosis and diastolic dysfunction in pressure-overloaded rats.* Circulation, 2002. **106**(1): p. 130-5.
290. Sun, Y. and K.T. Weber, *Infarct scar: a dynamic tissue.* Cardiovasc Res, 2000. **46**(2): p. 250-6.
291. Hao, J., et al., *Interaction between angiotensin II and Smad proteins in fibroblasts in failing heart and in vitro.* Am J Physiol Heart Circ Physiol, 2000. **279**(6): p. H3020-30.
292. Ju, H., et al., *Effect of AT1 receptor blockade on cardiac collagen remodeling after myocardial infarction.* Cardiovasc Res, 1997. **35**(2): p. 223-32.
293. Weber, K.T., *Extracellular matrix remodeling in heart failure: a role for de novo angiotensin II generation.* Circulation, 1997. **96**(11): p. 4065-82.
294. Soon, E., et al., *Elevated levels of inflammatory cytokines predict survival in idiopathic and familial pulmonary arterial hypertension.* Circulation, 2010. **122**(9): p. 920-7.
295. Li, A., et al., *IL-8 directly enhanced endothelial cell survival, proliferation, and matrix metalloproteinases production and regulated angiogenesis.* J Immunol, 2003. **170**(6): p. 3369-76.

296. Li, A., et al., *Autocrine role of interleukin-8 in induction of endothelial cell proliferation, survival, migration and MMP-2 production and angiogenesis.* Angiogenesis, 2005. **8**(1): p. 63-71.
297. Yue, T.L., et al., *Interleukin-8 is chemotactic for vascular smooth muscle cells.* Eur J Pharmacol, 1993. **240**(1): p. 81-4.
298. Yue, T.L., et al., *Interleukin-8. A mitogen and chemoattractant for vascular smooth muscle cells.* Circ Res, 1994. **75**(1): p. 1-7.
299. Rosca, M.G. and C.L. Hoppel, *Mitochondria in heart failure.* Cardiovasc Res, 2010. **88**(1): p. 40-50.
300. Belch, J.J., et al., *Oxygen free radicals and congestive heart failure.* Br Heart J, 1991. **65**(5): p. 245-8.
301. Hill, M.F. and P.K. Singal, *Antioxidant and oxidative stress changes during heart failure subsequent to myocardial infarction in rats.* Am J Pathol, 1996. **148**(1): p. 291-300.
302. Hill, M.F. and P.K. Singal, *Right and left myocardial antioxidant responses during heart failure subsequent to myocardial infarction.* Circulation, 1997. **96**(7): p. 2414-20.
303. Mallat, Z., et al., *Elevated levels of 8-iso-prostaglandin F2alpha in pericardial fluid of patients with heart failure: a potential role for in vivo oxidant stress in ventricular dilatation and progression to heart failure.* Circulation, 1998. **97**(16): p. 1536-9.
304. Tsutsui, H., S. Kinugawa, and S. Matsushima, *Mitochondrial oxidative stress and dysfunction in myocardial remodelling.* Cardiovasc Res, 2009. **81**(3): p. 449-56.
305. Ide, T., et al., *Direct evidence for increased hydroxyl radicals originating from superoxide in the failing myocardium.* Circ Res, 2000. **86**(2): p. 152-7.
306. Rosca, M.G., et al., *Cardiac mitochondria in heart failure: decrease in respirasomes and oxidative phosphorylation.* Cardiovasc Res, 2008. **80**(1): p. 30-9.
307. Davila-Roman, V.G., et al., *Altered myocardial fatty acid and glucose metabolism in idiopathic dilated cardiomyopathy.* J Am Coll Cardiol, 2002. **40**(2): p. 271-7.
308. de las Fuentes, L., et al., *Myocardial fatty acid metabolism: independent predictor of left ventricular mass in hypertensive heart disease.* Hypertension, 2003. **41**(1): p. 83-7.
309. Sochor, H., et al., *Studies of fatty acid metabolism with positron emission tomography in patients with cardiomyopathy.* Eur J Nucl Med, 1986. **12 Suppl**: p. S66-9.
310. Allard, M.F., et al., *Contribution of oxidative metabolism and glycolysis to ATP production in hypertrophied hearts.* Am J Physiol, 1994. **267**(2 Pt 2): p. H742-50.
311. Christe, M.E. and R.L. Rodgers, *Altered glucose and fatty acid oxidation in hearts of the spontaneously hypertensive rat.* J Mol Cell Cardiol, 1994. **26**(10): p. 1371-5.
312. Recchia, F.A., et al., *Reduced nitric oxide production and altered myocardial metabolism during the decompensation of pacing-induced heart failure in the conscious dog.* Circ Res, 1998. **83**(10): p. 969-79.
313. Mearini, G., et al., *Atrogin-1 and MuRF1 regulate cardiac MyBP-C levels via different mechanisms.* Cardiovasc Res, 2010. **85**(2): p. 357-66.

314. Birks, E.J., et al., *Elevated p53 expression is associated with dysregulation of the ubiquitin-proteasome system in dilated cardiomyopathy.* Cardiovasc Res, 2008. **79**(3): p. 472-80.
315. Hitomi, J., et al., *Involvement of caspase-4 in endoplasmic reticulum stress-induced apoptosis and Abeta-induced cell death.* J Cell Biol, 2004. **165**(3): p. 347-56.
316. Pelletier, N., et al., *The endoplasmic reticulum is a key component of the plasma cell death pathway.* J Immunol, 2006. **176**(3): p. 1340-7.
317. Ito, A., et al., *Tbx3 expression is related to apoptosis and cell proliferation in rat bladder both hyperplastic epithelial cells and carcinoma cells.* Cancer Lett, 2005. **219**(1): p. 105-12.
318. Geraci, M.W., et al., *Gene expression patterns in the lungs of patients with primary pulmonary hypertension: a gene microarray analysis.* Circ Res, 2001. **88**(6): p. 555-62.
319. McMurtry, M.S., et al., *Dichloroacetate prevents and reverses pulmonary hypertension by inducing pulmonary artery smooth muscle cell apoptosis.* Circ Res, 2004. **95**(8): p. 830-40.
320. Drake, J.I., et al., *Molecular Signature of a Right Heart Failure Program in Chronic Severe Pulmonary Hypertension.* Am J Respir Cell Mol Biol.
321. Peng, J., et al., *The transcription factor EPAS-1/hypoxia-inducible factor 2alpha plays an important role in vascular remodeling.* Proc Natl Acad Sci U S A, 2000. **97**(15): p. 8386-91.
322. Compernolle, V., et al., *Loss of HIF-2alpha and inhibition of VEGF impair fetal lung maturation, whereas treatment with VEGF prevents fatal respiratory distress in premature mice.* Nat Med, 2002. **8**(7): p. 702-10.
323. Kotch, L.E., et al., *Defective vascularization of HIF-1alpha-null embryos is not associated with VEGF deficiency but with mesenchymal cell death.* Dev Biol, 1999. **209**(2): p. 254-67.
324. Ema, M., et al., *A novel bHLH-PAS factor with close sequence similarity to hypoxia-inducible factor 1alpha regulates the VEGF expression and is potentially involved in lung and vascular development.* Proc Natl Acad Sci U S A, 1997. **94**(9): p. 4273-8.
325. Hu, C.J., et al., *Differential roles of hypoxia-inducible factor 1alpha (HIF-1alpha) and HIF-2alpha in hypoxic gene regulation.* Mol Cell Biol, 2003. **23**(24): p. 9361-74.
326. Wang, V., et al., *Differential gene up-regulation by hypoxia-inducible factor-1alpha and hypoxia-inducible factor-2alpha in HEK293T cells.* Cancer Res, 2005. **65**(8): p. 3299-306.
327. Oktay, Y., et al., *Hypoxia-inducible factor 2alpha regulates expression of the mitochondrial aconitase chaperone protein frataxin.* J Biol Chem, 2007. **282**(16): p. 11750-6.
328. Scortegagna, M., et al., *Multiple organ pathology, metabolic abnormalities and impaired homeostasis of reactive oxygen species in Epas1-/- mice.* Nat Genet, 2003. **35**(4): p. 331-40.

329. Shinojima, T., et al., *Renal cancer cells lacking hypoxia inducible factor (HIF)-1alpha expression maintain vascular endothelial growth factor expression through HIF-2alpha.* Carcinogenesis, 2007. **28**(3): p. 529-36.
330. Gale, D.P., et al., *Autosomal dominant erythrocytosis and pulmonary arterial hypertension associated with an activating HIF2 alpha mutation.* Blood, 2008. **112**(3): p. 919-21.
331. Sano, M., et al., *p53-induced inhibition of Hif-1 causes cardiac dysfunction during pressure overload.* Nature, 2007. **446**(7134): p. 444-8.
332. Kidoya, H., et al., *Spatial and temporal role of the apelin/APJ system in the caliber size regulation of blood vessels during angiogenesis.* Embo J, 2008. **27**(3): p. 522-34.
333. Blom, I.E., R. Goldschmeding, and A. Leask, *Gene regulation of connective tissue growth factor: new targets for antifibrotic therapy?* Matrix Biol, 2002. **21**(6): p. 473-82.
334. Grotendorst, G.R., *Connective tissue growth factor: a mediator of TGF-beta action on fibroblasts.* Cytokine Growth Factor Rev, 1997. **8**(3): p. 171-9.
335. Au, C.G., et al., *Increased connective tissue growth factor associated with cardiac fibrosis in the mdx mouse model of dystrophic cardiomyopathy.* Int J Exp Pathol, 2011. **92**(1): p. 57-65.
336. Hayata, N., et al., *Connective tissue growth factor induces cardiac hypertrophy through Akt signaling.* Biochem Biophys Res Commun, 2008. **370**(2): p. 274-8.
337. Panek, A.N., et al., *Connective tissue growth factor overexpression in cardiomyocytes promotes cardiac hypertrophy and protection against pressure overload.* PLoS One, 2009. **4**(8): p. e6743.
338. Bennett, V. and A.J. Baines, *Spectrin and ankyrin-based pathways: metazoan inventions for integrating cells into tissues.* Physiol Rev, 2001. **81**(3): p. 1353-92.
339. Matsuoka, Y., X. Li, and V. Bennett, *Adducin: structure, function and regulation.* Cell Mol Life Sci, 2000. **57**(6): p. 884-95.
340. Cusi, D., et al., *Polymorphisms of alpha-adducin and salt sensitivity in patients with essential hypertension.* Lancet, 1997. **349**(9062): p. 1353-7.
341. Naydenov, N.G. and A.I. Ivanov, *Adducins regulate remodeling of apical junctions in human epithelial cells.* Mol Biol Cell, 2010. **21**(20): p. 3506-17.
342. Deacon, D.C., et al., *The miR-143-adducin3 pathway is essential for cardiac chamber morphogenesis.* Development, 2010. **137**(11): p. 1887-96.
343. Chang, A., et al., *BRENDA, AMENDA and FRENDA the enzyme information system: new content and tools in 2009.* Nucleic Acids Res, 2009. **37**(Database issue): p. D588-92.
344. Humbert, M., et al., *Increased interleukin-1 and interleukin-6 serum concentrations in severe primary pulmonary hypertension.* Am J Respir Crit Care Med, 1995. **151**(5): p. 1628-31.
345. Voelkel, N.F., et al., *Interleukin-1 receptor antagonist treatment reduces pulmonary hypertension generated in rats by monocrotaline.* Am J Respir Cell Mol Biol, 1994. **11**(6): p. 664-75.
346. Steiner, M.K., et al., *Interleukin-6 overexpression induces pulmonary hypertension.* Circ Res, 2009. **104**(2): p. 236-44, 28p following 244.

347. Fujita, M., et al., *Pulmonary hypertension in TNF-alpha-overexpressing mice is associated with decreased VEGF gene expression.* J Appl Physiol, 2002. **93**(6): p. 2162-70.
348. Selimovic, N., et al., *Growth factors and interleukin-6 across the lung circulation in pulmonary hypertension.* Eur Respir J, 2009. **34**(3): p. 662-8.
349. Ito, T., et al., *Interleukin-10 expression mediated by an adeno-associated virus vector prevents monocrotaline-induced pulmonary arterial hypertension in rats.* Circ Res, 2007. **101**(7): p. 734-41.
350. Hecker, M., et al., *Dysregulation of the IL-13 receptor system: a novel pathomechanism in pulmonary arterial hypertension.* Am J Respir Crit Care Med, 2010. **182**(6): p. 805-18.
351. Hsu, E., et al., *Lung tissues in patients with systemic sclerosis have gene expression patterns unique to pulmonary fibrosis and pulmonary hypertension.* Arthritis Rheum, 2011. **63**(3): p. 783-94.
352. Pucci, A., et al., *Myocardial insulin-like growth factor-1 and insulin-like growth factor binding protein-3 gene expression in failing hearts harvested from patients undergoing cardiac transplantation.* J Heart Lung Transplant, 2009. **28**(4): p. 402-5.
353. Abe, N., et al., *Increased level of pericardial insulin-like growth factor-1 in patients with left ventricular dysfunction and advanced heart failure.* J Am Coll Cardiol, 2006. **48**(7): p. 1387-95.
354. Ingwall, J.S., *Energy metabolism in heart failure and remodelling.* Cardiovasc Res, 2009. **81**(3): p. 412-9.
355. Bouillaud, F., *UCP2, not a physiologically relevant uncoupler but a glucose sparing switch impacting ROS production and glucose sensing.* Biochim Biophys Acta, 2009. **1787**(5): p. 377-83.
356. Wu, F., J. Zhang, and D.A. Beard, *Experimentally observed phenomena on cardiac energetics in heart failure emerge from simulations of cardiac metabolism.* Proc Natl Acad Sci U S A, 2009. **106**(17): p. 7143-8.
357. Gurel, E., et al., *Ischemic preconditioning affects hexokinase activity and HKII in different subcellular compartments throughout cardiac ischemia-reperfusion.* J Appl Physiol, 2009. **106**(6): p. 1909-16.
358. Zuurbier, C.J., K.M. Smeele, and O. Eerbeek, *Mitochondrial hexokinase and cardioprotection of the intact heart.* J Bioenerg Biomembr, 2009. **41**(2): p. 181-5.
359. May, D., et al., *Transgenic system for conditional induction and rescue of chronic myocardial hibernation provides insights into genomic programs of hibernation.* Proc Natl Acad Sci U S A, 2008. **105**(1): p. 282-7.
360. Bogaard, H.J., et al., *Adrenergic receptor blockade reverses right heart remodeling and dysfunction in pulmonary hypertensive rats.* American Journal of Respiratory and Critical Care Medicine, 2010. **182**(5): p. 652-660.
361. Eyries, M., et al., *Hypoxia-induced apelin expression regulates endothelial cell proliferation and regenerative angiogenesis.* Circ Res, 2008. **103**(4): p. 432-40.
362. Sheikh, A.Y., et al., *In vivo genetic profiling and cellular localization of apelin reveals a hypoxia-sensitive, endothelial-centered pathway activated in ischemic heart failure.* Am J Physiol Heart Circ Physiol, 2008. **294**(1): p. H88-98.

363. Andersen, C.U., et al., *Pulmonary apelin levels and effects in rats with hypoxic pulmonary hypertension.* Respir Med, 2009. **103**(11): p. 1663-71.
364. Dallabrida, S.M., et al., *Angiopoietin-1 promotes cardiac and skeletal myocyte survival through integrins.* Circ Res, 2005. **96**(4): p. e8-24.
365. Kim, I., et al., *Angiopoietin-1 regulates endothelial cell survival through the phosphatidylinositol 3'-Kinase/Akt signal transduction pathway.* Circ Res, 2000. **86**(1): p. 24-9.
366. McLaughlin, V.V., et al., *ACCF/AHA 2009 expert consensus document on pulmonary hypertension a report of the American College of Cardiology Foundation Task Force on Expert Consensus Documents and the American Heart Association developed in collaboration with the American College of Chest Physicians; American Thoracic Society, Inc.; and the Pulmonary Hypertension Association.* J Am Coll Cardiol, 2009. **53**(17): p. 1573-619.
367. Sandoval, J., et al., *Survival in primary pulmonary hypertension. Validation of a prognostic equation.* Circulation, 1994. **89**(4): p. 1733-44.
368. Toyooka, S., et al., *Right but not left ventricular function recovers early after living-donor lobar lung transplantation in patients with pulmonary arterial hypertension.* J Thorac Cardiovasc Surg, 2009. **138**(1): p. 222-6.
369. Griffith, B.P., et al., *Heart-lung transplantation: lessons learned and future hopes.* Ann Thorac Surg, 1987. **43**(1): p. 6-16.
370. Christie, J.D., et al., *The Registry of the International Society for Heart and Lung Transplantation: Twenty-sixth Official Adult Lung and Heart-Lung Transplantation Report-2009.* J Heart Lung Transplant, 2009. **28**(10): p. 1031-49.
371. Bando, K., et al., *Indications for and results of single, bilateral, and heart-lung transplantation for pulmonary hypertension.* J Thorac Cardiovasc Surg, 1994. **108**(6): p. 1056-65.
372. Kramer, M.R., et al., *Recovery of the right ventricle after single-lung transplantation in pulmonary hypertension.* Am J Cardiol, 1994. **73**(7): p. 494-500.
373. Mendeloff, E.N., et al., *Lung transplantation for pulmonary vascular disease.* Ann Thorac Surg, 2002. **73**(1): p. 209-17; discussion 217-9.
374. Pasque, M.K., et al., *Single-lung transplantation for pulmonary hypertension. Three-month hemodynamic follow-up.* Circulation, 1991. **84**(6): p. 2275-9.
375. Orens, J.B., et al., *Thoracic organ transplantation in the United States, 1995-2004.* Am J Transplant, 2006. **6**(5 Pt 2): p. 1188-97.
376. Hosenpud, J.D., et al., *The Registry of the International Society for Heart and Lung Transplantation: seventeenth official report-2000.* J Heart Lung Transplant, 2000. **19**(10): p. 909-31.
377. Hosenpud, J.D., et al., *The Registry of the International Society for Heart and Lung Transplantation: fifteenth official report--1998.* J Heart Lung Transplant, 1998. **17**(7): p. 656-68.
378. Hunt, S.A., *ACC/AHA 2005 guideline update for the diagnosis and management of chronic heart failure in the adult: a report of the American College of Cardiology/American Heart Association Task Force on Practice Guidelines (Writing Committee to Update the 2001 Guidelines for the Evaluation and Management of Heart Failure).* J Am Coll Cardiol, 2005. **46**(6): p. e1-82.

379. Brodde, O.E. and M.C. Michel, *Adrenergic and muscarinic receptors in the human heart.* Pharmacol Rev, 1999. **51**(4): p. 651-90.
380. Rockman, H.A., W.J. Koch, and R.J. Lefkowitz, *Seven-transmembrane-spanning receptors and heart function.* Nature, 2002. **415**(6868): p. 206-12.
381. Ungerer, M., et al., *Altered expression of beta-adrenergic receptor kinase and beta 1-adrenergic receptors in the failing human heart.* Circulation, 1993. **87**(2): p. 454-63.
382. Xiang, Y. and B.K. Kobilka, *Myocyte adrenoceptor signaling pathways.* Science, 2003. **300**(5625): p. 1530-2.
383. DeWire, S.M., et al., *Beta-arrestins and cell signaling.* Annu Rev Physiol, 2007. **69**: p. 483-510.
384. Rajagopal, S., K. Rajagopal, and R.J. Lefkowitz, *Teaching old receptors new tricks: biasing seven-transmembrane receptors.* Nat Rev Drug Discov, 2010. **9**(5): p. 373-86.
385. Jarpe, M.B., et al., *Anti-apoptotic versus pro-apoptotic signal transduction: checkpoints and stop signs along the road to death.* Oncogene, 1998. **17**(11 Reviews): p. 1475-82.
386. McKay, M.M. and D.K. Morrison, *Integrating signals from RTKs to ERK/MAPK.* Oncogene, 2007. **26**(22): p. 3113-21.
387. Rakesh, K., et al., *beta-Arrestin-biased agonism of the angiotensin receptor induced by mechanical stress.* Sci Signal, 2010. **3**(125): p. ra46.
388. Beanlands, R.S., et al., *The effects of beta(1)-blockade on oxidative metabolism and the metabolic cost of ventricular work in patients with left ventricular dysfunction: A double-blind, placebo-controlled, positron-emission tomography study.* Circulation, 2000. **102**(17): p. 2070-5.
389. Prabhu, S.D., et al., *beta-adrenergic blockade in developing heart failure: effects on myocardial inflammatory cytokines, nitric oxide, and remodeling.* Circulation, 2000. **101**(17): p. 2103-9.
390. Holverda, S., et al., *Impaired stroke volume response to exercise in pulmonary arterial hypertension.* J Am Coll Cardiol, 2006. **47**(8): p. 1732-3.
391. Provencher, S., et al., *Deleterious effects of beta-blockers on exercise capacity and hemodynamics in patients with portopulmonary hypertension.* Gastroenterology, 2006. **130**(1): p. 120-6.
392. Feuerstein, G.Z., A. Bril, and R.R. Ruffolo, Jr., *Protective effects of carvedilol in the myocardium.* Am J Cardiol, 1997. **80**(11A): p. 41L-45L.
393. Collaboration, T.A.-N.Z.H.F.R., *Randomised, placebo-controlled trial of carvedilol in patients with congestive heart failure due to ischaemic heart disease. Australia/New Zealand Heart Failure Research Collaborative Group.* Lancet, 1997. **349**(9049): p. 375-80.
394. Dargie, H.J., *Effect of carvedilol on outcome after myocardial infarction in patients with left-ventricular dysfunction: the CAPRICORN randomised trial.* Lancet, 2001. **357**(9266): p. 1385-90.
395. Packer, M., et al., *The effect of carvedilol on morbidity and mortality in patients with chronic heart failure. U.S. Carvedilol Heart Failure Study Group.* N Engl J Med, 1996. **334**(21): p. 1349-55.

396. Barone, F.C., et al., *Carvedilol prevents severe hypertensive cardiomyopathy and remodeling.* J Hypertens, 1998. **16**(6): p. 871-84.
397. Kiriazis, H., et al., *Knockout of beta(1)- and beta(2)-adrenoceptors attenuates pressure overload-induced cardiac hypertrophy and fibrosis.* Br J Pharmacol, 2008. **153**(4): p. 684-92.
398. Brusselmans, K., et al., *Heterozygous deficiency of hypoxia-inducible factor-2alpha protects mice against pulmonary hypertension and right ventricular dysfunction during prolonged hypoxia.* J Clin Invest, 2003. **111**(10): p. 1519-27.
399. Yu, A.Y., et al., *Impaired physiological responses to chronic hypoxia in mice partially deficient for hypoxia-inducible factor 1alpha.* J Clin Invest, 1999. **103**(5): p. 691-6.
400. Semenza, G.L., *Targeting HIF-1 for cancer therapy.* Nat Rev Cancer, 2003. **3**(10): p. 721-32.
401. Warburg, O., *On respiratory impairment in cancer cells.* Science, 1956. **124**(3215): p. 269-70.
402. Mochizuki, Y., et al., *Angiopoietin 2 stimulates migration and tube-like structure formation of murine brain capillary endothelial cells through c-Fes and c-Fyn.* J Cell Sci, 2002. **115**(Pt 1): p. 175-83.
403. Lobov, I.B., P.C. Brooks, and R.A. Lang, *Angiopoietin-2 displays VEGF-dependent modulation of capillary structure and endothelial cell survival in vivo.* Proc Natl Acad Sci U S A, 2002. **99**(17): p. 11205-10.
404. Zhu, Y., et al., *Angiopoietin-2 facilitates vascular endothelial growth factor-induced angiogenesis in the mature mouse brain.* Stroke, 2005. **36**(7): p. 1533-7.
405. Kumpers, P., et al., *Circulating angiopoietins in idiopathic pulmonary arterial hypertension.* Eur Heart J, 2010. **31**(18): p. 2291-300.
406. Grimshaw, M.J., et al., *A role for endothelin-2 and its receptors in breast tumor cell invasion.* Cancer Res, 2004. **64**(7): p. 2461-8.
407. Grimshaw, M.J., S. Naylor, and F.R. Balkwill, *Endothelin-2 is a hypoxia-induced autocrine survival factor for breast tumor cells.* Mol Cancer Ther, 2002. **1**(14): p. 1273-81.
408. Na, G., et al., *Role of hypoxia in the regulation of periovulatory EDN2 expression in the mouse.* Can J Physiol Pharmacol, 2008. **86**(6): p. 310-9.
409. Klipper, E., et al., *Induction of endothelin-2 expression by luteinizing hormone and hypoxia: possible role in bovine corpus luteum formation.* Endocrinology, 2010. **151**(4): p. 1914-22.
410. Giaid, A., et al., *Expression of endothelin-1 in the lungs of patients with pulmonary hypertension.* N Engl J Med, 1993. **328**(24): p. 1732-9.
411. Kimura, K., et al., *Cardiac sympathetic rejuvenation: a link between nerve function and cardiac hypertrophy.* Circ Res, 2007. **100**(12): p. 1755-64.
412. Tsutsui, H., K. Ishihara, and G.t. Cooper, *Cytoskeletal role in the contractile dysfunction of hypertrophied myocardium.* Science, 1993. **260**(5108): p. 682-7.
413. Simon, R., et al., *Analysis of gene expression data using BRB-ArrayTools.* Cancer Inform, 2007. **3**: p. 11-7.
414. Korn, E.L., et al., *Controlling the number of false discoveries: application to high-dimensional genomic data.* Journal of Statistical Planning and Inference, 2004. **124**(2): p. 379-398.

415. Jagus, R., W.F. Anderson, and B. Safer, *The regulation of initiation of mammalian protein synthesis.* Prog Nucleic Acid Res Mol Biol, 1981. **25**: p. 127-85.
416. Sugden, P.H. and A. Clerk, *Cellular mechanisms of cardiac hypertrophy.* J Mol Med, 1998. **76**(11): p. 725-46.
417. Li, S.Y. and J. Ren, *Cardiac overexpression of alcohol dehydrogenase exacerbates chronic ethanol ingestion-induced myocardial dysfunction and hypertrophy: role of insulin signaling and ER stress.* J Mol Cell Cardiol, 2008. **44**(6): p. 992-1001.
418. Shahbazian, D., et al., *eIF4B controls survival and proliferation and is regulated by proto-oncogenic signaling pathways.* Cell Cycle, 2010. **9**(20): p. 4106-9.
419. Flynn, A. and C.G. Proud, *The role of eIF4 in cell proliferation.* Cancer Surv, 1996. **27**: p. 293-310.
420. Prenzel, N., et al., *EGF receptor transactivation by G-protein-coupled receptors requires metalloproteinase cleavage of proHB-EGF.* Nature, 1999. **402**(6764): p. 884-8.
421. Shah, B.H. and K.J. Catt, *A central role of EGF receptor transactivation in angiotensin II -induced cardiac hypertrophy.* Trends Pharmacol Sci, 2003. **24**(5): p. 239-44.
422. Virdis, A. and E.L. Schiffrin, *Vascular inflammation: a role in vascular disease in hypertension?* Curr Opin Nephrol Hypertens, 2003. **12**(2): p. 181-7.
423. Andersen, P., et al., *EGFR induces expression of IRF-1 via STAT1 and STAT3 activation leading to growth arrest of human cancer cells.* Int J Cancer, 2008. **122**(2): p. 342-9.
424. Asakura, M., et al., *Cardiac hypertrophy is inhibited by antagonism of ADAM12 processing of HB-EGF: metalloproteinase inhibitors as a new therapy.* Nat Med, 2002. **8**(1): p. 35-40.
425. Thomas, W.G., et al., *Adenoviral-directed expression of the type 1A angiotensin receptor promotes cardiomyocyte hypertrophy via transactivation of the epidermal growth factor receptor.* Circ Res, 2002. **90**(2): p. 135-42.
426. Le Cras, T.D., et al., *Disrupted pulmonary vascular development and pulmonary hypertension in transgenic mice overexpressing transforming growth factor-alpha.* Am J Physiol Lung Cell Mol Physiol, 2003. **285**(5): p. L1046-54.
427. Finck, B.N. and D.P. Kelly, *PGC-1 coactivators: inducible regulators of energy metabolism in health and disease.* J Clin Invest, 2006. **116**(3): p. 615-22.
428. Puigserver, P. and B.M. Spiegelman, *Peroxisome proliferator-activated receptor-gamma coactivator 1 alpha (PGC-1 alpha): transcriptional coactivator and metabolic regulator.* Endocr Rev, 2003. **24**(1): p. 78-90.
429. Burkart, E.M., et al., *Nuclear receptors PPARbeta/delta and PPARalpha direct distinct metabolic regulatory programs in the mouse heart.* J Clin Invest, 2007. **117**(12): p. 3930-9.
430. Huss, J.M., et al., *The nuclear receptor ERRalpha is required for the bioenergetic and functional adaptation to cardiac pressure overload.* Cell Metab, 2007. **6**(1): p. 25-37.

431. Lehman, J.J., et al., *The transcriptional coactivator PGC-1alpha is essential for maximal and efficient cardiac mitochondrial fatty acid oxidation and lipid homeostasis.* Am J Physiol Heart Circ Physiol, 2008. **295**(1): p. H185-96.
432. Gomez-Arroyo, J.G., et al. *Adrenergic receptor blockage improves metabolic modeling in experimental right ventricular failure due to pulmonary hypertension*. in *American Thoracic Society International Conference*. 2011. Denver, CO, USA.
433. Reiterer, G., M. Toborek, and B. Hennig, *Quercetin protects against linoleic acid-induced porcine endothelial cell dysfunction.* J Nutr, 2004. **134**(4): p. 771-5.
434. Ronaldson, P.T., T. Ashraf, and R. Bendayan, *Regulation of multidrug resistance protein 1 by tumor necrosis factor alpha in cultured glial cells: involvement of nuclear factor-kappaB and c-Jun N-terminal kinase signaling pathways.* Mol Pharmacol, 2010. **77**(4): p. 644-59.
435. Sharom, F.J., *ABC multidrug transporters: structure, function and role in chemoresistance.* Pharmacogenomics, 2008. **9**(1): p. 105-27.
436. van der Deen, M., et al., *Diminished expression of multidrug resistance-associated protein 1 (MRP1) in bronchial epithelium of COPD patients.* Virchows Arch, 2006. **449**(6): p. 682-8.
437. Sia, Y.T., et al., *Long-term effects of carvedilol on left ventricular function, remodeling, and expression of cardiac cytokines after large myocardial infarction in the rat.* J Cardiovasc Pharmacol, 2002. **39**(1): p. 73-87.
438. Li, B., et al., *Effects of carvedilol on cardiac cytokines expression and remodeling in rat with acute myocardial infarction.* Int J Cardiol, 2006. **111**(2): p. 247-55.
439. Pauschinger, M., et al., *Carvedilol improves left ventricular function in murine coxsackievirus-induced acute myocarditis association with reduced myocardial interleukin-1beta and MMP-8 expression and a modulated immune response.* Eur J Heart Fail, 2005. **7**(4): p. 444-52.
440. Rossig, L., et al., *Congestive heart failure induces endothelial cell apoptosis: protective role of carvedilol.* J Am Coll Cardiol, 2000. **36**(7): p. 2081-9.
441. Fujio, H., et al., *Carvedilol inhibits proliferation of cultured pulmonary artery smooth muscle cells of patients with idiopathic pulmonary arterial hypertension.* J Cardiovasc Pharmacol, 2006. **47**(2): p. 250-5.
442. Reiter, E. and R.J. Lefkowitz, *GRKs and beta-arrestins: roles in receptor silencing, trafficking and signaling.* Trends Endocrinol Metab, 2006. **17**(4): p. 159-65.
443. Szczepanek, K., et al., *Mitochondrial-targeted signal transducer and activator of transcription (STAT3) protects against ischemia-induced changes in the electron transport chain and the generation of reactive oxygen species.* J Biol Chem, 2011.
444. Chen, Q., et al., *Ischemic defects in the electron transport chain increase the production of reactive oxygen species from isolated rat heart mitochondria.* Am J Physiol Cell Physiol, 2008. **294**(2): p. C460-6.
445. Krahenbuhl, S., et al., *Decreased activities of ubiquinol:ferricytochrome c oxidoreductase (complex III) and ferrocytochrome c:oxygen oxidoreductase (complex IV) in liver mitochondria from rats with hydroxycobalamin[c-lactam]-induced methylmalonic aciduria.* J Biol Chem, 1991. **266**(31): p. 20998-1003.

446. Lesnefsky, E.J., et al., *Myocardial ischemia decreases oxidative phosphorylation through cytochrome oxidase in subsarcolemmal mitochondria.* Am J Physiol, 1997. **273**(3 Pt 2): p. H1544-54.
447. Rosenbloom, A.L., *Mecasermin (recombinant human insulin-like growth factor I).* Adv Ther, 2009. **26**(1): p. 40-54.
448. Ezzat, V.A., et al., *The role of IGF-I and its binding proteins in the development of type 2 diabetes and cardiovascular disease.* Diabetes Obes Metab, 2008. **10**(3): p. 198-211.
449. Marleau, S., et al., *Cardiac and peripheral actions of growth hormone and its releasing peptides: relevance for the treatment of cardiomyopathies.* Cardiovasc Res, 2006. **69**(1): p. 26-35.
450. Cupps, T.R. and A.S. Fauci, *Corticosteroid-mediated immunoregulation in man.* Immunol Rev, 1982. **65**: p. 133-55.
451. DeKruyff, R.H., Y. Fang, and D.T. Umetsu, *Corticosteroids enhance the capacity of macrophages to induce Th2 cytokine synthesis in CD4+ lymphocytes by inhibiting IL-12 production.* J Immunol, 1998. **160**(5): p. 2231-7.
452. Guo, C., et al., *Correction of Th1-dominant cytokine profiles by high-dose dexamethasone in patients with chronic idiopathic thrombocytopenic purpura.* J Clin Immunol, 2007. **27**(6): p. 557-62.
453. Ramirez, F., et al., *Glucocorticoids promote a TH2 cytokine response by CD4+ T cells in vitro.* J Immunol, 1996. **156**(7): p. 2406-12.
454. Bellotto, F., et al., *Effective immunosuppressive therapy in a patient with primary pulmonary hypertension.* Thorax, 1999. **54**(4): p. 372-4.
455. Wang, W., et al., *Dexamethasone attenuates development of monocrotaline-induced pulmonary arterial hypertension.* Mol Biol Rep, 2011. **38**(5): p. 3277-84.
456. Heineke, J. and J.D. Molkentin, *Regulation of cardiac hypertrophy by intracellular signalling pathways.* Nat Rev Mol Cell Biol, 2006. **7**(8): p. 589-600.
457. Muslin, A.J., *MAPK signalling in cardiovascular health and disease: molecular mechanisms and therapeutic targets.* Clin Sci (Lond), 2008. **115**(7): p. 203-18.
458. Wang, Y., *Mitogen-activated protein kinases in heart development and diseases.* Circulation, 2007. **116**(12): p. 1413-23.
459. Yang, X., M.V. Cohen, and J.M. Downey, *Mechanism of cardioprotection by early ischemic preconditioning.* Cardiovasc Drugs Ther, 2010. **24**(3): p. 225-34.

Appendix A: Probes identified by prediction analysis with 100% across LOOCV

# of Probes	Gene Name	Description
1	40060	Rattus norvegicus septin 4 (Sept4), mRNA [NM_001011893]
1	A_44_P105213	Unknown
1	A_44_P314231	Unknown
1	A_44_P384688	Unknown
1	A_44_P431358	Unknown
1	A_44_P459484	Unknown
1	A_44_P546267	Unknown
1	A_44_P575763	Unknown
1	A_44_P704947	Unknown
1	A_44_P729183	Unknown
1	A_44_P921710	Unknown
1	A_44_P944159	Unknown
1	AA900990	AA900990 UI-R-E0-dj-f-04-0-UI.s1 UI-R-E0 Rattus norvegicus cDNA clone UI-R-E0-dj-f-04-0-UI 3' similar to gi [AA900990]
1	AA963280	AA963280 UI-R-E1-gh-h-04-0-UI.s1 UI-R-E1 Rattus norvegicus cDNA clone UI-R-E1-gh-h-04-0-UI 3', mRNA sequence [AA963280]
1	Aars	PREDICTED: Rattus norvegicus alanyl-tRNA synthetase (Aars), mRNA [XM_214690]
1	Abtb2	Rattus norvegicus ankyrin repeat and BTB (POZ) domain containing 2 (Abtb2), mRNA [NM_134403]
2	Acaa1	Rattus norvegicus acetyl-Coenzyme A acyltransferase 1 (Acaa1), mRNA [NM_012489]
1	Actn4	Rattus norvegicus actinin alpha 4 (Actn4), mRNA [NM_031675]
1	Add2	Rattus norvegicus adducin 2 (beta) (Add2), mRNA [NM_012491]
1	Afg3l1_predicted	PREDICTED: Rattus norvegicus AFG3(ATPase family gene 3)-like 1 (yeast) (predicted) (Afg3l1_predicted), mRNA [XM_341714]
1	AI010816	EST205267 Normalized rat muscle, Bento Soares Rattus sp. cDNA clone RMUAS84 3' end, mRNA sequence [AI010816]
1	AI043579	UI-R-C1-jt-e-10-0-UI.s1 UI-R-C1 Rattus norvegicus cDNA clone UI-R-C1-jt-e-10-0-UI 3', mRNA sequence [AI043579]
1	AI045508	AI045508 UI-R-C1-kj-g-08-0-UI.s1 UI-R-C1 Rattus norvegicus cDNA clone UI-R-C1-kj-g-08-0-UI 3', mRNA sequence [AI045508]
1	AI229412	AI229412 EST226107 Normalized rat embryo, Bento Soares Rattus sp. cDNA clone REMCG02 3' end, mRNA sequence [AI229412]
1	Akap2	Rattus norvegicus A kinase (PRKA) anchor protein 2 (Akap2), mRNA [NM_001011974]
1	Akt1	Rattus norvegicus thymoma viral proto-oncogene 1 (Akt1), mRNA [NM_033230]
1	Aldoa	Rattus norvegicus aldolase A (Aldoa), mRNA [NM_012495]
1	Aldoal1	Rattus norvegicus aldolase A-like 1 (Aldoal1), mRNA [NM_001013943]
1	Anp32b	Rattus norvegicus acidic nuclear phosphoprotein 32 family, member B (Anp32b), mRNA [NM_131911]
1	Anxa5	Rattus norvegicus annexin A5 (Anxa5), mRNA [NM_013132]
10	Aqp1	Rattus norvegicus aquaporin 1 (Aqp1), mRNA [NM_012778]
1	Arhgap21_predicted	PREDICTED: Rattus norvegicus Rho GTPase activating protein 21 (predicted) (Arhgap21_predicted), mRNA [XM_225628]

1	Arpc1b	Rattus norvegicus actin related protein 2/3 complex, subunit 1B (Arpc1b), mRNA [NM_019289]
1	Atox1	Rattus norvegicus ATX1 (antioxidant protein 1) homolog 1 (yeast) (Atox1), mRNA [NM_053359]
1	Atp2b2	Rattus norvegicus ATPase, Ca++ transporting, plasma membrane 2 (Atp2b2), mRNA [NM_012508]
1	AW141147	AW141147 EST291183 Normalized rat brain, Bento Soares Rattus sp. cDNA clone RGIBE08 5' end similar to C-1, putative transcription factor, mRNA sequence [AW141147]
1	AW142959	AW142959 EST293251 Normalized rat kidney, Bento Soares Rattus sp. cDNA clone RGIBA46 5' end, mRNA sequence [AW142959]
1	AW143194	AW143194 EST293490 Normalized rat brain, Bento Soares Rattus sp. cDNA clone RGIBF39 5' end, mRNA sequence [AW143194]
1	AW143900	AW143900 EST294196 Normalized rat embryo, Bento Soares Rattus sp. cDNA clone RGICC51 5' end, mRNA sequence [AW143900]
1	AW144158	AW144158 EST294454 Normalized rat ovary, Bento Soares Rattus sp. cDNA clone RGICK08 5' end, mRNA sequence [AW144158]
1	AW144236	AW144236 EST294532 Normalized rat ovary, Bento Soares Rattus sp. cDNA clone RGICN59 5' end, mRNA sequence [AW144236]
1	AW253396	AW253396 UI-R-BJ0-aen-d-08-0-UI.s1 UI-R-BJ0 Rattus norvegicus cDNA clone UI-R-BJ0-aen-d-08-0-UI 3', mRNA sequence [AW253396]
1	AW433572	AW433572 UI-R-BJ0p-aez-g-10-0-UI.s1 UI-R-BJ0p Rattus norvegicus cDNA clone UI-R-BJ0p-aez-g-10-0-UI 3', mRNA sequence [AW433572]
1	AW529005	AW529005 UI-R-BT1-aka-a-11-0-UI.s1 UI-R-BT1 Rattus norvegicus cDNA clone UI-R-BT1-aka-a-11-0-UI 3', mRNA sequence [AW529005]
1	AW915016	AW915016 EST346320 Normalized rat ovary, Bento Soares Rattus sp. cDNA clone RGIBN51 5' end, mRNA sequence [AW915016]
1	AW915635	AW915635 EST346939 Normalized rat embryo, Bento Soares Rattus sp. cDNA clone RGICY71 5' end, mRNA sequence [AW915635]
1	AW916021	AW916021 EST347325 Rat gene index, normalized rat, norvegicus, Bento Soares Rattus norvegicus cDNA clone RGIDF02 5' end, mRNA sequence [AW916021]
1	AW917132	EST348436 Rat gene index, normalized rat, norvegicus, Bento Soares Rattus norvegicus cDNA clone RGIDZ63 5' end, mRNA sequence [AW917132]
1	AW917894	AW917894 EST349198 Rat gene index, normalized rat, norvegicus, Bento Soares Rattus norvegicus cDNA clone RGIEJ82 5' end, mRNA sequence [AW917894]
1	AW918202	AW918202 EST349506 Rat gene index, normalized rat, norvegicus, Bento Soares Rattus norvegicus cDNA clone RGIEN76 5' end, mRNA sequence [AW918202]
1	AW918729	AW918729 EST350033 Rat gene index, normalized rat, norvegicus, Bento Soares Rattus norvegicus cDNA clone RGIEX24 5' end, mRNA sequence [AW918729]
1	AW919096	AW919096 EST350400 Rat gene index, normalized rat, norvegicus, Bento Soares Rattus norvegicus cDNA clone RGIFC69 5' end, mRNA sequence [AW919096]
1	AW919109	AW919109 EST350413 Rat gene index, normalized rat, norvegicus, Bento Soares Rattus norvegicus cDNA clone RGIFC89 5' end, mRNA sequence [AW919109]

1	AW920343	AW920343 EST351647 Rat gene index, normalized rat, norvegicus, Bento Soares Rattus norvegicus cDNA clone RGIGU32 5' end, mRNA sequence [AW920343]
1	Bat1a	Rattus norvegicus HLA-B-associated transcript 1A (Bat1a), mRNA [NM_133300]
1	Bat3	Rattus norvegicus HLA-B-associated transcript 3 (Bat3), transcript variant 2, mRNA [NM_053609]
1	Bcam	Rattus norvegicus basal cell adhesion molecule (Bcam), mRNA [NM_031752]
1	BF395647	BF395647 UI-R-CM0-bjp-e-07-0-UI.s1 UI-R-CM0 Rattus norvegicus cDNA clone UI-R-CM0-bjp-e-07-0-UI 3', mRNA sequence [BF395647]
1	BF404842	BF404842 UI-R-CA1-bic-d-02-0-UI.s1 UI-R-CA1 Rattus norvegicus cDNA clone UI-R-CA1-bic-d-02-0-UI 3', mRNA sequence [BF404842]
1	BF563221	BF563221 UI-R-BO1-ajh-a-06-0-UI.r1 UI-R-BO1 Rattus norvegicus cDNA clone UI-R-BO1-ajh-a-06-0-UI 5', mRNA sequence [BF563221]
1	BG376818	UI-R-CA1-blh-e-03-0-UI.s1 UI-R-CA1 Rattus norvegicus cDNA clone UI-R-CA1-blh-e-03-0-UI 3', mRNA sequence [BG376818]
1	BI274747	BI274747 UI-R-CX0-bxd-e-07-0-UI.s1 UI-R-CX0 Rattus norvegicus cDNA clone UI-R-CX0-bxd-e-07-0-UI 3', mRNA sequence [BI274747]
1	BI294916	BI294916 UI-R-DK0-ced-f-05-0-UI.s1 UI-R-DK0 Rattus norvegicus cDNA clone UI-R-DK0-ced-f-05-0-UI 3', mRNA sequence [BI294916]
1	BM389289	BM389289 UI-R-DZ0-cko-f-18-0-UI.s1 NCI_CGAP_DZ0 Rattus norvegicus cDNA clone IMAGE:7338356 3', mRNA sequence [BM389289]
1	BM986517	BM986517 EST594111 Rat gene index, normalized rat, norvegicus Rattus norvegicus cDNA clone RGOAC85 3' end similar to diphosphoinositol polyphosphate phosphohydrolase, mRNA sequence [BM986517]
1	BQ210430	UI-R-DY1-coi-g-14-0-UI.s1 UI-R-DY1 Rattus norvegicus cDNA clone UI-R-DY1-coi-g-14-0-UI 3', mRNA sequence [BQ210430]
1	Bsg	Rattus norvegicus basigin (Bsg), mRNA [NM_012783]
2	Bst2	Rattus norvegicus bone marrow stromal cell antigen 2 (Bst2), mRNA [NM_198134]
1	C1r	C1r protein (Fragment). [Source:Uniprot/SPTREMBL;Acc:Q4G030] [ENSRNOT00000015897]
1	Casp4	Rattus norvegicus caspase 4, apoptosis-related cysteine peptidase (Casp4), mRNA [NM_053736]
1	CB606450	CB606450 AMGNNUC:TRXP1-00001-B1-A trxp1 (10556) Rattus norvegicus cDNA clone trxp1-00001-b1 5', mRNA sequence [CB606450]
1	CB615257	AMGNNUC:SRCS1-00113-G5-A srcs1 (10883) Rattus norvegicus cDNA clone srcs1-00113-g5 5', mRNA sequence [CB615257]
1	CB759117	AMGNNUC:SRPG2-00040-D8-A srpg2 (10238) Rattus norvegicus cDNA clone srpg2-00040-d8 5', mRNA sequence [CB759117]
1	Ccnd2	Rattus norvegicus cyclin D2 (Ccnd2), mRNA [NM_022267]
1	Cd63	Rattus norvegicus CD63 antigen (Cd63), mRNA [NM_017125]
1	Cdc42ep2	Rattus norvegicus CDC42 effector protein (Rho GTPase binding) 2 (Cdc42ep2), mRNA [NM_001009689]
4	Cdkn1a	Rattus norvegicus cyclin-dependent kinase inhibitor 1A (Cdkn1a), mRNA [NM_080782]
1	Cebpd	Rattus norvegicus CCAAT/enhancer binding protein (C/EBP), delta (Cebpd), mRNA [NM_013154]

1	CF107866	Shultzomica01117 Rat lung airway and parenchyma cDNA libraries Rattus norvegicus cDNA clone NA9257 5', mRNA sequence [CF107866]
1	CF111029	Shultzomica04280 Rat lung airway and parenchyma cDNA libraries Rattus norvegicus cDNA clone Contig3797 5', mRNA sequence [CF111029]
1	CF111207	Shultzomica04458 Rat lung airway and parenchyma cDNA libraries Rattus norvegicus cDNA clone Contig3944 5', mRNA sequence [CF111207]
1	Chrac1_predicted	PREDICTED: Rattus norvegicus chromatin accessibility complex 1 (predicted) (Chrac1_predicted), mRNA [XM_235400]
1	Cilp_predicted	PREDICTED: Rattus norvegicus cartilage intermediate layer protein, nucleotide pyrophosphohydrolase (predicted) (Cilp_predicted), mRNA [XM_236348]
1	Ciz1_predicted	PREDICTED: Rattus norvegicus CDKN1A interacting zinc finger protein 1 (predicted) (Ciz1_predicted), mRNA [XM_216034]
1	Col4a2_predicted	PREDICTED: Rattus norvegicus procollagen, type IV, alpha 2 (predicted) (Col4a2_predicted), mRNA [XM_225043]
1	COX1	Cytochrome c oxidase subunit 1 (EC 1.9.3.1) (Cytochrome c oxidase polypeptide I). [Source:Uniprot/SWISSPROT;Acc:P05503] [ENSRNOT00000050156]
1	CR469283	CR469283 Rat pBluescript Lion Rattus norvegicus cDNA clone LIONp463E09157 3', mRNA sequence [CR469283]
1	Creld1	Rattus norvegicus cysteine-rich with EGF-like domains 1 (Creld1), mRNA [NM_001024783]
1	Crim1_predicted	PREDICTED: Rattus norvegicus cysteine-rich motor neuron 1 (predicted) (Crim1_predicted), mRNA [XM_233798]
1	Cst3	Rattus norvegicus cystatin C (Cst3), mRNA [NM_012837]
1	Cstb	Rattus norvegicus cystatin B (Cstb), mRNA [NM_012838]
10	Ctgf	Rattus norvegicus connective tissue growth factor (Ctgf), mRNA [NM_022266]
1	CV102701	AGENCOURT_31523961 NIH_MGC_270 Rattus norvegicus cDNA clone IMAGE:7446235 5', mRNA sequence [CV102701]
6	Cyp1a1	Rattus norvegicus cytochrome P450, family 1, subfamily a, polypeptide 1 (Cyp1a1), mRNA [NM_012540]
1	Cyp27a1	Rattus norvegicus cytochrome P450, family 27, subfamily a, polypeptide 1 (Cyp27a1), mRNA [NM_178847]
1	Dbnl	Rattus norvegicus drebrin-like (Dbnl), mRNA [NM_031352]
1	Dctn1	Rattus norvegicus dynactin 1 (Dctn1), mRNA [NM_024130]
1	Dhrs4	Rattus norvegicus dehydrogenase/reductase (SDR family) member 4 (Dhrs4), mRNA [NM_153315]
1	Dlx1	PREDICTED: Rattus norvegicus distal-less homeobox 1 (Dlx1), mRNA [XM_230987]
1	Dnajb5_predicted	BF558851 UI-R-A1-dv-f-06-0-UI.r1 UI-R-A1 Rattus norvegicus cDNA clone UI-R-A1-dv-f-06-0-UI 5', mRNA sequence [BF558851]
1	Dst_predicted	PREDICTED: Rattus norvegicus dystonin (predicted) (Dst_predicted), mRNA [XM_237042]
1	DV718416	RVL9000 Wackym-Soares normalized rat vestibular cDNA library Rattus norvegicus cDNA 5', mRNA sequence [DV718416]
1	DV722942	RVL14623 Wackym-Soares normalized rat vestibular cDNA library Rattus norvegicus cDNA 5', mRNA sequence [DV722942]
1	DV728620	RVL21285 Wackym-Soares normalized rat vestibular cDNA library Rattus norvegicus cDNA 5', mRNA sequence [DV728620]

1	Dvl1	Rattus norvegicus dishevelled, dsh homolog 1 (Drosophila) (Dvl1), mRNA [NM_031820]
1	Edg2	Rattus norvegicus endothelial differentiation, lysophosphatidic acid G-protein-coupled receptor, 2 (Edg2), mRNA [NM_053936]
1	Edn2	Rattus norvegicus endothelin 2 (Edn2), mRNA [NM_012549]
1	Eef2	Rattus norvegicus eukaryotic translation elongation factor 2 (Eef2), mRNA [NM_017245]
1	Eef2k	Rattus norvegicus eukaryotic elongation factor-2 kinase (Eef2k), mRNA [NM_012947]
1	Egln3	Rattus norvegicus EGL nine homolog 3 (C. elegans) (Egln3), mRNA [NM_019371]
6	Eif4b	Rattus norvegicus eukaryotic translation initiation factor 4B (Eif4b), mRNA [NM_001008324]
1	Eif4g3_predicted	PREDICTED: Rattus norvegicus eukaryotic translation initiation factor 4 gamma, 3 (predicted) (Eif4g3_predicted), mRNA [XM_216563]
1	Eml2	Rattus norvegicus echinoderm microtubule associated protein like 2 (Eml2), mRNA [NM_138921]
1	Enah	Rattus norvegicus enabled homolog (Drosophila) (Enah), mRNA [NM_001012150]
1	Eno1	Rattus norvegicus enolase 1, alpha (Eno1), mRNA [NM_012554]
1	ENSRNOT00000000707	Myristoylated alanine-rich C-kinase substrate (MARCKS) (Protein kinase C substrate 80 kDa protein). [Source:Uniprot/SWISSPROT;Acc:P30009] [ENSRNOT00000000707]
1	ENSRNOT00000005432	Unknown
1	ENSRNOT00000007351	PREDICTED: Rattus norvegicus similar to Small nuclear ribonucleoprotein F (snRNP-F) (Sm protein F) (Sm-F) (SmF) (LOC680737), mRNA [XM_001058626]
1	ENSRNOT00000008057	PREDICTED: Rattus norvegicus similar to small unique nuclear receptor co-repressor (predicted) (RGD1560600_predicted), mRNA [XM_214099]
1	ENSRNOT00000009344	PREDICTED: Rattus norvegicus similar to Calsequestrin-1 precursor (Calsequestrin, skeletal muscle isoform) (LOC686019), mRNA [XM_001063867]
1	ENSRNOT00000013672	PREDICTED: Rattus norvegicus similar to proline arginine rich coiled coil 1, transcript variant 5 (LOC681287), mRNA [XM_001058826]
1	ENSRNOT00000015113	LOC501069 protein (Fragment). [Source:Uniprot/SPTREMBL;Acc:Q5U4E6] [ENSRNOT00000015113]
1	ENSRNOT00000017043	PREDICTED: Rattus norvegicus similar to mKIAA1604 protein (predicted) (RGD1565385_predicted), mRNA [XM_342453]
2	ENSRNOT00000017422	Mago-nashi-like proliferation-associated protein (Fragment). [Source:Uniprot/SPTREMBL;Acc:Q27W02] [ENSRNOT00000017422]
1	ENSRNOT00000023601	Memory related protein-1 (Fragment). [Source:Uniprot/SPTREMBL;Acc:Q78E25] [ENSRNOT00000023601]
1	ENSRNOT00000023696	E3 ubiquitin-protein ligase MIB2 (EC 6.3.2.-) (Mind bomb homolog 2) (RBSC-skeletrophin/dystrophin-like polypeptide). [Source:Uniprot/SWISSPROT;Acc:Q68LP1] [ENSRNOT00000023696]
1	ENSRNOT00000028121	Unknown
1	ENSRNOT00000029141	similar to Fructose-bisphosphate aldolase A (Muscle-type aldolase) (Aldolase 1) (LOC290761), mRNA [Source:RefSeq_dna;Acc:XR_007988] [ENSRNOT00000029141]

1	ENSRNOT00000037887	Alpha-mannosidase 2 (EC 3.2.1.114) (Alpha-mannosidase II) (Mannosyl- oligosaccharide 1,3-1,6-alpha-mannosidase) (MAN II) (Golgi alpha- mannosidase II) (Mannosidase alpha class 2A member 1) (Fragment). [Source:Uniprot/SWISSPROT;Acc:P28494]...
1	ENSRNOT00000040029	PREDICTED: Rattus norvegicus eukaryotic translation initiation factor 4 gamma, 1 (Eif4g1), mRNA [XM_213569]
1	ENSRNOT00000041388	Unknown
1	ENSRNOT00000041594	Unknown
1	ENSRNOT00000048684	similar to RIKEN cDNA 5031410I06 (LOC686886), mRNA [Source:RefSeq_dna;Acc:XR_009064] [ENSRNOT00000048684]
1	ENSRNOT00000051257	PREDICTED: Rattus norvegicus dysferlin (predicted) (Dysf_predicted), mRNA [XM_232123]
1	ENSRNOT00000055469	similar to nemo like kinase (LOC365949), mRNA [Source:RefSeq_dna;Acc:XR_009210] [ENSRNOT00000055469]
1	ENSRNOT00000056257	LOC360570 protein (Fragment). [Source:Uniprot/SPTREMBL;Acc:Q3B8R3] [ENSRNOT00000056257]
1	ENSRNOT00000057386	Col4a1 protein (Fragment). [Source:Uniprot/SPTREMBL;Acc:Q5FWY9] [ENSRNOT00000057386]
1	ENSRNOT00000058206	TSC22 domain family protein 1 (Transforming growth factor beta-1-induced transcript 4 protein) (Regulatory protein TSC-22) (TGFB-stimulated clone 22 homolog). [Source:Uniprot/SWISSPROT;Acc:P62501] [ENSRNOT00000058206]
1	Fads3	Rattus norvegicus fatty acid desaturase 3 (Fads3), mRNA [NM_173137]
3	Fdps	Rattus norvegicus farensyl diphosphate synthase (Fdps), mRNA [NM_031840]
2	Fhl1	Rattus norvegicus four and a half LIM domains 1 (Fhl1), transcript variant 2, mRNA [NM_145669]
1	Fkbp5	Rattus norvegicus FK506 binding protein 5 (Fkbp5), mRNA [NM_001012174]
1	Fkrp	Rattus norvegicus fukutin related protein (Fkrp), mRNA [NM_001025678]
1	Fliih	Rattus norvegicus flightless I homolog (Drosophila) (Fliih), mRNA [NM_001008279]
1	Fln29	Fln29 protein. [Source:Uniprot/SPTREMBL;Acc:Q5M806] [ENSRNOT00000033984]
1	Flnc_predicted	PREDICTED: Rattus norvegicus filamin C, gamma (actin binding protein 280) (predicted) (Flnc_predicted), mRNA [XM_342653]
1	Flot1	Rattus norvegicus flotillin 1 (Flot1), mRNA [NM_022701]
1	Ftl1	Rattus norvegicus ferritin light chain 1 (Ftl1), mRNA [NM_022500]
1	Fts	Rattus norvegicus fused toes (Fts), mRNA [NM_001011926]
1	Gadd45a	Rattus norvegicus growth arrest and DNA-damage-inducible 45 alpha (Gadd45a), mRNA [NM_024127]
2	Gas6	Rattus norvegicus growth arrest specific 6 (Gas6), mRNA [NM_057100]
1	Gata4	Rattus norvegicus GATA binding protein 4 (Gata4), mRNA [NM_144730]
1	Gcdh_predicted	Rattus norvegicus similar to glutaryl-CoA dehydrogenase precursor (LOC364975), mRNA [XM_344744]
1	Gchfr	Rattus norvegicus GTP cyclohydrolase I feedback regulator (Gchfr), mRNA [NM_133595]
1	Gdnf	Rattus norvegicus glial cell line derived neurotrophic factor (Gdnf), mRNA [NM_019139]

1	Gng11	Rattus norvegicus guanine nucleotide binding protein (G protein), gamma 11 (Gng11), mRNA [NM_022396]
1	Gnpda2_predicted	PREDICTED: Rattus norvegicus glucosamine-6-phosphate deaminase 2 (predicted) (Gnpda2_predicted), mRNA [XM_214029]
1	Gorasp1	Rattus norvegicus golgi reassembly stacking protein 1 (Gorasp1), mRNA [NM_019385]
1	Gpc1	Rattus norvegicus glypican 1 (Gpc1), mRNA [NM_030828]
1	Gpsm1	Rattus norvegicus G-protein signalling modulator 1 (AGS3-like, C. elegans) (Gpsm1), mRNA [NM_144745]
1	Gyg1	Rattus norvegicus glycogenin 1 (Gyg1), mRNA [NM_031043]
1	Gzmc	Rattus norvegicus granzyme C (Gzmc), mRNA [NM_134332]
1	H2-T18	Rattus norvegicus histocompatibility 2, T region locus 18 (H2-T18), mRNA [NM_001002821]
3	Hcrt	Rattus norvegicus hypocretin (Hcrt), mRNA [NM_013179]
1	Hdac5	Rattus norvegicus histone deacetylase 5, mRNA (cDNA clone IMAGE:7301599), partial cds. [BC086431]
1	Hip1	HIP1 protein (Fragment). [Source:Uniprot/SPTREMBL;Acc:Q8VHU1] [ENSRNOT00000001967]
1	Hipk2_predicted	Rattus norvegicus similar to nuclear body associated kinase 1a (LOC362342), mRNA [XM_342662]
1	Hk1	Rattus norvegicus hexokinase 1 (Hk1), mRNA [NM_012734]
1	Hmgb1	Rattus norvegicus high mobility group box 1 (Hmgb1), mRNA [NM_012963]
1	Hps6	Rattus norvegicus Hermansky-Pudlak syndrome 6 (Hps6), mRNA [NM_181432]
1	Hrmt1l2	Rattus norvegicus heterogeneous nuclear ribonucleoproteins methyltransferase-like 2 (S. cerevisiae) (Hrmt1l2), mRNA [NM_024363]
1	Hspa12b_predicted	PREDICTED: Rattus norvegicus heat shock protein 70kDa 12B (predicted) (Hspa12b_predicted), mRNA [XM_230610]
1	Hspa5bp1	Rattus norvegicus heat shock 70kDa protein 5 binding protein 1 (Hspa5bp1), mRNA [NM_178021]
1	Hspb3	Rattus norvegicus heat shock 27kDa protein 3 (Hspb3), mRNA [NM_031750]
1	Hspca	Rattus norvegicus heat shock protein 1, alpha (Hspca), mRNA [NM_175761]
1	Hspcb	Rattus norvegicus heat shock 90kDa protein 1, beta (Hspcb), mRNA [NM_001004082]
1	Hspd1	Rattus norvegicus heat shock protein 1 (chaperonin) (Hspd1), mRNA [NM_022229]
1	Idh3B	Rattus norvegicus isocitrate dehydrogenase 3 (NAD+) beta (Idh3B), mRNA [NM_053581]
1	Ilvbl_predicted	PREDICTED: Rattus norvegicus ilvB (bacterial acetolactate synthase)-like (predicted) (Ilvbl_predicted), mRNA [XM_343174]
1	Inha	Rattus norvegicus inhibin alpha (Inha), mRNA [NM_012590]
1	Inpp5a_predicted	Rattus norvegicus similar to Type I inositol-1,4,5-trisphosphate 5-phosphatase (5PTASE) (LOC365382), mRNA [XM_344971]
2	Ipo13	Rattus norvegicus importin 13 (Ipo13), mRNA [NM_053778]
4	Itgb1	Rattus norvegicus integrin beta 1 (fibronectin receptor beta) (Itgb1), mRNA [NM_017022]
1	Josd3	Rattus norvegicus Josephin domain containing 3 (Josd3), mRNA [NM_001014207]
1	Ka15	Rattus norvegicus type I keratin KA15 (Ka15), mRNA

		[NM_001004022]
1	Ke2	Rattus norvegicus MHC class II region expressed gene KE2 (Ke2), mRNA [NM_212506]
1	Kif3b_predicted	PREDICTED: Rattus norvegicus kinesin family member 3B (predicted) (Kif3b_predicted), mRNA [XM_215883]
1	Klf9	Rattus norvegicus Kruppel-like factor 9 (Klf9), mRNA [NM_057211]
1	Krt1-18	Rattus norvegicus keratin complex 1, acidic, gene 18 (Krt1-18), mRNA [NM_053976]
1	Lamb2	Rattus norvegicus laminin, beta 2 (Lamb2), mRNA [NM_012974]
1	Ldhd	Rattus norvegicus lactate dehydrogenase D (Ldhd), mRNA [NM_001008893]
1	LOC288526	LOC288526 protein (Fragment). [Source:Uniprot/SPTREMBL;Acc:Q496Y9] [ENSRNOT00000037829]
1	LOC289517	PREDICTED: Rattus norvegicus similar to Alpha-enolase (2-phospho-D-glycerate hydro-lyase) (Non-neural enolase) (NNE) (Enolase 1) (LOC289517), mRNA [XR_008796]
1	LOC290721	PREDICTED: Rattus norvegicus similar to Alpha-enolase (2-phospho-D-glycerate hydro-lyase) (Non-neural enolase) (NNE) (Enolase 1) (LOC290721), mRNA [XR_005691]
1	LOC291205	PREDICTED: Rattus norvegicus similar to 60 kDa heat shock protein, mitochondrial precursor (Hsp60) (60 kDa chaperonin) (CPN60) (Heat shock protein 60) (HSP-60) (Mitochondrial matrix protein P1) (HSP-65) (LOC291205), mRNA [XR_007380]
1	LOC294154	Rattus norvegicus similar to chromosome 6 open reading frame 106 isoform a (LOC294154), mRNA [NM_001039607]
1	LOC297826	PREDICTED: Rattus norvegicus similar to Alpha-enolase (2-phospho-D-glycerate hydro-lyase) (Non-neural enolase) (NNE) (Enolase 1) (LOC297826), mRNA [XM_001066983]
1	LOC298606	Rattus norvegicus similar to RIKEN cDNA 1810012H11 (LOC298606), mRNA [NM_001013936]
1	LOC308950	PREDICTED: Rattus norvegicus similar to heat shock protein 1 (chaperonin) (LOC308950), mRNA [XR_009038]
1	LOC309169	Rattus norvegicus tangerin (LOC309169), mRNA [NM_001025117]
1	LOC361399	Rattus norvegicus similar to autoantigen (LOC361399), mRNA [NM_001033068]
1	LOC364556	Rattus norvegicus Ab1-351 mRNA, complete cds. [AY325145]
1	LOC365354	PREDICTED: Rattus norvegicus similar to Alpha-enolase (2-phospho-D-glycerate hydro-lyase) (Non-neural enolase) (NNE) (Enolase 1) (LOC365354), mRNA [XR_009200]
1	LOC365511	PREDICTED: Rattus norvegicus similar to zinc finger protein 296 (LOC365511), mRNA [XM_345065]
1	LOC499022	Quaking protein. [Source:Uniprot/SWISSPROT;Acc:Q91XU1] [ENSRNOT00000023304]
1	LOC499778	PREDICTED: Rattus norvegicus similar to 60S ribosomal protein L7a (LOC499778), mRNA [XR_006491]
1	LOC499779	Rattus norvegicus similar to RIKEN cDNA 2900010J23, mRNA (cDNA clone MGC:105672 IMAGE:7304460), complete cds. [BC082799]
1	LOC499856	Rattus norvegicus hypothetical protein LOC499856 (LOC499856), mRNA [NM_001025042]
1	LOC679923	PREDICTED: Rattus norvegicus similar to voltage-dependent anion channel 1 (LOC679923), mRNA [XM_001054981]
1	LOC680319	PREDICTED: Rattus norvegicus hypothetical protein LOC680319 (LOC680319), mRNA [XM_001056630]

1	LOC686892	Muscleblind-like protein BLES04 (Fragment). [Source:Uniprot/SPTREMBL;Acc:Q8CIQ0] [ENSRNOT00000014315]
1	LOC690516	PREDICTED: Rattus norvegicus similar to Smad ubiquitination regulatory factor 1 isoform 2 (LOC690516), mRNA [XM_001074660]
1	Maoa	Amine oxidase [flavin-containing] A (EC 1.4.3.4) (Monoamine oxidase type A) (MAO-A). [Source:Uniprot/SWISSPROT;Acc:P21396] [ENSRNOT00000003910]
1	Mapk12	Rattus norvegicus mitogen-activated protein kinase 12 (Mapk12), mRNA [NM_021746]
1	Mapk14	Rattus norvegicus p38 mitogen activated protein kinase mRNA, complete cds. [U73142]
1	Mbd3_predicted	PREDICTED: Rattus norvegicus methyl-CpG binding domain protein 3 (predicted) (Mbd3_predicted), mRNA [XM_343162]
1	MGC109491	Rattus norvegicus similar to 1110007F12Rik protein (MGC109491), mRNA [NM_001009709]
1	MGC116197	Rattus norvegicus similar to RIKEN cDNA 1700001E04 (MGC116197), mRNA [NM_001025755]
1	MGC94736	Rattus norvegicus similar to hypothetical protein MGC35097 (MGC94736), mRNA [NM_001007685]
1	Msc_predicted	RVL633 Wackym-Soares normalized rat vestibular cDNA library Rattus norvegicus cDNA 5', mRNA sequence [CX569607]
1	Mtch1	Rattus norvegicus mitochondrial carrier homolog 1 (C. elegans), mRNA (cDNA clone IMAGE:7377090), partial cds. [BC098813]
1	Mvp	Rattus norvegicus major vault protein (Mvp), mRNA [NM_022715]
1	Myd116	Rattus norvegicus myeloid differentiation primary response gene 116 (Myd116), mRNA [NM_133546]
1	Myh14	Putative myosin IIC (Fragment). [Source:Uniprot/SPTREMBL;Acc:Q9EPH4] [ENSRNOT00000027132]
1	Nck1_predicted	PREDICTED: Rattus norvegicus non-catalytic region of tyrosine kinase adaptor protein 1 (predicted) (Nck1_predicted), mRNA [XM_217246]
1	Ncl	Rattus norvegicus nucleolin (Ncl), mRNA [NM_012749]
1	Neu1	Rattus norvegicus neuraminidase 1 (Neu1), mRNA [NM_031522]
1	Nppb	Rattus norvegicus natriuretic peptide precursor type B (Nppb), mRNA [NM_031545]
1	Nrxn1	Rattus norvegicus neurexin 1 (Nrxn1), mRNA [NM_021767]
1	Ogt	Rattus norvegicus O-linked N-acetylglucosamine (GlcNAc) transferase (UDP-N-acetylglucosamine:polypeptide-N-acetylglucosaminyl transferase) (Ogt), mRNA [NM_017107]
1	Olr1273_predicted	Rattus norvegicus olfactory receptor 1273 (predicted) (Olr1273_predicted), mRNA [NM_001000458]
1	Olr1583_predicted	Rattus norvegicus olfactory receptor 1583 (predicted) (Olr1583_predicted), mRNA [NM_001000080]
1	Olr3_predicted	Rattus norvegicus olfactory receptor 3 (predicted) (Olr3_predicted), mRNA [NM_001000110]
1	Olr53_predicted	Rattus norvegicus olfactory receptor 53 (predicted) (Olr53_predicted), mRNA [NM_001001008]
1	Olr778_predicted	Rattus norvegicus olfactory receptor 778 (predicted) (Olr778_predicted), mRNA [NM_001000607]
1	Ostf1	Rattus norvegicus osteoclast stimulating factor 1 (Ostf1), mRNA [NM_148892]
1	Oxnad1_predicted	PREDICTED: Rattus norvegicus oxidoreductase NAD-binding domain containing 1 (predicted) (Oxnad1_predicted), mRNA [XM_224623]
1	Pabpc4	Pabpc4 protein (Fragment). [Source:Uniprot/SPTREMBL;Acc:Q5I0G7]

		[ENSRNOT00000056592]
1	Paf1	Rattus norvegicus Paf1, RNA polymerase II associated factor, homolog (S. cerevisiae) (Paf1), mRNA [NM_001024898]
1	Pbk_predicted	Rattus norvegicus PDZ binding kinase (predicted) (Pbk_predicted), mRNA [NM_001079937]
1	Pbxip1	Rattus norvegicus pre-B-cell leukemia transcription factor interacting protein 1, mRNA (cDNA clone IMAGE:7097507) [BC085776]
1	Pcbp2	Rattus norvegicus poly(rC) binding protein 2 (Pcbp2), mRNA [NM_001013223]
1	Pcbp3	Rattus norvegicus poly(rC) binding protein 3 (Pcbp3), mRNA [NM_001011945]
1	Pcgf1	Rattus norvegicus polycomb group ring finger 1 (Pcgf1), mRNA [NM_001007000]
1	Pdzrn3_predicted	PDZ domain-containing RING finger protein 3 (Semaphorin cytoplasmic domain-associated protein 3) (Protein SEMACAP3). [Source:Uniprot/SWISSPROT;Acc:P68907] [ENSRNOT00000008032]
1	Pex14	Rattus norvegicus peroxisomal biogenesis factor 14 (Pex14), mRNA [NM_172063]
1	Pik3r2	Rattus norvegicus phosphatidylinositol 3-kinase, regulatory subunit, polypeptide 2 (Pik3r2), mRNA [NM_022185]
3	Plat	Rattus norvegicus plasminogen activator, tissue (Plat), mRNA [NM_013151]
1	Plekha3	Rattus norvegicus pleckstrin homology domain-containing, family A (phosphoinositide binding specific) member 3 (Plekha3), mRNA [NM_001013077]
1	Pnpla2_predicted	PREDICTED: Rattus norvegicus patatin-like phospholipase domain containing 2 (predicted) (Pnpla2_predicted), mRNA [XM_341960]
1	Pop7_predicted	PREDICTED: Rattus norvegicus processing of precursor 7, ribonuclease P family, (S. cerevisiae) (predicted) (Pop7_predicted), mRNA [XM_213733]
1	Por	Rattus norvegicus P450 (cytochrome) oxidoreductase (Por), mRNA [NM_031576]
1	Postn_predicted	PREDICTED: Rattus norvegicus periostin, osteoblast specific factor (predicted) (Postn_predicted), mRNA [XM_342245]
1	Pou2f3	POU domain, class 2, transcription factor 3 (Octamer-binding transcription factor 11) (Oct-11) (Transcription factor Skn-1). [Source:Uniprot/SWISSPROT;Acc:P42571] [ENSRNOT00000012170]
1	Ppargc1b	Rattus norvegicus peroxisome proliferative activated receptor, gamma, coactivator 1 beta (Ppargc1b), mRNA [NM_176075]
1	Ppfia4	PREDICTED: Rattus norvegicus protein tyrosine phosphatase, receptor type, f polypeptide (PTPRF), interacting protein (liprin), alpha 4 (Ppfia4), mRNA [XM_573454]
1	Ppp1r9b	Rattus norvegicus protein phosphatase 1, regulatory subunit 9B (Ppp1r9b), mRNA [NM_053474]
1	Prkaa2	Rattus norvegicus protein kinase, AMP-activated, alpha 2 catalytic subunit (Prkaa2), mRNA [NM_023991]
1	Prpf38a_predicted	PREDICTED: Rattus norvegicus PRP38 pre-mRNA processing factor 38 (yeast) domain containing A (predicted) (Prpf38a_predicted), mRNA [XM_216475]
1	Prss15	Rattus norvegicus protease, serine, 15 (Prss15), mRNA [NM_133404]
1	Psap	Rattus norvegicus prosaposin (Psap), mRNA [NM_013013]
1	Psme4	Rattus norvegicus proteasome (prosome, macropain) activator subunit 4, mRNA (cDNA clone IMAGE:7128175), complete cds. [BC090326]

1	Rab15	RATRAB15X Sprague-Dawley (clone LRB9) RAB15 mRNA, complete cds [M83679]
1	Rab6ip1_predicted	PREDICTED: Rattus norvegicus Rab6 interacting protein 1 (predicted) (Rab6ip1_predicted), mRNA [XM_219270]
1	Rad23b	Rattus norvegicus RAD23b homolog (S. cerevisiae) (Rad23b), mRNA [NM_001025275]
1	Raly	Rattus norvegicus hnRNP-associated with lethal yellow (Raly), mRNA [NM_001011958]
1	Rasl10b_predicted	PREDICTED: Rattus norvegicus RAS-like, family 10, member B (predicted) (Rasl10b_predicted), mRNA [XM_220782]
1	Rcsd1_predicted	PREDICTED: Rattus norvegicus RCSD domain containing 1 (predicted) (Rcsd1_predicted), mRNA [XM_341147]
1	RGD1304827	Rattus norvegicus hypothetical LOC316091 (RGD1304827), mRNA [NM_001009437]
1	RGD1306959_predicted	PREDICTED: Rattus norvegicus similar to C11orf17 protein (predicted) (RGD1306959_predicted), mRNA [XM_341902]
1	RGD1307395	PREDICTED: Rattus norvegicus similar to SR rich protein (RGD1307395), mRNA [XM_001060221]
1	RGD1307401	Rattus norvegicus similar to RIKEN cDNA 2310005P05 (RGD1307401), mRNA [NM_001014088]
1	RGD1307772	RGD1307772 protein (Fragment). [Source:Uniprot/SPTREMBL;Acc:Q4FZU8] [ENSRNOT00000023710]
1	RGD1307973_predicted	PREDICTED: Rattus norvegicus similar to 2900002H16Rik protein (predicted) (RGD1307973_predicted), mRNA [XM_222150]
1	RGD1309054_predicted	PREDICTED: Rattus norvegicus similar to FKSG26 protein (predicted) (RGD1309054_predicted), mRNA [XM_214707]
1	RGD1309410_predicted	PREDICTED: Rattus norvegicus LOC363020 (predicted) (RGD1309410_predicted), mRNA [XM_347094]
1	RGD1309471	Rattus norvegicus similar to hypothetical protein MGC6696 (RGD1309471), mRNA [NM_001034829]
1	RGD1309906	Rattus norvegicus similar to RIKEN cDNA 2310004I24 gene (RGD1309906), mRNA [NM_001009246]
1	RGD1310147_predicted	PREDICTED: Rattus norvegicus similar to TBC1 domain family, member 8; BUB2-like protein 1; vascular Rab-GAP [XM_340793]
1	RGD1310470	RGD1310470 protein (Fragment). [Source:Uniprot/SPTREMBL;Acc:Q5BJL1] [ENSRNOT00000003001]
1	RGD1311267	Rattus norvegicus similar to RIKEN cDNA 4931426K16 gene (RGD1311267), mRNA [NM_001039024]
1	RGD1311307	Rattus norvegicus similar to 1300014I06Rik protein (RGD1311307), mRNA [NM_001025719]
1	RGD1311849_predicted	PREDICTED: Rattus norvegicus similar to mKIAA1797 protein (predicted) (RGD1311849_predicted), mRNA [XM_233144]
1	RGD1311939_predicted	PREDICTED: Rattus norvegicus similar to AI115348 protein (predicted) (RGD1311939_predicted), mRNA [XM_233838]
1	RGD1560731_predicted	Unknown
1	RGD1561232_predicted	PREDICTED: Rattus norvegicus similar to Keratin, type II cytoskeletal 8 (Cytokeratin 8) (Cytokeratin endo A) (predicted) (RGD1561232_predicted), mRNA [XM_001070211]
1	RGD1561296_predicted	PREDICTED: Rattus norvegicus similar to cDNA sequence BC022133 (predicted) (RGD1561296_predicted), mRNA [XM_575607]
1	RGD1562658_predicted	PREDICTED: Rattus norvegicus similar to RIKEN cDNA 1700009P17 (predicted) (RGD1562658_predicted), mRNA [XM_573504]

1	RGD1562755_predicted	PREDICTED: Rattus norvegicus similar to 60S ribosomal protein L23a (predicted) (RGD1562755_predicted), mRNA [XM_223453]
1	RGD1562778_predicted	Rattus norvegicus similar to tripartite motif protein 50 (predicted) (RGD1562778_predicted), mRNA [NM_001077675]
1	RGD1562936_predicted	PREDICTED: Rattus norvegicus similar to Heat shock protein HSP 90-beta (HSP 84) (predicted) (RGD1562936_predicted), mRNA [XR_007989]
1	RGD1563344_predicted	PREDICTED: Rattus norvegicus similar to OTU domain containing 1 (predicted) (RGD1563344_predicted), mRNA [XM_574086]
1	RGD1563524_predicted	PREDICTED: Rattus norvegicus similar to 60 kDa heat shock protein, mitochondrial precursor (Hsp60) (predicted) (RGD1563524_predicted), mRNA [XM_229115]
1	RGD1563532_predicted	PREDICTED: Rattus norvegicus similar to ankyrin repeat domain 25 (predicted) (RGD1563532_predicted), mRNA [XM_001077488]
1	RGD1563990_predicted	Rattus norvegicus similar to 8430411H09Rik protein (LOC300146), mRNA [XM_217014]
1	RGD1564981_predicted	PREDICTED: Rattus norvegicus similar to Nonspecific lipid-transfer protein, mitochondrial precursor (NSL-TP) (predicted) (RGD1564981_predicted), mRNA [XR_008599]
1	RGD1565022_predicted	PREDICTED: Rattus norvegicus similar to calmodulin regulated spectrin-associated protein 1 (predicted) (RGD1565022_predicted), mRNA [XM_216007]
1	RGD1565350_predicted	PREDICTED: Rattus norvegicus similar to Shb protein (predicted) (RGD1565350_predicted), mRNA [XR_008772]
1	RGD1565584_predicted	BG673264 DRNBRC09 Rat DRG Library Rattus norvegicus cDNA clone DRNBRC09 5', mRNA sequence [BG673264]
1	RGD1565602_predicted	PREDICTED: Rattus norvegicus similar to PLU1 (predicted) (RGD1565602_predicted), mRNA [XM_239761]
1	RGD1566014_predicted	PREDICTED: Rattus norvegicus similar to Factor VIII associated protein (predicted) (RGD1566014_predicted), mRNA [XM_577058]
1	Rnaseh1	Rattus norvegicus ribonuclease H1 (Rnaseh1), mRNA [NM_001013097]
2	Rnd1	Rattus norvegicus Rho family GTPase 1 (Rnd1), mRNA [NM_001013222]
1	Rnf3_predicted	PREDICTED: Rattus norvegicus ring finger protein 3 (predicted) (Rnf3_predicted), mRNA [XM_223729]
1	Rpa3_predicted	PREDICTED: Rattus norvegicus replication protein A3 (predicted) (Rpa3_predicted), mRNA [XM_216097]
1	Rpl4	Rattus norvegicus ribosomal protein L4 (Rpl4), mRNA [NM_022510]
1	Rps25	UI-R-FS0-cqo-a-09-0-UI.s1 UI-R-FS0 Rattus norvegicus cDNA clone UI-R-FS0-cqo-a-09-0-UI 3', mRNA sequence [CA508544]
1	Rrad	Rattus norvegicus Ras-related associated with diabetes (Rrad), mRNA [NM_053338]
1	Rsn	Rattus norvegicus restin (Reed-Steinberg cell-expressed intermediate filament-associated protein) (Rsn), mRNA [NM_031745]
1	RT1-A2	Rattus norvegicus RT1 class Ia, locus A2 (RT1-A2), mRNA [NM_001008829]
1	RT1-CE1	Rattus norvegicus RT1 class I, CE1 (RT1-CE1), mRNA [NM_001008832]
1	RT1-CE16	Rattus norvegicus RT1 class I, CE16 (RT1-CE16), mRNA [NM_001008839]
1	RT1-CE2	Rattus norvegicus RT1 class I, CE2 (RT1-CE2), mRNA [NM_001008840]

1	RT1-CE3	Rattus norvegicus RT1 class I, CE3 (RT1-CE3), mRNA [NM_001008841]
1	RT1-CE4	Rattus norvegicus RT1 class I, CE4 (RT1-CE4), mRNA [NM_001008842]
1	RT1-CE7	Rattus norvegicus RT1 class I, CE7 (RT1-CE7), mRNA [NM_001008845]
1	RT1-Cl	Rattus norvegicus RT1 class Ib, locus Cl (RT1-Cl), mRNA [NM_206848]
1	RT1-Db1	Rattus norvegicus RT1 class II, locus Db1 (RT1-Db1), mRNA [NM_001008884]
1	S63519	S63519 Rattus sp. membrane protein-73 mRNA, partial cds; mitochondrial gene for mitochondrial product [S63519]
1	Scly	Rattus norvegicus selenocysteine lyase (Scly), mRNA [NM_001007755]
1	Serbp1	Rattus norvegicus Serpine1 mRNA binding protein 1 (Serbp1), mRNA [NM_145086]
1	Serping1	Rattus norvegicus serine (or cysteine) peptidase inhibitor, clade G, member 1 (Serping1), mRNA [NM_199093]
1	Sfrs14_predicted	Rattus norvegicus similar to arginine/serine-rich 14 splicing factor (LOC361126), mRNA [XM_341413]
1	Sgcg	Rattus norvegicus sarcoglycan, gamma (dystrophin-associated glycoprotein) (Sgcg), mRNA [NM_001006993]
1	Slc12a7	PREDICTED: Rattus norvegicus solute carrier family 12 (potassium [XM_001071999]
1	Slc25a5	Rattus norvegicus solute carrier family 25 (mitochondrial carrier; adenine nucleotide translocator), member 5 (Slc25a5), mRNA [NM_057102]
1	Spag7_predicted	PREDICTED: Rattus norvegicus sperm associated antigen 7 (predicted) (Spag7_predicted), mRNA [XM_220574]
1	Spg7	Rattus norvegicus spastic paraplegia 7 homolog (human) (Spg7), mRNA [NM_181388]
1	Spink5_predicted	PREDICTED: Rattus norvegicus serine protease inhibitor, Kazal type 5 (predicted) (Spink5_predicted), mRNA [XM_001056195]
1	Spsb4_predicted	PREDICTED: Rattus norvegicus splA [XM_236555]
1	Srp68_predicted	Rattus norvegicus similar to signal recognition particle 68kDa (LOC363707), mRNA [XM_343986]
1	Stat3	Rattus norvegicus signal transducer and activator of transcription 3 (Stat3), mRNA [NM_012747]
1	Taf9	Rattus norvegicus TAF9 RNA polymerase II, TATA box binding protein (TBP)-associated factor (Taf9), transcript variant 2, mRNA [NM_184048]
1	Tagln2	Rattus norvegicus transgelin 2 (Tagln2), mRNA [NM_001013127]
1	TC583295	Unknown
1	TC584984	Unknown
1	TC587305	Unknown
1	TC588650	Q3UE36_MOUSE (Q3UE36) Bone marrow macrophage cDNA, RIKEN full-length enriched library, clone:G530015L18 product:TFIIIC2 subunit homolog, partial (3%) [TC588650]
1	TC590435	Unknown
1	TC595486	Q2KZQ6_BORA1 (Q2KZQ6) Mannose-6-phosphate isomerase , partial (6%) [TC595486]
1	TC598739	Q8LP76_9SOLN (Q8LP76) HT-A protein (Fragment), partial (17%) [TC598739]
1	TC599269	Unknown

1	TC599311	Unknown
1	TC601277	Unknown
1	TC601898	Q7TQ12_RAT (Q7TQ12) Aa1114, partial (9%) [TC601898]
1	TC602662	Unknown
1	TC603711	Q9DEY1_CYPCA (Q9DEY1) Ovarian fibroin-like substance-1, partial (5%) [TC603711]
1	TC606685	Unknown
1	TC607876	Unknown
1	TC610053	Unknown
1	TC611036	Unknown
1	TC611785	Unknown
1	TC613062	Q6PED9_MOUSE (Q6PED9) Rai16 protein (Fragment), partial (63%) [TC613062]
1	TC616203	Q33PR9_9GAMM (Q33PR9) Adenylyl cyclase CyaB, partial (10%) [TC616203]
1	TC634117	Q5NA53_ORYSA (Q5NA53) Glycogenin-like protein, partial (3%) [TC634117]
1	TC635003	Unknown
1	TC637917	Q5SSP7_MOUSE (Q5SSP7) T-box 2, partial (8%) [TC637917]
1	TC641622	Unknown
1	TC642107	Q81D10_BACCR (Q81D10) Phage protein, partial (21%) [TC642107]
1	TC647139	Q3C866_9CLOT (Q3C866) Helicase, C-terminal:DEAD/DEAH box helicase, N-terminal, partial (4%) [TC647139]
1	Tcp11	Rattus norvegicus t-complex protein 11 (mouse) (Tcp11), mRNA [NM_001007695]
1	Tex264	Rattus norvegicus testis expressed gene 264 homolog (mouse) (Tex264), mRNA [NM_001007665]
1	Tex9_predicted	PREDICTED: Rattus norvegicus testis expressed gene 9 (predicted) (Tex9_predicted), mRNA [XM_001054229]
1	Tgfb1i4	Rattus norvegicus transforming growth factor beta 1 induced transcript 4, mRNA (cDNA clone IMAGE:6918096), complete cds. [BC059146]
1	Thoc1	Rattus norvegicus THO complex 1 (Thoc1), mRNA [NM_001047850]
1	Thrap5_predicted	PREDICTED: Rattus norvegicus thyroid hormone receptor associated protein 5 (predicted) (Thrap5_predicted), mRNA [XM_216837]
2	Tmed9	Rattus norvegicus transmembrane emp24 protein transport domain containing 9 (Tmed9), mRNA [NM_001009703]
1	Tmem110	Rattus norvegicus transmembrane protein 110 (Tmem110), mRNA [NM_198774]
1	Tmf1	Rattus norvegicus TATA element modulatory factor 1 (Tmf1), mRNA [NM_053671]
1	Tollip_predicted	PREDICTED: Rattus norvegicus toll interacting protein (predicted) (Tollip_predicted), mRNA [XM_341961]
1	Trak2	Rattus norvegicus trafficking protein, kinesin binding 2 (Trak2), mRNA [NM_133560]
1	Trhde	Thyrotropin-releasing hormone-degrading ectoenzyme (EC 3.4.19.6) (TRH- degrading ectoenzyme) (TRH-DE) (TRH-specific aminopeptidase) (Thyroliberinase) (Pyroglutamyl-peptidase II) (PAP-II). [Source:Uniprot/SWISSPROT;Acc:Q10836] [ENSRNOT00000007461]
1	Trim63	Rattus norvegicus tripartite motif protein 63 (Trim63), mRNA [NM_080903]
1	Ttr	Rattus norvegicus transthyretin (Ttr), mRNA [NM_012681]

1	Tuba6	Rattus norvegicus tubulin, alpha 6 (Tuba6), mRNA [NM_001011995]
1	Tubb2b	Rattus norvegicus tubulin, beta 2b (Tubb2b), mRNA [NM_001013886]
1	Tubb2c	Rattus norvegicus tubulin, beta 2c (Tubb2c), mRNA [NM_199094]
1	Tubb5	Rattus norvegicus tubulin, beta 5 (Tubb5), mRNA [NM_173102]
1	Ube2e2	PREDICTED: Rattus norvegicus ubiquitin-conjugating enzyme E2E 2 (UBC4 [XM_341288]
2	Ube2q_predicted	PREDICTED: Rattus norvegicus ubiquitin-conjugating enzyme E2Q (putative) (predicted) (Ube2q_predicted), mRNA [XM_215612]
5	Ucp2	Rattus norvegicus uncoupling protein 2 (mitochondrial, proton carrier) (Ucp2), mRNA [NM_019354]
1	Unc45b_predicted	PREDICTED: Rattus norvegicus unc-45 homolog B (C. elegans) (predicted) (Unc45b_predicted), mRNA [XM_220771]
1	Vil2	Rattus norvegicus villin 2 (Vil2), mRNA [NM_019357]
1	Vim	Rattus norvegicus vimentin (Vim), mRNA [NM_031140]
1	Wdr27_predicted	PREDICTED: Rattus norvegicus WD repeat domain 27 (predicted) (Wdr27_predicted), mRNA [XM_001055617]
1	XM_215841	Rattus norvegicus similar to hypothetical protein FLJ32800 (LOC296118), mRNA [XM_215841]
1	XM_222132	Rattus norvegicus similar to Spindlin-like protein 2 (SPIN-2) (LOC288640), mRNA [XM_222132]
1	XM_229703	Rattus norvegicus similar to cDNA sequence BC003993 (LOC317034), mRNA [XM_229703]
1	XM_230279	Rattus norvegicus similar to protein kinase C and casein kinase substrate in neurons 3 (LOC311187), mRNA [XM_230279]
1	XM_230768	Rattus norvegicus similar to 60S ribosomal protein L7a (Surfeit locus protein 3) (PLA-X polypeptide) (LOC311565), mRNA [XM_230768]
1	XM_236784	Rattus norvegicus similar to sex-determination protein homolog Fem1a (LOC316131), mRNA [XM_236784]
1	XM_340847	Rattus norvegicus similar to myosin containing PDZ domain (LOC360570), mRNA [XM_340847]
1	XM_342024	Rattus norvegicus similar to DNA damage binding protein 1 (Damage-specific DNA binding protein 1) (DDB p127 subunit) (DDBa) (UV-damaged DNA-binding protein 1) (UV-DDB 1) (Xeroderma pigmentosum group E complementing protein) (XPCe) (X-associated...
1	XM_343598	Rattus norvegicus similar to titin isoform N2-A; connectin; CMH9, included; cardiomyopathy, dilated 1G (autosomal dominant) (LOC363258), mRNA [XM_343598]
1	XM_345660	Rattus norvegicus similar to RIKEN cDNA 1100001I23 (LOC366602), mRNA [XM_345660]
1	Zbtb17	Rattus norvegicus zinc finger and BTB domain containing 17 (Zbtb17), mRNA [NM_001012105]
1	Zdhhc2	Rattus norvegicus zinc finger, DHHC domain containing 2 (Zdhhc2), mRNA [NM_145096]

Appendix B: Genes selected as significant by class comparison analysis

Parametric p-value	Geom mean of ratios in class 1 : Failure	Geom mean of ratios in class 2 : Unknown	Fold difference of geom means	Agilent ID	Gene Name
1.00E-07	0.648	0.367	1.766	A_44_P490277	ENSRNOT00000048403
3.00E-07	1.108	0.594	1.865	A_44_P998312	NM_001037652
4.00E-07	0.545	0.298	1.829	A_44_P234378	XR_006502
5.00E-07	0.744	1.278	0.582	A_44_P250319	ENSRNOT00000031045
5.00E-07	0.636	0.383	1.661	A_44_P232265	XM_346093
6.00E-07	1.372	0.888	1.545	A_44_P196685	XM_341907
7.00E-07	0.629	0.333	1.889	A_44_P222660	XM_226568
7.00E-07	0.597	0.363	1.645	A_44_P447766	ENSRNOT00000050331
1.10E-06	0.893	1.819	0.491	A_44_P992854	NM_057132
1.10E-06	2.174	5.398	0.403	A_44_P210440	ENSRNOT00000014802
1.10E-06	1.098	2.404	0.457	A_44_P929695	XM_228203
1.20E-06	0.59	0.355	1.662	A_44_P351714	ENSRNOT00000043501
1.40E-06	0.296	0.117	2.53	A_43_P14682	NM_022674
1.70E-06	1.11	2.063	0.538	A_44_P131240	ENSRNOT00000050411
2.30E-06	0.587	0.351	1.672	A_44_P342208	A_44_P342208
3.00E-06	0.595	0.35	1.7	A_44_P203838	XM_225531
3.30E-06	0.344	0.631	0.545	A_44_P860396	ENSRNOT00000047510
3.30E-06	2.135	0.973	2.194	A_43_P10269	NM_001025712
3.70E-06	0.85	0.515	1.65	A_42_P496649	DV727080
4.70E-06	0.71	0.4	1.775	A_44_P651922	NM_017150
4.70E-06	0.675	1.019	0.662	A_44_P348868	NM_019226
5.30E-06	0.84	0.415	2.024	A_44_P511324	NM_053982
5.70E-06	0.958	0.518	1.849	A_44_P1013385	ENSRNOT00000022065
6.20E-06	0.937	1.78	0.526	A_44_P992854	NM_057132
7.20E-06	0.748	0.304	2.461	A_43_P12806	NM_053439
7.70E-06	0.578	0.361	1.601	A_44_P548455	ENSRNOT00000032995
7.90E-06	0.383	1.049	0.365	A_44_P622201	BC098778
9.40E-06	0.927	1.72	0.539	A_44_P992854	NM_057132
9.70E-06	0.617	0.39	1.582	A_42_P793008	NM_130432
1.01E-05	24.293	101.384	0.24	A_44_P864923	AW916836
1.02E-05	2.828	9.214	0.307	A_44_P336664	CF108444
1.02E-05	1.829	4.532	0.404	A_44_P226208	AI170501
1.03E-05	1.059	0.565	1.874	A_42_P493785	ENSRNOT00000001419
1.08E-05	1.211	0.773	1.567	A_44_P714524	CX570178
1.09E-05	0.938	1.708	0.549	A_44_P992854_2348	NM_057132
1.18E-05	0.06	0.218	0.275	A_44_P594411	CB804485
1.18E-05	0.946	1.812	0.522	A_44_P992854	NM_057132
1.23E-05	1.507	2.463	0.612	A_44_P1033739	XM_573823
1.24E-05	0.171	0.82	0.209	A_44_P900646	TC627022
1.34E-05	0.11	0.63	0.175	A_44_P930730	TC585294
1.37E-05	0.92	1.763	0.522	A_44_P992854	NM_057132
1.52E-05	0.258	0.139	1.856	A_44_P525250	XM_227370

1.55E-05	1.761	5.304	0.332	A_43_P20704	ENSRNOT00000050411
1.56E-05	0.686	1.61	0.426	A_44_P109998	XM_227287
1.70E-05	0.631	0.39	1.618	A_44_P368365	XM_235395
1.74E-05	0.159	0.782	0.203	A_44_P579214	TC633900
1.85E-05	0.928	1.78	0.521	A_44_P992854	NM_057132
1.89E-05	0.614	0.428	1.435	A_44_P852623	ENSRNOT00000060788
2.02E-05	0.266	0.173	1.538	A_44_P432965	NM_031840
2.20E-05	1.269	2.067	0.614	A_44_P361380	ENSRNOT00000038715
2.26E-05	0.823	1.559	0.528	A_43_P12215	NM_022386
2.28E-05	1.715	1.035	1.657	A_44_P1042125	XM_001060585
2.35E-05	0.358	0.716	0.5	A_44_P142352	ENSRNOT00000003707
2.36E-05	0.725	1.627	0.446	A_44_P868828	TC628052
2.38E-05	0.572	0.378	1.513	A_44_P302676	XM_221003
2.43E-05	1.585	0.915	1.732	A_43_P10161	XM_213920
2.49E-05	0.974	0.524	1.859	A_42_P632328	ENSRNOT00000003556
2.59E-05	4.614	2.432	1.897	A_44_P387587	NM_022585
2.63E-05	0.649	0.446	1.455	A_44_P391688	ENSRNOT00000034681
2.65E-05	0.765	0.399	1.917	A_44_P360946	XR_008195
2.66E-05	0.773	1.075	0.719	A_44_P446556	XM_342906
3.07E-05	5.783	14.662	0.394	A_44_P550237	NM_017212
3.07E-05	1.493	0.981	1.522	A_42_P547945	BC098813
3.10E-05	0.532	0.351	1.516	A_44_P215788	NM_001005905
3.22E-05	0.985	1.722	0.572	A_44_P992854	NM_057132
3.26E-05	3.015	1.02	2.956	A_44_P118075	XM_575227
3.46E-05	1.747	0.713	2.45	A_44_P214873	NM_024362
3.59E-05	1.225	1.972	0.621	A_44_P288997	AW916759
3.76E-05	1.42	0.112	12.679	A_44_P264230	XM_001062165
3.81E-05	0.586	0.39	1.503	A_42_P728472	NM_001007600
3.89E-05	0.855	1.821	0.47	A_44_P165817	NP798075
4.14E-05	0.896	0.638	1.404	A_42_P709819	XM_001063185
4.29E-05	5.716	3.546	1.612	A_42_P793598	NM_194354
4.41E-05	0.65	0.476	1.366	A_43_P14875	NM_031324
4.45E-05	0.77	0.48	1.604	A_42_P777285	AI013497
4.46E-05	1.641	22.759	0.072	A_44_P435618_1878	NM_017333
4.46E-05	1.331	0.147	9.054	A_44_P701240	TC620596
4.58E-05	1.702	3.585	0.475	A_44_P153979	NM_013164
4.62E-05	0.828	0.499	1.659	A_44_P745027	XR_009438
4.92E-05	0.661	0.497	1.33	A_43_P10034	NM_053928
5.11E-05	1.725	3.759	0.459	A_44_P188729	ENSRNOT00000046108
5.18E-05	0.713	0.52	1.371	A_43_P11181	XM_001077170
5.24E-05	3.478	1.775	1.959	A_42_P499282	NM_001031660
5.61E-05	0.565	1.319	0.428	A_44_P342075	ENSRNOT00000027314
5.84E-05	0.363	0.225	1.613	A_44_P189065	ENSRNOT00000027123
5.87E-05	1.754	3.263	0.538	A_44_P466111	AB012231
5.91E-05	0.938	0.68	1.379	A_44_P997815	NM_001079698
5.96E-05	1.087	1.508	0.721	A_44_P203421	U45479
6.20E-05	0.184	0.453	0.406	A_44_P837560	TC583130
6.29E-05	1.045	0.674	1.55	A_44_P207907	NM_022498

6.30E-05	0.522	0.355	1.47	A_44_P290905	ENSRNOT00000049230
6.30E-05	0.337	0.561	0.601	A_44_P340977	ENSRNOT00000047510
6.30E-05	0.484	0.333	1.453	A_44_P698581	A_44_P698581
6.44E-05	0.508	0.31	1.639	A_44_P199482	XR_005657
6.64E-05	1.887	0.867	2.176	A_43_P16650	XM_214107
6.80E-05	1.28	3.862	0.331	A_43_P12612	Y12259
6.89E-05	0.523	0.696	0.751	A_44_P1059422	NM_001009268
6.92E-05	1.178	0.77	1.53	A_44_P606810	TC593084
6.97E-05	0.653	0.322	2.028	A_44_P304752	XR_008958
7.07E-05	1.148	0.82	1.4	A_44_P329688	XM_240915
7.14E-05	0.538	1.185	0.454	A_43_P11613	NM_012903
7.30E-05	0.453	0.299	1.515	A_44_P192364	ENSRNOT00000057412
7.37E-05	0.543	0.317	1.713	A_42_P780097	NM_001008280
7.43E-05	0.499	0.723	0.69	A_44_P553980	ENSRNOT00000047510
7.49E-05	1.092	0.816	1.338	A_44_P193221	CK471009
7.71E-05	0.771	1.227	0.628	A_44_P482595	NM_053796
7.80E-05	0.562	0.369	1.523	A_42_P487031	NM_001009539
7.83E-05	0.938	2.439	0.385	A_44_P745617	TC603676
8.00E-05	0.277	0.086	3.221	A_42_P751720	XR_009563
8.67E-05	0.856	1.937	0.442	A_44_P400591	A_44_P400591
8.72E-05	0.097	0.059	1.644	A_43_P16774	NM_001006995
8.75E-05	0.728	0.544	1.338	A_42_P839036	ENSRNOT00000013359
8.79E-05	0.334	0.922	0.362	A_44_P853879	TC624399
9.06E-05	0.425	0.307	1.384	A_44_P271643	NM_053970
9.30E-05	1.648	0.983	1.677	A_44_P343303	NM_019367
9.37E-05	0.556	0.343	1.621	A_44_P867677	XR_005504
9.66E-05	0.759	0.607	1.25	A_43_P10477	CF108377
9.70E-05	0.64	0.441	1.451	A_44_P482749	XR_008366
9.87E-05	0.95	0.552	1.721	A_44_P1054708	NM_001009538
9.93E-05	1.22	2.358	0.517	A_44_P834734	AB026259
9.93E-05	1.993	2.741	0.727	A_44_P853685	TC589959
9.94E-05	0.668	0.456	1.465	A_44_P339867	NM_017199
0.0001072	0.497	1.359	0.366	A_44_P434859	BC090353
0.0001092	0.25	0.906	0.276	A_44_P158079	BI395434
0.0001105	0.508	0.345	1.472	A_44_P523261	ENSRNOT00000049805
0.000112	0.656	0.471	1.393	A_44_P389243	ENSRNOT00000000433
0.0001123	1.57	0.984	1.596	A_43_P12047	NM_019380
0.0001133	0.388	0.25	1.552	A_44_P1002452	NM_001009271
0.0001135	3.389	6.42	0.528	A_42_P799113	NM_139104
0.0001136	0.975	1.901	0.513	A_44_P363090	NM_001008725
0.0001146	0.979	1.792	0.546	A_44_P992854	NM_057132
0.0001147	1.178	0.834	1.412	A_42_P512252	NM_201421
0.0001157	0.682	0.319	2.138	A_42_P674598	NM_013067
0.0001168	0.505	0.35	1.443	A_44_P361504	ENSRNOT00000036109
0.0001195	0.601	0.408	1.473	A_42_P596503	NM_053334
0.0001215	0.223	0.93	0.24	A_44_P1018098	ENSRNOT00000019724
0.0001224	0.17	0.633	0.269	A_44_P449108	AI043579
0.0001245	1.379	0.967	1.426	A_44_P325376	XM_574706

0.0001265	0.651	0.939	0.693	A_44_P1059334	NM_133398
0.0001267	3.05	7.281	0.419	A_44_P278113	ENSRNOT00000043693
0.0001273	0.732	0.408	1.794	A_44_P959692	XM_001066878
0.0001292	0.659	0.41	1.607	A_42_P827124	ENSRNOT00000007351
0.0001293	1.729	0.534	3.238	A_44_P125226	AW532988
0.00013	3.517	1.958	1.796	A_44_P667648	ENSRNOT00000010055
0.000131	1.014	0.544	1.864	A_44_P728932	ENSRNOT00000028742
0.0001314	0.592	0.39	1.518	A_44_P301863	ENSRNOT00000007403
0.0001331	1.498	2.948	0.508	A_44_P337606	ENSRNOT00000016804
0.0001364	0.577	1.342	0.43	A_44_P820184	AI030973
0.0001369	0.286	0.659	0.434	A_44_P187830	ENSRNOT00000002851
0.0001378	1.616	6.76	0.239	A_44_P254016	NM_016992
0.0001378	0.966	1.964	0.492	A_44_P992854	NM_057132
0.0001384	1.38	2.301	0.6	A_44_P436528	ENSRNOT00000014310
0.0001386	1.122	2.241	0.501	A_44_P261450	ENSRNOT00000009894
0.0001404	1.302	10.509	0.124	A_42_P631453	XM_216941
0.0001434	1.186	0.786	1.509	A_44_P427523	NM_057140
0.0001444	0.06	0.026	2.308	A_44_P400494	NM_053976
0.0001445	1.093	0.806	1.356	A_43_P12732	NM_033097
0.0001446	0.769	0.392	1.962	A_44_P450149	ENSRNOT00000042609
0.0001461	2.655	1.521	1.746	A_42_P660068	NM_031350
0.0001487	0.661	0.44	1.502	A_43_P17696	NM_001004257
0.00015	0.519	0.331	1.568	A_44_P536545	XM_001055461
0.0001504	0.8	0.527	1.518	A_42_P552233	XM_213765
0.0001515	0.673	1.313	0.513	A_43_P22613	ENSRNOT00000018266
0.0001528	0.848	0.479	1.77	A_42_P675659	NM_001004276
0.0001537	5.155	1.245	4.141	A_44_P921710	A_44_P921710
0.0001545	1.18	0.638	1.85	A_43_P10614	TC600099
0.0001564	0.339	0.141	2.404	A_44_P786208	CF111551
0.0001565	0.535	1.129	0.474	A_44_P196933	NM_001014031
0.0001573	0.474	0.879	0.539	A_44_P442733	NM_022386
0.0001594	2.009	1.049	1.915	A_44_P329357	NM_017112
0.0001647	0.453	0.305	1.485	A_44_P182913	XR_008450
0.0001653	1.04	2.104	0.494	A_44_P154245	ENSRNOT00000003146
0.0001655	1.678	0.851	1.972	A_43_P13146	NM_131907
0.0001674	2.593	3.827	0.678	A_44_P876215	CF109454
0.0001682	2.156	1.4	1.54	A_43_P12438	NM_024387
0.0001685	0.667	0.292	2.284	A_44_P483888	XM_001060262
0.0001701	1.918	0.856	2.241	A_44_P583151	A_44_P583151
0.0001703	0.621	0.436	1.424	A_44_P222865	ENSRNOT00000005711
0.0001708	1.326	0.949	1.397	A_43_P16523	XM_341861
0.0001709	0.754	1.847	0.408	A_44_P1059789	ENSRNOT00000010118
0.0001718	0.721	0.415	1.737	A_44_P185138	A_44_P185138
0.0001723	79.722	9.691	8.226	A_42_P669388	NM_001039011
0.0001727	6.952	1.625	4.278	A_43_P15602	NM_134391
0.0001739	0.922	1.539	0.599	A_44_P264988	ENSRNOT00000016784
0.0001765	0.138	0.558	0.247	A_44_P900178	TC584409
0.0001765	0.912	0.618	1.476	A_44_P1051965	NM_053877

0.0001815	2.15	4.277	0.503	A_44_P466108	AB012231
0.0001816	0.904	1.848	0.489	A_44_P551919	ENSRNOT00000057681
0.0001828	2.017	3.39	0.595	A_44_P536282	NM_001013130
0.0001831	1.209	0.791	1.528	A_43_P10634	NM_001025123
0.0001843	0.162	0.082	1.976	A_44_P236187	NM_022582
0.0001867	0.624	0.356	1.753	A_42_P604121	NM_001012144
0.0001884	0.147	0.945	0.156	A_44_P590051	AW917697
0.0001884	0.87	1.917	0.454	A_44_P884555	BE113337
0.0001902	2.419	1.013	2.388	A_44_P975513	TC588827
0.0001914	3.919	8.831	0.444	A_44_P1043059	NM_001013130
0.0001925	2.125	6.128	0.347	A_44_P463064	ENSRNOT00000043693
0.0001928	1.157	2.057	0.562	A_44_P1044499	ENSRNOT00000006333
0.000193	3.994	8.596	0.465	A_44_P685899	TC601880
0.0001952	0.409	0.273	1.498	A_44_P226029	ENSRNOT00000016184
0.0002013	1.53	0.82	1.866	A_44_P704874	AA963844
0.0002062	0.143	0.553	0.259	A_44_P824467	TC599815
0.0002067	2.292	1.435	1.597	A_42_P563553	XM_001081219
0.0002067	0.504	0.345	1.461	A_44_P432139	NM_031099
0.0002096	0.502	0.369	1.36	A_44_P473449	XM_227913
0.0002105	0.708	0.488	1.451	A_43_P15307	NM_030859
0.0002112	2.561	5.391	0.475	A_44_P792220	TC590891
0.0002143	0.19	0.938	0.203	A_44_P251787	AW142969
0.0002161	0.584	0.446	1.309	A_44_P222865	ENSRNOT00000005711
0.0002176	3.499	6.148	0.569	A_44_P668313	ENSRNOT00000017233
0.0002187	0.345	2.9	0.119	A_44_P901264	TC607281
0.0002198	0.412	0.313	1.316	A_44_P337088	NM_133609
0.0002214	1	1.42	0.704	A_42_P642507	ENSRNOT00000037829
0.0002236	5.698	3.824	1.49	A_43_P10709	XM_215728
0.0002255	0.147	0.818	0.18	A_44_P959890	AABR03000060
0.0002268	0.507	0.34	1.491	A_44_P232113	A_44_P232113
0.0002277	11.947	19.659	0.608	A_44_P333010	ENSRNOT00000014193
0.000232	3.682	2.729	1.349	A_44_P561113	TC615156
0.0002321	0.506	0.854	0.593	A_44_P245665	NM_053311
0.0002328	0.246	0.43	0.572	A_44_P532389	CF110666
0.0002348	0.619	0.409	1.513	A_44_P100996	NM_017150
0.0002359	1.098	0.215	5.107	A_44_P913155	AW915016
0.0002366	0.976	1.851	0.527	A_44_P261874	NM_175761
0.0002384	1.809	1.245	1.453	A_44_P138347	NM_001034958
0.0002443	2.253	5.507	0.409	A_44_P463071	ENSRNOT00000043693
0.0002464	5.152	18.322	0.281	A_44_P177704	AF370889
0.0002469	0.506	0.289	1.751	A_42_P644278	NM_001037349
0.0002472	0.631	0.43	1.467	A_44_P283941	NM_001009600
0.0002482	0.187	0.547	0.342	A_43_P19515	NM_001014207
0.0002483	0.787	0.504	1.562	A_42_P506402	NM_145677
0.0002486	0.985	0.654	1.506	A_44_P132470	NM_022511
0.00025	0.286	0.172	1.663	A_44_P928928	ENSRNOT00000044499
0.0002505	0.486	0.305	1.593	A_44_P537303	NM_022510
0.0002521	0.955	1.426	0.67	A_44_P238257	NM_053920

0.0002547	0.709	0.999	0.71	A_44_P976320	TC593051
0.0002628	0.178	0.824	0.216	A_44_P978172	TC602645
0.0002628	0.935	1.239	0.755	A_42_P726994	XM_001072149
0.0002634	0.198	0.733	0.27	A_44_P458987	AY325145
0.000264	1.182	2.933	0.403	A_43_P21507	ENSRNOT00000049300
0.0002649	0.787	0.565	1.393	A_44_P116172	ENSRNOT00000019107
0.0002671	0.954	0.599	1.593	A_44_P271416	NM_138708
0.0002683	1.508	1.103	1.367	A_44_P1033023	NM_013063
0.0002704	0.232	0.63	0.368	A_44_P670611	TC632008
0.0002726	0.966	0.519	1.861	A_44_P248083	XM_221978
0.000273	2.021	2.922	0.692	A_42_P516640	NM_019124
0.0002735	0.244	0.659	0.37	A_43_P11261	XM_234572
0.0002739	0.456	1.464	0.311	A_44_P1012333	BC090353
0.0002755	0.657	0.468	1.404	A_44_P1003072	NM_001025650
0.0002793	1.032	1.751	0.589	A_44_P416633	NM_175754
0.0002822	1.115	0.882	1.264	A_44_P213392	NM_057122
0.0002859	10.514	34.313	0.306	A_44_P320617	NM_019131
0.0002863	1.527	0.974	1.568	A_44_P1046705	ENSRNOT00000025008
0.0002899	6.676	12.342	0.541	A_43_P16895	XM_224672
0.0002909	36.413	141.416	0.257	A_42_P832832	NM_012530
0.0002968	1.585	0.897	1.767	A_44_P555042	NM_001000169
0.0002974	0.558	0.217	2.571	A_44_P714409	NM_001047907
0.0003003	0.585	0.373	1.568	A_44_P455065	ENSRNOT00000045295
0.0003037	0.184	0.145	1.269	A_44_P143567	NM_031840
0.0003084	0.738	0.455	1.622	A_43_P11682	NM_013050
0.0003151	0.934	0.626	1.492	A_44_P760650	ENSRNOT00000024085
0.0003151	2.559	1.51	1.695	A_44_P988460	AW142021
0.000317	0.621	2.902	0.214	A_44_P140378	ENSRNOT00000015232
0.00032	0.637	0.277	2.3	A_44_P1042876	NM_031971
0.0003219	0.792	0.964	0.822	A_44_P396522	NM_021840
0.0003236	0.618	0.766	0.807	A_44_P227361	ENSRNOT00000008741
0.0003237	2.451	4.11	0.596	A_44_P790431	ENSRNOT00000060252
0.0003257	0.638	1.024	0.623	A_43_P11241	ENSRNOT00000055970
0.0003319	0.716	1.052	0.681	A_42_P760177	XM_342906
0.0003362	0.149	0.698	0.213	A_44_P420869	BM391518
0.0003365	0.488	0.348	1.402	A_44_P203746	XM_344416
0.0003413	0.941	1.493	0.63	A_42_P548791	NM_021762
0.000342	1.123	0.849	1.323	A_44_P291060	ENSRNOT00000015257
0.000346	0.944	0.69	1.368	A_44_P991484	CA510796
0.0003462	1.128	1.574	0.717	A_44_P741147	AW917588
0.0003479	0.228	0.125	1.824	A_44_P531129	M12822
0.0003516	0.663	0.318	2.085	A_44_P319256	ENSRNOT00000056171
0.0003551	3.825	1.003	3.814	A_44_P219447	BM986234
0.0003557	1.527	1.108	1.378	A_44_P1033023_781	NM_013063
0.0003559	0.496	0.329	1.508	A_44_P168184	AF507943
0.0003598	0.733	1.223	0.599	A_44_P313431	ENSRNOT00000009755
0.0003698	3.122	1.846	1.691	A_44_P358361	NM_001002821
0.0003701	0.684	0.547	1.25	A_42_P519910	ENSRNOT00000021017

0.0003711	3.307	0.461	7.174	A_44_P299109	DV723665
0.0003724	0.923	0.7	1.319	A_44_P1025944	NM_147140
0.0003761	1.487	2.525	0.589	A_44_P622978	TC590816
0.0003781	1.5	0.986	1.521	A_44_P457447	CF112427
0.0003797	5.77	12.365	0.467	A_42_P588944	NM_012862
0.0003873	0.722	0.432	1.671	A_44_P278829	XR_006025
0.0003898	10.847	19.02	0.57	A_44_P1007347	NM_019386
0.0003921	0.539	0.369	1.461	A_44_P535706	ENSRNOT00000017422
0.0004022	0.809	0.569	1.422	A_42_P699937	NM_001034134
0.0004052	12.474	1.408	8.859	A_44_P510951	ENSRNOT00000028443
0.000406	2.185	1.357	1.61	A_44_P460797	AF020046
0.0004067	1.068	1.407	0.759	A_44_P745393	ENSRNOT00000023274
0.0004081	1.399	1.003	1.395	A_43_P13808	NM_001017477
0.0004191	0.636	0.441	1.442	A_44_P222865	ENSRNOT00000005711
0.0004193	6.874	57.055	0.12	A_44_P353708	ENSRNOT00000016663
0.0004206	1.752	0.77	2.275	A_44_P289312	CB567518
0.0004286	0.652	0.435	1.499	A_44_P458241	ENSRNOT00000024406
0.000432	1.416	0.984	1.439	A_42_P770458	NM_134414
0.0004337	3.073	1.522	2.019	A_43_P12741	NM_052798
0.0004367	1.827	3.496	0.523	A_44_P1031034	NM_031745
0.0004393	1.694	0.462	3.667	A_42_P577938	NM_001014218
0.0004399	5.044	7.923	0.637	A_44_P505180	NM_057202
0.0004401	1.384	2.066	0.67	A_44_P309215	NM_001024771
0.0004435	1.067	1.575	0.677	A_44_P351563	A_44_P351563
0.0004462	1.389	2.253	0.617	A_43_P15794	NM_053766
0.000449	0.474	0.303	1.564	A_44_P397495	NM_024359
0.0004502	0.697	0.479	1.455	A_44_P457053	XR_007987
0.0004569	0.759	0.478	1.588	A_44_P522482	NM_001013928
0.0004598	0.194	0.629	0.308	A_44_P261444	XM_343065
0.0004599	2.978	5.425	0.549	A_44_P137187	ENSRNOT00000042098
0.0004624	1.187	0.715	1.66	A_43_P10498	XM_237039
0.0004634	1.279	0.637	2.008	A_44_P605194	XM_340890
0.0004683	0.945	0.537	1.76	A_44_P281457	XM_001054883
0.0004689	0.963	0.494	1.949	A_44_P1020018	ENSRNOT00000016882
0.0004718	1.103	0.797	1.384	A_42_P645110	NM_001029919
0.0004743	0.759	0.561	1.353	A_44_P461944	NM_001007714
0.0004832	1.048	0.68	1.541	A_44_P288826	ENSRNOT00000025491
0.000487	0.09	0.044	2.045	A_44_P154298	XM_573787
0.000488	0.33	0.732	0.451	A_44_P714885	TC589847
0.0004887	0.665	0.465	1.43	A_44_P112237	ENSRNOT00000052249
0.0004887	0.677	0.464	1.459	A_44_P311247	NM_212515
0.00049	0.553	0.413	1.339	A_44_P318941	XM_225467
0.0004909	1.338	0.723	1.851	A_44_P941132	ENSRNOT00000030569
0.0004926	3.139	1.996	1.573	A_44_P318029	ENSRNOT00000035618
0.0004966	0.672	1.102	0.61	A_44_P1006988	ENSRNOT00000025335
0.0004978	1.531	1.322	1.158	A_44_P494483	XM_215528
0.0004985	1.186	1.542	0.769	A_44_P311945	ENSRNOT00000013471
0.000499	0.625	0.444	1.408	A_44_P222865	ENSRNOT00000005711

0.0005041	0.333	0.232	1.435	A_43_P10069	DV717672
0.0005044	0.58	0.375	1.547	A_43_P12406	NM_024151
0.0005062	5.765	10.524	0.548	A_44_P451627	XM_237286
0.0005085	0.739	0.382	1.935	A_44_P503579	NM_201415
0.0005109	50.115	140.76	0.356	A_44_P1021630	ENSRNOT00000058312
0.0005193	1.844	0.455	4.053	A_44_P394119	BG663439
0.0005209	0.245	0.151	1.623	A_44_P183694	AB072614
0.0005241	1.352	0.88	1.536	A_44_P243604	ENSRNOT00000055588
0.0005308	3.899	6.584	0.592	A_44_P299247	NM_012778
0.0005309	0.61	1.014	0.602	A_44_P477446	ENSRNOT00000043942
0.0005328	3.973	6.483	0.613	A_44_P299247	NM_012778
0.0005329	0.09	0.179	0.503	A_44_P233080	NM_012551
0.0005337	0.658	0.405	1.625	A_44_P121682	XM_230870
0.000536	1.501	0.349	4.301	A_44_P822078	XM_576832
0.0005408	1.369	0.858	1.596	A_44_P494652	NM_001013431
0.0005419	1.076	1.693	0.636	A_44_P258751	NM_031081
0.0005452	0.239	0.152	1.572	A_42_P710738	NM_031620
0.0005461	0.885	0.388	2.281	A_44_P157045	ENSRNOT00000045196
0.0005473	0.812	0.474	1.713	A_44_P194925	ENSRNOT00000043365
0.00055	0.564	0.754	0.748	A_44_P105791	BF548544
0.0005565	0.894	0.466	1.918	A_42_P561580	NM_031113
0.0005579	0.664	0.323	2.056	A_44_P1042876	NM_031971
0.000562	0.364	0.675	0.539	A_44_P808557	TC604543
0.0005674	1.57	1.118	1.404	A_44_P1033023	NM_013063
0.0005693	0.588	1.221	0.482	A_44_P505500	ENSRNOT00000052393
0.0005738	0.125	0.523	0.239	A_44_P1016061	DV729072
0.0005842	1.138	1.517	0.75	A_44_P302012	ENSRNOT00000007173
0.0005852	0.071	0.014	5.071	A_44_P975250	BC099121
0.0005871	2.911	4.225	0.689	A_44_P748217	ENSRNOT00000046038
0.0005956	0.849	0.339	2.504	A_43_P17988	NM_001025018
0.0006055	0.706	0.55	1.284	A_43_P11046	TC581726
0.0006068	1.143	2.011	0.568	A_42_P489167	XM_224963
0.0006188	1.096	1.32	0.83	A_44_P1040854	NM_153628
0.0006236	0.662	0.495	1.337	A_44_P116176	ENSRNOT00000019107
0.0006237	0.347	0.233	1.489	A_44_P370645	ENSRNOT00000008329
0.0006247	0.614	0.177	3.469	A_44_P1042876	NM_031971
0.0006283	0.694	1.011	0.686	A_42_P638128	NM_012893
0.0006297	1.096	0.664	1.651	A_42_P592059	ENSRNOT00000001922
0.0006318	0.23	0.887	0.259	A_44_P741769	AI555513
0.0006338	2.896	1.439	2.013	A_44_P556586	BC086580
0.0006366	1.549	5.636	0.275	A_44_P152290	ENSRNOT00000007761
0.0006397	2.824	0.699	4.04	A_43_P15470	NM_012701
0.0006409	0.492	0.342	1.439	A_44_P165918	ENSRNOT00000061986
0.0006414	0.895	0.581	1.54	A_44_P1006655	NM_053597
0.0006515	0.916	1.599	0.573	A_44_P217774	NM_001009698
0.0006579	0.5	0.327	1.529	A_44_P461657	XM_001071880
0.0006591	0.78	0.56	1.393	A_44_P948037	NM_001039196
0.0006702	1.206	0.809	1.491	A_43_P11040	NM_001009639

0.0006711	0.734	1.822	0.403	A_44_P312309	NM_001047087
0.0006715	2.514	2.11	1.191	A_43_P15205	ENSRNOT00000061430
0.0006795	3.769	1.25	3.015	A_44_P135424	XM_223116
0.0006824	0.611	0.413	1.479	A_44_P370335	NM_001011911
0.0006851	1.209	0.795	1.521	A_44_P1037886	NM_001033685
0.0006855	0.269	0.709	0.379	A_43_P10405	ENSRNOT00000002523
0.0006931	0.392	0.286	1.371	A_44_P234500	XR_006077
0.0006933	1.588	3.094	0.513	A_44_P1046263	ENSRNOT00000022583
0.0006943	1.143	0.762	1.5	A_44_P433367	AF546755
0.0006943	0.871	0.682	1.277	A_44_P1022403	NM_001004204
0.0007009	0.931	0.151	6.166	A_44_P175786	XM_228865
0.0007016	0.083	0.169	0.491	A_44_P233080	NM_012551
0.0007019	1.991	0.684	2.911	A_43_P11951	NM_019150
0.0007079	0.87	0.602	1.445	A_43_P11423	XM_342470
0.0007097	1.127	0.75	1.503	A_44_P158216	NM_022185
0.00071	3.671	7.301	0.503	A_44_P463069	ENSRNOT00000043693
0.0007128	0.656	0.445	1.474	A_44_P454993	XM_346127
0.0007163	1.589	2.327	0.683	A_44_P159191	ENSRNOT00000025756
0.0007208	0.635	0.964	0.659	A_43_P10601	XM_220207
0.0007215	3.918	6.476	0.605	A_44_P299247	NM_012778
0.0007277	0.646	0.851	0.759	A_44_P153206	NM_031515
0.000728	0.681	1.338	0.509	A_44_P239985	NM_013217
0.0007292	1.008	0.765	1.318	A_44_P390454	NM_017276
0.0007296	1.423	0.757	1.88	A_44_P515360	L22079
0.0007313	0.331	0.6	0.552	A_43_P14802	ENSRNOT00000024714
0.0007316	0.908	1.477	0.615	A_44_P386840	NM_001013209
0.0007354	0.78	0.389	2.005	A_44_P944832	BG671311
0.0007392	2.26	3.308	0.683	A_43_P11924	NM_017338
0.000741	0.068	0.038	1.789	A_44_P416695	NM_001004022
0.0007431	1.82	1.003	1.815	A_44_P220301	ENSRNOT00000061270
0.0007464	9.266	23.758	0.39	A_44_P489468	ENSRNOT00000030661
0.0007495	2.262	1.529	1.479	A_44_P716323	TC591828
0.0007501	1.181	0.874	1.351	A_43_P15303	NM_030836
0.0007565	0.756	1.17	0.646	A_44_P411362	NM_001039026
0.0007576	0.23	0.12	1.917	A_44_P461130	NM_183333
0.0007586	0.551	0.707	0.779	A_44_P822616	ENSRNOT00000000206
0.0007637	0.886	0.502	1.765	A_44_P100565	A_44_P100565
0.0007641	0.803	0.61	1.316	A_44_P1046566	ENSRNOT00000004150
0.0007686	0.815	0.46	1.772	A_44_P194928	XM_213602
0.0007756	2.185	2.991	0.731	A_44_P607486	ENSRNOT00000006604
0.0007756	1.032	0.673	1.533	A_44_P520509	NM_001033868
0.0007863	7.244	10.812	0.67	A_43_P21455	ENSRNOT00000014917
0.0007939	0.482	0.35	1.377	A_44_P393422	NM_001013188
0.0007996	38.447	159.751	0.241	A_44_P994686	NM_012676
0.0007998	1.712	3.107	0.551	A_44_P615732	ENSRNOT00000017156
0.0008021	0.087	0.197	0.442	A_44_P233080	NM_012551
0.0008066	0.473	1.037	0.456	A_44_P651794	ENSRNOT00000034463
0.0008103	12.067	2.062	5.852	A_44_P424218	ENSRNOT00000017151

0.0008159	1.181	2.543	0.464	A_44_P801044	NM_001025775
0.0008183	2.309	1.108	2.084	A_44_P1060444	XM_216368
0.0008223	0.912	0.491	1.857	A_44_P280410	NM_183325
0.0008245	1.483	2.58	0.575	A_44_P492321	ENSRNOT00000023710
0.0008271	0.881	0.563	1.565	A_44_P374011	NM_001017489
0.0008273	3.685	7.419	0.497	A_44_P851230	BF558478
0.0008282	0.613	0.422	1.453	A_44_P603427	BC104707
0.0008457	1.202	0.786	1.529	A_44_P336714	XM_341545
0.0008476	1.465	3.048	0.481	A_44_P649177	ENSRNOT00000017391
0.0008498	0.57	1.239	0.46	A_43_P16715	NM_001024903
0.0008532	0.663	1.022	0.649	A_43_P11226	XM_217381
0.0008595	19.682	2.38	8.27	A_44_P533672	BG670971
0.0008611	0.717	0.488	1.469	A_44_P473220	XM_344177
0.0008641	2.707	1.324	2.045	A_43_P22696	A_43_P22696
0.0008691	3.961	6.366	0.622	A_44_P299247	NM_012778
0.0008726	0.242	0.493	0.491	A_44_P160113	AW918729
0.0008742	0.531	0.354	1.5	A_44_P992404	NM_001039004
0.0008769	0.464	0.991	0.468	A_44_P994454	ENSRNOT00000006370
0.0008791	0.791	0.468	1.69	A_44_P266340	AW918765
0.0008836	0.466	1.036	0.45	A_44_P252417	NM_022281
0.000884	0.537	0.904	0.594	A_44_P836445	NM_001014255
0.000886	3.275	2.127	1.54	A_43_P16740	ENSRNOT00000020532
0.0008876	1.052	0.794	1.325	A_42_P525962	ENSRNOT00000005402
0.0008878	0.173	0.66	0.262	A_44_P652332	NM_001025023
0.0008896	0.181	0.398	0.455	A_44_P542887	NM_001014207
0.000898	1.185	0.787	1.506	A_43_P17564	NM_001013044
0.0009006	1.381	0.916	1.508	A_44_P510659	NM_019380
0.0009066	1.43	6.28	0.228	A_43_P16346	U89745
0.0009075	1.158	1.518	0.763	A_44_P309052	NM_001008853
0.0009099	2.08	0.966	2.153	A_43_P10593	NM_032612
0.0009113	1.891	0.339	5.578	A_44_P473020	AF321133
0.0009123	0.787	1.106	0.712	A_42_P800669	BF289687
0.0009146	0.992	0.73	1.359	A_44_P1054213	NM_013083
0.0009199	0.488	0.363	1.344	A_44_P494862	NM_001008309
0.0009207	0.576	0.405	1.422	A_42_P544965	NM_031104
0.0009226	0.301	0.79	0.381	A_44_P352123	NM_001014215
0.0009235	1.072	0.652	1.644	A_44_P334709	NM_022672
0.0009309	0.372	0.295	1.261	A_44_P149036	NM_017138
0.0009324	0.804	1.355	0.593	A_44_P533778	NM_030830
0.0009348	0.574	1.476	0.389	A_44_P747226	TC620374
0.0009367	0.303	1.137	0.266	A_44_P639148	TC605165
0.0009367	2.121	1.49	1.423	A_43_P10326	CF110545
0.0009437	4.067	6.81	0.597	A_44_P299247	NM_012778
0.0009481	0.72	0.393	1.832	A_44_P200630	AA851208
0.0009491	0.863	0.643	1.342	A_44_P191784	NM_031969
0.0009521	0.08	0.506	0.158	A_44_P730758	TC609403
0.0009522	2.17	0.77	2.818	A_44_P190226	ENSRNOT00000019919
0.0009556	0.353	0.163	2.166	A_42_P641234	NM_001008303

0.0009583	0.627	0.389	1.612	A_44_P446539	ENSRNOT00000011456
0.0009585	1.394	1.004	1.388	A_44_P995085	NM_001007801
0.0009597	1.368	0.74	1.849	A_44_P777199	NM_001008354
0.0009631	2.75	4.731	0.581	A_42_P524370	NM_053369
0.0009668	0.221	0.512	0.432	A_44_P566856	TC639666
0.0009714	0.625	0.444	1.408	A_42_P639337	NM_001014272
0.000974	1.862	0.905	2.057	A_44_P376683	BF548232
0.0009758	1.034	2.247	0.46	A_43_P20159	ENSRNOT00000033355
0.000983	0.868	0.597	1.454	A_44_P533172	AI535535
0.0009837	0.982	3.155	0.311	A_44_P796993	TC626901
0.0009876	1.968	5.095	0.386	A_43_P18603	ENSRNOT00000024296
0.00099	0.592	0.853	0.694	A_44_P1057074	XM_221050
0.0009937	3.106	1.057	2.939	A_42_P666809	DV725602
0.0009963	0.615	0.407	1.511	A_44_P238891	ENSRNOT00000014993
0.0009988	2.723	1.304	2.088	A_44_P538989	NM_001014010

Vita

Jennifer Irene Drake (born Jennifer Irene Mazurek) was born on July 22, 1981 in Milwaukee, WI. She graduated from Divine Savior Holy Angels High School, Milwaukee, WI in 1999. She received her Bachelor of Sciences in Molecular Biology and Biochemistry from the University of Wisconsin – Madison in 2002. After graduation, she worked for Epic Systems Corporation, Madison, WI testing electronic medical record software. In 2004, she joined the Bioinformatics program at Virginia Commonwealth University and received her Master of Bioinformatics degree in 2006, after which she joined the Integrative Life Sciences Ph.D. program in VCU Life Sciences at Virginia Commonwealth University.

Publications:

Drake JI, Bogaard HJ, Mizuno S, Clifton B, Xie B, Gao Y, Dumur CI, Fawcett P, Voelkel NF, and Natarajan R. Molecular Signature of a Right Heart Failure Program in Chronic Severe Pulmonary Hypertension. *Am. J. Respir. Cell Mol. Biol.,* in press.

Voekel NF, Natarajan R, Drake JI, and Bogaard HJ. Right Ventricle in Pulmonary Hypertension. *Comprehensive Physiology*, 2011, 1:1-16.

Wegrzyn J, Potla R, Chwae Y-J, Sepur NBV, Zhang Q, Koeck T, Derecka M, Szczepanek K, Szelag M, Gornicka A, Moh A, Moghaddas S, Chen Q, Bobbili S, Cichy J, Dulak J, Baker DP, Wolfman A, Stuehr D, Hassan MO, Fu X-Y, Avadhani N, Drake JI, Fawcett P, Lesnefsky EJ, Larner AC. Function of mitochondrial Stat3 in cellular respiration. *Science*, 2009 Feb 6, 323(5915):793-797.

Poster Presentations:

Drake JI, Bogaard HJ, Natarajan R, Kraskausakas D, Fawcett, P, and Voelkel NF. *Role of Adducin 3 in an Experimental Model of Right Ventricular Failure and Pulmonary Hypertension*. American Thoracic Society Conference, May 17, 2011.

Drake JI, Natarajan R, Voelkel NF, and Fawcett P. *Gene Expression Profiling of Pulmonary Hypertension*, Graduate Student Research Forum, Virginia Council of Graduate Schools, February 19, 2010.